Compton Scattering and Renormalization of Twist Four Operators

by

Yao Ji

A Dissertation Presented in Partial Fulfillment
of the Requirements for the Degree
Doctor of Philosophy

Approved February 2016 by the
Graduate Supervisory Committee:

Andrei Belitsky, Chair
Richard Lebed
Kevin Schmidt
Tanmay Vachaspati

ARIZONA STATE UNIVERSITY

May 2016

ABSTRACT

In this thesis, I present the study of nucleon structure from distinct perspectives in the framework of Quantum Chromodynamics (QCD). I start by elaborating the motivations behind the endeavors and then introducing the key concept, namely the generalized parton distribution functions (GPDs), which serves as the framework describing hadronic particles in terms of their fundamental constituents. The second chapter is then devoted to a detailed phenomenological study of the Virtual Compton Scattering (VCS) process, where a more comprehensive parametrization is suggested. In the third chapter, the renormalization kernels that enters the QCD evolution equations at twist-4 accuracy are computed in terms of Feynman diagrams in momentum space, which can be viewed as an extension of the work by Bukhvostov, Frolov, Lipatov, and Kuraev (BKLK). The results can be used for determining the QCD background interaction for future precision measurements.

I would like to dedicate this dissertation to the memory of my grandfather Ruiqing Liu, and my best friend Ming Wang who passed away last year. May eternal peace be always with them.

ACKNOWLEDGMENTS

First of all, I would like to give sincere thanks to my advisor, Dr. Andrei Belitsky. He is one of the most important people in my life. I thank him not only for his direction, assistance, and guidance but also for his patience, preciseness and warmth. He steered me into particle physics, shared with me knowledge of physics and introduced me to scientific research. He also gave me many suggestions on how to solve problems in my daily life. My appreciation can't be conveyed in words. Thank you sir for these seven years I have known you.

I would also like to thank my friends Francis Duplessis, Jeffery Hyde, Henry Lamm IV, Chufeng Li, Nikhil Monga, Jayden Newstead, Dr. Saugata Chatterjee, Dr. Xinyang Wang, Dr. Lang Yu, Yun Zhao and Shuchen Zhu for their enlightening discussion on various topics in physics and mathematics. Special thanks are due to Prof. Richard Lebed, Henry Lamm IV, Jeffery Hyde and Shuchen Zhu for proofreading this thesis and valuable comments.

Furthermore, I would like to thank all my committee members, Prof. Richard Lebed, Prof. Kevin Schmidt and Prof. Tanmay Vachaspati for their valuable time and advice.

Thanks are also due to all the faculty, staff and classmates in the Physics Department at the Arizona State University for their assistance and friendship.

Finally, thanks to my family for their support, understanding and encouragement.

TABLE OF CONTENTS

APPENDIX Page

LIST OF FIGURES

CHAPTER 1

INTRODUCTION

Protons and neutrons, collectively known as nucleons, are the fundamental building blocks of the ordinary matter, which give rise to 99.9% of the total mass of our observable universe. As the name suggests, the neutron carries no electric charge while the proton is a positively charged particle. In 1933, the exceptionally large magnetic moment of the proton was firstly measured by Otto Stern, et.al. [1, 2] and a year later, a group led by Isidor Isaac Rabi and Otto Stern [3, 4, 5] conducted the experiment concluding that the neutron carries negative magnetic moment. These significant discoveries led physicists to realize that the nucleons are not elementary particles, but instead they are composite particles made up by fundamental particles. This realization was further confirmed by the study of elastic electron-proton scattering experiment [6, 7] pioneered by Robert Hofstadter et.al., where they demonstrated that the electron-proton scattering cross section deviated significantly from both what the single-particle theory predicted and the electron-electron experimental data. Moreover, during the 1950s and 1960s, a zoo of hadronic particles was discovered, and the classification of these newly discovered particles eventually led to the proposal of the quark model constructed by Murray Gell-Mann and George Zweig in 1964 [8]. In this model, the nucleons, or baryons in general, are postulated to be composite of three elementary particles called quarks, while the mesons are particles made up of two quarks. A few years later, in order to describe the deep inelastic scattering data obtained by the Stanford Linear Accelerator in 1968 -1969, James Bjorken and Richard Feynman [9] developed the parton model, in which the nucleons are made of strongly interacting constituents (partons), which are known today as quarks and gluons.

In the framework of the simple quark model, the anomalous magnetic moments of the nucleons were believed to be explained fairly well by assuming that the up and down

quarks have similar masses, which together account for a large proportion of the nucleon mass. However, as the current understanding goes, the majority of the nucleon's mass could not be attributed to the constituent quarks, but instead originates from the strong interactions within the nucleon. The simple quark model also postulated that the spin of the nucleon is entirely built up from the quark spins, in accordance with the Pauli exclusion principle. This conclusion, however, was challenged by the European Muon Collaboration at CERN in 1987, where it was discovered that the valence quarks – quarks that are present within the nucleon at low energy scales – are responsible for only a small fraction of the total spin of the nucleon. Later experiments confirmed this discovery with higher-precision measurements. This discovery puzzled high-energy physicist for quite some time and is now known as the "proton spin crisis" [10]. This inconsistency of the simple quark model with experimental results has motivated a great amount of discussion and research interest since then, and the HERMES experiment was constructed dedicated to the study of nucleon spin structure, and concluded the spin contribution of the valence quarks to be roughly 33% [11].

On the theoretical side, it became obvious that it is necessary to include the spin contributions that had previously been unaccounted for. One of the very first attempts for solving the nucleon spin puzzle in general was proposed by Robert L. Jaffe and Aneesh V. Manohar, in the form of the sum rule for nucleon spin [12],

$$\frac{1}{2} = \frac{1}{2}\Delta\Sigma + \mathcal{L}_q + \Delta G + \mathcal{L}_g \,, \tag{1.1}$$

where $\Delta\Sigma, \mathcal{L}_q, \Delta G$ and $\mathcal{L}_g$ represent the contributions of quark spin, quark angular momentum, gluon spin and gluon angular momentum to the total nucleon spin, respectively. Each term in eqn.1.1 is defined in the infinite-momentum frame, and the last three terms have gauge dependence which have to be fixed in the light-cone gauge in order to have them unambiguously defined. Despite these shortcomings, it retains a clear physical pic-

ture, in which direct connections between the nucleon's spin content and the high-energy experiments can be made.

Another well-known sum rule for the nucleon spin was proposed by Xiangdong Ji in 1997, which is frame independent and manifestly gauge invariant [13],

$$\frac{1}{2} = J_q + J_g = \frac{1}{2}\Delta\Sigma + L_q + J_g\,, \tag{1.2}$$

and explicitly the angular momentum density along the z-direction for an arbitrary frame can be written as,

$$M^{012} = \frac{1}{2}\bar{\psi}\gamma^0\sigma^{12}\psi + \bar{\psi}\gamma^0(\vec{x}\times(-i\vec{D}))^3\psi + [\vec{x}\times(\vec{E}\times\vec{B})]^3\,, \tag{1.3}$$

where $\vec{D} = \vec{\nabla} - ig\vec{A}$, $\vec{E}$ and $\vec{B}$ is the electric and magnetic field for the gluon field, respectively.

As simple and elegant eqn.1.3 may look, it relies on the information of strong interaction in the low-energy regime in the form of quark and gluon distribution functions, together known as parton distribution functions [13, 14, 15, 16]. Since a comprehensive theoretical technique for the studies of low-energy strong interactions is still beyond our reach, input from experimental data, and more recently, the development of lattice QCD is a must. From the experimental perspective, the best tool for getting access to the parton distribution functions is through the so-called Deep Inelastic Scattering (DIS).

1.1 Generalized Parton Distribution Functions and Deeply Virtual Compton Scattering

Most of our knowledge about the nucleon structure is obtained from the scattering processes of high-energy leptons with nucleons. The primary reasons that make lepton-nucleon scattering stand out in the study of nucleon structures is mulitfold: the structureless nature of the leptons, their well-understood behaviors under the electromagnetic interaction, their immunity to strong-interaction contaminations, and their availability.

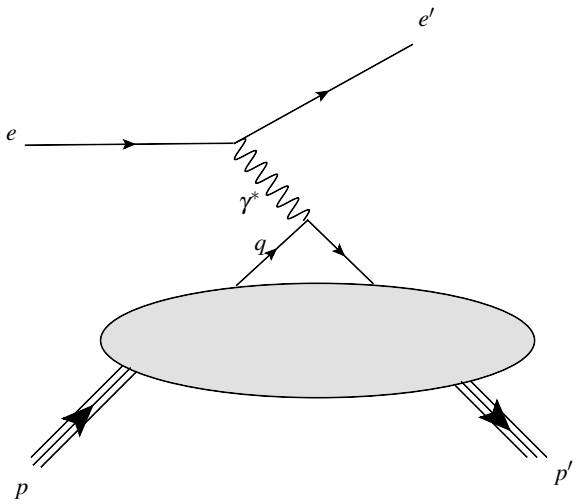

Figure 1.1: Electron-nucleon Elastic Scattering described as interaction via a virtual photon exchange between an electron and a single quark within the nucleon.

In general, lepton-nucleon scattering can be classified into two generic categories: either *inclusive* or *exclusive*. In an inclusive experiment, the final state of the scattered lepton is measured, while the final hadronic states are left undetected. In an exclusive experiment, however, the final states of the lepton as well as the hadronic particles of the scattering process are recorded.

In the following, a descriptive introduction will be given on how experimental results can be interpreted theoretically in the framework of Quantum Chromodynamics (QCD), and how the generalized parton distribution originated (For details, see [17, 18, 19]).

1.1.1 Elastic Scattering and Form Factors

As previously mentioned, the first elastic electron-nucleon scattering experiments were conducted by Hofstadter and collaborators at the Stanford Linear Accelerator in the 1950s. The process can be written as $eN \rightarrow e'N'$, as shown in fig. 1.1.

Theoretically, this process is described in the form of a QCD matrix element,

$$\langle p'|\bar{\psi}_q(x)\mathcal{O}\psi_q(x)|p\rangle\,. \tag{1.4}$$

This is a *local non-forward* QCD matrix element in the sense that only one space-time point is involved (x in the present case, and it is often set to be 0 without losing generality) and *non-forward* refers to the fact that the four-momentum of the nucleon has been changed in the process (i.e., $p \to p'$). In simple terms, eqn.1.4 describes the process of creating a quark at spacetime point x in a nucleon with momentum p and then creating another quark at the same spacetime point in a nucleon whose four-momentum has changed into p'. The operator $\mathcal{O}$ elucidates how the two quarks are related to each other via relevant interactions. In a special reference frame, the so-called Breit frame, in which the energy of the virtual photon transferred between the lepton and the nucleon is zero, eqn.1.4 retains a simpler picture as the probability of probing a constituent quark absorbing the virtual photon γ^* at spacetime x, disregarding the momentum of the nucleon itself.

The matrix elements for the cases of vector and axial vector currents in momentum space, eqn.1.4 gives rise to the so-called Form Factors (FFs), in analogy to the electron form factors in Quantum Electrodynamics (QED) [20]. By applying Dirac's Equation as well as an analysis of the available physical quantities and operators at hand, namely, the kinematical variable of 4-vectors p^μ and $\Delta^\mu = p' - p$, γ^μ and $\sigma^{\mu\nu}$ for the vector case and γ^5, $\gamma^\mu\gamma^5$ for the axial current case, the most general matrix element decomposition that the Lorentz symmetry dictates reads,

$$\langle p'|\bar{\psi}_q(0)\gamma^\mu\psi_q(0)|p\rangle = F_1^q(t)\bar{N}(p')\gamma^\mu N(p) + F_2^q(t)\bar{N}(p')i\sigma^{\mu\nu}\frac{\Delta_\nu}{2M_N}N(p)\,, \tag{1.5}$$

$$\langle p'|\bar{\psi}_q(0)\gamma^\mu\gamma^5\psi_q(0)|p\rangle = G_A^q(t)\bar{N}(p')\gamma^\mu\gamma^5 N(p) + G_P^q(t)\bar{N}(p')\gamma^5\frac{\Delta^\mu}{2M_N}N(p)\,. \tag{1.6}$$

where $t = \Delta^2$ and M_N is the mass of the nucleon under consideration. $F_1^q(t)$, $F_2^q(t)$, $G_A^q(t)$ and $G_P^q(t)$ are called the Dirac, Pauli, axial and induced pseudo-scalar form factors, respectively and they are the basic observables in lepton-nucleon scattering.

The information of the quark and gluon distributions are then encoded in the four form factors illustrated above. A linear combination of $F_1^q(t)$ and $F_2^q(t)$ can be related to the electric and magnetic nucleon form factors denoted as $G_E^q(t)$ and and $G_M^q(t)$, respectively. Fourier transforming G_E and G_M into coordinate space in the Breit frame, they have simple physical interpretations as electric and magnetic densities in the nucleon.

1.1.2 Inclusive Scattering and Parton Distribution Functions

Lepton-nucleon scattering experiments, generally called "Deep inelastic Scattering (DIS)" and written as $eN \to eX$, were first carried out by the Stanford Linear Accelerator Center in the late 1960s [21]. The result of this experiment led to the proposal of the nucleon parton model.

The kinematics involved in this process include the squared four-momentum, transferred between the electron and the nucleon, denoted as $Q^2 = -q^2 \equiv -(k' - k)^2 < 0$, where $p_{e'}$ and p_e are the four-momenta of the outgoing and incoming electron, the energy-loss variable $\nu \equiv \dfrac{p_N \cdot q}{M_N}$, and the Bjorken variable $x_B = \dfrac{Q^2}{2p_N \cdot q}$. In the picture of the parton model, the virtual photon emitted from the interacting electron interacts with a singe parton (or a quark as it is understood today) inside the nucleon, which then goes through a series of interactions that finally leads to hadronization (Fig. 1.2).

This simple picture, however, relies heavily on the concept of QCD "factorization"[1] [13, 15], where the part of the quantum-mechanical amplitude representing a hard

[1] QCD factorization has been explicitly proved for the leading order in $1/Q^2$ expansion, i.e., for a transversely polarized virtual photon in Deeply Virtual Compton Scattering [15, 22] and longitudinal polarized

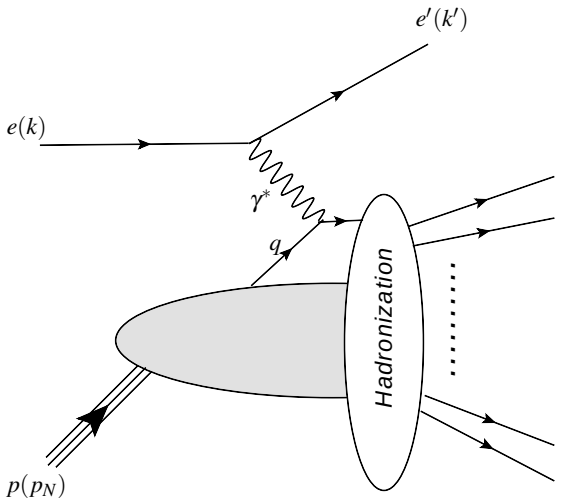

Figure 1.2: Electron-nucleon Inelastic Scattering depicted as single quark-electron interaction.

process calculable in perturbation theory, e.g., the virtual photon and quark interacting with large momenta, can be factored out from the sea of soft interacting particles. This phenomenon can be physically interpreted as the decoherence between large-scale/low energy physics (long-wavelength partons inside the nucleons) and the small scale/high-energy physics (the-high resolution scale of the virtual photon).

The amplitude of the lepton-nucleon interaction can be generally written as,

$$\mathcal{A}_n = L_\mu(k,k')\langle n|j^\mu(0)|p_N\rangle\,, \tag{1.7}$$

where $\langle n|j^\mu(0)|p\rangle$ is the hadronic transition amplitude induced by the local quark electromagnetic current $j^\mu(0)$. The leptonic current reads,

$$L^\mu(k,k') = \frac{ie}{q^2}\bar{u}(k')\gamma^\mu u(k)\,. \tag{1.8}$$

Inclusive processes require us to sum over all final hadronic states, and as a result, the squared amplitude of the lepton-nucleon interaction is written,

$$|\mathcal{A}|^2 = \sum_n \frac{e^2}{q^4} L_\mu^\dagger L_\nu W^{\mu\nu}$$

photons in deeply virtual meson production [23], while higher-order behaviors are still not fully understood yet.

$$= \sum_n \frac{e^2}{q^4} L_\mu^\dagger L_\nu \langle p_N | j^{\mu\dagger}(0) | n \rangle \langle n | j^\mu(0) | p_N \rangle \,. \tag{1.9}$$

Summation over all hadronic state is achieved by applying the completeness relation $\sum_n |n\rangle\langle n| = 1$, and then a Fourier transform yields,

$$W^{\mu\nu} = \frac{1}{4\pi} \int d^4z \, e^{iq\cdot z} \langle p_N | j^\mu(z) j^\nu(0) | p_N \rangle \,. \tag{1.10}$$

By Lorentz and gauge invariance arguments, the deep inelastic scattering nucleon electromagnetic tensor $W^{\mu\nu}$ can be described in terms of four structure functions, denoted as $F_{1,2}$ and $g_{1,2}$.

$$\begin{aligned} W^{\mu\nu} = & -\left(g^{\mu\nu} - \frac{q^\mu q^\nu}{q^2} \right) F_1(x_B, Q^2) \\ & + \frac{1}{p_N \cdot q} \left(p_N^\mu - \frac{p_N \cdot q}{q^2} q^\mu \right) \left(p_N^\nu - \frac{p_N \cdot q}{q^2} q^\nu \right) F_2(x_B, Q^2) \\ & - \frac{i}{p_N \cdot q} \varepsilon^{\mu\nu\rho\sigma} q_\rho s_\sigma g_1(x_B, Q^2) - \frac{i}{p_N \cdot q} \varepsilon^{\mu\nu\rho\sigma} q_\rho \left(s_\sigma - \frac{s \cdot q}{p_N \cdot q} p_\sigma \right) g_2(x_B, Q^2) \,, \end{aligned} \tag{1.11}$$

where s^μ is the nucleon polarization vector.

The QCD factorization principle allows us to make connections between the physical observables $F_{1,2}$ defined above with the quark distribution functions $q(x)$ given by,

$$F_i(x, x_B) = \int_{x_B}^1 \frac{dx}{x} C_i(x_B/x, Q^2/\mu^2) q(x; \mu^2) \,, \tag{1.12}$$

where C_i is the coefficient function perturbatively computable from the high-energy quark-photon interaction. μ^2 is the arbitrary factorization cut-off scale normally set between $1 GeV$ and Q^2. This equation lays the foundation for the values of perturbative QCD calculations [19].

In the Bjorken limit, where $Q^2 \to +\infty$ with $x_B = const$, only two independent functions $F_1(x_B, Q^2)$ and $g_1(x_B, Q^2)$ in eqn.1.10 survive, corresponding to unpolarized $q(x_B, Q^2)$

and polarized $\Delta q(x_B, Q^2)$ parton distribution functions, respectively, and the convolution equation 1.12 receives huge simplifications [24].

$$F_1(x_B, Q^2) = \frac{1}{2}\sum_q e_q^2(q(x_B, Q^2) + \bar{q}(x_B, Q^2))\,, \tag{1.13}$$

$$g_1(x_B, Q^2) = \frac{1}{2}\sum_q e_q^2(\Delta q(x_B, Q^2) + \Delta\bar{q}(x_B, Q^2))\,, \tag{1.14}$$

where e_q is the charge of the quark of each flavor and $\bar{q}$ and $\Delta\bar{q}$ are the anti-quark counterparts of q and Δq, respectively.

The fact that the analysis is on an inclusive process enables us to invoke a powerful tool, namely, the Optical Theorem, which asserts that

$$2\,\mathrm{Im}(\mathcal{M}(a \to b)) = \sum_f \int d\Pi_f \mathcal{M}^*(b \to f)\mathcal{M}(a \to f)\,, \tag{1.15}$$

where f represents all possible intermediate states in the process of $a \to b$.

The Optical Theorem allows us to identify the cross section of the deep inelastic scattering with the forward amplitude of the double-virtual Compton scattering of nucleons.

$$\sigma(\gamma^* p_N \to \text{hardonization}) \propto \mathrm{Im}\,\mathcal{M}(\gamma^* p_N \to \gamma p_N)\,, \tag{1.16}$$

where the ratio is determined by the kinematics in the process in a frame-dependent way.

As long as the premise of the QCD factorization applies, and base on the Optical Theorem the study of deep inelastic scattering is converted to the study of matrix element written as,

$$\langle p|\bar{\psi}_q(0)\mathcal{O}\psi_q(z)|p\rangle\,. \tag{1.17}$$

Here eqn.1.17 is called "non-local" "forward" matrix element, which refers to the fact that the operator between the nucleon states involves two separate points in space-time (0 and z) and "forward" signifies the nucleon does not change its momentum in the process.

The investigation of deep inelastic scattering is generally carried out in the frame where the momenta of incoming and outing nucleons are collinear along the z-axis. One could then proceed to define the light-cone frame l^μ related to the nucleon frame z^μ by[2] $(l^+,l^1,l^2,l^-) = ((z^0+z^3)/\sqrt{2}, z^1, z^2, (z^0-z^3)/\sqrt{2})$. This frame redefinition reduces the number of coordinates on which the massless particles traveling along the z-direction depend to only one, either l^+ or l^- according to their direction along z-axis. At leading order for fast-moving nucleons, the two quark distribution functions $q(x)$ and $\Delta q(x)$, where $x = p_q^+/p_N^+$ is the momentum fraction of the nucleon the quark carries, are written as [25],

$$q(x) = \frac{p^+}{4\pi}\int dz^- e^{ixp^+z^-}\langle p|\bar{\psi}_q(0)\gamma^+[0,z]\psi_q(z)|p\rangle\Big|_{z^+=z_\perp=0}, \tag{1.18}$$

$$\Delta q(x) = \frac{p^+}{4\pi}\int dz^- e^{ixp^+z^-}\langle pS_{||}|\bar{\psi}_q(0)\gamma^+\gamma^5[0,z]\psi_q(z)|pS_{||}\rangle\Big|_{z^+=z_\perp=0}. \tag{1.19}$$

where $S_{||}$ is nucleon spin projection in the longitudinal direction, and $[0,z] = P\int_0^z dz^-\cdot A^+$ is the gauge link between the two distinct spacetime points[3]. Here, at leading order, one counts only the number of particles traveling along the light-cone, while more generally for a DIS process, however, one is required to integrate out the dynamics on the transverse plane $l^\perp$. The function $q(x)$ can be interpreted as the quark density along the z^- direction for positive x, while for $x<0$, it represents the antiquark density traveling along the z^- direction. $\Delta q(x)$ is understood in a similar way except that in this case, it counts the quark/anti-quark number differences of different spin polarization.

Of course, one could also insert other Dirac bilinear operators, i.e., $\sigma^{\mu\nu}$, into eqn.1.17, and their contribution will occur at leading twist[4] expansion as well. The pro-

[2]Other definitions regarding l^1 and l^2 are also applicable, e.g. $l_\perp = \frac{1}{\sqrt{2}}(z^1+iz^2)$ and $\bar{l}_\perp = \frac{1}{\sqrt{2}}(z^1-iz^2)$ which can be easily connected to the helicity operator eqn. 3.8.

[3]Physically, the gauge link correspond to the summation of a series quark-gluon interactions between the two points.

[4]The twist t of an operator is defined as $t = d-s$, where d is the dimension of the operator and s is its spin. For example, the fermion current operator $\bar{\psi}\gamma^\mu\psi$ is a twist-2 operator since each Dirac spinor carries dimension $\frac{3}{2}$ while the current operator transforms as a vector under Lorentz group, as seen by the index μ.

cess involving $\sigma^{\mu\nu}$ will not however conserve the quark helicity. These processes are less experimentally accessible and as a result less well studied.

1.1.3 Exclusive Scattering and Generalized Parton Distribution Functions

With the concepts of Form Factors and Parton distribution function established, Dieter Müller, et.al., Xiangdong Ji and Anatoly Radyushin in the 1990s came to the idea to generalize these two distinct concepts into one single framework conveniently named *Generalized Parton Distribution Functions* (GPDs) [13, 15, 16]. A GPD is defined as the matrix element of a nonlocal non-forward process, written as,

$$\langle p_2|\bar{\psi}_q(0)\mathcal{O}\psi_q(y)|p_1\rangle\,, \tag{1.20}$$

where "non-forward" refers to the momentum change of the nucleon $p_2 \to p_1$, and nonlocal translates into the fact that two points 0 and y in spacetime are involved. Similar to the matrix element decomposition in the elastic scattering case, the leading twist-2 quark operators can be written as follows [13, 26],

$$\begin{aligned}\langle p_2|\bar{\psi}_q(-z^-)\gamma^+[-z^-,z^-]\psi_q(z^-)|p_1\rangle = \int_{-1}^{1} dx\, \mathrm{e}^{-ixp^+z^-}\Big\{&H^q(x,\eta,\Delta^2)\bar{u}(p_2)\gamma^+u(p_1)\\ &+E^q(x,\eta,\Delta^2)\bar{u}(p_2)\frac{i\sigma^{\nu+}\Delta_\nu}{2M_N}u(p_1)\Big\}\,,\end{aligned} \tag{1.21}$$

$$\begin{aligned}\langle p_2|\bar{\psi}_q(-z^-)\gamma^+\gamma^5[-z^-,z^-]\psi_q(z^-)|p_1\rangle = \int_{-1}^{1} dx\, \mathrm{e}^{-ixp^+z^-}\Big\{&\tilde{H}^q(x,\eta,\Delta^2)\bar{u}(p_2)\gamma^+\gamma^5u(p_1)\\ &-\tilde{E}^q(x,\eta,\Delta^2)\bar{u}(p_2)\gamma^5\frac{\Delta^+}{2M_N}u(p_1)\Big\}\,,\end{aligned} \tag{1.22}$$

$$\begin{aligned}\langle p_2|\bar{\psi}_q(-z^-)\sigma_\mu^{+\perp}[-z^-,z^-]\psi_q(z^-)|p_1\rangle = \int_{-1}^{1} dx\, \mathrm{e}^{-ixp^+z^-}\Big\{&H_T^q(x,\eta,\Delta^2)\bar{u}(p_2)i\sigma_\mu^{+\perp}u(p_1)\\ &+\tilde{H}_T^q(x,\eta,\Delta^2)\bar{u}(p_2)\frac{ip^+\Delta_\nu\sigma_\mu^{\nu\perp}}{2M_N^2}u(p_1)\\ &-E_T^q(x,\eta,\Delta^2)\bar{u}(p_2)\frac{\gamma^+\Delta_\mu^\perp-\Delta^+\gamma_\mu^\perp}{2M_N}u(p_1)\\ &-\tilde{E}_T^q(x,\eta,\Delta^2)\bar{u}(p_1)\frac{p^+\gamma_\mu^\perp}{2M_N}u(p_1)\Big\}\,,\end{aligned} \tag{1.23}$$

where M_N is the average mass of the incoming and going hadrons. $p = p_1 + p_2$, $\Delta = p_1 - p_2$ and $\eta = \dfrac{\Delta^+}{p^+}$ is called skewness. The first two operators conserve the helicity between the initial and final states of the hadrons, while the inclusion of the last operator illustrates the possibility of a helicity-flipping nucleon transition. This process can be physically understood as a helicity/orbital angular momentum conversion operation, and is due to the fact that the mass of the nucleons are not negligible.

Time reversal symmetry and hermiticity imply the following constraints on the GPDs. For $F^q = H^q, \tilde{H}^q, E, \tilde{E}^q, H_T, E_T$, one finds [20, 26, 27],

$$F^q(x,\eta,\Delta^2) = F^q(x,-\eta,\Delta^2)\,, \tag{1.24}$$

and

$$\tilde{E}_T^q(x,\eta,\Delta^2) = -\tilde{E}_T^q(x,-\eta,\Delta^2)\,, \tag{1.25}$$

while

$$\left(F^q(x,\eta,\Delta^2)\right)^* = F^q(x,-\eta,\Delta^2)\,, \tag{1.26}$$

for all leading twist GPDs except $\tilde{E}_T^q$ in which case, one finds,

$$\left(\tilde{E}_T^q(x,\eta,\Delta^2)\right)^* = -\tilde{E}_T^q(x,-\eta,\Delta^2)\,. \tag{1.27}$$

The leading-twist gluon operators are subjected to the same decomposition procedure, which yields [26, 28, 29, 30],

$$\begin{aligned}
&\langle p_2|F_a^{+\mu}(-z^-)[-z^-,z^-]^{ab} g_{\mu\nu}^{\perp} F_b^{\nu+}(z^-)|p_1\rangle \\
&\qquad = \frac{p^+}{4}\int_{-1}^{1} dx\, \mathrm{e}^{-ixp^+z^-}\Big\{H^g(x,\eta,\Delta^2)\bar{u}(p_2)\gamma^+u(p_1) \\
&\qquad\qquad + E^g(x,\eta,\Delta^2)\bar{u}(p_2)\frac{i\sigma^{\nu+}\Delta_\nu}{2M_N}u(p_1)\Big\}\,, \qquad (1.28)\\
&\langle p_2|F_a^{+\mu}(-z^-)[-z^-,z^-]^{ab} i\varepsilon_{\mu\nu}^{\perp} F_b^{\nu+}(z^-)|p_1\rangle
\end{aligned}$$

$$= \frac{p^+}{4}\int_{-1}^{1} dx\, \mathrm{e}^{-ixp^+z^-}\Big\{\tilde{H}^g(x,\eta,\Delta^2)\bar{u}(p_2)\gamma^+\gamma^5 u(p_1) - \tilde{E}^g(x,\eta,\Delta^2)\bar{u}(p_2)\gamma^5\frac{\Delta^+}{2M_N}u(p_1)\Big\}, \tag{1.29}$$

$$\langle p_2|F_a^{+\rho}(-z^-)[-z^-,z^-]^{ab}\tau^{\perp}_{\mu\nu;\rho\sigma}F_b^{\sigma+}(z^-)|p_1\rangle = \frac{p^+}{4}\int_{-1}^{1} dx\, \mathrm{e}^{-ixp^+z^-}\Big\{H_T^q(x,\eta,\Delta^2)\bar{u}(p_2)i\sigma_\sigma^{+\perp}u(p_1) + \tilde{H}_T^g(x,\eta,\Delta^2)\bar{u}(p_2)\frac{ip^+\Delta_\nu\sigma_\sigma^{\nu\perp}}{2M_N^2}u(p_1) - E_T^g(x,\eta,\Delta^2)\bar{u}(p_2)\frac{\gamma^+\Delta_\mu^\perp-\Delta^+\gamma_\sigma^\perp}{2M_N}u(p_1) - \tilde{E}_T^g(x,\eta,\Delta^2)\bar{u}(p_2)\frac{p^+\gamma_\sigma^\perp}{2M_N}u(p_1)\Big\}\tau^\perp_{\mu\nu}{}^{\sigma\rho}\frac{-\Delta_\rho}{2M_N}, \tag{1.30}$$

where $g^\perp_{\mu\nu}\equiv g_{\mu\nu}-n_\mu\bar{n}_\nu-n_\nu\bar{n}_\mu$[5], $\varepsilon^\perp_{\mu\nu}\equiv\varepsilon^{\alpha\beta\rho\sigma}g^\perp_{\mu\alpha}g^\perp_{\nu\beta}\bar{n}_\rho n_\sigma$[6], and $\tau^\perp_{\mu\nu;\rho\sigma}\equiv\frac{1}{2}g_{\mu\rho}g^\perp_{\nu\sigma}+\frac{1}{2}g_{\mu\sigma}g^\perp_{\nu\rho}-\frac{1}{2}g^\perp_{\mu\nu}g^\perp_{\rho\sigma}$.

Since anti-gluons are identical to gluons themselves, and the exchange of $x\to -x$ is identified as an exchange between particle-antiparticle paris, one finds the following constraints for the gluonic GPDs,

$$H^g(-x,\eta,\Delta^2)=H^g(x,\eta,\Delta^2), \qquad E^g(-x,\eta,\Delta^2)=E^g(x,\eta,\Delta^2), \tag{1.31}$$

$$\tilde{H}^g(-x,\eta,\Delta^2)=-\tilde{H}^g(x,\eta,\Delta^2), \qquad \tilde{E}^g(-x,\eta,\Delta^2)=-\tilde{E}^g(x,\eta,\Delta^2). \tag{1.32}$$

Although the GPDs are not directly accessible experimentally, as a unifying concept, its limits and moments in x have been studied extensively both experimentally and theoretically, and can be linked to the nonlocal forward and local non-forward processes, as has been discussed earlier. First of all, it is apparent that at the limit of $\Delta\to 0$, the nonlocal non-forward process which gives rise to GPDs reduces to the nonlocal forward case in which the parton distribution functions (PDFs) (1.18) are introduced. It is quite clear that

[5] $n_\mu=\frac{1}{\sqrt{2}}(1,0,0,1), \bar{n}_\mu=n^\mu$ are the light-cone null vectors.

[6] One adopts the convention $\varepsilon^{0123}=1$.

as $\Delta \to 0$, the skewness parameter $\eta = \Delta^+/p^+$ approaches 0 as well, and thus one obtains,

$$H^q(x,0,0) = q(x) = f^q(x)\theta(x) - \bar{f}^q(x)\theta(-x)\,, \tag{1.33}$$

$$\tilde{H}^q(x,0,0) = \Delta q(x) = \Delta f^q(x)\theta(x) - \Delta \bar{f}^q(x)\theta(-x)\,, \tag{1.34}$$

where $f^q(x)$ represents the quark distribution function while $\bar{f}^q(x)$ parametrize the distribution of antiquarks. Similarly, the gluonic GPDs obtain a physical interpretation in the forward limit as [19]

$$H^g(x,0,0) = g(x) = xf^g(x)\theta(x) - xf^g(-x)\theta(-x)\,, \tag{1.35}$$

$$\tilde{H}^g(x,0,0) = \Delta g(x) = x\Delta f^g(x)\theta(x) + x\Delta f^g(-x)\theta(-x)\,. \tag{1.36}$$

In order to retrieve the form factors defined in eqn.1.5 for local nonfoward processes, simply setting $z^- = 0$ in eqns.1.21 and 1.22 and contracting eqn.1.5 with the light-cone null vector $\bar{n}^\mu$, one arrives at,

$$F_1^q(\Delta^2) = \int_{-1}^{1} dx H^q(x,\eta,\Delta^2)\,, \qquad F_2^q(\Delta^2) = \int_{-1}^{1} dx E^q(x,\eta,\Delta^2)\,, \tag{1.37}$$

$$G_A^q(\Delta^2) = \int_{-1}^{1} dx \tilde{H}^q(x,\eta,\Delta^2)\,, \qquad G_P^q(\Delta^2) = \int_{-1}^{1} dx \tilde{E}^q(x,\eta,\Delta^2)\,. \tag{1.38}$$

With eqns.1.33 - 1.36, 1.37, and 1.38 established, one starts to realize the power of GPDs. As a matter of fact, more constraints and physical observables can be derived for the GPDs, as one finds on the following section.

1.1.4 GPD Polynomiality and Nucleon Spin Puzzle

Now one may proceed to investigate the higher x moments of the GPDs. To simplify our discussion, it is conventional to adopt the so called light-cone gauge, where the plus component of the gluon field A^+ is set to be zero, i.e., $A^+ = 0$ [31]. Then the gauge links appearing in eqns.1.21-1.23 and eqns.1.28-1.30 vanish. Take eqn.1.21 for example,

$$\int_{-1}^{1} dx x^n \, \mathrm{e}^{-ixp^+z^-} \left\{ H^q(x,\eta,\Delta^2)\bar{u}(p_2)\gamma^+ u(p_1) + E^q(x,\eta,\Delta^2)\bar{u}(p_2)\frac{i\sigma^{\nu+}\Delta_\nu}{2M_N}u(p_1) \right\}$$

$$= (i\partial_-)^n \int_{-1}^{1} dx \frac{e^{xp^+z^-}}{(p^+)^n} \Big\{ H^q(x,\eta,\Delta^2)\bar{u}(p_2)\gamma^+ u(p_1) + E^q(x,\eta,\Delta^2)\bar{u}(p_2)\frac{i\sigma^{\nu+}\Delta_\nu}{2M_N}u(p_1) \Big\}$$
$$= \frac{(i\partial_-)^n}{(p^+)^n}\langle p_2|\bar{\psi}_q(-z_1^-)\gamma^+\psi_q(z^-)|p_1\rangle$$
$$= \frac{1}{(p^+)^n}\langle p_2|\bar{\psi}_q(-z^-)\gamma^+(i\overleftrightarrow{\partial_-})^n\psi_q(z^-)|p_1\rangle\,, \tag{1.39}$$

where $\overleftrightarrow{\partial_-} = \overleftarrow{\partial_-} - \overrightarrow{\partial_-}$. For general purposes, one replaces the partial derivative $\overleftrightarrow{\partial_-}$ with the covariant derivative $\overleftrightarrow{D_-}$. Setting $z^- = 0$, one immediate finds,

$$\int_{-1}^{1} dx x^n \Big\{ H^q(x,\eta,\Delta^2)\bar{u}(p_2)\gamma^+ u(p_1) + E^q(x,\eta,\Delta^2)\bar{u}(p_2)\frac{i\sigma^{\nu+}\Delta_\nu}{2M_N}u(p_1) \Big\} \tag{1.40}$$
$$= \frac{1}{(p^+)^n}\langle p_2|\bar{\psi}_q(0)\gamma^+(i\overleftrightarrow{D}_-)^n\psi_q(0)|p_1\rangle$$
$$= \frac{1}{(p^+)^n}\langle p_2|\bar{\psi}_q(0)\gamma^+(i\overleftrightarrow{D}_-)^n\psi_q(0)|p_1\rangle$$
$$= \frac{1}{(p^+)^n} n_\mu n_{\mu_1}...n_{\mu_n}\langle p_2|\bar{\psi}_q(0)\gamma^\mu i\overleftrightarrow{D}^{\mu_1}...i\overleftrightarrow{D}^{\mu_n}\psi_q(0)|p_1\rangle$$
$$= \frac{1}{(p^+)^n} n_\mu n_{\mu\mu_1}...n_{\mu_n}\langle p_2|\mathcal{O}^{\mu_1...\mu_n}(0)|p_1\rangle\,, \tag{1.41}$$

where n_μ is the null vector in the light-cone frame.

As one wishes to focus on the studies of twist-2 operator $\mathcal{O}_{t_2}^{\mu\mu_1...\mu_2}$, the general operator $\mathcal{O}^{\mu\mu_1...\mu_n}$ appeared above is subjected to symmetrization over Lorentz indices in addition to a subtraction of trace its term, namely,

$$\mathcal{O}_{t_2}^{\mu\mu_1...\mu_2} = \overset{\mu\mu_1...\mu_n}{\mathbf{S}}\mathcal{O}^{\mu\mu_1...\mu_n} = \overset{\mu\mu_1...\mu_n}{\mathbf{S}}\bar{\psi}_q(0)i\gamma^\mu i\overleftrightarrow{D}^{\mu_1}...i\overleftrightarrow{D}^{\mu_n}\psi_q(0)\,, \tag{1.42}$$

and

$$\overset{\mu\mu_1...\mu_n}{\mathbf{S}}T_{\mu\mu_1...\mu_n} = T_{\{\mu\mu_1...\mu_n\}} - \frac{2\mathrm{mod}(n,2)}{(n+3)!!(n+1)!}$$
$$\times g_{\{\mu\mu_1}\cdots g_{\mu_{n-1}\mu_n\}}g^{\nu\nu_1}...g^{\nu_{n-1}\nu_n}T_{\{\nu\nu_1...\nu_n\}}\,, \tag{1.43}$$

where $\{...\}$ represents the symmetrization operation, and now a decomposition of eqn.1.41 in terms of Dirac bilinears is possible [18],

$$\langle p_2|\mathcal{O}^{\mu\mu_1...\mu_n}(0)|p_1\rangle = \overset{\mu\mu_1...\mu_n}{\mathbf{S}}\bar{u}(p_2)\gamma^\mu u(p_1)\sum_{\substack{i=0\\ \text{i even}}}^{n} A^q_{n+1,i}\Delta^{\mu_1}...\Delta^{\mu_i}p^{\mu_{i+1}}...p^{\mu_n}$$

$$+ \overset{\mu\mu_1\ldots\mu_n}{\mathbf{S}} \bar{u}(p_2)\frac{i\sigma^{\mu\alpha}\Delta_\alpha}{2M_N}u(p_1)\sum_{\substack{i=0\\ \text{i even}}}^{n} B^q_{n+1}(\Delta^2)\Delta^{\mu_1}\ldots\Delta^{\mu_i}p^{\mu_{i+1}}p^{\mu_n}$$

$$+ \overset{\mu\mu_1\ldots\mu_n}{\mathbf{S}} \bar{u}(p_2)u(p_1)\mathrm{mod}(n,2)C^q_{n+1}(\Delta^2)\Delta^{\mu_1}\ldots\Delta^{\mu_n}. \tag{1.44}$$

Plugging eqn.1.44 back into eqn.1.41 where all the Lorentz indices are contracted with the light cone null vectors n_μ ,..., n_{μ_n} and setting $\eta = \Delta^+/p^+$, one finally arrives at the following formulae,

$$\int_{-1}^{1} dx x^n H^q(x,\eta,\Delta^2) = \sum_{\substack{i=0\\ i\,\text{even}}}^{n} \eta^i A^q_{n+1,i}(\Delta^2) + \mathrm{mod}(n,2)\eta^{n+1}C^q_{n+1,i}(\Delta^2), \tag{1.45}$$

$$\int_{-1}^{1} dx x^n E^q(x,\eta,\Delta^2) = \sum_{\substack{i=0\\ i\,\text{even}}}^{n} \eta^i B^q_{n+1,i}(\Delta^2) - \mathrm{mod}(n,2)\eta^{n+1}C^q_{n+1,i}(\Delta^2). \tag{1.46}$$

This property of GPDs is called *polynomiality*, which states that the n-th moments of the GPDs are polynomials in η to the order of $n+1$. As one has observed, this identity is a direct consequence of Lorentz symmetry invoked in the form factor decomposition for twist-two operators. Similar equations apply for H^g, E^g and $\tilde{E}^{q,g}$ and $\tilde{H}^{q,g}$ of twist-two operators as well.

$$\int_{-1}^{1} dx x^n \tilde{H}^q(x,\eta,\Delta^2) = \sum_{\substack{i=0\\ i\,\text{even}}}^{n} \eta^i \tilde{A}^q_{n+1,i}(\Delta^2), \tag{1.47}$$

$$\int_{-1}^{1} dx x^n \tilde{E}^q(x,\eta,\Delta^2) = \sum_{\substack{i=0\\ i\,\text{even}}}^{n} \eta^i \tilde{B}^q_{n+1,i}(\Delta^2), \tag{1.48}$$

$$\int_{0}^{1} dx x^{n-1} H^g(x,\eta,\Delta^2) = \sum_{\substack{i=0\\ i\,\text{even}}}^{n} \eta^i A^g_{n+1,i}(\Delta^2) + \mathrm{mod}(n,2)\eta^{n+1}C^g_{n+1,i}(\Delta^2), \tag{1.49}$$

$$\int_{0}^{1} dx x^{n-1} E^g(x,\eta,\Delta^2) = \sum_{\substack{i=0\\ i\,\text{even}}}^{n} \eta^i B^g_{n+1,i}(\Delta^2) - \mathrm{mod}(n,2)\eta^{n+1}C^g_{n+1,i}(\Delta^2), \tag{1.50}$$

$$\int_{0}^{1} dx x^n \tilde{H}^q(x,\eta,\Delta^2) = \sum_{\substack{i=0\\ i\,\text{even}}}^{n} \eta^i \tilde{A}^q_{n+1,i}(\Delta^2), \tag{1.51}$$

$$\int_{0}^{1} dx x^n \tilde{E}^q(x,\eta,\Delta^2) = \sum_{\substack{i=0\\ i\,\text{even}}}^{n} \eta^i \tilde{B}^q_{n+1,i}(\Delta^2), \tag{1.52}$$

where one has used the symmetry properties expressed in eqns.1.31 and 1.32 to change the lower limit of the integration for gluon GPDs from -1 to 0. Also note that the reduction of moments from n to $n-1$ going between the corresponding quark and gluon GPDs is a direct consequence of the higher spin numbers for the gluonic operators compared to their quark counterparts. Polynomiality properties can also be derived for the helicity-nonconserving twist-2 operators, which give rise to $H_T^{q,g}$, $E_T^{q,g}$, $\tilde{H}_T^{q,g}$ and $\tilde{H}_T^{q,g}$; details can be found in [32].

Having established the polynomialities for higher moments of GPDs and motived by the fact that the 0-th moments of the GPDs are in fact the physical observables of form factors as shown in1.37 and 1.38, one may proceed to investigate the physical significance of their higher-moments counterparts. In fact, the first moments of the GPDs are deeply connected to the parton's angular momentum, which was firstly realized by Xiangdong Ji[13] in 1997. Staring form the Belinfante improved energy momentum tensor [13],

$$T^{\mu\nu} = \sum_{i=q,g} T_i^{\mu\nu}\,, \tag{1.53}$$

where the contributions of each individual particle are written as,

$$T_q^{\mu\nu} = \bar{\psi}_q \gamma^{\{\mu} i \overleftrightarrow{D}^{\nu\}} \psi_q\,, \qquad T_g^{\mu\nu} = G^{\mu\alpha} G_\alpha^{\ \nu} + \frac{1}{4} g^{\mu\nu} G^{\alpha\beta} G_{\alpha\beta}\,, \tag{1.54}$$

as a result, the angular momentum density is written,

$$M^{\alpha\mu\nu} = T^{\alpha\nu} x^\mu - T^{\alpha^\nu} x^\mu\,. \tag{1.55}$$

Then the total angular momentum of the nucleon along the z-axis is given by,

$$\vec{J}^3 = \int dx^3\, M^{012}(x)\,, \tag{1.56}$$

and a similar equation for the light-cone helicity operator applies if the light-cone frame is adopted [33],

$$J^3 = \int dx^- d^2x_\perp\, M^{+12}(x)\,. \tag{1.57}$$

In this case, the previous discussions on parton distributions and form factors arise and all the techniques one has encountered before apply, namely, the parton energy-momentum tensor is decomposed as,

$$\langle p_2|T^{\mu\nu}_{q,g}|p_1\rangle = A_{q,g}(\Delta^2)\bar{u}(p_2)p^{\{\mu}\gamma^{\nu\}}u(p_1) + B_{q,g}(\Delta^2)\frac{p^{\{\mu}i\sigma^{\nu\}}\Delta_\alpha}{2m}u(p_1) + C_{q,g}(\Delta^2)\frac{\Delta^{\mu\nu}-g^{\mu\nu}\Delta^2}{m}\bar{u}(p_2)u(p_1) + \bar{C}_{q,g}(\Delta^2)mg^{\mu\nu}\bar{u}(p_2)u(p_1)\,. \quad (1.58)$$

Then plugging eqns.1.55 and 1.58 into eqn.1.57; contracting with the light-cone null vector and projectors in the transverse plane and making use of the Fourier transform, one finds the following results [13, 14],

$$\langle J^3_q\rangle = \frac{1}{2}[A_q(0)+B_q(0)]\,, \qquad \langle J^3_g\rangle = \frac{1}{2}[A_g(0)+B_g(0)]\,, \quad (1.59)$$

which can be rewritten in terms of the first moments of the GPDs, as one has discovered in eqn.1.45-1.52,

$$\langle J^3_q\rangle = \frac{1}{2}\lim_{\Delta^2\to 0}\int_{-1}^{1} dx\, x[H_q(x,\eta,\Delta^2)+E_q(x,\eta,\Delta^2)]\,, \quad (1.60)$$

$$\langle J^3_g\rangle = \frac{1}{2}\lim_{\Delta^2\to 0}\int_{-1}^{1} dx\,[H_g(x,\eta,\Delta^2)+E_g(x,\eta,\Delta^2)]\,. \quad (1.61)$$

This mismatch between the quark and gluon counterparts is apparent as has been discussed earlier. The formulae 1.59 and 1.60 are conventionally called Ji's sum rule. They are in parallel to the momentum sum rules,

$$\langle p^+_q\rangle = A_q(0) = \int_0^1 dx\, x[q(x)+\bar{q}(x)]\,, \quad (1.62)$$

$$\langle p^+_g\rangle = A_g(0) = \int_0^1 dx\, x g(x)\,. \quad (1.63)$$

Typically, the exception values $\langle p^+_{q,g}\rangle$ and $\langle J_{q,g}\rangle$ are dependent on the renormalization scale μ, physically interpreted as the resolution scale of the process.

Obviously, due to momentum and angular momentum conservation, one has,

$$\langle p^+_g\rangle + \sum_q \langle p^+_q\rangle = 1\,, \qquad \langle J^3_g\rangle + \sum_q \langle J^3_q\rangle = \frac{1}{2}\,, \quad (1.64)$$

which combined with eqn.1.59, 1.62, and 1.63 gives the following equations that constrain B_g and B_q,

$$B_g(0) + \sum_q B_q(0) = \sum_q \int_{-1}^{1} dx x E^q(x,0,0) + \int_0^1 dx E^g(x,0,0) = 0\,. \tag{1.65}$$

The independence of the renormalization scale, which may be chosen arbitrarily, of eqn. 1.65 was confirmed by Stanley J. Brodsky et. al. [34] for the case of one-loop QED scenario.

Clearly, eqn.1.59,1.60, 1.62 and 1.63 generate huge interest in the studies of GPDs which are physically accessible, at certain limits of the GPDs, through Deep Inelastic Scattering experiments.

CHAPTER 2

COMPTON SCATTERING: FROM DEEPLY VIRTUAL TO QUASI-REAL

In this chapter, the question of interpolation of the virtual Compton scattering process off a polarized nucleon target is investigated between the deeply virtual regime for the initial-state photon and its near on-shell kinematics, making use of the photon helicity-dependent Compton Form Factors (CFFs) as a main ingredient of the formalism. The five-fold differential cross section for the reaction with all possible polarization options for the lepton and nucleon spins is evaluated in terms of CFFs in the rest reference frame of the initial-state nucleon. Here a rather simple parametrization is suggested for the Compton hadronic tensor in terms of CFFs which are free from kinematical singularities and are directly related, at large photon virtualities, to Generalized Parton Distributions. A relation of the basis spanned by a minimal number of Dirac bilinears to the one introduced by Tarrach for the parametrization of the virtual Compton tensor is also suggested, and the former is utilized to establish a set of equalities among our CFFs and Generalized Polarizabilities. As a complementary result, one expresses Compton scattering in the Born approximation in terms of CFFs as well [35].

2.1 Motivation

As it was enunciated previously, Compton scattering on a nucleon involving one virtual photon exchange, $\gamma^*(q_1)N(p_1) \to \gamma(q_2)N(p_2)$, plays a distinguished role in the quest to access its internal content and unravel the mysteries of strong interactions. The reason for this is multifold. Experimentally, the scattering process off a proton can be measured in a straightforward fashion, free of complications of composite probes, via scattering of leptons on a hydrogen target. The five-fold differential cross section for the emission of an

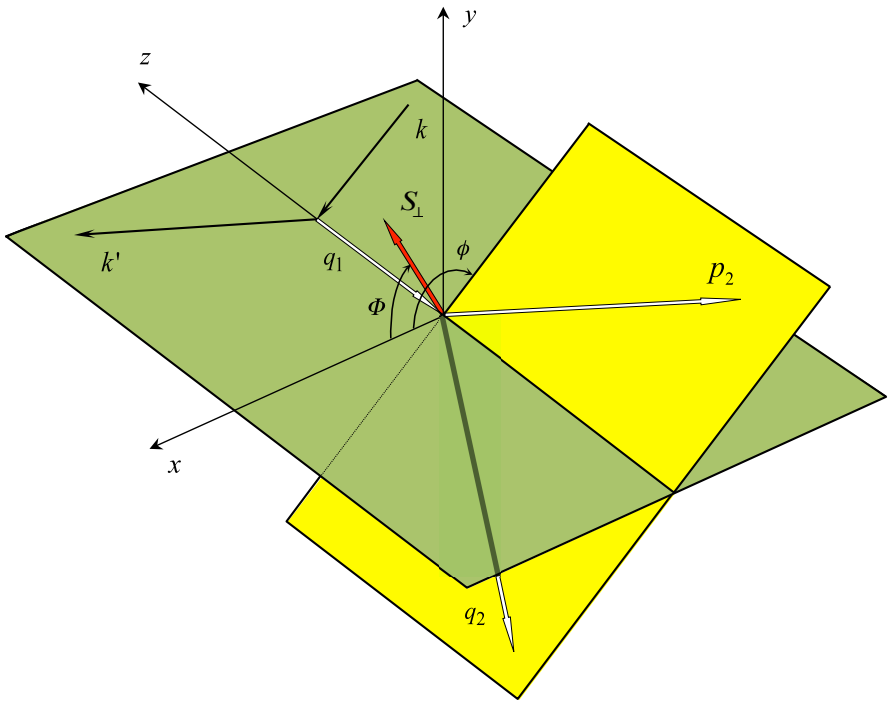

Figure 2.1: The target rest frame, used in this work, is the same as adopted in the previous consideration [36]. The z-axis is counter-along the photon three-momentum $\boldsymbol{q}_1$ direction, and the x-component of the incoming electron momentum $\boldsymbol{k}$ is chosen to be positive. The angles parametrizing the five-fold cross section (2.1) are defined as follows: ϕ is the azimuthal angle between the lepton plane and the recoiled proton momentum, while the difference $\varphi \equiv \Phi - \phi$ for fixed ϕ is determined by the direction of the transverse nucleon polarization vector component $\boldsymbol{S}_\perp = (\cos\Phi, \sin\Phi)$.

on-shell photon to the final state, $\ell(k)N(p_1) \to \ell(k')N(p_2)\gamma(q_2)$, reads

$$d\sigma = \frac{\alpha_{\rm em}^3 x_{\rm B} y^2}{16\pi^2\, \mathcal{Q}^4 \sqrt{1+\varepsilon^2}} \left|\frac{\mathcal{T}}{e^3}\right|^2 dx_{\rm B} d\mathcal{Q}^2 d|t| d\phi d\varphi\,, \tag{2.1}$$

in the approximation that neglects the mass of the lepton. The phase space is parameterized by the Bjorken variable $x_{\rm B} = \mathcal{Q}^2/(2p_1\cdot q_1)$, which is in turn determined by the momentum $q_1 = k - k'$ of the initial-state photon of virtuality $\mathcal{Q}^2 = -q_1^2$, the square of the t-channel momentum $t{=}(p_2 - p_1)^2$, the azimuthal angle ϕ of the recoiled nucleon, and for a transversally polarized target yet another (relative) angle φ, where the latter two are defined in the rest frame of the target as depicted in Fig. 2.1. Finally, the variable $y = p_1\cdot q_1/p_1\cdot k$ is introduced for the lepton energy loss and a shorthand nation for $\varepsilon = 2x_{\rm B}M/\mathcal{Q}$ that incorporates nonvanishing target mass effects is introduced. In the above five-fold cross section,

the leptoproduction amplitude $\mathcal{T}$ is a linear superposition of the Bethe-Heitler (BH) and virtual Compton scattering (VCS) amplitudes, depending on whether the real photon is emitted off the lepton or nucleon, respectively. In the scattering amplitude

$$\mathcal{T} = \mathcal{T}^{\rm BH} + \mathcal{T}^{\rm VCS}\,, \tag{2.2}$$

the former is determined in terms of the nucleon matrix element of the quark electromagnetic current j_μ

$$J_\mu = \langle p_2|j_\mu(0)|p_1\rangle\,, \tag{2.3}$$

while the hadronic Compton tensor,

$$T_{\mu\nu} = i\int d^4z\, {\rm e}^{\frac{i}{2}(q_1+q_2)\cdot z}\langle p_2|T\left\{j_\mu(z/2)j_\nu(-z/2)\right\}|p_1\rangle\,, \tag{2.4}$$

encodes information on more intricate long-distance dynamics. This is the main observable for our subsequent analysis.[7]

The variation of the virtuality $\mathcal{Q}^2$ of the initial-state photon allows one to probe a wide range of distance scales, interpolating between short- and long-wavelength structures of the nucleon. A number of observables are available to achieve this goal, all representing different facets of the same reaction. For real to slightly virtual initial-state photons, produced as a bremsstrahlung off the lepton beam, and a low energy $\omega' = q_2^0$ of the outgoing photon, the Compton amplitude admits a conventional multipole expansion, with leading the contributions defining the electric α and magnetic β polarizabilities of the nucleon, see, e.g., Ref. [37] for a review. The latter characterize the linear response of the nucleon to the electric and magnetic fields of the incoming photon, which slightly distorts the hadron and as a consequence, induces (in the quasi-static approximation) nontrivial electric $d = \alpha\mathcal{E}_{\rm in}$ and magnetic $\mu = \beta\mathcal{B}_{\rm in}$ dipole moments. The latter then interact with the electromagnetic

[7]Note here one adopts a different convention for the hadronic electromagnetic tensor compared to eqn.1.10. The two conventions are related by a simple spacetime translation with minor changes in normalization coefficients.

fields of the outgoing photon through multipole couplings $d \cdot \mathcal{E}_{\rm out} + \mu \cdot \mathcal{B}_{\rm out}$. The experimental values for the coefficients α and β are very small, indicating that the nucleon is a very rigid object allowing only for a very small deformation. Understanding of their magnitude within effective field theories comes about as a result of a subtle cancelation of the pion cloud and quark-core effects. For an off-shell initial-state photon with virtuality $\mathcal{Q}^2$ that scatters on a polarized spin one-half target, one can introduce ten [38] generalized, — referring to the functional dependence on $\mathcal{Q}^2$ rather than being mere numbers, — polarizabilities which reduce to six, once one imposes charge conjugation and crossing symmetry constraints [39].

Increasing the momentum transfer in the $t-$channel results in large-angle scattering of the emitted real photon in the final state. As a consequence, one enters the domain of the wide-angle Compton scattering. In this kinematics, the process receives quantitative description within the QCD factorization approach with the leading asymptotic behavior driven by the hard gluon exchanges between the nucleon's constituents [40] and by the Feynman soft mechanism at moderate t with the amplitude arguably described by a handbag diagram [26, 41] (see Fig. 2.2). The real Compton form factors emerging in the latter framework are actually moments of more general functions encoding the partonic degrees of freedom in the nucleon.

In the deeply virtual regime of large Euclidean $\mathcal{Q}^2$ and fixed t, the probe resolves an individual nucleon's constituents, and the process admits a full-fledged description in terms of the Generalized Parton Distributions (GPDs) [28, 42, 43]. However, the Compton amplitude itself is only determined by an integral of GPDs accompanied by a perturbatively computable coefficient function. These convolutions are known as Compton Form Factors (CFFs) [36]. Making use of gauge invariance, discrete symmetries and crossing, one can establish that there are twelve independent CFFs when the outgoing photon is real. They describe information about the hadron for all possible polarization settings of the nucleon

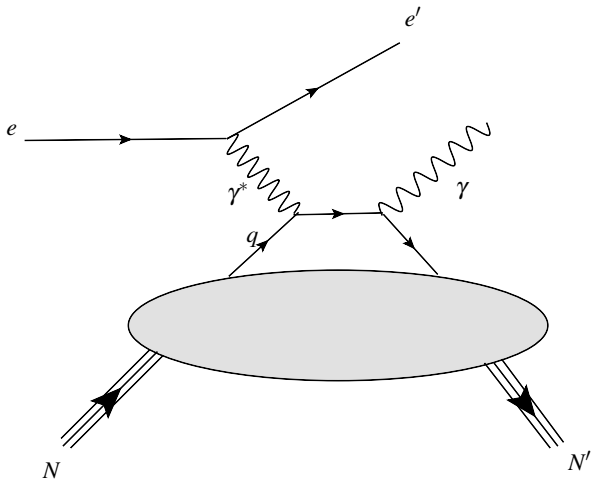

Figure 2.2: Handbag diagram in leading twist expansion which survives the Bjorken limit

and the resolving photons. Since this decomposition is general, the CFFs define the amplitude in all kinematical regimes, interpolating between the aforementioned polarizabilities at low energies, and thus describing the response of the nucleon as a whole to the external probes, all the way up to probing partonic degrees of freedom at high energies.

The goal of this chapter is to elaborate on the previous analysis [44] and provide a complete set of exact results for helicity amplitudes describing the virtual Compton scattering, on the one hand, filling the gap for transversely polarized targets as well as contributions of the double helicity-flip effects that were not entirely worked out before, as well as deliver a set of relations between CFFs and polarizabilities introduced in earlier studies [39], making use of the Tarrach's decomposition of the Compton tensor [45], on the other. Thus, a useful dictionary is established that can be used to re-express the results of experimental measurements in terms of the same observables, Compton form factors.

The subsequent part of this chapter is organized as follows. In the next section, a review the formalism of helicity amplitudes, used previously in the literature in deeply virtual kinematics is given, and a set of exact concise formulas for all polarization settings, unpolarized, longitudinal and transverse, of the nucleon target is provided. In Sect. 2.3, the

question of gauge-invariant decomposition of the hadronic tensor is addressed. An exactly solvable toy example of a point particle is introduced, and then a rather simple parameterization of the Compton tensor in terms of CFFs that are free of kinematical singularities is suggested. The connection to the structure functions defined by Tarrach and the form of CFFs in the Born approximation is established by means of helicity amplitudes. In Sect. 2.4, based on the findings in previous chapters, the low-energy expansion of the CFFs is developed and a complete set of relations to the generalized polarizabilities of Guichon et al., introduced in Ref. [38], is provided.

2.2 Cross Section in Terms of Helicity Amplitudes

In recent investigations [44, 46], the authors demonstrated that the deviation between the data on hard electroproduction of photons and theoretical estimates for corresponding observables within the approximation scheme of Ref. [36] could be reconciled by calculating kinematical corrections in the hard scale exactly, while ignoring dynamical high-twist contributions altogether. The neglect of the latter was motivated by the hierarchy of low-energy scales associated with hadronic matrix elements of high-twist operators, which are smaller than soft kinematical scales encountered in the problem, i.e., the nucleon mass and the t-channel momentum transfer. Incorporation of the kinematical power-suppressed effects was achieved by separating them between the leptonic and hadronic parts independently, and by evaluating photon helicity amplitudes utilizing the polarization vectors for the incoming and outgoing photons in the target rest frame. In addition to providing an efficient computational scheme, it has another advantage of localizing the azimuthal angular dependence in the lepton helicity amplitudes for the choice of the reference frame with the z-axis counter-aligned with the incoming photon three-momentum, as shown in Fig. 2.1. It also allows for a straightforward reduction to the harmonic expansion introduced in Refs. [36, 47].

2.2.1 Form Factor Parameterization of Hadronic Helicity Amplitudes

Taking the hadronic component of the leptoproduction amplitude of a real photon as the starting point, the nucleon helicity amplitudes for the (deeply virtual or quasi-real) Compton scattering is defined as

$$\mathcal{T}_{ab}^{\rm VCS}(\phi) = (-1)^{a-1}\varepsilon_2^{\mu *}(b) T_{\mu\nu}\varepsilon_1^{\nu}(a)\,, \tag{2.5}$$

by contracting the VCS tensor (2.4) with the photon polarization vectors. Here, the overall phase $(-1)^{a-1}$ accounts for the signature factor in the completeness relation for the photon polarization vectors. The a and b indices take the values $a \in \{0, \pm 1\}$ and $b = \pm 1$. The ε-vectors for the virtual photon are given in the reference frame by

$$\varepsilon_1^{\mu}(\pm) \;=\; \frac{e^{\mp i\phi}}{\sqrt{2}}(0,1,\pm i,0)\,, \qquad \varepsilon_1^{\mu}(0) = \frac{1}{\varepsilon}(-\sqrt{1+\varepsilon^2},0,0,1), \tag{2.6}$$

while for the real photon they are

$$\begin{aligned}\varepsilon_2^{\mu *}(\pm) = \frac{1}{\sqrt{2}}\Bigg(0, \frac{1+\frac{\varepsilon^2}{2}\frac{\mathcal{Q}^2+t}{\mathcal{Q}^2+x_{\rm B}t}}{\sqrt{1+\varepsilon^2}}\cos\phi \pm i\sin\phi,& \\ \mp i\cos\phi + \frac{1+\frac{\varepsilon^2}{2}\frac{\mathcal{Q}^2+t}{\mathcal{Q}^2+x_{\rm B}t}}{\sqrt{1+\varepsilon^2}}\sin\phi, \frac{-\varepsilon\mathcal{Q}\widetilde{K}/\sqrt{1+\varepsilon^2}}{\mathcal{Q}^2+x_{\rm B}t}\Bigg)&.\end{aligned} \tag{2.7}$$

Here, for later convenience a kinematical factor with mass dimension one is introduced as,

$$\widetilde{K} = \sqrt{(1-x_{\rm B})x_{\rm B} + \frac{\varepsilon^2}{4}}\,\sqrt{\frac{(t_{\rm min}-t)(t-t_{\rm max})}{\mathcal{Q}^2}}\,, \tag{2.8}$$

which vanishes at the minimally (maximally) allowed value of the t-channel momentum transfer $-t = -t_{\rm min}$ ($-t = -t_{\rm max}$), with

$$\begin{aligned} t_{\rm min} &= -\mathcal{Q}^2\frac{2(1-x_{\rm B})\left(1-\sqrt{1+\varepsilon^2}\right)+\varepsilon^2}{4x_{\rm B}(1-x_{\rm B})+\varepsilon^2}\,, \\ t_{\rm max} &= -\mathcal{Q}^2\frac{2(1-x_{\rm B})\left(1+\sqrt{1+\varepsilon^2}\right)+\varepsilon^2}{4x_{\rm B}(1-x_{\rm B})+\varepsilon^2}\,. \end{aligned} \tag{2.9}$$

In turn, $\widetilde{K}$ vanishes if $x_{\rm B}$ reaches for fixed $-t$ and $\mathcal{Q}^2$ the maximal allowed value

$$x_{\rm B\,max} = 1 - \frac{\mathcal{Q}^2 + t}{\mathcal{Q}^2 + t + \left(\sqrt{-t\,(4M^2 - t)} - t\right)\frac{\mathcal{Q}^2}{2M^2}}. \tag{2.10}$$

Consequently, this factor encodes the phase-space boundary in hadronic variables. In the explicit computation of Eq. (2.5), the Lorentz-covariant decomposition for the ε-vectors in terms of momentum four-vectors defining the process is used, which is often written for convenience in terms of the t-channel momentum transfer, the sum of nucleons' momenta, the averaged momentum of the photons, and a vector orthogonal to the previous three[8]:

$$\Delta^\mu = p_2^\mu - p_1^\mu\,, \quad p^\mu = p_1^\mu + p_2^\mu\,, \qquad q^\mu = \tfrac{1}{2}(q_1^\mu + q_2^\mu)\,, \quad \varepsilon^\mu{}_{pq\Delta} \equiv \varepsilon^\mu{}_{\alpha\beta\gamma} p^\alpha q^\beta \Delta^\gamma\,. \tag{2.11}$$

The coefficients in such an expansion are given in terms of the kinematical invariants introduced above. A complete set of relations is deferred to the Appendix A.1.

The computations of the cross section (2.1) by means of the hadron helicity amplitudes (2.5), presented in the following two sections, require an explicit tensor decomposition of the Compton amplitude. Unfortunately, no consensus exists on the form of parametrization of such a tensor, even for DVCS kinematics. In the latter case, the partonic interpretation of $T_{\mu\nu}$ arises from the application of Operator Product Expansion (OPE) techniques which are valid to a given accuracy in the $1/\mathcal{Q}$-expansion, and this leaves a substantial ambiguity in the parametrization of the hadronic amplitude, depending on the fashion that one restores its gauge invariance broken by the leading-order approximation.

To get around this problem, one first parameterizes directly the photon helicity amplitudes (2.5). Thereby, one describes the nucleon-to-nucleon transition for given photon helicities in terms of two even-parity and two odd-parity bilinear Dirac spinor covariants, analogously to the manner they appear in the standard form-factor parameterization of

[8] One adopts here to the conventions of Itzykson and Zuber [48], i.e., the normalization choice for the Levi-Civita tensor is given by $\varepsilon^{0123} = +1$.

the vector and axial-vector currents. Moreover, the above helicity amplitudes taken into account for opposite pairs of helicities are not independent of each other and are rather related by parity conservation, generically written as

$$\begin{aligned}
\mathcal{T}^{\mathrm{VCS}}_{--}(\mathcal{F}) &= \mathcal{T}^{\mathrm{VCS}}_{++}(\mathcal{F})\Big|_{\mathcal{F}^{P=\pm1}\to\pm\mathcal{F}^{P=\pm1}}, \\
\mathcal{T}^{\mathrm{VCS}}_{0-}(\mathcal{F}) &= \mathcal{T}^{\mathrm{VCS}}_{0+}(\mathcal{F})\Big|_{\mathcal{F}^{P=\pm1}\to\pm\mathcal{F}^{P=\pm1}}, \\
\mathcal{T}^{\mathrm{VCS}}_{-+}(\mathcal{F}) &= \mathcal{T}^{\mathrm{VCS}}_{+-}(\mathcal{F})\Big|_{\mathcal{F}^{P=\pm1}\to\pm\mathcal{F}^{P=\pm1}},
\end{aligned} \tag{2.12}$$

where $\mathcal{F}^P$ stands for CFFs with definite parity $P=\pm1$ (even parity $P=1$ refers to the vector case, while the odd one $P=-1$ refers to the axial-vector case). As a consequence, a set $\mathcal{F}$ of three times four independent CFFs are present, and the helicity amplitudes can be expressed in terms of six linear functions, three depending on two even (or two odd) CFFs. Furthermore, it is possible to summarize diverse formulations in a single parametrization since the representation of the photon polarization vectors in terms of kinematical variables allows us to use the Dirac equation for the free nucleon spinors. Consequently, the helicity amplitudes (2.5) can be written in following form

$$\mathcal{T}^{\mathrm{VCS}}_{ab} = \mathcal{V}(\mathcal{F}_{ab}) - b\,\mathcal{A}(\mathcal{F}_{ab}) \quad \text{for} \quad b\in\{+,-\}, \tag{2.13}$$

in terms of the vector and axial-vector form factor parametrization,

$$\mathcal{V}(\mathcal{F}_{ab}) = \bar{u}_2\left(\not{m}\mathcal{H}_{ab} + i\sigma_{\alpha\beta}\frac{m^\alpha\Delta^\beta}{2M}\mathcal{E}_{ab}\right)u_1, \tag{2.14}$$

$$\mathcal{A}(\mathcal{F}_{ab}) = \bar{u}_2\left(\not{m}\gamma_5\widetilde{\mathcal{H}}_{ab} + \gamma_5\frac{m\cdot\Delta}{2M}\widetilde{\mathcal{E}}_{ab}\right)u_1, \tag{2.15}$$

with a convention-dependent vector m^μ and bispinors $u_i \equiv u(p_i,S_i)$, normalized as $\bar{u}(p,S)u(p,S) = 2M$. Such a uniform functional form for all photon helicity options, which closely matches the GPD notation, is very convenient for the evaluation of the cross section. However, one has to take special care tracing potential kinematical singularities. Emphasizing the simplicity of the underlying analysis, Sect. 2.3 is dedicated to describing how CFFs can be defined in a singularity free manner.

A few other comments are in order. Our conventions imply the relations

$$\mathcal{F}_{--} = \mathcal{F}_{++}\,, \quad \mathcal{F}_{0-} = \mathcal{F}_{0+}\,, \text{ and } \mathcal{F}_{-+} = \mathcal{F}_{+-} \quad \text{for} \quad \mathcal{F} \in \{\mathcal{H}, \mathcal{E}, \widetilde{\mathcal{H}}, \widetilde{\mathcal{E}}\}\,. \tag{2.16}$$

The above vector m^μ in the GPD framework is often equated to a fixed light-like vector and reflects, loosely speaking, also the accuracy in restoring gauge invariance lost within the twist-two accuracy. A couple of fixed light-like vector choices were explored in the literature, see, e.g., discussion in Ref. [19]. Going beyond the leading twist approximation, the choice $m^\mu = q^\mu/p\cdot q$ is physically motivated and guarantees a proper behavior under Lorentz transformations, as well as allowing for a simple implementation of the Bose symmetry [36]. Another choice $m^\mu = q_1^\mu/p_1\cdot q_1$ can be advocated by the fact that, in the present reference frame, this vector contains only longitudinal degrees of freedom. Finally, $m^\mu \propto q_2^\mu$ can also be taken as a light-like vector in the GPD framework [49, 50]. Using the free Dirac equation for the nucleon spinors, it becomes obvious that the parameterization (2.13)–(2.15) in terms of spinor bilinears is complete and, hence, different choices of m^μ correspond to a linear transformation in the space of CFFs. As in previous work, the following vector

$$m^\mu = q^\mu/p\cdot q\,,$$

is used throughout the current analysis.

The above helicity CFFs can be expressed in terms of the ones emerging in the GPD framework. However, since the latter relies on a truncation of the $1/\mathcal{Q}$-expansion, the resulting relations will depend on a particular parametrization of the Compton tensor and identification of CFFs as a convolution of GPDs and perturbative coefficient functions valid only to a very low accuracy in the $1/\mathcal{Q}$-expansion. While in Sect. 2.3 an exact set of CFF relations will be given, see below Eqs. (2.131)–(2.132), here the leading contribution to the helicity form factors from twist-two $\mathcal{F}\,(\equiv \mathcal{F}^{\text{tw}-2})$ is quoted, as well as the effective

twist-three $\mathcal{F}^{\rm eff}$ and gluon-transversity $\mathcal{F}_T$ CFFs,

$$\mathcal{F}_{++} = \mathcal{F} + \mathcal{O}\left(1/\mathcal{Q}^2\right) \tag{2.17}$$

$$\mathcal{F}_{0+} = \frac{\sqrt{2}\widetilde{K}}{\sqrt{1+\varepsilon^2}\mathcal{Q}\left(2-x_{\rm B}+\frac{x_{\rm B}t}{\mathcal{Q}^2}\right)}\mathcal{F}^{\rm eff} + \mathcal{O}\left(1/\mathcal{Q}^2\right) + \mathcal{O}(\alpha_s)\,, \tag{2.18}$$

$$\mathcal{F}_{+-} = \frac{\widetilde{K}^2}{2M^2\left(2-x_{\rm B}+\frac{x_{\rm B}t}{\mathcal{Q}^2}\right)^2}\mathcal{F}_T + \mathcal{O}\left(1/\mathcal{Q}^2\right)\,, \tag{2.19}$$

where some typical kinematical factors were treated here exactly, preparing the stage for full-fledged formulas. In the amplitude $\mathcal{F}_{0+}$, an effective GPD-inspired CFF is used,

$$\mathcal{F}^{\rm eff} = -2\xi\left(\frac{1}{1+\xi}\mathcal{F} + \mathcal{F}_+^{\rm tw-3} - \mathcal{F}_-^{\rm tw-3}\right) + \mathcal{O}\left(1/\mathcal{Q}^2\right) + \mathcal{O}\left(\alpha_s/\mathcal{Q}\right)\,. \tag{2.20}$$

These contain a twist-two induced part and twist-three quantities $\mathcal{F}_\pm^3$ that are given in Ref. [36], see Eqs. (84)–(87) there. Note, however, that these effective CFFs are also affected by the twist-two gluon transversity, formally suppressed by α_s, and also high-twist contributions. As has been discussed in Ref. [46] for a scalar target, the transversity admixture to the longitudinal helicity-flip amplitudes presently is not under theoretical control, and its clarification requires a twist-three analysis at NLO accuracy. Above one made use of the generalized Bjorken variable ξ that is expressed via $x_{\rm B}$ as follows: $\xi \simeq x_{\rm B}/(2-x_{\rm B})$. Further insights on the interplay between current conservation, the choice of the partonic scaling variables and, respectively, the choice of the auxiliary light-like vectors and kinematical effects can be found in Ref. [46] and below in Sect. 2.3.2.

Having fixed the parametrization of the hadronic helicity amplitudes (2.13)–(2.15) by the choice $m^\mu \equiv q^\mu/p\cdot q$, one will turn now in the next two sections to how they are incorporated into the square of the VCS amplitude as well as its interference with the Bethe-Heitler process. it should be emphasized once more that the uncertainties from kinematical and dynamical higher twist contributions, appearing in the relation of hadronic and partonic quantities for deeply virtual kinematics, are entirely encoded in the relations of helicity-

dependent CFFs $\mathcal{F}_{ab}$ to the set of CFFs that one adopts for the evaluation of the hadronic tensor. Thus, the results that follow are exact, free of any approximations.

2.2.2 *Squared Compton Scattering Amplitude*

It is now possible to calculate the square of the (D)VCS amplitude, that enters the cross section (2.1), where the lepton mass is set to zero and the polarization of the final-state lepton remains unobserved. Using the completeness relations for the photon polarization vectors, this square as can rewritten as,

$$|\mathcal{T}^{\rm VCS}|^2 = \frac{1}{\mathcal{Q}^2} \sum_{a=-,0,+} \sum_{b=-,0,+} \mathcal{L}_{ab}(\lambda,\phi)\mathcal{W}_{ab}\,, \tag{2.21}$$

in terms of the hadronic,

$$\mathcal{W}_{ab} = \mathcal{T}^{\rm VCS}_{a+} \left(\mathcal{T}^{\rm VCS}_{b+}\right)^* + \mathcal{T}^{\rm VCS}_{a-} \left(\mathcal{T}^{\rm VCS}_{b-}\right)^*\,, \tag{2.22}$$

and leptonic,

$$\mathcal{L}_{ab}(\lambda,\phi) = \varepsilon_1^{\mu *}(a) L_{\mu\nu}(\lambda) \varepsilon_1^{\nu}(b)\,, \tag{2.23}$$

squared amplitudes, labeled by the helicity states of the initial and final photons. Here, the familiar leptonic tensor for the initial-state lepton with helicity $\lambda = \pm 1$ reads

$$L_{\mu\nu} = 2\mathcal{Q}^{-2}\left(k_\mu k'_\nu + k_\nu k'_\mu - k\cdot k' g_{\mu\nu} + i\lambda\varepsilon_{\mu\nu kk'}\right)\,. \tag{2.24}$$

Note that $|\lambda| \leq 1$ can be also regarded as the polarizability of the lepton beam. More explicitly, one finds for the squared VCS amplitude (2.21)

$$\begin{aligned}
\mathcal{Q}^2|\mathcal{T}^{\rm VCS}|^2 \;=\;& \mathcal{L}_{++}(\lambda)\mathcal{W}_{++} + \mathcal{L}_{++}(-\lambda)\mathcal{W}_{--} + \mathcal{L}_{00}\mathcal{W}_{00} \\
+\;& \mathcal{L}_{0+}(\lambda,\phi)\mathcal{W}_{0+} + \mathcal{L}_{0+}(-\lambda,-\phi)\mathcal{W}_{0-} + \mathcal{L}_{0+}(-\lambda,\phi)\mathcal{W}_{+0} + \mathcal{L}_{0+}(\lambda,-\phi)\mathcal{W}_{-0} \\
+\;& \mathcal{L}_{+-}(\phi)\mathcal{W}_{+-} + \mathcal{L}_{+-}(-\phi)\mathcal{W}_{-+}\,.
\end{aligned} \tag{2.25}$$

The squared leptonic helicity amplitudes can be calculated exactly yielding known results, e.g., in the form already presented in Ref. [46]:

$$\mathcal{L}_{++}(\lambda) \;=\; \frac{1}{y^2(1+\varepsilon^2)}\left(2-2y+y^2+\frac{\varepsilon^2}{2}y^2\right)-\frac{2-y}{\sqrt{1+\varepsilon^2}y}\lambda\,, \tag{2.26}$$

$$\mathcal{L}_{00} \;=\; \frac{4}{y^2(1+\varepsilon^2)}\left(1-y-\frac{\varepsilon^2}{4}y^2\right), \tag{2.27}$$

$$\mathcal{L}_{0+}(\lambda,\phi) \;=\; \frac{2-y-\lambda y\sqrt{1+\varepsilon^2}}{y^2(1+\varepsilon^2)}\sqrt{2}\sqrt{1-y-\frac{\varepsilon^2}{4}y^2}\,e^{-i\phi}\,, \tag{2.28}$$

$$\mathcal{L}_{+-}(\phi) \;=\; \frac{2}{y^2(1+\varepsilon^2)}\left(1-y-\frac{\varepsilon^2}{4}y^2\right)e^{i2\phi}\,. \tag{2.29}$$

The remaining squared amplitudes are related to the above by parity- and time-reversal invariance,

$$\begin{aligned}
&\mathcal{L}_{0-}(\lambda,\phi)=\mathcal{L}_{0+}(-\lambda,-\phi)\,, \qquad && \mathcal{L}_{\pm,0}(\lambda,\phi)=\mathcal{L}_{0,\pm}(-\lambda,\phi)\,,\\
&\mathcal{L}_{--}(\lambda)=\mathcal{L}_{++}(-\lambda)\,, && \mathcal{L}_{-+}(\phi)=\mathcal{L}_{+-}(-\phi)\,.
\end{aligned} \tag{2.30}$$

The squared helicity amplitudes of the hadronic tensor (2.22) take the following form in the spinor representation (2.13)–(2.15),

$$\mathcal{W}_{ab} \;=\; \sum_{S'}\sum_{c=\pm1}\Big[\mathcal{V}(\mathcal{F}_{ac})-c\,\mathcal{A}(\mathcal{F}_{ac})\Big]\Big[\mathcal{V}^\dagger(\mathcal{F}^*_{bc})-c\,\mathcal{A}^\dagger(\mathcal{F}^*_{bc})\Big]\,,$$

and will be evaluated exactly for given nucleon polarizations. The polarization vector of the initial nucleon is decomposed in its transverse and longitudinal components,

$$S^\mu(\Phi,\theta)=\sin\theta\,S^\mu_{\rm T}(\Phi)+\cos\theta\,S^\mu_{\rm L}\,, \tag{2.31}$$

where the angle is $\Phi=\varphi+\phi$ is introduced in Fig. 2.1, while the individual vectors

$$S^\mu_{\rm T}(\varphi+\phi)=(0,\cos(\varphi+\phi),\sin(\varphi+\phi),0)\,, \qquad S^\mu_{\rm L}=(0,0,0,1)\,, \tag{2.32}$$

can be expressed in the basis of momenta (2.11), see Appendix A.1. The outgoing nucleon will be treated in our considerations as unpolarized, since there seems to be no plans to perform recoil polarization measurements in experiments for a rather challenging virtual Compton scattering reaction. If needed, our work can be generalized along these lines.

The Fourier coefficients, given by the square of the VCS helicity amplitudes, can be re-expressed as bilinear combinations of CFFs with their functional dependence reflecting the nucleon polarization states. Consequently, the square of the VCS amplitude is decomposed into four terms exhibiting the spin of the target as follows,

$$\sum_{S'}\Big[\mathcal{V}(\mathcal{F})+\mathcal{A}(\mathcal{F})\Big]\Big[\mathcal{V}^{\dagger}(\mathcal{F}^{*})+\mathcal{A}^{\dagger}(\mathcal{F}^{*})\Big] \;=\; \Bigg[\mathcal{C}^{\rm VCS}_{\rm unp}+\Lambda\cos(\theta)\frac{1}{\sqrt{1+\varepsilon^2}}\mathcal{C}^{\rm VCS}_{\rm LP} \\ +\Lambda\sin(\theta)\sin(\varphi)\frac{i\widetilde{K}}{2M}\mathcal{C}^{\rm VCS}_{\rm TP-}+\Lambda\sin(\theta)\cos(\varphi)\frac{\widetilde{K}}{2M\sqrt{1+\varepsilon^2}}\mathcal{C}^{\rm VCS}_{\rm TP+}\Bigg](\mathcal{F},\mathcal{F}^{*})\,, \tag{2.33}$$

where the polarizability Λ of the nucleon target is shown explicitly. The naming of different $\mathcal{C}^{\rm VCS}_{\cdots}(\mathcal{F},\mathcal{F}^{*})$ functions is self-explanatory. These arise as bilinear combinations of CFFs, making use of the definition (2.13). Their form will be given below. Moreover, one may consider $\mathcal{F}$ and $\mathcal{F}^{*}$ as independent variables so that a uniform functional form can be employed in the evaluation of all initial-to-final photon-helicity state transitions: spanning the range between conserved helicity, longitudinal-to-transverse, and transverse-to-transverse helicity-flip contributions.

It would be a good idea to spell out some of the changes in definitions given here compared to the ones used in earlier studies. Note that in comparison to Ref. [44], the combination $\mathcal{C}^{\rm VCS}_{\rm LP}$ was redefined by pulling out an overall factor of $1/\sqrt{1+\varepsilon^2}$. Moreover, with respect to the approximate expressions of Ref. [36], the overall normalization of the transversity contributions is also changed here. Note also that in the relations (2.18) and (2.19) between the longitudinal and transverse helicity flip CFFs and GPD-inspired CFFs there appears a factor $\widetilde{K}$ and $\widetilde{K}^2$, respectively. Compared to Ref. [36], such kinematical factors are now stripped off if the first- and second- order harmonics in terms of helicity-dependent CFFs are expressed. Another modification is that the leptonic part for exact kinematics can be simply obtained by a set of substitution rules from our previous DVCS results that have been already discussed in Ref. [44] and will not be repeated here. Finally,

it should also be noted that some of the remaining corrections in the hadronic part can be considered as a reparametrization of the scaling variable, i.e.,

$$\xi \simeq \frac{x_{\rm B}}{2-x_{\rm B}} \quad \to \quad \xi = \frac{x_{\rm B}}{2-x_{\rm B}+\frac{x_{\rm B}t}{\mathcal{Q}^2}}\,.$$

Now it is possible to cast our findings into the form suggested in Ref. [36]. Namely, from the squared VCS amplitude (2.25), the computed leptonic helicity amplitudes (2.29) and the definition of the hadronic coefficients $\mathcal{C}^{\rm DVCS}$ as functions of the helicity-dependent CFFs, one can immediately read off the harmonic expansion, which is written here by analogy to Ref. [36] as

$$|\mathcal{T}^{\rm VCS}(\phi,\varphi)|^2 = \frac{e^6}{y^2\mathcal{Q}^2}\left\{c_0^{\rm VCS}(\varphi)+\sum_{n=1}^{2}\left[c_n^{\rm VCS}(\varphi)\cos(n\phi)+s_n^{\rm VCS}(\varphi)\sin(n\phi)\right]\right\}. \tag{2.34}$$

The evaluation of the Fourier harmonics in Eq. (2.34) is straightforward and provides for the coefficients in the decomposition

$$c_n^{\rm VCS}(\varphi) = c_{n,\rm unp}^{\rm VCS}+\cos\theta\, c_{n,\rm LP}^{\rm VCS}+\sin\theta\, c_{n,\rm TP}^{\rm VCS}(\varphi) \tag{2.35}$$

$$s_n^{\rm VCS}(\varphi) = s_{n,\rm unp}^{\rm VCS}+\cos\theta\, s_{n,\rm LP}^{\rm VCS}+\sin\theta\, s_{n,\rm TP}^{\rm VCS}(\varphi) \tag{2.36}$$

the following results:

- Unpolarized target

$$\begin{aligned} c_{0,\rm unp}^{\rm VCS} &= 2\frac{2-2y+y^2+\frac{\varepsilon^2}{2}y^2}{1+\varepsilon^2}\,\mathcal{C}_{\rm unp}^{\rm VCS}(\mathcal{F}_{++},\mathcal{F}_{++}^*\big|\mathcal{F}_{-+},\mathcal{F}_{-+}^*) \\ &\quad +8\frac{1-y-\frac{\varepsilon^2}{4}y^2}{1+\varepsilon^2}\,\mathcal{C}_{\rm unp}^{\rm VCS}(\mathcal{F}_{0+},\mathcal{F}_{0+}^*)\,, \end{aligned} \tag{2.37}$$

$$\begin{aligned} \begin{Bmatrix} c_{1,\rm unp}^{\rm VCS} \\ s_{1,\rm unp}^{\rm VCS} \end{Bmatrix} &= \frac{4\sqrt{2}\sqrt{1-y-\frac{\varepsilon^2}{4}y^2}}{1+\varepsilon^2} \\ &\quad\times \begin{Bmatrix} 2-y \\ -\lambda y\sqrt{1+\varepsilon^2} \end{Bmatrix}\begin{Bmatrix} \mathrm{Re}\,e \\ \mathrm{Im}\,m \end{Bmatrix}\mathcal{C}_{\rm unp}^{\rm VCS}\left(\mathcal{F}_{0+}\big|\mathcal{F}_{++}^*,\mathcal{F}_{-+}^*\right), \end{aligned} \tag{2.38}$$

$$c_{2,\mathrm{unp}}^{\mathrm{VCS}} \;=\; 8\frac{1-y-\frac{\varepsilon^2}{4}y^2}{1+\varepsilon^2}\,\mathrm{Re\,e}\mathcal{C}_{\mathrm{unp}}^{\mathrm{VCS}}\left(\mathcal{F}_{-+},\mathcal{F}_{++}^{*}\right). \tag{2.39}$$

- Longitudinally polarized target

$$c_{0,\mathrm{LP}}^{\mathrm{VCS}} \;=\; \frac{2\lambda\Lambda y(2-y)}{1+\varepsilon^2}\mathcal{C}_{\mathrm{LP}}^{\mathrm{VCS}}(\mathcal{F}_{++},\mathcal{F}_{++}^{*}\big|\mathcal{F}_{-+},\mathcal{F}_{-+}^{*}), \tag{2.40}$$

$$\begin{aligned}\begin{Bmatrix} c_{1,\mathrm{LP}}^{\mathrm{VCS}} \\ s_{1,\mathrm{LP}}^{\mathrm{VCS}} \end{Bmatrix} \;&=\; -4\sqrt{2}\Lambda\frac{\sqrt{1-y-\frac{\varepsilon^2}{4}y^2}}{(1+\varepsilon^2)^{3/2}} \\ &\times\; \begin{Bmatrix} -\lambda y\sqrt{1+\varepsilon^2} \\ 2-y \end{Bmatrix}\begin{Bmatrix} \mathrm{Re\,e} \\ \mathrm{Im\,m} \end{Bmatrix}\mathcal{C}_{\mathrm{LP}}^{\mathrm{VCS}}\left(\mathcal{F}_{0+}\big|\mathcal{F}_{++}^{*},\mathcal{F}_{-+}^{*}\right), \end{aligned} \tag{2.41}$$

$$s_{2,\mathrm{LP}}^{\mathrm{VCS}} \;=\; -8\Lambda\frac{1-y-\frac{\varepsilon^2}{4}y^2}{(1+\varepsilon^2)^{3/2}}\,\mathrm{Im\,m}\mathcal{C}_{\mathrm{LP}}^{\mathrm{VCS}}\left(\mathcal{F}_{-+},\mathcal{F}_{++}^{*}\right). \tag{2.42}$$

- Transversally polarized target

$$\begin{aligned} c_{0,\mathrm{TP}}^{\mathrm{VCS}} \;&=\; -4\frac{1-y-\frac{\varepsilon^2}{4}y^2}{1+\varepsilon^2}\,\frac{\widetilde{K}}{M}\Lambda\sin(\varphi)\,\mathrm{Im\,m}\mathcal{C}_{\mathrm{TP}_-}^{\mathrm{VCS}}(\mathcal{F}_{0+},\mathcal{F}_{0+}^{*}) \\ &+\; \frac{2-y}{1+\varepsilon^2}\frac{\widetilde{K}}{M}\Bigg[\lambda\Lambda\cos(\varphi)\,y\mathcal{C}_{\mathrm{TP}+}^{\mathrm{VCS}} \\ &\quad -\Lambda\sin(\varphi)\frac{2-2y+y^2+\frac{1}{2}\varepsilon^2y^2}{2-y}\,\mathrm{Im\,m}\mathcal{C}_{\mathrm{TP}-}^{\mathrm{VCS}}\Bigg](\mathcal{F}_{++},\mathcal{F}_{++}^{*}\big|\mathcal{F}_{-+},\mathcal{F}_{-+}^{*}), \end{aligned} \tag{2.43}$$

$$\begin{aligned}\begin{Bmatrix} c_{1,\mathrm{TP}}^{\mathrm{VCS}} \\ s_{1,\mathrm{TP}}^{\mathrm{VCS}} \end{Bmatrix} \;&=\; -2\sqrt{2}\frac{\sqrt{1-y-\frac{\varepsilon^2}{4}y^2}}{1+\varepsilon^2}\,\frac{\widetilde{K}}{M}\Bigg[\frac{\Lambda\cos(\varphi)}{\sqrt{1+\varepsilon^2}}\begin{Bmatrix} -\lambda y\sqrt{1+\varepsilon^2} \\ 2-y \end{Bmatrix}\begin{Bmatrix} \mathrm{Re\,e} \\ \mathrm{Im\,m} \end{Bmatrix}\mathcal{C}_{\mathrm{TP}+}^{\mathrm{VCS}} \\ &+\; \Lambda\sin(\varphi)\begin{Bmatrix} 2-y \\ \lambda y\sqrt{1+\varepsilon^2} \end{Bmatrix}\begin{Bmatrix} \mathrm{Im\,m} \\ \mathrm{Re\,e} \end{Bmatrix}\mathcal{C}_{\mathrm{TP}-}^{\mathrm{VCS}}\Bigg]\left(\mathcal{F}_{0+}\big|\mathcal{F}_{++}^{*},\mathcal{F}_{-+}^{*}\right), \end{aligned} \tag{2.44}$$

$$\left\{\begin{matrix} c_{2,\mathrm{TP}}^{\mathrm{VCS}} \\ s_{2,\mathrm{TP}}^{\mathrm{VCS}} \end{matrix}\right\} \;=\; -4\frac{1-y-\frac{\varepsilon^2}{4}y^2}{(1+\varepsilon^2)^{3/2}}\frac{\widetilde{K}}{M}\,\mathrm{Im}\,\mathrm{m}\left\{\begin{matrix} \sqrt{1+\varepsilon^2}\,\Lambda\sin(\varphi)\,\mathcal{C}_{\mathrm{TP}-}^{\mathrm{VCS}} \\ \Lambda\cos(\varphi)\,\mathcal{C}_{\mathrm{TP}+}^{\mathrm{VCS}} \end{matrix}\right\}\left(\mathcal{F}_{-+},\mathcal{F}_{++}^{*}\right). \tag{2.45}$$

Here incoherent sums of transverse helicity-flip and non-flip CFFs are introduced:

$$\mathcal{C}_{\mathrm{S}}^{\mathrm{VCS}}(\mathcal{F}_{++},\mathcal{F}_{++}^{*}\big|\mathcal{F}_{-+},\mathcal{F}_{-+}^{*}) \;=\; \mathcal{C}_{\mathrm{S}}^{\mathrm{VCS}}(\mathcal{F}_{++},\mathcal{F}_{++}^{*}) \pm \mathcal{C}_{\mathrm{S}}^{\mathrm{VCS}}(\mathcal{F}_{-+},\mathcal{F}_{-+}^{*}), \tag{2.46}$$

$$\mathcal{C}_{\mathrm{S}}^{\mathrm{VCS}}(\mathcal{F}_{0+}\big|\mathcal{F}_{++}^{*},\mathcal{F}_{-+}^{*}) \;=\; \mathcal{C}_{\mathrm{S}}^{\mathrm{VCS}}(\mathcal{F}_{0+},\mathcal{F}_{++}^{*}) \pm \mathcal{C}_{\mathrm{S}}^{\mathrm{VCS}}(\mathcal{F}_{0+},\mathcal{F}_{-+}^{*}), \tag{2.47}$$

where the $+$ and $-$ signs apply for $\mathrm{S}\in\{\mathrm{unp},\mathrm{TP}-\}$ and $\mathrm{S}\in\{\mathrm{LP},\mathrm{TP}+\}$ cases, respectively.

By means of Eq. (2.25), the following exact results for the bilinear CFF combinations that enter the VCS squared term are discovered:

- Unpolarized target

$$\begin{aligned}\mathcal{C}_{\mathrm{unp}}^{\mathrm{VCS}} \;=\;& \frac{4(1-x_{\mathrm{B}})\left(1+\frac{x_{\mathrm{B}}t}{\mathcal{Q}^2}\right)}{\left(2-x_{\mathrm{B}}+\frac{x_{\mathrm{B}}t}{\mathcal{Q}^2}\right)^2}\left[\mathcal{H}\mathcal{H}^{*}+\widetilde{\mathcal{H}}\widetilde{\mathcal{H}}^{*}\right]+\frac{\left(2+\frac{t}{\mathcal{Q}^2}\right)\varepsilon^2}{\left(2-x_{\mathrm{B}}+\frac{x_{\mathrm{B}}t}{\mathcal{Q}^2}\right)^2}\widetilde{\mathcal{H}}\widetilde{\mathcal{H}}^{*}-\frac{t}{4M^2}\mathcal{E}\mathcal{E}^{*} \\ &-\frac{x_{\mathrm{B}}^2}{\left(2-x_{\mathrm{B}}+\frac{x_{\mathrm{B}}t}{\mathcal{Q}^2}\right)^2}\left\{\left(1+\frac{t}{\mathcal{Q}^2}\right)^2\left[\mathcal{H}\mathcal{E}^{*}+\mathcal{E}\mathcal{H}^{*}+\mathcal{E}\mathcal{E}^{*}\right]\right. \\ &\left.+\widetilde{\mathcal{H}}\widetilde{\mathcal{E}}^{*}+\widetilde{\mathcal{E}}\widetilde{\mathcal{H}}^{*}+\frac{t}{4M^2}\widetilde{\mathcal{E}}\widetilde{\mathcal{E}}^{*}\right\},\end{aligned} \tag{2.48}$$

- Longitudinally polarized target

$$\begin{aligned}\mathcal{C}_{\mathrm{LP}}^{\mathrm{VCS}} \;=\;& \frac{4(1-x_{\mathrm{B}})\left(1+\frac{x_{\mathrm{B}}t}{\mathcal{Q}^2}\right)+2\left(1-x_{\mathrm{B}}+\frac{\mathcal{Q}^2+t}{2\mathcal{Q}^2}\right)\varepsilon^2}{\left(2-x_{\mathrm{B}}+\frac{x_{\mathrm{B}}t}{\mathcal{Q}^2}\right)^2}\left[\mathcal{H}\widetilde{\mathcal{H}}^{*}+\widetilde{\mathcal{H}}\mathcal{H}^{*}\right] \\ &-\frac{x_{\mathrm{B}}^2\left(1+\frac{x_{\mathrm{B}}t}{\mathcal{Q}^2}-(1-x_{\mathrm{B}})\frac{t}{\mathcal{Q}^2}\right)}{\left(2-x_{\mathrm{B}}+\frac{x_{\mathrm{B}}t}{\mathcal{Q}^2}\right)^2}\left[\mathcal{H}\widetilde{\mathcal{E}}^{*}+\widetilde{\mathcal{E}}\mathcal{H}^{*}+\widetilde{\mathcal{H}}\mathcal{E}^{*}+\mathcal{E}\widetilde{\mathcal{H}}^{*}\right]\end{aligned}$$

$$-\frac{4x_{\rm B}(1-x_{\rm B})\left(1+\frac{x_{\rm B}t}{\mathcal{Q}^2}\right)\frac{t}{\mathcal{Q}^2}+x_{\rm B}\left(1+\frac{t}{\mathcal{Q}^2}\right)^2\varepsilon^2}{2\left(2-x_{\rm B}+\frac{x_{\rm B}t}{\mathcal{Q}^2}\right)^2}\left[\widetilde{\mathcal{H}}\mathcal{E}^*+\mathcal{E}\widetilde{\mathcal{H}}^*\right]$$
$$-\frac{x_{\rm B}}{2-x_{\rm B}+\frac{x_{\rm B}t}{\mathcal{Q}^2}}\left(\frac{x_{\rm B}^2\left(1+\frac{t}{\mathcal{Q}^2}\right)^2}{2\left(2-x_{\rm B}+\frac{x_{\rm B}t}{\mathcal{Q}^2}\right)}+\frac{t}{4M^2}\right)\left[\mathcal{E}\widetilde{\mathcal{E}}^*+\widetilde{\mathcal{E}}\mathcal{E}^*\right], \qquad (2.49)$$

- Transversally polarized target

$$\mathcal{C}^{\rm VCS}_{\rm TP+} = \frac{2}{\left(2-x_{\rm B}+\frac{x_{\rm B}t}{\mathcal{Q}^2}\right)^2}\Bigg\{x_{\rm B}\left[\mathcal{H}\widetilde{\mathcal{E}}^*+\widetilde{\mathcal{E}}\mathcal{H}^*\right]+\frac{4x_{\rm B}(1-2x_{\rm B})M^2}{\mathcal{Q}^2}\left[\mathcal{H}\widetilde{\mathcal{H}}^*+\widetilde{\mathcal{H}}\mathcal{H}^*\right]$$
$$-\left(2-x_{\rm B}+\frac{x_{\rm B}t}{\mathcal{Q}^2}+\left(3+\frac{t}{\mathcal{Q}^2}\right)\frac{\varepsilon^2}{2}\right)\left[\widetilde{\mathcal{H}}\mathcal{E}^*+\mathcal{E}\widetilde{\mathcal{H}}^*\right]$$
$$+\frac{x_{\rm B}^2}{2}\left(1-\frac{t}{\mathcal{Q}^2}\right)\left[\mathcal{E}\widetilde{\mathcal{E}}^*+\widetilde{\mathcal{E}}\mathcal{E}^*\right]\Bigg\}, \qquad (2.50)$$

$$\mathcal{C}^{\rm VCS}_{\rm TP-} = \frac{2}{2-x_{\rm B}+\frac{x_{\rm B}t}{\mathcal{Q}^2}}\left[\mathcal{H}\mathcal{E}^*-\mathcal{E}\mathcal{H}^*\right]-\frac{2x_{\rm B}}{\left(2-x_{\rm B}+\frac{x_{\rm B}t}{\mathcal{Q}^2}\right)^2}\left[\widetilde{\mathcal{H}}\widetilde{\mathcal{E}}^*-\widetilde{\mathcal{E}}\widetilde{\mathcal{H}}^*\right]. \qquad (2.51)$$

Let us point out at this moment that the transverse double-flip CFFs, given in the approximation (2.19), can be expressed by the gluon transversity CFFs which were introduced in Ref. [51] via the following linear map (cf. (2.122) and (2.126)–(2.129) below)

$$\mathcal{H}_T = \mathcal{H}_T^{[51]}+\mathcal{E}_T^{[51]}+2\widetilde{\mathcal{H}}_T^{[51]}+\frac{t}{\widetilde{K}^2}\Bigg[\left(1-x_{\rm B}+\frac{x_{\rm B}t}{2\mathcal{Q}^2}\right)\left(1+\frac{x_{\rm B}t}{2\mathcal{Q}^2}\right)\mathcal{H}_T^{[51]}$$
$$-\frac{x_{\rm B}^2}{4}\mathcal{E}_T^{[51]}+\frac{x_{\rm B}}{4}\left(2-x_{\rm B}+\frac{x_{\rm B}t}{\mathcal{Q}^2}\right)\widetilde{\mathcal{E}}_T^{[51]}\Bigg], \qquad (2.52)$$

$$\mathcal{E}_T = -2\widetilde{\mathcal{H}}_T^{[51]}-\frac{4M^2}{\widetilde{K}^2}\Bigg[\left(1-x_{\rm B}+\frac{x_{\rm B}t}{2\mathcal{Q}^2}\right)\left(1+\frac{x_{\rm B}t}{2\mathcal{Q}^2}\right)\mathcal{H}_T^{[51]}$$
$$-\frac{x_{\rm B}^2}{4}\mathcal{E}_T^{[51]}+\frac{x_{\rm B}}{4}\left(2-x_{\rm B}+\frac{x_{\rm B}t}{\mathcal{Q}^2}\right)\widetilde{\mathcal{E}}_T^{[51]}\Bigg], \qquad (2.53)$$

$$\widetilde{\mathcal{H}}_T = \frac{M^2\left(2-x_{\rm B}+\frac{x_{\rm B}t}{\mathcal{Q}^2}\right)}{\widetilde{K}^2}\Bigg[x_{\rm B}\mathcal{H}_T^{[51]}+\frac{x_{\rm B}t}{4M^2}\mathcal{E}_T^{[51]}$$
$$-\left(2-x_{\rm B}+\frac{x_{\rm B}t}{\mathcal{Q}^2}\right)\frac{t}{4M^2}\widetilde{\mathcal{E}}_T^{[51]}\Bigg], \qquad (2.54)$$

$$\widetilde{\mathcal{E}}_T \;=\; \frac{M^2\left(2-x_{\rm B}+\frac{x_{\rm B}t}{\mathcal{Q}^2}\right)}{\widetilde{K}^2}\Bigg[\left(2-x_{\rm B}+\frac{x_{\rm B}t}{\mathcal{Q}^2}\right)\widetilde{\mathcal{E}}_T^{[51]} \\ -\frac{4M^2x_{\rm B}^2+4\widetilde{K}^2}{x_{\rm B}t}\mathcal{H}_T^{[51]}-x_{\rm B}\mathcal{E}_T^{[51]}\Bigg]. \qquad (2.55)$$

These obviously suffer from kinematical $1/\widetilde{K}^2$ singularities. In the case of our unaltered twist-three CFF definitions such kinematical singularities cancel each other, while for gluon transversity contributions a partial cancelation in all four expressions for $\mathcal{C}$-functions (2.48)–(2.51) is observed:

$$\mathcal{C}_{\rm S}^{\rm VCS}(\mathcal{F}_T,\mathcal{F}_T^*)\propto\widetilde{K}^{-2}\quad\text{for}\quad S\in\{\text{unp},\text{LP},\text{TP}+,\text{TP}-\}$$

and

$$\mathcal{C}_{\rm S}^{\rm VCS}(\mathcal{F}_T,\mathcal{F}^*)\propto\left\{\begin{array}{c}\widetilde{K}^0\\ \widetilde{K}^{-2}\end{array}\right\}\quad\text{for}\quad S\in\left\{\begin{array}{c}\text{unp},\text{LP}\\ \text{TP}+,\text{TP}-\end{array}\right\}.$$

If power-suppressed contributions are neglected, one retrieves for the $\mathcal{C}$-functions the same functional form that was already found in Ref. [36]. Moreover, the behavior of helicity-flip CFFs, indicated by the additional $\widetilde{K}$ and $\widetilde{K}^2$ factors in the relations (2.18), (2.19), ensure that all first- (second-) and second- (first-) order harmonics for unp and LP (TP+ and TP−) cases vanish in the limit $t\to t_{\rm min}$ as $\sqrt{t_{\rm min}-t}$ and $t_{\rm min}-t$, respectively. Finally, it should pointed out that the results given here are consistent with the expanded ones of Ref. [36] and that they have been numerically cross checked by means of the leptonic tensor (2.24) and a hadronic Compton scattering tensor, given below in Eq. (2.136).

2.2.3 Interference Term

Let us now turn to the interference term. Inserting the completeness condition for the initial and final photon polarization states, one finds the interference term $\mathcal{I}$ as a linear superposition

$$\mathcal{I}=\frac{\pm e^6}{t\,\mathcal{P}_1(\phi)\mathcal{P}_2(\phi)}\sum_{a=\pm,0}\sum_{b=\pm}\sum_{S'}\left\{\mathcal{L}^{\rho}_{ab}(\lambda,\phi)\mathcal{T}_{ab}J^{\dagger}_{\rho}+\left(\mathcal{L}^{\rho}_{ab}(\lambda,\phi)\mathcal{T}_{ab}J^{\dagger}_{\rho}\right)^*\right\}, \qquad (2.56)$$

of the products of hadronic and leptonic helicity amplitudes. The former were defined earlier in Eq. (2.13), and the matrix element of the quark electromagnetic current (2.3),

$$J_\rho = \bar{u}_2 \Gamma_\rho(\Delta) u_1 \qquad \text{with} \qquad \Gamma_\rho(\Delta) = \gamma_\rho F_1(t) + i\sigma_{\rho\sigma}\frac{\Delta^\sigma}{2M} F_2(t)\,, \tag{2.57}$$

is determined by the Dirac and Pauli form factors F_1 and F_2. Moreover, $1/\mathcal{P}_1(\phi)\mathcal{P}_2(\phi)$ stands for the product of rescaled propagators of the Bethe-Heitler amplitude, specified in Eqs. (28)–(31) of Ref. [36].

First, the hadronic part $\mathcal{T}_{ab} J_\rho^\dagger$ of the interference term (2.56) is considered which, similarly to the leptonic part, has one open Lorentz index. The former is given by the VCS helicity amplitudes (2.13)–(2.15) and the electromagnetic current (2.57). The resulting (axial-) vector amplitudes will be decomposed in the basis (2.11) of the physical momenta. Due to electromagnetic current conservation, terms that are proportional to Δ_ρ are neglected, which vanish upon contraction with the leptonic part $\mathcal{L}^\rho_{ab}$. The summation over the final-nucleon polarization states yields the following expression in the vector sector:

$$\begin{aligned}
\sum_{S'} \mathcal{V}(\mathcal{F}) J_\rho^\dagger \;=\; & p_\rho \left[\mathcal{C}^{\mathcal{I}}_{\text{unp}}(\mathcal{F}) - \mathcal{C}^{\mathcal{I},A}_{\text{unp}}\right](\mathcal{F}) + 2q_\rho \frac{t}{\mathcal{Q}^2}\mathcal{C}^{\mathcal{I},V}_{\text{unp}}(\mathcal{F}) \\
& + \frac{2i\varepsilon_{pq\Delta\rho}}{\mathcal{Q}^2}\left[\frac{\Lambda\cos(\theta)}{\sqrt{1+\varepsilon^2}}\mathcal{C}^{\mathcal{I},V}_{\text{LP}} + \frac{\Lambda\sin(\theta)\cos(\varphi)M}{\sqrt{1+\varepsilon^2}\widetilde{K}}\mathcal{C}^{\mathcal{I},V}_{\text{TP}+}\right](\mathcal{F}) \\
& - p_\rho \frac{\Lambda\sin(\theta)\sin(\varphi)M}{i\widetilde{K}}\left[\mathcal{C}^{\mathcal{I}}_{\text{TP}-} - \mathcal{C}^{\mathcal{I},A}_{\text{TP}-}\right](\mathcal{F}) \\
& - 2q_\rho \frac{t}{\mathcal{Q}^2}\frac{\Lambda\sin(\theta)\sin(\varphi)M}{i\widetilde{K}}\mathcal{C}^{\mathcal{I},V}_{\text{TP}-}(\mathcal{F})\,,
\end{aligned} \tag{2.58}$$

and analogously in the axial-vector case

$$\begin{aligned}
\sum_{S'} \mathcal{A}(\mathcal{F}) J_\rho^\dagger \;=\; & p_\rho \frac{\Lambda\cos(\theta)}{\sqrt{1+\varepsilon^2}}\left[\mathcal{C}^{\mathcal{I}}_{\text{LP}} - \mathcal{C}^{\mathcal{I},V}_{\text{LP}}\right](\mathcal{F}) + 2q_\rho \frac{t}{\mathcal{Q}^2}\frac{\Lambda\cos(\theta)}{\sqrt{1+\varepsilon^2}}\mathcal{C}^{\mathcal{I},A}_{\text{LP}}(\mathcal{F}) \\
& + p_\rho \frac{\Lambda\sin(\theta)\cos(\varphi)M}{\sqrt{1+\varepsilon^2}\widetilde{K}}\left[\mathcal{C}^{\mathcal{I}}_{\text{TP}+} - \mathcal{C}^{\mathcal{I},V}_{\text{TP}+}\right](\mathcal{F}) \\
& + 2q_\rho \frac{t}{\mathcal{Q}^2}\frac{\Lambda\sin(\theta)\cos(\varphi)M}{\sqrt{1+\varepsilon^2}\widetilde{K}}\mathcal{C}^{\mathcal{I},A}_{\text{TP}+}(\mathcal{F}) \\
& + \frac{2i\varepsilon_{pq\Delta\rho}}{\mathcal{Q}^2}\left[\mathcal{C}^{\mathcal{I},A}_{\text{unp}} - \frac{\Lambda\sin(\theta)\sin(\varphi)M}{i\widetilde{K}}\mathcal{C}^{\mathcal{I},A}_{\text{TP}-}\right](\mathcal{F})\,.
\end{aligned} \tag{2.59}$$

As becomes obvious from these two equations, the result for the transversely polarized target can be obtained from the ones of unpolarized and longitudinally polarized cases by the following substitutions

$$\mathcal{C}^{\mathcal{I},\cdots}_{\rm unp}(\mathcal{F}) \quad \Rightarrow \quad -\Lambda\sin(\theta)\sin(\varphi)\frac{M}{i\widetilde{K}}\mathcal{C}^{\mathcal{I},\cdots}_{\rm TP_-}(\mathcal{F}), \tag{2.60}$$

$$\frac{\Lambda\cos(\theta)}{\sqrt{1+\varepsilon^2}}\mathcal{C}^{\mathcal{I},\cdots}_{\rm LP}(\mathcal{F}) \quad \Rightarrow \quad \frac{\Lambda\sin(\theta)\cos(\varphi)}{\sqrt{1+\varepsilon^2}}\frac{M}{\widetilde{K}}\mathcal{C}^{\mathcal{I},\cdots}_{\rm TP_+}(\mathcal{F}). \tag{2.61}$$

Now turn to the leptonic helicity amplitudes,

$$\mathcal{L}^{\rho}_{ab}(\lambda,\phi) = \varepsilon_1^{\mu *}(a) L_{\mu}{}^{\rho}{}_{\nu}\varepsilon_2^{\nu}(b), \tag{2.62}$$

where

$$L_{\mu\rho\nu} = \frac{(k-q_2)^2(k-\Delta)^2}{\mathcal{Q}^6}\,\mathrm{tr}\,\tfrac{1}{2}(1-\lambda\gamma_5)\left[\gamma_\rho(\not{k}-\not{\Delta})^{-1}\gamma_\nu + \gamma_\rho(\not{k}'+\not{\Delta})^{-1}\gamma_\nu\right]\gamma_\mu\not{k}. \tag{2.63}$$

This amplitude contains the entire azimuthal angular dependence of the interference term. Its contraction with the Lorentz vectors entering the decomposition of the hadronic amplitudes (2.58) and (2.59) introduces the coefficients for the lepton helicity-independent,

$$\left\{\begin{array}{c} C_{ab} \\ C^V_{ab} \\ C^A_{ab} \end{array}\right\} = \mathrm{Re\,e}\,\mathcal{L}^{\rho}_{ab}(\lambda=0,\phi)\left\{\begin{array}{c} p_\rho \\ 2q_\rho\frac{t}{\mathcal{Q}^2} \\ \frac{2i\varepsilon_{pq\Delta\rho}}{\mathcal{Q}^2} \end{array}\right\},$$

$$\left\{\begin{array}{c} \delta S_{ab} \\ \delta S^V_{ab} \\ \delta S^A_{ab} \end{array}\right\} = \mathrm{Im\,m}\frac{\mathcal{L}^{\rho}_{ab}(\lambda=0,\phi)}{\sqrt{1+\varepsilon^2}}\left\{\begin{array}{c} p_\rho \\ 2q_\rho\frac{t}{\mathcal{Q}^2} \\ \frac{2i\varepsilon_{pq\Delta\rho}}{\mathcal{Q}^2} \end{array}\right\}, \tag{2.64}$$

and helicity-dependent components

$$\left\{\begin{array}{c} S_{ab} \\ S^V_{ab} \\ S^A_{ab} \end{array}\right\} = \mathrm{Im\,m}\frac{\partial}{\partial\lambda}\mathcal{L}^{\rho}_{ab}(\lambda,\phi)\left\{\begin{array}{c} p_\rho \\ 2q_\rho\frac{t}{\mathcal{Q}^2} \\ \frac{2i\varepsilon_{pq\Delta\rho}}{\mathcal{Q}^2} \end{array}\right\},$$

$$\left\{\begin{array}{c}\delta C_{ab}\\ \delta C^{V}_{ab}\\ \delta C^{A}_{ab}\end{array}\right\} = \mathrm{Re}\,\mathrm{e}\,\frac{\partial}{\partial\lambda}\frac{\mathcal{L}^{\rho}_{ab}(\lambda,\phi)}{\sqrt{1+\varepsilon^2}}\left\{\begin{array}{c}p_\rho\\ 2q_\rho\,\frac{t}{\mathcal{Q}^2}\\ \frac{2i\varepsilon_{pq\Delta\rho}}{\mathcal{Q}^2}\end{array}\right\}, \tag{2.65}$$

respectively. Notice that in the deeply virtual regime, the leptonic coefficients with V and A superscripts are power suppressed. The harmonic expansion of these coefficients are also introduced,

$$\begin{aligned}(\delta)C_{ab}(\phi) &= \frac{1}{x_{\mathrm{B}}y^3}\sum_{n=0}^{3}\cos(n\phi)\,(\delta)C_{ab}(n)\,,\\ (\delta)S_{ab}(\phi) &= \frac{1}{x_{\mathrm{B}}y^3}\sum_{n=1}^{3}\sin(n\phi)\,(\delta)S_{ab}(n)\,,\end{aligned} \tag{2.66}$$

where a conventional factor $1/(x_{\mathrm{B}}y^3)$ is included.

As for the square of the virtual Compton scattering amplitude, listed in Sect. 2.2.2, the interference term is decomposed in a Fourier harmonic sum, and entering contributions $c^{\mathcal{I}}_{k,\mathrm{S}}$ are labeled with respect to the polarization of the incoming nucleon state $\mathrm{S}\in\{\mathrm{unp},\mathrm{LP},\mathrm{TP}+,\mathrm{TP}-\}$,

$$\mathcal{I}(\phi,\varphi) = \frac{\pm e^6}{x_{\mathrm{B}}y^3 t\mathcal{P}_1(\phi)\mathcal{P}_2(\phi)}\left[\sum_{n=0}^{3}c^{\mathcal{I}}_{n,\mathrm{S}}(\varphi)\cos(n\phi)+\sum_{n=1}^{3}s^{\mathcal{I}}_{n,\mathrm{S}}(\varphi)\sin(n\phi)\right]. \tag{2.67}$$

The Fourier coefficients $c^{\mathcal{I}}_{n,\mathrm{S}}$ and $s^{\mathcal{I}}_{n,\mathrm{S}}$ are straightforwardly obtained from the definitions given in this section, and can be exactly expressed in terms of effective linear combinations of helicity-dependent CFFs (2.13).

However, as follows from Eqs. (2.58), (2.59) together with (2.64), (2.65), an exact calculation of the interference term (2.56) yields a result that is given by a superposition of factorized leptonic and hadronic components. Hence, one may introduce "effective" hadronic linear combinations of CFFs that read for the unpolarized and transversally polarized TP$-$ components as follows:

$$\mathcal{C}^{\mathcal{I}}_{ab,\mathrm{S}}(n|\mathcal{F}_{ab}) \;=\; \mathcal{C}^{\mathcal{I}}_{\mathrm{S}}(\mathcal{F}_{ab}) + \frac{C^{V}_{ab}(n)}{C_{ab}(n)}\mathcal{C}^{\mathcal{I},V}_{\mathrm{S}}(\mathcal{F}_{ab}) + \frac{C^{A}_{ab}(n)}{C_{ab}(n)}\mathcal{C}^{\mathcal{I},A}_{\mathrm{S}}(\mathcal{F}_{ab})\,,$$

$$\mathcal{S}^{\mathcal{I}}_{ab,\mathrm{S}}(n|\mathcal{F}_{ab}) \;=\; \mathcal{C}^{\mathcal{I}}_{\mathrm{S}}(\mathcal{F}_{ab}) + \frac{S^{V}_{ab}(n)}{S_{ab}(n)}\,\mathcal{C}^{\mathcal{I},V}_{\mathrm{S}}(\mathcal{F}_{ab}) + \frac{S^{A}_{ab}(n)}{S_{ab}(n)}\,\mathcal{C}^{\mathcal{I},A}_{\mathrm{S}}(\mathcal{F}_{ab})\,, \tag{2.68}$$

where $\mathrm{S} \in \{\mathrm{unp}, \mathrm{TP}-\}$, and for the longitudinally and transversally polarized TP+ parts as:

$$\begin{aligned}
\mathcal{C}^{\mathcal{I}}_{ab,\mathrm{S}}(n|\mathcal{F}_{ab}) \;&=\; \mathcal{C}^{\mathcal{I}}_{\mathrm{S}}(\mathcal{F}_{ab}) + \frac{\delta C^{V}_{ab}(n)}{\delta C_{ab}(n)}\,\mathcal{C}^{\mathcal{I},V}_{\mathrm{S}}(\mathcal{F}_{ab}) + \frac{\delta C^{A}_{ab}(n)}{\delta C_{ab}(n)}\,\mathcal{C}^{\mathcal{I},A}_{\mathrm{S}}(\mathcal{F}_{ab})\,, \\
\mathcal{S}^{\mathcal{I}}_{ab,\mathrm{S}}(n|\mathcal{F}_{ab}) \;&=\; \mathcal{C}^{\mathcal{I}}_{\mathrm{S}}(\mathcal{F}_{ab}) + \frac{\delta S^{V}_{ab}(n)}{\delta S_{ab}(n)}\,\mathcal{C}^{\mathcal{I},V}_{\mathrm{S}}(\mathcal{F}_{ab}) + \frac{\delta S^{A}_{ab}(n)}{\delta S_{ab}(n)}\,\mathcal{C}^{\mathcal{I},A}_{\mathrm{S}}(\mathcal{F}_{ab})\,,
\end{aligned} \tag{2.69}$$

with $\mathrm{S} \in \{\mathrm{LP}, \mathrm{TP}+\}$. The explicit results of the calculation of the leptonic coefficients $(\delta)C^{\cdots}_{ab}(n)$ and $(\delta)S^{\cdots}_{ab}(n)$, defined in Eqs. (2.64)–(2.66), are listed in Appendix A.2. From what was said above, it follows that the dominant term in the deeply virtual kinematics is given by the coefficients $\mathcal{C}^{\mathcal{I}}_{\mathrm{S}}$. Also, it turns out that for a given harmonic all helicity amplitudes will contribute. However, in the regime of large photon virtualities, the first harmonics are dominated by the helicity-conserved CFFs $\mathcal{F}_{++}$ (of twist-two in power counting), while the second ones receive a leading contribution from the longitudinal-to-transverse CFFs $\mathcal{F}_{0+}$ (twist-three). The third harmonic is governed by the transverse-to-transvers, CFFs $\mathcal{F}_{-+}$, determined at twist-two level by the gluon-transversity GPDs. The latter contribution yields a $\cos(3\phi)$ harmonic for unpolarized scattering, given by the real part of the CFFs, and $\sin(3\phi)$ harmonic for the longitudinally polarized part, this time expressed in terms of the imaginary part. The transversally polarized part is determined by the imaginary part of CFF combinations, leading to $\cos(\varphi)\sin(3\phi)$ and $\sin(\varphi)\cos(3\phi)$ harmonics. There also appear constant terms that are relatively suppressed by $1/\mathcal{Q}$ in the amplitudes and are dominated by twist-two operator matrix elements.

Now the explicit expressions for the Fourier coefficients in terms of linear photon helicity-dependent CFF combinations are listed, where the separate terms are ordered with respect to their importance in the deeply virtual region:

- Unpolarized target

$$c_{0,\mathrm{unp}}^{\mathcal{I}} = C_{++}(0)\,\mathrm{Ree}\mathcal{C}_{++,\mathrm{unp}}^{\mathcal{I}}(0|\mathcal{F}_{++}) + \{_{++} \to {}_{0+}\} + \{_{++} \to {}_{-+}\}, \tag{2.70}$$

$$\begin{Bmatrix} c_1^{\mathcal{I}} \\ s_1^{\mathcal{I}} \end{Bmatrix}_{\mathrm{unp}} = \begin{Bmatrix} C_{++}(1) \\ \lambda\, S_{++}(1) \end{Bmatrix} \begin{Bmatrix} \mathrm{Ree} \\ \mathrm{Imm} \end{Bmatrix} \begin{Bmatrix} \mathcal{C}_{++}^{\mathcal{I}}(1|\mathcal{F}_{++}) \\ \mathcal{S}_{++}^{\mathcal{I}}(1|\mathcal{F}_{++}) \end{Bmatrix}_{\mathrm{unp}} + \{_{++} \to {}_{0+}\} + \{_{++} \to {}_{-+}\}, \tag{2.71}$$

$$\begin{Bmatrix} c_2^{\mathcal{I}} \\ s_2^{\mathcal{I}} \end{Bmatrix}_{\mathrm{unp}} = \begin{Bmatrix} C_{0+}(2) \\ \lambda\, S_{0+}(2) \end{Bmatrix} \begin{Bmatrix} \mathrm{Ree} \\ \mathrm{Imm} \end{Bmatrix} \begin{Bmatrix} \mathcal{C}_{0+}^{\mathcal{I}}(2|\mathcal{F}_{0+}) \\ \mathcal{S}_{0+}^{\mathcal{I}}(2|\mathcal{F}_{0+}) \end{Bmatrix}_{\mathrm{unp}} + \{_{0+} \to {}_{++}\} + \{_{0+} \to {}_{-+}\}, \tag{2.72}$$

$$c_{3,\mathrm{unp}}^{\mathcal{I}} = C_{-+}(3)\,\mathrm{Ree}\mathcal{C}_{-+,\mathrm{unp}}^{\mathcal{I}}(3|\mathcal{F}_{-+}) + \{_{-+} \to {}_{++}\} + \{_{-+} \to {}_{0+}\}, \tag{2.73}$$

where the CFF combinations $\mathcal{C}_{ab,\mathrm{unp}}^{\mathcal{I}}$ and $\mathcal{S}_{ab,\mathrm{unp}}^{\mathcal{I}}$ are defined in Eqs. (2.68) and (2.83)–(2.85), together with $C_{ab}^{\mathcal{I},\cdots}$ and $S_{ab}^{\mathcal{I},\cdots}$, listed in Appendix A.2.1.

- Longitudinally polarized target [i.e., $\cos\theta$ proportional part]

$$c_{0,\mathrm{LP}}^{\mathcal{I}} = \Lambda\lambda\,\delta C_{++}(0)\,\mathrm{Ree}\mathcal{C}_{++,\mathrm{LP}}^{\mathcal{I}}(0|\mathcal{F}_{++}) + \{_{++} \to {}_{0+}\} + \{_{++} \to {}_{-+}\}, \tag{2.74}$$

$$\begin{Bmatrix} c_1^{\mathcal{I}} \\ s_1^{\mathcal{I}} \end{Bmatrix}_{\mathrm{LP}} = \Lambda \begin{Bmatrix} \lambda\,\delta C_{++}(1) \\ \delta S_{++}(1) \end{Bmatrix} \begin{Bmatrix} \mathrm{Ree} \\ \mathrm{Imm} \end{Bmatrix} \begin{Bmatrix} \mathcal{C}_{++}^{\mathcal{I}}(1|\mathcal{F}_{++}) \\ \mathcal{S}_{++}^{\mathcal{I}}(1|\mathcal{F}_{++}) \end{Bmatrix}_{\mathrm{LP}} + \{_{++} \to {}_{0+}\} + \{_{++} \to {}_{-+}\}, \tag{2.75}$$

$$\begin{Bmatrix} c_2^{\mathcal{I}} \\ s_2^{\mathcal{I}} \end{Bmatrix}_{\mathrm{LP}} = \Lambda \begin{Bmatrix} \lambda\,\delta C_{0+}(2) \\ \delta S_{0+}(2) \end{Bmatrix} \begin{Bmatrix} \mathrm{Ree} \\ \mathrm{Imm} \end{Bmatrix} \begin{Bmatrix} \mathcal{C}_{0+}^{\mathcal{I}}(2|\mathcal{F}_{0+}) \\ \mathcal{S}_{0+}^{\mathcal{I}}(2|\mathcal{F}_{0+}) \end{Bmatrix}_{\mathrm{LP}} + \{_{0+} \to {}_{++}\} + \{_{0+} \to {}_{-+}\}, \tag{2.76}$$

$$s_{3,\mathrm{LP}}^{\mathcal{I}} = \Lambda\,\delta S_{-+}(3)\,\mathrm{Imm}\mathcal{C}_{-+,\mathrm{LP}}^{\mathcal{I}}(3|\mathcal{F}_{-+}) + \{_{-+} \to {}_{++}\} + \{_{-+} \to {}_{0+}\}, \tag{2.77}$$

where the CFF combinations $\mathcal{C}^{\mathcal{I}}_{ab,\mathrm{LP}}$ and $\mathcal{S}^{\mathcal{I}}_{ab,\mathrm{LP}}$ are defined in Eqs. (2.69) and (2.86)–(2.88) together with $\delta C^{\mathcal{I},\cdots}_{ab}$ and $\delta S^{\mathcal{I},\cdots}_{ab}$, listed in Appendix A.2.2.

- Transversally polarized target [i.e., $\sin\theta$ proportional part]

$$
\begin{aligned}
c^{\mathcal{I}}_{0,\mathrm{TP}} &= \lambda\,\Lambda\cos(\varphi)\,\frac{M}{\widetilde{K}}\,\delta C_{++}(0)\,\mathrm{Re}\mathcal{C}^{\mathcal{I}}_{++,\mathrm{TP}+}(0|\mathcal{F}_{++}) \\
&- \Lambda\sin(\varphi)\,\frac{M}{\widetilde{K}}\,C_{++}(0)\,\mathrm{Im}\mathcal{C}^{\mathcal{I}}_{++,\mathrm{TP}-}(0|\mathcal{F}_{++}) \\
&\qquad + \{{}_{++}\to{}_{0+}\} + \{{}_{++}\to{}_{-+}\}, \qquad (2.78)\\
\begin{Bmatrix} c^{\mathcal{I}}_1 \\ s^{\mathcal{I}}_1 \end{Bmatrix}_{\mathrm{TP}} &= \Lambda\cos(\varphi)\,\frac{M}{\widetilde{K}}\begin{Bmatrix} \lambda\,\delta C_{++}(1) \\ \delta S_{++}(1) \end{Bmatrix}\begin{Bmatrix} \mathrm{Re} \\ \mathrm{Im} \end{Bmatrix}\begin{Bmatrix} \mathcal{C}^{\mathcal{I}}_{++}(1|\mathcal{F}_{++}) \\ \mathcal{S}^{\mathcal{I}}_{++}(1|\mathcal{F}_{++}) \end{Bmatrix}_{\mathrm{TP}+} \\
&+ \Lambda\sin(\varphi)\,\frac{M}{\widetilde{K}}\begin{Bmatrix} -C_{++}(1) \\ \lambda\,S_{++}(1) \end{Bmatrix}\begin{Bmatrix} \mathrm{Im} \\ \mathrm{Re} \end{Bmatrix}\begin{Bmatrix} \mathcal{C}^{\mathcal{I}}_{++}(1|\mathcal{F}_{++}) \\ \mathcal{S}^{\mathcal{I}}_{++}(1|\mathcal{F}_{++}) \end{Bmatrix}_{\mathrm{TP}-} \\
&\qquad + \{{}_{++}\to{}_{0+}\} + \{{}_{++}\to{}_{-+}\}, \qquad (2.79)\\
\begin{Bmatrix} c^{\mathcal{I}}_2 \\ s^{\mathcal{I}}_2 \end{Bmatrix}_{\mathrm{TP}} &= \Lambda\cos(\varphi)\,\frac{M}{\widetilde{K}}\begin{Bmatrix} \lambda\,\delta C_{0+}(2) \\ \delta S_{0+}(2) \end{Bmatrix}\begin{Bmatrix} \mathrm{Re} \\ \mathrm{Im} \end{Bmatrix}\begin{Bmatrix} \mathcal{C}^{\mathcal{I}}_{0+}(2|\mathcal{F}_{0+}) \\ \mathcal{S}^{\mathcal{I}}_{0+}(2|\mathcal{F}_{0+}) \end{Bmatrix}_{\mathrm{TP}+} \\
&+ \Lambda\sin(\varphi)\,\frac{M}{\widetilde{K}}\begin{Bmatrix} -C_{++}(2) \\ \lambda\,S_{++}(2) \end{Bmatrix}\begin{Bmatrix} \mathrm{Im} \\ \mathrm{Re} \end{Bmatrix}\begin{Bmatrix} \mathcal{C}^{\mathcal{I}}_{0+}(2|\mathcal{F}_{0+}) \\ \mathcal{S}^{\mathcal{I}}_{0+}(2|\mathcal{F}_{0+}) \end{Bmatrix}_{\mathrm{TP}-} \\
&\qquad + \{{}_{0+}\to{}_{++}\} + \{{}_{0+}\to{}_{-+}\}, \qquad (2.80)\\
s^{\mathcal{I}}_{3,\mathrm{TP}} &= \Lambda\cos(\varphi)\,\frac{M}{\widetilde{K}}\,\delta S_{-+}(3)\,\mathrm{Im}\mathcal{C}^{\mathcal{I}}_{-+,\mathrm{TP}+}(3|\mathcal{F}_{-+}) \\
&\qquad + \{{}_{-+}\to{}_{++}\} + \{{}_{-+}\to{}_{0+}\}, \qquad (2.81)\\
c^{\mathcal{I}}_{3,\mathrm{TP}} &= -\Lambda\sin(\varphi)\,\frac{M}{\widetilde{K}}\,C_{-+}(3)\,\mathrm{Im}\mathcal{C}^{\mathcal{I}}_{-+,\mathrm{TP}-}(3|\mathcal{F}_{-+}) \\
&\qquad + \{{}_{-+}\to{}_{++}\} + \{{}_{-+}\to{}_{0+}\}, \qquad (2.82)
\end{aligned}
$$

where the CFF combinations $\mathcal{C}^{\mathcal{I}}_{ab,\mathrm{TP}-}$ and $\mathcal{S}^{\mathcal{I}}_{ab,\mathrm{TP}-}$ [$\mathcal{C}^{\mathcal{I}}_{ab,\mathrm{TP}+}$ and $\mathcal{S}^{\mathcal{I}}_{ab,\mathrm{TP}+}$] are defined in Eqs. (2.68) and (2.89)–(2.91) [Eqs. (2.69) and (2.92)–(2.94)] together with $C^{\mathcal{I},\cdots}_{ab}$ and $S^{\mathcal{I},\cdots}_{ab}$ [$\delta C^{\mathcal{I},\cdots}_{ab}$ and $\delta S^{\mathcal{I},\cdots}_{ab}$], listed in Appendix A.2.1 [Appendix A.2.2].

For the linear combinations of CFFs, evaluated from Eqs. (2.58) and (2.59), for the helicity dependent CFFs the following exact expressions are found:

- Unpolarized target

$$\mathcal{C}^{\mathcal{I}}_{\rm unp}(\mathcal{F}) = F_1\mathcal{H} - \frac{t}{4M^2}F_2\mathcal{E} + \frac{x_{\rm B}}{2-x_{\rm B}+\frac{x_{\rm B}t}{\mathcal{Q}^2}}(F_1+F_2)\widetilde{\mathcal{H}}\,, \tag{2.83}$$

$$\mathcal{C}^{\mathcal{I},V}_{\rm unp}(\mathcal{F}) = \frac{x_{\rm B}}{2-x_{\rm B}+\frac{x_{\rm B}t}{\mathcal{Q}^2}}(F_1+F_2)(\mathcal{H}+\mathcal{E})\,, \tag{2.84}$$

$$\mathcal{C}^{\mathcal{I},A}_{\rm unp}(\mathcal{F}) = \frac{x_{\rm B}}{2-x_{\rm B}+\frac{x_{\rm B}t}{\mathcal{Q}^2}}(F_1+F_2)\widetilde{\mathcal{H}}\,, \tag{2.85}$$

- Longitudinally polarized target

$$\begin{aligned}\mathcal{C}^{\mathcal{I}}_{\rm LP}(\mathcal{F}) = {}& \frac{2}{2-x_{\rm B}+\frac{x_{\rm B}t}{\mathcal{Q}^2}}F_1\Bigg[\left\{(1-x_{\rm B})\left(1+\frac{x_{\rm B}t}{\mathcal{Q}^2}\right)+\frac{x_{\rm B}}{2}+\frac{x_{\rm B}^2M^2}{\mathcal{Q}^2}\left(3+\frac{t}{\mathcal{Q}^2}\right)\right\}\widetilde{\mathcal{H}}\\ &+ \frac{x_{\rm B}}{2-x_{\rm B}+\frac{x_{\rm B}t}{\mathcal{Q}^2}}(F_1+F_2)\Bigg[\mathcal{H}+\frac{x_{\rm B}}{2}\left(1-\frac{t}{\mathcal{Q}^2}\right)\mathcal{E}-\frac{(1-2x_{\rm B})t}{\mathcal{Q}^2}\widetilde{\mathcal{H}}\\ &-\frac{t}{4M^2}\widetilde{\mathcal{E}}\Bigg]+\frac{x_{\rm B}}{2}\left\{\frac{t}{4M^2}-\frac{x_{\rm B}}{2}\left(1-\frac{t}{\mathcal{Q}^2}\right)\right\}\widetilde{\mathcal{E}}\Bigg]\,,\end{aligned} \tag{2.86}$$

$$\mathcal{C}^{\mathcal{I},V}_{\rm LP}(\mathcal{F}) = \frac{x_{\rm B}}{2-x_{\rm B}+\frac{x_{\rm B}t}{\mathcal{Q}^2}}(F_1+F_2)\left[\mathcal{H}+\frac{x_{\rm B}}{2}\left(1-\frac{t}{\mathcal{Q}^2}\right)\mathcal{E}\right]\,, \tag{2.87}$$

$$\mathcal{C}^{\mathcal{I},A}_{\rm LP}(\mathcal{F}) = \frac{x_{\rm B}}{2-x_{\rm B}+\frac{x_{\rm B}t}{\mathcal{Q}^2}}(F_1+F_2)\left[\widetilde{\mathcal{H}}+2x_{\rm B}\frac{M^2}{\mathcal{Q}^2}\widetilde{\mathcal{H}}+\frac{x_{\rm B}}{2}\widetilde{\mathcal{E}}\right]\,. \tag{2.88}$$

- Transversally polarized target

$$\begin{aligned}\mathcal{C}^{\mathcal{I}}_{\rm TP-}(\mathcal{F}) = {}& \frac{1}{2-x_{\rm B}+\frac{x_{\rm B}t}{\mathcal{Q}^2}}\Bigg[\frac{\widetilde{K}^2}{M^2}(F_2\mathcal{H}-F_1\mathcal{E})\\ &+ x_{\rm B}^2(F_1+F_2)\left\{\left(1+\frac{t}{\mathcal{Q}^2}\right)^2\left(\mathcal{H}+\frac{t}{4M^2}\mathcal{E}\right)-\widetilde{\mathcal{H}}-\frac{t}{4M^2}\widetilde{\mathcal{E}}\right\}\Bigg]\,,\end{aligned} \tag{2.89}$$

$$\mathcal{C}^{\mathcal{I},V}_{\rm TP-}(\mathcal{F}) = x_{\rm B}(F_1+F_2)\left[\mathcal{H}+\frac{t}{4M^2}\mathcal{E}\right]\,, \tag{2.90}$$

$$\mathcal{C}^{\mathcal{I},A}_{\rm TP-}(\mathcal{F}) = -\frac{x_{\rm B}^2}{2-x_{\rm B}+\frac{x_{\rm B}t}{\mathcal{Q}^2}}(F_1+F_2)\left[\widetilde{\mathcal{H}}+\frac{t}{4M^2}\widetilde{\mathcal{E}}\right]\,, \tag{2.91}$$

$$\mathcal{C}^{\mathcal{I}}_{\rm TP+}(\mathcal{F}) = \frac{x_{\rm B}^2\left(1-(1-2x_{\rm B})\frac{t}{\mathcal{Q}^2}\right)}{2-x_{\rm B}+\frac{x_{\rm B}t}{\mathcal{Q}^2}}(F_1+F_2)\left[\mathcal{H}+\frac{t}{4M^2}\mathcal{E}-\widetilde{\mathcal{H}}-\frac{t}{4M^2}\widetilde{\mathcal{E}}\right]$$

$$- \frac{1}{2-x_B+\frac{x_B t}{Q^2}}\frac{\widetilde{K}^2}{M^2}\left[\frac{x_B}{2}F_1\left(\mathcal{E}-\widetilde{\mathcal{E}}-\frac{4M^2}{Q^2}\widetilde{\mathcal{H}}\right)+\frac{x_B}{2}F_2\mathcal{E}+F_2\widetilde{\mathcal{H}}\right], \qquad (2.92)$$

$$\mathcal{C}^{\mathcal{I},V}_{\mathrm{TP}+}(\mathcal{F}) = \frac{x_B}{2-x_B+\frac{x_B t}{Q^2}}(F_1+F_2)\left[x_B\left(1-\frac{t}{Q^2}(1-2x_B)\right)\left(\mathcal{H}+\frac{t}{4M^2}\mathcal{E}\right)\right.$$
$$\left.-\frac{\widetilde{K}^2}{2M^2}\mathcal{E}\right], \qquad (2.93)$$

$$\mathcal{C}^{\mathcal{I},A}_{\mathrm{TP}+}(\mathcal{F}) = -\frac{x_B}{2-x_B+\frac{x_B t}{Q^2}}(F_1+F_2)\left[\left\{2-x_B+2\frac{x_B t}{Q^2}+\left(3+\frac{t}{Q^2}-\frac{t}{M^2}\right)\frac{\varepsilon^2}{2}\right\}\widetilde{\mathcal{H}}\right.$$
$$\left.-\frac{x_B}{2}\left\{x_B\left(1-\frac{t}{Q^2}\right)-\frac{t}{2M^2}\right\}\widetilde{\mathcal{E}}\right]. \qquad (2.94)$$

This completes the full set of exact results for the electroproduction cross section with exact account for the kinematical power corrections, where the pure BH cross section is given in Ref. [36]. As in the case of DVCS $\mathcal{C}$-coefficients, the kinematical singularities appearing for twist-three and transversity CFFs (partially) cancel also in the interference term, and the expected behavior of the harmonics in the $-t \to -t_{\min}$ limit can be established. Thereby, the CFF combinations

$$\mathcal{H}_{a+}+\frac{t}{4M^2}\mathcal{E}_{a+}, \qquad \widetilde{\mathcal{H}}_{a+}+\frac{t}{4M^2}\widetilde{\mathcal{E}}_{a+},$$
$$\mathcal{H}_{a+}+\frac{x_B\left(1+\frac{t}{Q^2}\right)}{2-x_B+\frac{x_B t}{Q^2}}\widetilde{\mathcal{H}}_{a+}, \qquad \mathcal{E}_{a+}+\frac{x_B\left(1+\frac{t}{Q^2}\right)}{2-x_B+\frac{x_B t}{Q^2}}\widetilde{\mathcal{E}}_{a+}, \qquad (2.95)$$

behave as $\widetilde{K}^{1-a}$. Furthermore, with the map (2.52)–(2.55) the approximated results, given in Ref. [36], are restored. Again, a numerical cross check of our results is performed.

Let us add that the harmonics (2.70)–(2.82) can also be explicitly evaluated as function of the helicity-dependent CFFs. For instance, the exact results for the odd harmonics of an unpolarized target read in the fashion of [36] as follows,

$$s^{\mathcal{I}}_{1,\mathrm{unp}} = \frac{8\widetilde{K}\sqrt{1-y-\frac{y^2\varepsilon^2}{4}}\lambda(2-y)y}{Q(1+\varepsilon^2)^2}\,\mathrm{Im}\,\mathrm{m}\left\{\mathcal{C}'^{\mathcal{I}}_{\mathrm{unp}}\left(\left[\frac{1+\sqrt{1+\varepsilon^2}}{2\left(1+\frac{t}{Q^2}\right)^{-1}}+\varepsilon^2-\frac{x_B t}{Q^2}\right]\mathcal{F}_{++}\right.\right.$$
$$\left.\left.+\left[\frac{1-\sqrt{1+\varepsilon^2}}{2\left(1+\frac{t}{Q^2}\right)^{-1}}+\varepsilon^2-\frac{x_B t}{Q^2}\right]\mathcal{F}_{-+}+\frac{\sqrt{2}\widetilde{K}}{Q}\mathcal{F}_{0+}\right)\right.$$

$$+\Delta\mathcal{S}^{\mathcal{I}}_{1,\mathrm{unp}}\Bigg(\left[\frac{1-\sqrt{1+\varepsilon^2}}{2\left(1+\frac{t}{\mathcal{Q}^2}\right)^{-1}}-\frac{(1-x_{\mathrm{B}})t}{\mathcal{Q}^2}\right]\mathcal{F}_{++}$$
$$+\left[\frac{1+\sqrt{1+\varepsilon^2}}{2\left(1+\frac{t}{\mathcal{Q}^2}\right)^{-1}}-\frac{(1-x_{\mathrm{B}})t}{\mathcal{Q}^2}\right]\mathcal{F}_{-+}-\frac{\sqrt{2}\widetilde{K}}{\mathcal{Q}}\mathcal{F}_{0+}\Bigg)\Bigg\}, \tag{2.96}$$

$$\begin{aligned}s^{\mathcal{I}}_{2,\mathrm{unp}} \;=\; & \frac{16\widetilde{K}^2\left(1-y-\frac{y^2\varepsilon^2}{4}\right)\lambda y}{\mathcal{Q}^2\left(1+\varepsilon^2\right)^2}\,\mathrm{Im}\,\mathrm{m}\Bigg\{\mathcal{C}'^{\mathcal{I}}_{\mathrm{unp}}\Bigg(\frac{1+\frac{x_{\mathrm{B}}t}{\mathcal{Q}^2}+\frac{1}{2}\varepsilon^2\left(1+\frac{t}{\mathcal{Q}^2}\right)}{\sqrt{2}\widetilde{K}\mathcal{Q}^{-1}}\mathcal{F}_{0+}\\ &+\frac{\frac{1}{2}\left(\mathcal{Q}^2-t\right)\varepsilon^2-x_{\mathrm{B}}t}{2\widetilde{K}^2}\sum_{a\in\{1,-1\}}\left[\frac{1-a\sqrt{1+\varepsilon^2}}{2\left(1+\frac{t}{\mathcal{Q}^2}\right)^{-1}}-\frac{(1-x_{\mathrm{B}})t}{\mathcal{Q}^2}\right]\mathcal{F}_{a+}\Bigg)\\ &+\Delta\mathcal{S}^{\mathcal{I}}_{2,\mathrm{unp}}\Bigg(\frac{\mathcal{Q}}{\sqrt{2}\widetilde{K}}\mathcal{F}_{0+}-\frac{\mathcal{Q}^2}{2\widetilde{K}^2}\sum_{a\in\{1,-1\}}\left[\frac{1-a\sqrt{1+\varepsilon^2}}{2\left(1+\frac{t}{\mathcal{Q}^2}\right)^{-1}}-\frac{(1-x_{\mathrm{B}})t}{\mathcal{Q}^2}\right]\mathcal{F}_{a+}\Bigg)\Bigg\},\end{aligned} \tag{2.97}$$

where slightly different $\mathcal{C}$-coefficients and power-suppressed addenda are introduced,

$$\begin{aligned}\mathcal{C}'^{\mathcal{I}}_{\mathrm{unp}}(\mathcal{F}) &= \mathcal{C}^{\mathcal{I}}_{\mathrm{unp}}(\mathcal{F})+\frac{t}{\mathcal{Q}^2}\mathcal{C}^{\mathcal{I},A}_{\mathrm{unp}}(\mathcal{F}),\\ \Delta\mathcal{S}^{\mathcal{I}}_{1,\mathrm{unp}}(\mathcal{F}) &= \frac{2x_{\mathrm{B}}t}{\mathcal{Q}^2}\mathcal{C}^{\mathcal{I},V}_{\mathrm{unp}}(\mathcal{F})+\frac{2(1-x_{\mathrm{B}})t}{\mathcal{Q}^2}\mathcal{C}^{\mathcal{I},A}_{\mathrm{unp}}(\mathcal{F}),\end{aligned}$$

and

$$\begin{aligned}\Delta\mathcal{S}^{\mathcal{I}}_{2,\mathrm{unp}}(\mathcal{F}) \;=\; & -\left(1-\frac{t}{\mathcal{Q}^2}+\frac{2x_{\mathrm{B}}t}{\mathcal{Q}^2}\right)\left[\frac{x_{\mathrm{B}}t}{\mathcal{Q}^2}\mathcal{C}^{\mathcal{I},V}_{\mathrm{unp}}+\frac{(1-x_{\mathrm{B}})t}{\mathcal{Q}^2}\mathcal{C}^{\mathcal{I},A}_{\mathrm{unp}}\right](\mathcal{F})\\ &-\frac{t\left(1+\varepsilon^2\right)}{\mathcal{Q}^2}\left(1+\frac{t}{\mathcal{Q}^2}\right)\mathcal{C}^{\mathcal{I},A}_{\mathrm{unp}}(\mathcal{F}).\end{aligned}$$

The first harmonic (2.96), in particular the term $\widetilde{K}\mathcal{F}_{0+}/\mathcal{Q}$, is free of kinematical singularities. In the hadronic coefficients of the second harmonic (2.97), possible $1/\widetilde{K}^2$ singularities in the hadronic coefficients cancel each other, too, see (2.95). Similar expressions hold true for the even harmonics; however, the addenda will then also depend on the photon-polarization parameter.

2.3 Parametrization of the Compton Tensor

Experimental studies of the Compton effect on the nucleon target have a long history, with theoretical considerations preceding them. The efforts of the past decade focused on deep Euclidean kinematics giving access to partonic constituents of matter, as was pointed about in the previous few sections. Over the years various parametrizations of the hadronic tensor were devised, tailored to the specific needs of observables of interest. The story goes back to Prange [52], who provided a decomposition originally given in terms of bilinear combinations of Dirac spinors and often rewritten by means of two-dimensional Pauli spinors [53]. Another widely used Lorentz-invariant representation was introduced by Tarrach [45] and employed in recent years for consideration of quasi-real kinematics [39], since this decomposition is free from kinematical singularities, on the one hand, and with all hadronic functions of kinematical invariants admitting a well-defined dispersion representation that possesses correct analytical properties [37], on the other. Finally, the developments of the last decade of the formalism of the deeply-virtual Compton scattering were mimicking structures used in the analysis of the forward deep-inelastic scattering, and thus yet another parametrization was devised as a consequence. However, the emerging Lorentz structures were recovered making use of the OPE for the correlation function (2.4) of the quark electromagnetic currents, demonstrating that electromagnetic gauge invariance, broken in the leading twist approximation, can be approximately restored by accounting for twist-three effects. More recently this program was pushed beyond the first-subleading corrections in Ref. [49, 50] by incorporating dynamical effects in the target mass and momentum transfer in the t-channel. Seeking a unified picture for observables used at high and low energies, one will rely on the DVCS set-up for the Compton tensor and construct interpolation between different kinematical limits for CFFs. A gauge-invariant decomposition of the Compton tensor is provided, starting from the analysis of the deeply-virtual regime and

then a set of formulas connecting helicity CFFs (2.13) with the ordinary CFFs admitting a partonic interpretation are supplemented.

2.3.1 A Toy Example

As a pedagogical example, let us first consider a point particle with spin-1/2 as our target. In this case the electromagnetic current (2.57) reduces to $J_\mu = \overline{u}_2 \gamma_\mu u_1$. The Compton matrix element can be then obtained from familiar lowest-order QED diagrams, i.e., the s- and u-channel hand-bag graphs, see Eq. (2.136) below with $F_1 = 1$ and $F_2 = 0$. One can easily verify by means of the Dirac equation that the resulting Compton scattering tensor exactly respects current conservation. To find a representation in which gauge the symmetry is explicitly manifested, the following trick is employed,

$$1 = \frac{\not{p}\not{q} + \not{q}\not{p}}{2\,p\cdot q},$$

which is supplemented by the equations of motion

$$\not{p}\,u_1 = 2M u_1 + \not{\Delta} u_1\,, \qquad \bar{u}_2\,\not{p} = 2M\bar{u}_2 - \bar{u}_2\,\not{\Delta},$$

and subsequent use of the Dirac-matrix algebra. This procedure yields a tensor containing non-flip "transverse" contributions only, as a consequence of the leading-order approximation,

$$\begin{aligned} T^{\text{p.p.}}_{\mu\nu} \;=\; & -\left[g_{\mu\nu} - \frac{q_{1\mu}p_\nu}{p\cdot q} - \frac{q_{2\nu}p_\mu}{p\cdot q} + \frac{q_1\cdot q_2}{p\cdot q}\,\frac{p_\mu p_\nu}{p\cdot q}\right]\frac{q\cdot V_{\text{p.p.}}}{p\cdot q} \\ & -\left[\varepsilon_{\mu\nu q\rho} + \varepsilon_{q\Delta\nu\rho}\left(\frac{q_{2\mu}}{q_1\cdot q_2} - \frac{p_\mu}{2p\cdot q}\right)\right. \\ & \qquad \left. +\varepsilon_{q\Delta\mu\rho}\left(\frac{q_{1\nu}}{q_1\cdot q_2} - \frac{p_\nu}{2p\cdot q}\right)\right]\frac{2q_1\cdot q_2}{q_1^2+q_2^2}\,\frac{A^\rho_{\text{p.p.}}}{p\cdot q}\,. \end{aligned} \tag{2.98}$$

Note that the kinematical pole in the projection operators

$$\frac{q_{1\nu}}{q_1\cdot q_2} - \frac{p_\nu}{2p\cdot q} \quad \text{and} \quad \frac{q_{2\mu}}{q_1\cdot q_2} - \frac{p_\mu}{2p\cdot q},$$

is removed by the overall factor of $q_1 \cdot q_2$ in Eq. (2.98). The vector and axial-vector CFFs in the tensor (2.98) have a very simple form, and read for an on-shell final-state photon:

$$V^{\rho}_{\text{p.p.}} = \bar{u}_2 \gamma^{\rho} u_1 \mathcal{H}^{\text{p.p.}}, \qquad \mathcal{H}^{\text{p.p.}} = \frac{-(2-x_{\text{B}})\mathcal{Q}^2 - x_{\text{B}} t}{2\mathcal{Q}^2} \left[\frac{1}{1-x_{\text{B}}} + \frac{1}{1+\frac{x_{\text{B}} t}{\mathcal{Q}^2}} \right], \tag{2.99}$$

$$A^{\rho}_{\text{p.p.}} = \bar{u}_2 \gamma^{\rho} \gamma_5 u_1 \widetilde{\mathcal{H}}^{\text{p.p.}}, \qquad \widetilde{\mathcal{H}}^{\text{p.p.}} = \frac{-(2-x_{\text{B}})\mathcal{Q}^2 - x_{\text{B}} t}{2\mathcal{Q}^2 \left(1+\frac{t}{\mathcal{Q}^2}\right)} \left[\frac{1}{1-x_{\text{B}}} - \frac{1}{1+\frac{x_{\text{B}} t}{\mathcal{Q}^2}} \right]. \tag{2.100}$$

Here, the CFFs have only two physical poles at $s = M^2$ and $u = M^2$, showing up in our variables at $x_{\text{B}} = 1$ and $x_{\text{B}} = -\mathcal{Q}^2/t$, respectively, and they have the proper symmetry under $s \leftrightarrow u$ exchange. Moreover, these CFFS are free of kinematical singularities, and are related to each other by a multiplicative factor:

$$\widetilde{\mathcal{H}}^{\text{p.p.}} = \frac{x_{\text{B}}}{2 - x_{\text{B}} + \frac{x_{\text{B}} t}{\mathcal{Q}^2}} \mathcal{H}^{\text{p.p.}}, \quad \text{or} \quad \widetilde{\mathcal{H}}^{\text{p.p.}} = \frac{\mathcal{Q}^2}{s-u} \mathcal{H}^{\text{p.p.}}. \tag{2.101}$$

It should be emphasized that even with the definitions (2.99) and (2.100), the form of the hadronic tensor is not uniquely fixed: rather by means of the Dirac equation and the relation (2.101), one can find different out, however, equivalent forms of the Compton scattering tensor. On the other hand, if a frame of reference is chosen, the helicity amplitudes (2.13) are independent of any parametrization ambiguities. However, it is important to note that the relation between these helicity CFFs and "partonic" CFFs does heavily depend on the chosen tensor decomposition.

Let us employ our parametrization of the helicity-dependent CFFs (2.14)–(2.15), used for evaluation of the differential cross sections in the preceding section, where the projection of the (axial-) vector CFFs with the averaged photon momentum $m_\mu = q_\mu / q \cdot p$ is adopted. These CFFs can be straightforwardly computed from the original tree diagrams. Alternatively, one may stick to the (axial-)vector CFFs (2.99) and (2.100) and compute the helicity amplitudes starting from Eq. (2.98). This is the route that is chosen in the realistic case of composite target below. The result of this analysis can be summarized in

the following set of helicity CFFs,

$$\mathcal{H}^{\rm p.p.}_{+b} = \left[\frac{1+b\sqrt{1+\varepsilon^2}}{2\sqrt{1+\varepsilon^2}} + \frac{(1-x_{\rm B})\left(1+\frac{t}{\mathcal{Q}^2}\right)\varepsilon^2 - \left(2-x_{\rm B}+\frac{x_{\rm B}t}{\mathcal{Q}^2}\right)\frac{x_{\rm B}^2 t}{\mathcal{Q}^2}}{\sqrt{1+\varepsilon^2}\left(2-x_{\rm B}+\frac{x_{\rm B}t}{\mathcal{Q}^2}\right)^2}\right]\mathcal{H}^{\rm p.p.}\,, \quad (2.102)$$

$$\mathcal{E}^{\rm p.p.}_{+b} = \frac{\varepsilon^2\left(1+\frac{t}{\mathcal{Q}^2}-2(1-x_{\rm B})\frac{t}{\mathcal{Q}^2}\right)}{\sqrt{1+\varepsilon^2}\left(2-x_{\rm B}+\frac{x_{\rm B}t}{\mathcal{Q}^2}\right)^2}\mathcal{H}^{\rm p.p.}\,, \quad (2.103)$$

$$\widetilde{\mathcal{H}}^{\rm p.p.}_{+b} = \left[\frac{1+b\sqrt{1+\varepsilon^2}}{2\sqrt{1+\varepsilon^2}}\left(1-\frac{t}{\mathcal{Q}^2}\right)+\frac{1}{\sqrt{1+\varepsilon^2}}\frac{x_{\rm B}t}{\mathcal{Q}^2}\right]\widetilde{\mathcal{H}}^{\rm p.p.}\,, \quad (2.104)$$

$$\widetilde{\mathcal{E}}^{\rm p.p.}_{+b} = \frac{4M^2}{\mathcal{Q}^2}\left[\frac{1+b\sqrt{1+\varepsilon^2}}{2\sqrt{1+\varepsilon^2}}\left(3+\frac{t}{\mathcal{Q}^2}\right)-\frac{1+(1-x_{\rm B})\frac{t}{\mathcal{Q}^2}}{\sqrt{1+\varepsilon^2}}\right]\widetilde{\mathcal{H}}^{\rm p.p.}\,, \quad (2.105)$$

$$\mathcal{H}^{\rm p.p.}_{0+} = -\frac{\sqrt{2}x_{\rm B}\widetilde{K}\left(2-x_{\rm B}+\frac{x_{\rm B}t}{\mathcal{Q}^2}-2\varepsilon^2\right)}{\mathcal{Q}\sqrt{1+\varepsilon^2}\left(2-x_{\rm B}+\frac{x_{\rm B}t}{\mathcal{Q}^2}\right)^2}\mathcal{H}^{\rm p.p.}\,, \quad (2.106)$$

$$\mathcal{E}^{\rm p.p.}_{0+} = \frac{2\sqrt{2}\varepsilon^2\widetilde{K}}{\mathcal{Q}\sqrt{1+\varepsilon^2}\left(2-x_{\rm B}+\frac{x_{\rm B}t}{\mathcal{Q}^2}\right)^2}\mathcal{H}^{\rm p.p.}\,, \quad (2.107)$$

$$\widetilde{\mathcal{H}}^{\rm p.p.}_{0+} = \frac{\sqrt{2}\widetilde{K}}{\mathcal{Q}\sqrt{1+\varepsilon^2}}\widetilde{\mathcal{H}}^{\rm p.p.}\,, \quad (2.108)$$

$$\widetilde{\mathcal{E}}^{\rm p.p.}_{0+} = \frac{4M^2}{\mathcal{Q}^2}\frac{\sqrt{2}\widetilde{K}}{\mathcal{Q}\sqrt{1+\varepsilon^2}}\widetilde{\mathcal{H}}^{\rm p.p.}\,. \quad (2.109)$$

Several comments are in order. As observed in GPD calculations in the twist-three sector, see Eqs. (84)–(87) in Ref. [36], the CFFs in the vector and axial-vector sector mix with each other, while in our analysis of a point particle, these admixtures are eliminated by utilizing the relation (2.101). Notice that the longitudinal and transverse spin-flip CFFs are power suppressed in the DVCS kinematics. The longitudinal-to-transverse helicity-flip CFFs (2.106) and (2.108) have the anticipated kinematical $\widetilde{K}$-factor in front of them. The transverse-to-transverse helicity-flip CFFs also do not possess any kinematical singularities but do not have the anticipated kinematical $\widetilde{K}^2$ factor in front of them, i.e., they do also not vanish at the kinematical boundary $t = t_{\rm min}$. Hence, if one chooses to switch to the definitions such as (2.19), spurious kinematical $1/\widetilde{K}^2$ singularities appear in expressions for transversity CFFs, see also the map (2.52)–(2.55) of such CFFs. Obviously, such spurious

kinematical singularities can be simply pulled out by a redefinition of transversity CFFs and then they trivially will not appear in cross section expressions. Plugging in our point-particle results (2.102)–(2.109) in the expression for the higher harmonics in the Fourier expansion, given in Sect. 2.2.2 and 2.2.3, one realizes that they vanish in the kinematical limit $t \to t_{\rm min}$ as expected. The basis of helicity dependent CFFs in which this behavior is explicit will be given in the next paragraph.

The helicity dependent CFFs associated with the so-called Born term for the Compton scattering off the nucleon (2.136) are also computed, see Eqs. (A.62)–(A.69) in the Appendix A.5. Again it was observed that the unpolarized and transverse-to-transverse spin-flip CFFs are free of kinematical singularities, however, certain longitudinal-to-transverse CFFs are suffering now from $1/\widetilde{K}$ poles in the representation of Ref. [36]. The absence of such spurious singularities can be made transparent by switching to the electric-like[9] combinations of CFFs

$$\mathcal{G}_{0b} = \mathcal{H}_{0b} + \frac{t}{4M^2}\mathcal{E}_{0b} \quad \text{and} \quad \widetilde{\mathcal{G}}_{0b} = \widetilde{\mathcal{H}}_{0b} + \frac{t}{4M^2}\widetilde{\mathcal{E}}_{0b}\,, \tag{2.110}$$

where $\mathcal{G}_{0b}$ and $\widetilde{\mathcal{G}}_{0b}$ are proportional to the desired kinematical factor $\widetilde{K}$, see expressions in Appendix A.5. For transverse helicity-flip CFFs it was found that $\mathcal{G}_{-+}$ and $\widetilde{\mathcal{G}}_{-+}$ are now proportional to $t - t_{\rm min}$ (not explicitly shown). The redefinitions (2.110) reparametrize the (axial-)vector matrix elements (2.14), (2.15) as follows:

$$\mathcal{V}(\mathcal{F}_{ab}) = \frac{1}{p\cdot q}\bar{u}_2\left(\not{q}\,\mathcal{G}_{ab} + \left[i\sigma_{\rho\sigma}\frac{q^\rho\Delta^\sigma}{2M} - \not{q}\,\frac{t}{4M^2}\right]\mathcal{E}_{ab}\right)u_1 \tag{2.111}$$

$$\mathcal{A}(\mathcal{F}_{ab}) = \frac{1}{p\cdot q}\bar{u}_2\left(\not{q}\,\gamma_5\,\widetilde{\mathcal{G}}_{ab} + \left[\gamma_5\frac{q\cdot\Delta}{2M} - \not{q}\,\gamma_5\,\frac{t}{4M^2}\right]\widetilde{\mathcal{E}}_{ab}\right)u_1\,. \tag{2.112}$$

It can be verified that the new nucleon helicity structures, proportional to $\mathcal{E}_{ab}$ or $\widetilde{\mathcal{E}}_{ab}$, will yield a kinematical factor $\widetilde{K}^2$ in the hadronic $\mathcal{C}$ coefficients of both the squared VCS and interference term. Hence, this guarantees that higher harmonics vanish in the limit $t \to t_{\rm min}$

[9] By analogy with the electric nucleon form factor.

as they should and, moreover, this factor can be reshuffled to yield a redefinition

$$\widetilde{K}^2\mathcal{E}_{0b} \quad \to \quad \mathcal{E}_{0b} \quad \text{and} \quad \widetilde{K}^2\widetilde{\mathcal{E}}_{0b} \quad \to \quad \widetilde{\mathcal{E}}_{0b}\,.$$

This guarantees that the new longitudinal helicity-flip amplitudes have the anticipated $\widetilde{K}$ factor as an overall factor, on the one hand, and that they are free of kinematical singularities, on the other. The corresponding modifications in Fourier coefficients $\mathcal{C}$ are straightforward and do not require any further comments.

2.3.2 Constructing Compton Scattering Tensor

To devise a general parametrization as was advertised above, one starts with the Compton scattering process off the nucleon for the case when both photons possess large virtualities, such that the hard scale is set by the Euclidean virtuality $Q^2 = -q^2$ with q_μ, defined in Eq. (2.11). As $Q^2 \to \infty$, the decoherence of the short- and long-range interactions allows one to probe partonic content of the nucleon via collinear factorization. This approach naturally introduces a pair of the light-cone vectors n_μ and n^*_μ, such that $n\cdot n = n^*\cdot n^* = 0$ and $n\cdot n^* = 1$, since partons propagate along the light cone. However, these cannot be fixed uniquely in terms of the external momenta of the process. Restricting to the leading terms in the $1/Q$-expansion, i.e., the so-called twist-two approximation, the result for the Compton scattering tensor is cast in the following form[10]

$$T_{\mu\nu} = -g^\perp_{\mu\nu}\, n\cdot V_{\rm T} - i\varepsilon^\perp_{\mu\nu}\, n\cdot A_{\rm T} + \left(\frac{q_2^2}{n^*\cdot q}\, n^*_\mu - q_{2\mu}\right)\left(\frac{q_1^2}{n^*\cdot q}\, n^*_\nu - q_{1\nu}\right) n\cdot V_{\rm L} + \tau^\perp_{\mu\nu;\rho\sigma}\,\frac{\Delta^\rho T^\sigma}{M^2}\,. \tag{2.113}$$

Here the first two terms on the r.h.s. were computed in numerous papers (in particular for DVCS kinematics). The third term after the equal sign contains a purely longitudinal part and appears at next-to-leading order in QCD coupling [54], mimicking the violation of the

[10]Notice that the T label used here does not have anything to do with the T-subscript adopted earlier to label the transversity CFFs in Eqs. (2.52)–(2.55), as well as (2.122) below.

Callan-Gross relation in deep-inelastic scattering. The fourth term stems from the double photon-helicity flip and is perturbatively induced at one-loop by the gluon transversity GPDs [30]. The projection on the leading-twist structures in Eq. (2.113) is achieved by the means of the tensors

$$g^{\perp}_{\mu\nu} = g_{\mu\nu} - n_\mu n^*_\nu - n_\nu n^*_\mu\,, \;\; \varepsilon^{\perp}_{\mu\nu} = \varepsilon_{\mu\nu-+}\,,$$
$$\tau^{\perp}_{\mu\nu;\rho\sigma} = \frac{1}{2}\left[g^{\perp}_{\mu\rho}g^{\perp}_{\nu\sigma} + g^{\perp}_{\mu\sigma}g^{\perp}_{\nu\rho} - g^{\perp}_{\mu\nu}g^{\perp}_{\rho\sigma}\right]. \tag{2.114}$$

The vector $V^\rho_{\rm T}$ ($V^\rho_{\rm L}$) and the axial-vector $A^\rho_{\rm T}$ CFFs describe transition amplitudes when the transverse (longitudinal) photon helicity is (nearly) conserved, while T^ρ is associated with the aforementioned transverse photon helicity-flip contribution. As a consequence of the leading-twist approximation, eight longitudinal–to–transverse and transverse–to–longitudinal photon helicity-flip amplitudes are absent and, moreover, the Compton scattering tensor (2.113) respects current conservation only to leading order in $1/Q$. However, once one goes beyond the twist-two approximation in the OPE analysis of the hadronic tensor, these missing amplitudes emerge and moreover, making use of QCD equations of motions, the electromagnetic current conservation gets restored up to the same accuracy. Thus the ambiguity in the construction of the Lorentz tensors is pushed up to the next order in the $1/Q^2$ expansion.

Since it is advantageous to stay as close as possible to the VCS tensor decomposed in terms of Lorentz structures that have a simple limit in the deeply virtual regime, below a parametrization motivated by Eq. (2.113) is proposed that can also be used for quasi-real (or real) photons without encountering kinematical singularities. Thereby, the following natural requirements are imposed:

- manifest current conservation and Bose symmetry;
- a close match with conventions used in deeply virtual Compton kinematics;

- singularity-free kinematical dependence.

Instead of the light-cone vectors, the external particle vectors are employed in the construction of the tensors. To make the tensors dimensionless, the scalar product used is $p\cdot q=(s-u)/2$, proportional to the positive energy variable ν, in denominators. Equipped with the above conditions and building blocks, the transverse metric tensor entering the leading-twist parametrization, which received corrections from the twist-three effects mentioned above, gets promoted to the following expression:

$$g^{\perp}_{\mu\nu} \;\to\; \widetilde{g}_{\mu\nu}=g_{\mu\nu}-\frac{q_{1\mu}p_\nu}{p\cdot q}-\frac{q_{2\nu}p_\mu}{p\cdot q}+\frac{q_1\cdot q_2}{p\cdot q}\,\frac{p_\mu p_\nu}{p\cdot q}\,, \tag{2.115}$$

where the twist-four component $p_\mu p_\nu$ follows from the expansion of $g^{\perp}_{\mu\nu}$. This tensor already appeared in our toy example (2.98) and its gauge invariance is easily verified by making use of the relations

$$p\cdot q_i=p\cdot q \quad \text{since} \quad q_1^\nu=q^\nu+\Delta^\nu/2 \;\text{ and }\; q_2^\mu=q^\mu-\Delta^\mu/2 \quad \text{with} \quad p\cdot\Delta=0\,.$$

Going to the Breit frame, where the transverse momentum is entirely carried by the nucleons, i.e., $p_2^\perp=-p_1^\perp$ and $q_i^\perp=0$, one realizes that the gauge-invariant tensor (2.115) projects onto photons with the same transverse helicity, having even parity in the t-channel. The counterpart of this contribution, having t-channel odd parity, is expressed in terms of the Levi-Civita tensor that generalizes the above $\varepsilon^{\perp}_{\mu\nu}$ beyond leading twist,

$$\varepsilon^{\perp}_{\mu\nu} \;\to\; \widetilde{\varepsilon}_{\mu\nu}=\frac{1}{p\cdot q}\left[\varepsilon_{\mu\nu pq}+\frac{p_\mu}{2\,p\cdot q}\varepsilon_{\Delta\nu pq}-\varepsilon_{\mu\Delta pq}\,\frac{p_\nu}{2\,p\cdot q}+\varepsilon_{\mu\nu\Delta q}\,\frac{p\cdot p}{2\,p\cdot q}\right]. \tag{2.116}$$

Here, for later convenience a power-suppressed $p\cdot p/p\cdot q$-term is added, which respects current conservation by itself. The coupling of longitudinal and transverse photon-helicity states may be naturally encoded in terms of the following tensor structures:

$$\left(q_{2\mu}-\frac{q_2^2}{p\cdot q}p_\mu\right)\left(g_{\nu\rho}-\frac{p_\nu\,q_1^\rho}{p\cdot q}\right) \quad \text{and} \quad \left(q_{1\nu}-\frac{q_1^2}{p\cdot q}p_\nu\right)\left(g_{\mu\rho}-\frac{p_\mu\,q_2^\rho}{p\cdot q}\right),$$

which are to be contracted with vector CFFs. Here the projectors, satisfying the relations

$$\left(g^{\mu\rho}-\frac{p^\mu q_2^\rho}{p\cdot q}\right)p_\rho=0\,,\qquad\qquad \left(g^{\nu\rho}-\frac{p^\nu q_1^\rho}{p\cdot q}\right)p_\rho=0\,, \tag{2.117}$$

$$\left(g^{\mu\rho}-\frac{p^\mu q_2^\rho}{p\cdot q}\right)\Delta_\rho=\Delta_\perp^\mu+\frac{t}{2p\cdot q}p^\mu\,,\qquad \left(g^{\nu\rho}-\frac{p^\nu q_1^\rho}{p\cdot q}\right)\Delta_\rho=\Delta_\perp^\nu-\frac{t}{2p\cdot q}p^\nu\,,$$

where $\Delta_\perp^\rho=\Delta^\rho-\eta\,p^\rho$, ensure electromagnetic gauge invariance. Notice that in the above tensors the longitudinal components were chosen in the form[11],

$$q_{2\mu}-\frac{q_2^2}{p\cdot q}p_\mu\quad\text{and}\quad q_{1\nu}-\frac{q_1^2}{p\cdot q}p_\nu\,.$$

Obviously, they do not contribute in the real photon limit. Last but not least, the current conservation in the transverse helicity-flip amplitudes can be implemented by utilizing the transverse projectors (2.117), yielding the substitution

$$\tau^\perp_{\mu\nu;\rho\sigma}\frac{\Delta^\rho T^\sigma}{M^2}\;\to\;\left(g_\mu{}^\alpha-\frac{p_\mu q_2^\alpha}{p\cdot q}\right)\left(g_\nu{}^\beta-\frac{p_\nu q_1^\beta}{p\cdot q}\right)\tau^\perp_{\alpha\beta;\rho\sigma}\frac{\Delta^\rho T^\sigma}{M^2}\,. \tag{2.118}$$

It is important to realize that a different choice of dual light-cone vectors will result in a parameterization, where the kinematically suppressed effects will be incorporated in a different fashion, see discussions in Ref. [46].

By analogy with the hadronic electromagnetic current, decomposed in terms of the Dirac bilinears accompanied by Dirac and Pauli form factors (2.57), a similar representation for the VCS in CFFs is now introduced, expanded in terms of the longitudinal and transverse components. To generalize the first three terms in the r.h.s. of Eq. (2.113) to the setup incorporating the exact kinematics, one replaces the light-cone vector n, projecting out the (axial-)vector CFFs by the average photon momentum q, whose leading component is indeed n, but it also encodes subleading-twist effects as well. Then the following expansion is used

$$V_i^\rho\;=\;\bar u_2\left(\frac{p^\rho}{p\cdot q}\left[\not q\,\mathcal{H}+i\sigma_{\alpha\beta}\,\frac{q^\alpha\Delta^\beta}{2M}\,\mathcal{E}\right]+\frac{\Delta_\perp^\rho}{p\cdot q}\left[\not q\,\mathcal{H}_i+i\sigma_{\alpha\beta}\,\frac{q^\alpha\Delta^\beta}{2M}\,\mathcal{E}_i\right]\right)u_1\,,$$

[11] In previous studies on the subject, the longitudinal pieces in terms of $q_{1\mu}-q_1\cdot q_2\,p_\mu/p\cdot q$ are written and $q_{2\nu}-q_1\cdot q_2\,p_\nu/p\cdot q$, which to twist-three accuracy can be replaced by the vectors that are displayed above.

$$A_i^\rho \;=\; \bar{u}_2\left(\frac{p^\rho}{p\cdot q}\left[\not{q}\gamma_5\,\widetilde{\mathcal{H}}+\frac{\Delta\cdot q}{2M}\gamma_5\,\widetilde{\mathcal{E}}\right]+\frac{\Delta_\perp^\rho}{p\cdot q}\left[\not{q}\gamma_5\,\widetilde{\mathcal{H}}_i+\frac{q\cdot\Delta}{2M}\gamma_5\,\widetilde{\mathcal{E}}_i\right]\right)u_1\,, \tag{2.120}$$

with the subscript i standing for $i\in\{\mathrm{T},\mathrm{L}\}$. The same expansion can be adopted for the $i\in\{\mathrm{LT},\mathrm{TL}\}$ cases. However, for these, the component proportional to p^ρ will not contribute to the VCS and can be ignored, while the transverse part is approximatly expressible in terms of twist-three CFFs introduced earlier, namely,

$$\mathcal{F}_{\mathrm{LT}}\overset{\mathrm{tw}-3}{=}\mathcal{F}_+^3-\mathcal{F}_-^3\,,\qquad \mathcal{F}_{\mathrm{TL}}\overset{\mathrm{tw}-3}{=}\mathcal{F}_+^3+\mathcal{F}_-^3\,. \tag{2.121}$$

To write the transversity CFFs in the same form, let us recall the following facts about the amplitude T_ρ entering the leading-twist DVCS tensor (2.113). It is parametrized by four transverse photon helicity-flip amplitudes [36] according to the suggestion of [51] as follows:

$$\begin{aligned}T_\sigma \;=\; \bar{u}_2\Bigg[&i\sigma_{\alpha\sigma}\frac{q^\alpha}{p\cdot q}\mathcal{H}_T^{[51]}+\frac{\Delta_{\perp\sigma}}{2M^2}\widetilde{\mathcal{H}}_T^{[51]}+\frac{1}{2M}\left(\frac{\not{q}}{p\cdot q}\Delta_\sigma-\frac{\Delta\cdot q}{p\cdot q}\gamma_\sigma\right)\mathcal{E}_T^{[51]}\\&+\frac{\not{q}p_\sigma-\gamma_\sigma p\cdot q}{2Mp\cdot q}\widetilde{\mathcal{E}}_T^{[51]}\Bigg]u_1\,.\end{aligned} \tag{2.122}$$

However, this can be represented analogously to Eqs. (2.119) and (2.120) in terms of two parity-even and -odd Dirac bilinears,

$$V_{\mathrm{TT}}^\rho=\frac{p^\rho}{p\cdot q}\bar{u}_2\left[\not{q}\,\mathcal{H}_T+i\sigma_{\alpha\beta}\,\frac{q^\alpha\Delta^\beta}{2M}\,\mathcal{E}_T\right]u_1\,, \tag{2.123}$$

$$A_{\mathrm{TT}}^\rho=\frac{p^\rho}{p\cdot q}\bar{u}_2\left[\not{q}\gamma_5\,\widetilde{\mathcal{H}}_T+\frac{\Delta\cdot q}{2M}\gamma_5\,\widetilde{\mathcal{E}}_T\right]u_1\,, \tag{2.124}$$

that are proportional to $\Delta_\sigma^\perp$ and $\widetilde{\Delta}_\sigma^\perp=\varepsilon_{\sigma\Delta pq}/p\cdot q$, respectively,

$$T_\rho\big(\mathcal{F}_T^{[51]}\big)=\Delta_\rho^\perp\,\frac{q\cdot V_{\mathrm{TT}}(\mathcal{F}_T)}{p\cdot q}+i\widetilde{\Delta}_\rho^\perp\,\frac{q\cdot A_{\mathrm{TT}}(\mathcal{F}_T)}{p\cdot q}+\mathcal{O}(1/Q^2)\,, \tag{2.125}$$

where $\widetilde{\Delta}_\mu^\perp$ is transverse with respect to both photon momenta q_1 and q_2. The relation among the two sets of CFFs, introduced in Eq. (2.122) and Eqs. (2.123), (2.124), respectively, is found to be

$$\mathcal{H}_T\;=\;\mathcal{H}_T^{[51]}+\mathcal{E}_T^{[51]}+2\widetilde{\mathcal{H}}_T^{[51]}$$

$$-\frac{t}{t+(4M^2-t)\left(\eta^2+\xi^2\frac{t}{Q^2}\right)}\left[(1-\eta^2)\mathcal{H}_T^{[51]}-\eta^2\mathcal{E}_{\rm T}^{[51]}-\eta\widetilde{\mathcal{E}}_T^{[51]}\right], \quad (2.126)$$

$$\mathcal{E}_T = -2\widetilde{\mathcal{H}}_T^{[51]} + \frac{4M^2}{t+(4M^2-t)\left(\eta^2+\xi^2\frac{t}{Q^2}\right)}\left[(1-\eta^2)\mathcal{H}_T^{[51]}-\eta^2\mathcal{E}_T^{[51]}-\eta\widetilde{\mathcal{E}}_T^{[51]}\right], \quad (2.127)$$

$$\widetilde{\mathcal{H}}_T = \frac{4M^2}{t+(4M^2-t)\left(\eta^2+\xi^2\frac{t}{Q^2}\right)}\left[\eta\mathcal{H}_T^{[51]}+\frac{\eta\, t}{4M^2}\mathcal{E}_T^{[51]}+\frac{t}{4M^2}\widetilde{\mathcal{E}}_T^{[51]}\right], \quad (2.128)$$

$$\widetilde{\mathcal{E}}_T = \frac{4M^2}{\eta\, t}\mathcal{H}_T^{[51]} - \frac{4M^2}{t+(4M^2-t)\left(\eta^2+\xi^2\frac{t}{Q^2}\right)}\left[\eta\,\frac{4M^2}{t}\mathcal{H}_T^{[51]}+\eta\mathcal{E}_T^{[51]}+\widetilde{\mathcal{E}}_T^{[51]}\right], \quad (2.129)$$

which reduce in the real photon case $q_2^2=0$ to Eqs. (2.126)–(2.129). Notice that the convenience of the representation (2.125) had forced us to introduce kinematical singularities into the transverse CFFs. These are exhibited in the VCS kinematics as poles in $t-t_{\rm min}$,

$$t+(4M^2-t)\left(\eta^2+\xi^2\frac{t}{Q^2}\right) = -\frac{4\widetilde{K}^2}{(2-x_{\rm B}+\frac{x_{\rm B}t}{Q^2})^2} \propto (t-t_{\rm min}).$$

Since in the helicity amplitudes the transversity CFFs are multiplied with $\widetilde{K}^2$, these poles will be canceled and, moreover, if changes are made in the expressions for the cross section back to the basis of Ref. [51], one will find in the transversity sector the CFFs are appropriately accompanied by a factor of $\widetilde{K}^2$, so that Fourier harmonics possess the expected behavior in the $t\to t_{\rm min}$ limit, see discussion in Sect. 2.2.2.

Having defined the tensor structures and the corresponding CFFs, now it is time to write down the complete Compton scattering tensor:

$$T_{\mu\nu} = -\widetilde{g}_{\mu\nu}\frac{q\cdot V_{\rm T}}{p\cdot q}+i\widetilde{\varepsilon}_{\mu\nu}\frac{q\cdot A_{\rm T}}{p\cdot q}+\left(q_{2\mu}-\frac{q_2^2}{p\cdot q}p_\mu\right)\left(q_{1\nu}-\frac{q_1^2}{p\cdot q}p_\nu\right)\frac{q\cdot V_{\rm L}}{p\cdot q} + \left(q_{1\nu}-\frac{q_1^2}{p\cdot q}p_\nu\right)\left(g_{\mu\rho}-\frac{p_\mu\, q_{2\rho}}{p\cdot q}\right)\left[\frac{V_{\rm LT}^\rho}{p\cdot q}+\frac{i\varepsilon^\rho{}_{qp\sigma}}{p\cdot q}\frac{A_{\rm LT}^\sigma}{p\cdot q}\right]$$

$$
\begin{aligned}
&+\left(q_{2\mu}-\frac{q_2^2}{p\cdot q}p_\mu\right)\left(g_{\nu\rho}-\frac{p_\nu q_{1\rho}}{p\cdot q}\right)\left[\frac{V_{\rm TL}^\rho}{p\cdot q}+\frac{i\varepsilon^\rho{}_{qp\sigma}}{p\cdot q}\frac{A_{\rm TL}^\sigma}{p\cdot q}\right]\\
&+\left(g_\mu{}^\rho-\frac{p_\mu q_2^\rho}{p\cdot q}\right)\left(g_\nu{}^\sigma-\frac{p_\nu q_1^\sigma}{p\cdot q}\right)\left[\frac{\Delta_\rho\Delta_\sigma+\widetilde{\Delta}_\rho^\perp\widetilde{\Delta}_\sigma^\perp}{2M^2}\frac{q\cdot V_{\rm TT}}{p\cdot q}\right.\\
&\qquad\left.+\frac{\Delta_\rho\widetilde{\Delta}_\sigma^\perp+\widetilde{\Delta}_\rho^\perp\Delta_\sigma}{2M^2}\frac{q\cdot A_{\rm TT}}{p\cdot q}\right],
\end{aligned}
\tag{2.130}
$$

where electromagnetic gauge invariance is implemented exactly. From our exact parameterization of the tensor (2.130), the helicity-dependent CFFs $\mathcal{F}_{ab}$ used in Sect. 2.2.2 and 2.2.3 can now be found for the evaluation of the cross sections in the target rest frame. Comparing Eq. (2.13) with (2.130) projected onto the photon polarization vectors, the following expressions are obtained,

$$
\begin{aligned}
\mathcal{F}_{+b} \;=\;& \left[\frac{1+b\sqrt{1+\varepsilon^2}}{2\sqrt{1+\varepsilon^2}}+\frac{(1-x_{\rm B})x_{\rm B}^2(4M^2-t)\left(1+\frac{t}{\mathcal{Q}^2}\right)}{\mathcal{Q}^2\sqrt{1+\varepsilon^2}\left(2-x_{\rm B}+\frac{x_{\rm B}t}{\mathcal{Q}^2}\right)^2}\right]\mathcal{F}_{\rm T}\\
&+\frac{1-b\sqrt{1+\varepsilon^2}}{2\sqrt{1+\varepsilon^2}}\frac{2\widetilde{K}^2}{M^2\left(2-x_{\rm B}+\frac{x_{\rm B}t}{\mathcal{Q}^2}\right)^2}\mathcal{F}_{\rm TT}\\
&+\frac{4x_{\rm B}^2\widetilde{K}^2}{\mathcal{Q}^2\sqrt{1+\varepsilon^2}\left(2-x_{\rm B}+\frac{x_{\rm B}t}{\mathcal{Q}^2}\right)^3}\mathcal{F}_{\rm LT},
\end{aligned}
\tag{2.131}
$$

$$
\begin{aligned}
\mathcal{F}_{0+} \;=\;& \frac{(-1)\sqrt{2}\,\widetilde{K}}{\sqrt{1+\varepsilon^2}\mathcal{Q}\left(2-x_{\rm B}+\frac{x_{\rm B}t}{\mathcal{Q}^2}\right)}\left\{\frac{2x_{\rm B}}{2-x_{\rm B}+\frac{x_{\rm B}t}{\mathcal{Q}^2}}\left[1+\frac{2x_{\rm B}^2\left(4M^2-t\right)}{\mathcal{Q}^2\left(2-x_{\rm B}+\frac{x_{\rm B}t}{\mathcal{Q}^2}\right)}\right]\mathcal{F}_{\rm LT}\right.\\
&\left.+x_{\rm B}\left[1+\frac{2x_{\rm B}(4M^2-t)}{\mathcal{Q}^2\left(2-x_{\rm B}+\frac{x_{\rm B}t}{\mathcal{Q}^2}\right)}\right]\mathcal{F}_{\rm T}+\frac{4x_{\rm B}^2M^2-\left(2x_{\rm B}+\varepsilon^2\right)t}{2M^2\left(2-x_{\rm B}+\frac{x_{\rm B}t}{\mathcal{Q}^2}\right)}\mathcal{F}_{\rm TT}\right\},
\end{aligned}
\tag{2.132}
$$

where $b=\pm1$ is the helicity of the real photon. Notice that the longitudinal helicity-flip CFFs (2.132) are proportional to the kinematical factor $\widetilde{K}$. Moreover, the transverse photon helicity-flip CFFs (2.131) with $b=-1$ are mostly proportional to $\widetilde{K}^2$, except for the term

$$
\frac{t_{\rm min}-t}{\mathcal{Q}^2}\,\frac{1+\sqrt{1+\varepsilon^2}-2x_{\rm B}}{2\left(2-x_{\rm B}+\frac{x_{\rm B}t}{\mathcal{Q}^2}\right)^2}\left[4(1-x_{\rm B})\frac{1-\sqrt{1+\varepsilon^2}}{2\sqrt{1+\varepsilon^2}}+\frac{\left(1+\frac{t}{\mathcal{Q}^2}\right)x_{\rm B}^2}{\sqrt{1+\varepsilon^2}}\right]
$$

$$= \frac{1-\sqrt{1+\varepsilon^2}}{2\sqrt{1+\varepsilon^2}} + \frac{(1-x_{\rm B})x_{\rm B}^2(4M^2-t)\left(1+\frac{t}{\mathcal{Q}^2}\right)}{\mathcal{Q}^2\sqrt{1+\varepsilon^2}\left(2-x_{\rm B}+\frac{x_{\rm B}t}{\mathcal{Q}^2}\right)^2}, \tag{2.133}$$

which is proportional to $t_{\rm min}-t$. Here, the r.h.s. of this relation may also be written as $\widetilde{K}^2/(t-t_{\rm max})$, see Eq. (2.8). It should also be pointed out that the transformations (2.131),(2.132) exist in the limit $s \to M^2$ or $u \to M^2$. In the simultaneous limit, where $(2-x_{\rm B}+x_{\rm B}t/\mathcal{Q}^2) \propto (s-u)$ vanishes, $1/(s-u)$ singularities appear that are associated with the longitudinal helicity-flip CFFs. This artifact may appear as an obstacle only in the low-energy expansion and can be overcome in a straightforward manner, either by removing this singularity by a simple reparametrization of the VCS tensor (2.130), e.g., $\mathcal{F}_{\rm LT} \to (p\cdot q/M^2)\mathcal{F}_{\rm LT}$, or be regarded as a constraint for the low energy behavior of its CFFs.

For completeness, in Appendix A.3 the form of the helicity transitions for the hadronic tensor parametrization introduced by Tarrach [45] are quoted. The latter does not suffer from kinematical singularities as well, and it will be used in the next section in the low-energy expansion. Thereby, it was found that with the CFF basis (2.110)–(2.112) the map is singularity-free for any values of kinematical variables, i.e., as for Born amplitudes the "electric" longitudinal helicity-flip CFFs are proportional to the kinematical factor $\widetilde{K}$, as one can read off from explicit formulae (A.31)–(A.42), while the $1/\widetilde{K}$- behavior of the remaining functions can be absorbed by their rescaling, as suggested in the preceding section. An analogous structure holds for the map of the transverse helicity-flip amplitudes [not explicitly shown in Eqs. (A.43)–(A.54)], where again the "electric" combination of CFFs is always anticipated with a factor $t-t_{\rm min}$.

2.4 Generalized Polarizabilities and Low-Energy Expansion

Having discussed at length the deeply-virtual regime that gives access to GPDs and provides a set of observables that exactly account for kinematically suppressed effects, let us turn to the opposite limit when the incoming photon becomes quasi-real or even real. In fact the formalism presented in the previous sections can also be utilized in these cases as well. In doing so, one sets $x_{\mathrm{B}} = \mathcal{Q}^2/(s+\mathcal{Q}^2-M^2)$ as the limit $\mathcal{Q}^2 \to 0$ is taken where $s=(p_1+q_1)^2$ is the center-of-mass energy in the real Compton scattering process. Obviously, the Bjorken and the ε variables vanish as $\mathcal{Q}^2$ tends to zero, while the $\widetilde{K}$-factor takes the value

$$\lim_{\mathcal{Q}^2\to 0} \widetilde{K} = \sqrt{-t\left(1+\frac{t\,s}{(s-M^2)^2}\right)}.$$

To start with, it is easy to verify that for a point-like particle the longitudinal spin-flip CFFs $\mathcal{H}_{0+}$, $\mathcal{E}_{0+}$, $\widetilde{\mathcal{H}}_{0+}$ and the combination $E_{0+} = (\Delta\cdot q/p\cdot q)\,\widetilde{\mathcal{E}}_{0+} \propto \mathcal{Q}^2\widetilde{\mathcal{E}}_{0+}$ entering the $\mathcal{C}$-coefficients all vanish as $\mathcal{Q}^2 \to 0$. The real-photon limit also exists for the remaining eight transverse-helicity CFFs, where $\overline{\mathcal{E}}_{\pm+}$ vanish. Thus, as is known, six amplitudes remain for real Compton scattering. No further peculiarities arise in the squared DVCS amplitudes presented in Sect. 2.2.2, and thus they can be used in a straightforward fashion to recover, e.g., the Klein-Nishina formula and its extension to a polarized point-like target from the helicity-dependent CFFs (2.102)–(2.109),

$$\begin{aligned}\frac{d^2\sigma}{d\cos(\theta_{\gamma\gamma})d\varphi} = \frac{R^2}{2}\left(\frac{\omega'}{\omega}\right)^2\Bigg[&\frac{\omega}{\omega'}+\frac{\omega'}{\omega}-\sin^2(\theta_{\gamma\gamma})\\ &+\lambda\,\Lambda\left(\frac{\omega}{\omega'}-\frac{\omega'}{\omega}\right)\cos(\theta_{\gamma\gamma})\cos(\theta)\\ &-\lambda\,\Lambda\left(1-\frac{\omega'}{\omega}\right)\sin(\theta_{\gamma\gamma})\sin(\theta)\cos(\varphi)\Bigg].\end{aligned} \tag{2.134}$$

Here $R = \alpha_{\rm em}/M$ is the classical radius of the point particle and ω is the energy of the initial-state photon,

$$\omega' = \frac{\omega}{1+\frac{\omega}{M}\left[1-\cos(\theta_{\gamma\gamma})\right]}$$

is the energy of the outgoing photon, while $\theta_{\gamma\gamma}$ is the photon scattering angle in the laboratory frame. This provides a further consistency cross-check on our analytical results.

Since a parametrization of the Compton tensor has been devised in the previous section that can be used for any kinematical settings, the CFFs presented here ca be related to polarizabilities, and their generalizations used in the description of the deformation response of the nucleon to the external long-wavelength electromagnetic probe. To define the generalized polarizabilities, let us recall that according to Low's theorem [55], in the low-energy expansion of the Compton amplitude in the energy of the outgoing photon $q_2^0 = \omega'$, the pole $(\omega')^{-1}$ and the constant $(\omega')^0$ terms are entirely determined by the elastic form factors of the nucleon F_1 and F_2. However, the linear in ω'-term in the expansion has yet another component that cannot be solely expressed in terms of the form factors and is encoded through generalized polarizabilities. These are functions of the incoming photon three-momentum. Depending on the polarization of the incoming and outgoing photons and their multipolarity, one can introduce ten different functions. To do it in a consistent fashion without the contamination from the form factor contributions, one conventionally splits the total Compton amplitude into the Born term and the rest,

$$T^{\mu\nu} = T^{\mu\nu}_{\rm Born} + T^{\mu\nu}_{\rm non-Born}\,, \tag{2.135}$$

where the first contribution $T^{\mu\nu}_{\rm Born}$ stems from the nucleon exchange between the electromagnetic vertices,

$$T^{\mu\nu}_{\rm Born} = -4\pi\alpha_{\rm em}\,\bar u_2\,\Gamma^\mu(-q_2)\,(\not p_2 + \not q_2 - M)^{-1}\,\Gamma^\nu(q_1)\,u_1 + (\text{cross term})\,, \tag{2.136}$$

with the Γ's defined in Eq. (2.57). As it was pointed out above, its low-energy expansion starts with the inverse power of the photon energy, while the leading term in $T^{\mu\nu}_{\rm non-Born}$ is

$O(\omega')$. In complete analogy with static multipoles that yield electric and magnetic dipoles for the linear coordinate moments of charge densities, in order to generate a linear-in-ω' effect, the outgoing photon should be either electric or magnetic. Thus the polarizabilities are labelled by the type $\rho_1(\rho_2)$ of the incoming (outgoing) photon, with $\rho \in \{0,1,2\}$ corresponding to scalar, magnetic and electric multipoles, respectively, the initial (final) orbital momentum $L_1(L_2)$ and spin-flip nature of the transitions, with $S \in \{0,1\}$ standing for non-flip and flip, accordingly, $P^{(\rho_2 L_2,\rho_1 L_1)S}$. The final state electric multipoles can be traded in terms of other charge multipoles the Siegert's theorem [56], while the initial-state electric sector reduces to the charged ones only up to an additional contribution from the so-called mixed generalized polarizabilities $P^{(\rho_2 L_2,L_1)S}$ [38].

The center-of-mass frame is used, as spelled out in the Appendix A.4, for relating our helicity CFFs to generalized polarizabilities. The low-energy expansion is performed with respect to the energy of the outgoing photon ω', with polarizabilities being functions of the momentum of the incoming virtual quantum $\bar{q}$. Two of the generalized polarizabilities are $\bar{q}^2$-generalization of the electric α and magnetic β polarizabilities measured in real Compton scattering,

$$P^{(01,01)0}(\bar{q}^2) = -\sqrt{\frac{2}{3}}\frac{\alpha(\bar{q}^2)}{\alpha_{\rm em}}, \qquad P^{(11,11)0}(\bar{q}^2) = -\sqrt{\frac{8}{3}}\frac{\beta(\bar{q}^2)}{\alpha_{\rm em}}, \tag{2.137}$$

with factored out dependence of the fine structure constant $\alpha_{\rm em}$. As an intermediate step, the low-energy expansion is constructed for CFFs in terms of twelve Tarrach's structure functions f_i. The results are presented in the Appendix A.4.1. However, imposing the implications of charge conjugation symmetry and nucleon crossing, some of the f's vanish at low energy, i.e., f_3, f_4, f_8, and f_{10} are of order $O(\omega')$ and thus vanish at leading order [39]. This yields a set of relations for the ten generalized polarizabilities resulting in just six independent ones. The low-energy expansion is verified along the way for the A amplitudes defined by Guichon et al. in terms of Tarrach's structure functions f_i calculated in Ref. [39].

The helicity CFFs then read in terms of generalized polarizabilities, where the Born contribution is neglected and suppressing all higher order terms in ω':

- (+1,+1) helicity CFFs

$$\mathcal{H}_{++} = \frac{\omega'}{2\sqrt{2}}\sqrt{\frac{E_i}{E_i+M}}\Big\{M\Big[6\bar{q}P^{(11,11)1}+\sqrt{6}(\bar{q}-\omega_0)P^{(11,11)0}(1+\cos\vartheta)\Big] + 3\bar{q}\Big[(\bar{q}\cos\vartheta-\omega_0)P^{(11,11)1}+\sqrt{2}\bar{q}(\bar{q}-\omega_0\cos\vartheta)P^{(01,12)1}\Big]\Big\}, \tag{2.138}$$

$$\mathcal{E}_{++} = \frac{\omega' M}{2\sqrt{2}\bar{q}}\sqrt{\frac{E_i}{E_i+M}}\Big\{6(2M-\omega_0)(2M-\omega_0+\bar{q}\cos\vartheta)P^{(11,11)1} + \sqrt{2}\bar{q}\Big[6\omega_0(\omega_0-2M)P^{(01,12)1}\cos\vartheta+\sqrt{3}\omega_0P^{(11,11)0}(1+\cos\vartheta) + \bar{q}\big[6(2M-\omega_0)P^{(01,12)1}-\sqrt{3}P^{(11,11)0}(1+\cos\vartheta)\big]\Big]\Big\}, \tag{2.139}$$

$$\widetilde{\mathcal{H}}_{++} = \frac{3\omega'\bar{q}^3(\bar{q}-\omega_0\cos\vartheta)}{4\omega_0^2}\sqrt{\frac{E_i}{E_i+M}}\Big\{\sqrt{2}P^{(11,11)1}-2\omega_0P^{(01,12)1}\Big\}, \tag{2.140}$$

$$\widetilde{\mathcal{E}}_{++} = \frac{3\omega' M\bar{q}^2(2M-\omega_0+\bar{q}\cos\vartheta)}{2\omega_0^2}\sqrt{\frac{E_i}{E_i+M}}\Big\{\sqrt{2}P^{(11,11)1}-2\omega_0P^{(01,12)1}\Big\}, \tag{2.141}$$

- (0,+1) helicity CFFs

$$\mathcal{H}_{0+} = -\frac{\omega'\sqrt{-M\omega_0}}{2\sqrt{2}q\sin\theta}\sqrt{\frac{E_i}{E_i+M}}\Big\{2\sqrt{3}(q-\omega_0\cos\theta)P^{(11,00)1} + q\Big[3\omega_0P^{(01,01)1}-6qP^{(01,01)1}\cos\theta+\sqrt{6}q(q-\omega_0\cos\theta)P^{(11,02)1} + 3\omega_0P^{(01,01)1}\cos2\theta+2\sqrt{6}MP^{(01,01)0}(1-\cos2\theta)\Big]\Big\}, \tag{2.142}$$

$$\mathcal{E}_{0+} = -\frac{\omega' M\sqrt{-M\omega_0}}{\sqrt{2}\omega_0q\sin\theta}\sqrt{\frac{E_i}{E_i+M}}\Big\{\omega_0\Big[(2M-\omega_0)\big(6P^{(01,01)1}+\sqrt{6}\omega_0P^{(11,02)1}\big) - 2\sqrt{3}P^{(11,00)1}\Big]\cos\theta+\omega_0\big[3P^{(01,01)1}-\sqrt{6}P^{(01,01)0}\big]\cos2\theta\Big] + q\Big[2\sqrt{3}P^{(11,00)1}+\omega_0\big[\sqrt{6}P^{(01,01)0}+3P^{(01,01)1}$$

$$+\sqrt{6}(\omega_0-2M)P^{(11,02)1}\big]\Big\}, \tag{2.143}$$

$$\widetilde{\mathcal{H}}_{0+}=-\frac{\omega' M(q-\omega_0\cos\theta)}{2\sqrt{2}b\sin\theta\sqrt{-M\omega_0}}\sqrt{\frac{E_i}{E_i+M}}\Big\{6qP^{(01,01)1}-\sqrt{3}\big(2P^{(11,00)1} +\sqrt{2}q^2P^{(11,02)1}\big)\cos\theta\big)\Big\}, \tag{2.144}$$

$$\widetilde{\mathcal{E}}_{0+}=-\frac{\omega' M(q-\omega_0\cos\theta)\sqrt{-M\omega_0}}{\sqrt{2}b\omega_0^2\sin\theta}\sqrt{\frac{E_i}{E_i+M}}\Big\{6qP^{(01,01)1}-\sqrt{3}\big(2P^{(11,00)1} +\sqrt{2}q^2P^{(11,02)1}\big)\cos\theta\Big\}. \tag{2.145}$$

- $(-1,+1)$ helicity CFFs

$$\mathcal{H}_{-+}=\frac{\omega'}{2\sqrt{2}}\sqrt{\frac{E_i}{E_i+M}}\Big\{3\sqrt{2}\bar{q}^3P^{(01,12)1}-3\omega_0\bar{q}P^{(11,11)1} -\Big[\sqrt{6}M(\omega_0+\bar{q})P^{(11,11)0}-3\bar{q}^2\big(P^{(11,11)1}-\sqrt{2}\omega_0P^{(01,12)1}\big)\Big]\cos\vartheta +M\Big[6\bar{q}P^{(11,11)1}+\sqrt{6}(\omega_0+\bar{q})P^{(11,11)0}\Big]\Big\}, \tag{2.146}$$

$$\mathcal{E}_{-+}=\frac{\omega' M}{2\sqrt{2}\bar{q}}\sqrt{\frac{E_i}{E_i+M}}\Big\{\sqrt{6}\bar{q}(\omega_0+\bar{q})P^{(11,11)0}(\cos\vartheta-1) \tag{2.147}$$

$$+6(2M-\omega_0)(2M-\omega_0+\bar{q}\cos\vartheta)P^{(11,11)1} -6\sqrt{2}\Big[\omega_0(\omega_0-2M)^2-\bar{q}^3\cos\vartheta\Big]P^{(01,12)1}\Big\}, \tag{2.148}$$

$$\widetilde{\mathcal{H}}_{-+}=\frac{3\omega'\bar{q}^3(\bar{q}-\omega_0\cos\vartheta)}{4\omega_0^2}\sqrt{\frac{E_i}{E_i+M}}\Big\{2\omega_0P^{(01,12)1}-\sqrt{2}P^{(11,11)1}\Big\}, \tag{2.149}$$

$$\widetilde{\mathcal{E}}_{-+}=\frac{3\omega' M\bar{q}^2(\omega_0-2M-\bar{q}\cos\vartheta)}{2\omega_0^2}\sqrt{\frac{E_i}{E_i+M}}\Big\{\sqrt{2}P^{(11,11)1}-2\omega_0P^{(01,12)1}\Big\}, \tag{2.150}$$

where the convention for the initial-state energy is used under the condition of the vanishing final-state one [39],

$$\omega_0\equiv\omega|_{\omega'=0}=M-E_i=M-\sqrt{M^2+\bar{q}^2}\,, \tag{2.151}$$

where E_i is the incoming nucleon's energy.

CHAPTER 3

RENORMALIZATION OF TWIST-FOUR OPERATORS IN LIGHT-CONE GAUGE

In this chapter one computes the one-loop renormalization group equations for non-singlet twist-four operators in QCD. The calculation heavily relies on the light-cone gauge formalism in momentum fraction space, that essentially rephrases the analysis of all two-to-two and two-to-three transition kernels to purely algebraic manipulations both for non- and quasipartonic operators. Fourier transforming the findings to the coordinate space, one checked them against available results obtained within a conformal symmetry-based formalism that bypasses explicit diagrammatic calculations, and confirmed agreement with the latter [65].

3.1 Motivation

The leading-power approximation to QCD processes with large momentum transfer, such as the deep-inelastic and deeply-virtual Compton scattering, admits an intuitive probabilistic description in the framework of the Feynman parton model [66], as was elaborated previously. According to the latter, physical cross sections are expressible in terms of (generalized) parton distribution functions. The QCD-improved picture arises via systematic inclusions of quantum corrections to probe-parton scattering amplitudes, as well as renormalization effects of leading-twist Wilson operators that parametrize Feynman parton densities. More subtle effects arise from power-suppressed contributions to hadronic cross sections, since they encode information on interference of hadronic wave functions with different numbers of partons. On the one hand, these are of interest in their own right since they provide access to intricate QCD dynamics [67]. On the other hand, they can be regarded as a QCD contaminating background to high-precision measurements of New Physics, see, e.g., [68]. In either case, understanding these contributions quantitatively is

indispensable at the precision frontier. Since data is typically taken at different values of the momentum transfer, at some point one has to incorporate effects of logarithmic scaling violation stemming from renormalization of higher-twist operators. The task of their unravelling at twist-four level will be undertaken in the present chapter.

Until very recently, only partial results for certain subsets of operators were available in the literature [69, 70]. A special class of operators out of all higher twists is known as quasipartonic. They can be characterized either as composite fields built from on-shell fields of the Feynman parton model or understood as operators with their twist equal to their length, i.e., the number of fields that form them. For this class of operators a systematic approach to constructing high-twist evolution equations was developed about three decades ago by Bukhvostov, Frolov, Lipatov and Kuraev in Ref. [71]. At leading order in QCD coupling, the evolution kernel for these was found as a sum of pairwise interaction kernels between elementary fields comprising the operators in question. The particle number-preserving nature allows one to map it to a Hamiltonian quantum-mechanical problem. This advantage was explored in a number of works at the twist-three level [72][12] starting from [74]. Eventually, the problem was mapped into an exactly solvable lattice model [75, 76]. However, while the quasipartonic operators form a subset closed under the renormalization group evolution [71, 77], they do not exhaust the set of all operators contributing at a given twist. The remaining ones are dubbed non-quasipartonic and they contain at least one "bad" field component in the formalism of light-cone quantization. These operators are characterized by the property that their twist is greater than their length. Their evolution does not preserve the number of fields in quantum transitions, and thus their study is more elaborate. In the twist-three case alluded to above, this was not a pressing issue since the use of QCD equations of motion allows one to remove all non-quasipartonic operators from the basis. For even higher twists, this is not sufficient, and particle number-changing

[12]For a more recent discussion of operator renormalization arising in certain single-spin asymmetries, see [73].

transitions involved in the analysis of non-quasipartonic operators have to be addressed explicitly.

The analysis of the renormalization problem for twist-four operators was completed recently in coordinate space [78], i.e., in terms of light-ray composite operators. The formalism is based on the use of conformal symmetry preserved by leading-order QCD evolution equations, Poincaré transformations in the transverse plane, and a minimal input from Feynman graphs. Presently one performs a direct computation of Feynman diagrams in the light-cone gauge and relies on the momentum-space technique, which makes the underlying calculation rather straightforward. With the exception of a few subtleties with the use of QCD equations of motion to recover the particle-number increasing transitions, it reduces to a few algebraic, though rather tedious, steps.

The choice of the operator basis at higher twists is not unique, due to multiple relations among a redundant set of operators via QCD equations of motion. Thus it is driven by requirements of simpler transformation properties under residual (conformal) symmetry, as well as simplicity of the underlying calculations. Here one adopts the basis of twist-four operators suggested in Ref. [78]. This will allow us to verify our results obtained by an independent calculation based on a different technique. Since one focuses on on the twist-four sector, one had three types of building blocks at our disposal as two-particle elements of operators in question: "good-good", "good-bad" and "bad-bad" light-cone field components. According to traditional classification, they possess twists two, (at least) three and (at least) four, respectively. We will address only the first two types, since the last one can be eliminated in hadronic matrix elements in favor of the other ones containing more fields via QCD equations of motion, as discussed below. Our consideration will be limited to the QCD nonsinglet sector, though partial results for two-to-two transitions will be reported for the singlet sector as well.

Our subsequent presentation is organized as follows. In the next section, the operator basis used in the current calculation is speled out and a dictionary between the twistor notations adopted in Ref. [78] and the light-cone conventions used in the present analysis is provided. Then, the general structure of twist-four evolution equations is discussed and a Fourier-transform bridge between the light-ray and momentum fraction space representations is provided. In Secs. 3.4.1, 3.4.2 and 3.4.3, one presents evolution kernels for two-to-two quasipartonic, non-quasipartonic and two-to-three transitions, respectively. As a result of this analysis, a simplified form of light-ray evolution kernels is found for certain evolution kernels which are reported in the Appendices. The latter also contain technical details on the calculation of Feynman diagrams defining operator mixing, as well as singlet two-to-two transitions.

3.2 Operator Basis

The light-cone dominated processes are parametrized by matrix elements of composite operators built up by fields localized on a light-cone ray defined by the vector $n_\mu = (1,0,0,1)/\sqrt{2}$ that is reciprocal to the large light-cone component of the momentum transfer. Thus they have the following generic form

$$\mathbb{O}(z_1,\dots,z_N) = C^{I_1\dots I_N}[z_0^-,z_1^-]_{I_1J_1}X_1^{J_1}(z_1^-)\dots[z_0^-,z_N^-]_{I_NJ_N}X_N^{J_N}(z_N^-)\,, \tag{3.1}$$

where the X-field cumulatively stands for certain components of quark and gluon fields as explained below. The positions $z_k^- = \bar{n}\cdot z_k$ of the fields on the light-cone are defined with the help of a tangent null vector $\bar{n}^\mu = (1,0,0,-1)/\sqrt{2}$ to the light-cone normalized such that $n\cdot\bar{n} = 1$. The gauge invariance of $\mathbb{O}$ is achieved by means of an appropriate contraction of the color indices I_k (either in the (anti-)fundamental $I_k = i_k$ or adjoint representation $I_k = a_k$ of the color group) into an $SU(N)$ singlet with a tensor $C_{I_1I_2\dots I_N}$ and field coordinates

parallel-transported to an arbitrary position z_0^- with the help of the Wilson line on the light-cone,

$$[z_0^-, z_k^-] = P\exp\left(ig\int_{z_k^-}^{z_0^-} dz^- A^+(z^-) \right). \tag{3.2}$$

Here

$$A^+ = n\cdot A = \tfrac{1}{\sqrt{2}}(A^0 + A^3) \tag{3.3}$$

is the light-cone projection of the gauge field.

3.2.1 Good and Bad Light-Cone Fields

It is well-known that the light-cone gauge

$$A^+ = 0\,, \tag{3.4}$$

has a number of advantages. First, one observes that the gauge links are gone in Eq. (3.1) and, as a consequence, this results in reducing of the number of diagrams contributing to loop amplitudes. Second, the Feynman parton model arises naturally from the light-cone gauge QCD. Namely, one decomposes the quark Ψ and gluon fields A^μ,

$$\Psi = \tfrac{1}{2}\gamma^-\gamma^+\Psi + \tfrac{1}{2}\gamma^+\gamma^-\Psi \equiv \Psi_+ + \Psi_-\,, \qquad A^\mu = n^\mu A^- - \bar{e}^\mu_\perp A_\perp - e^\mu_\perp \bar{A}_\perp\,, \tag{3.5}$$

in terms of the "good" $X_+ = \{\Psi_+, A_\perp, \bar{A}_\perp\}$ and the "bad" $X_- = \{\Psi_-, A^-\}$ components, respectively. Note that for the vector A^μ one defined its minus projection as follows

$$A^- = \bar{n}\cdot A = \tfrac{1}{\sqrt{2}}(A^0 - A^3)\,, \tag{3.6}$$

and, in addition, one decomposed the transverse gauge field in terms of its anti- and holomorphic components

$$\bar{A}_\perp = \bar{e}_\perp\cdot A = \tfrac{1}{\sqrt{2}}(A^1 - iA^2)\,, \qquad A_\perp = e_\perp\cdot A = \tfrac{1}{\sqrt{2}}(A^1 + iA^2) \tag{3.7}$$

with the help of the vector $e_\perp^\mu = (0,-1,-i,0)/\sqrt{2}$ (and its complex conjugate $\bar{e} = e^*$). These possess helicity $h = \pm 1$, respectively, being eigenvalues of the helicity operator [79]

$$H \equiv \bar{e}_\perp^\mu e_\perp^\nu \Sigma_{\mu\nu}\,, \tag{3.8}$$

that is built from the spin tensor $\Sigma_{\mu\nu}$ entering the Lorentz generators $iM_{\mu\nu}$. The "bad" components, being non-dynamical in the light-cone time z^+, can be integrated out in the path integral and, thus, only the on-shell propagating modes Ψ_+, $A_\perp$ and $\bar{A}_\perp$ are left. We will not perform this step, however, and keep all non-propagating degrees of freedom in the QCD Lagrangian, since the classification of operators will be easier in this case and moreover, one does not lose Lorentz covariance. Finally, it is straightforward to construct an operator basis making use of the above building blocks, namely, the field X in Eq. (3.1) will have the following components (as well as their Hermitian conjugates $X^\dagger$)

$$X = \{X_+, X_-, D_\perp X_+\}\,, \tag{3.9}$$

with $D_\perp = e_\perp \cdot D$ being the holomorphic covariant derivative $D_\mu = \partial_\mu - igA_\mu$.

3.2.2 Twistor Representation

To make a connection to the basis of Ref. [80], let us recall the twistor formalism used there. We pass to the spinor representation for Lorentz vectors by contracting them with the two-dimensional block σ^μ of four-dimensional Dirac matrices in the chiral representation $\gamma^\mu = \text{antidiag}(\bar{\sigma}^\mu, \sigma^\mu)$, e.g.,

$$x_{\alpha\dot{\alpha}} = x_\mu \sigma^\mu_{\alpha\dot{\alpha}}\,, \tag{3.10}$$

where $\sigma^\mu = (1, \vec{\sigma})$ and $\vec{\sigma}$ is the three-vector of Pauli matrices, while $\bar{\sigma}^\mu = (1, -\vec{\sigma})$. The light-cone vectors n and $\bar{n}$ can be factorized into two twistors λ_α and μ_α

$$n_{\alpha\dot{\alpha}} = \lambda_\alpha \bar{\lambda}_{\dot{\alpha}}\,, \qquad \bar{n}_{\alpha\dot{\alpha}} = \mu_\alpha \bar{\mu}_{\dot{\alpha}}\,, \tag{3.11}$$

where $\lambda^*_\alpha = \lambda_{\dot\alpha}$ and $\mu^*_\alpha = \mu_{\dot\alpha}$. For the light-cone vectors introduced in the previous section, one can choose the two-dimensional spinors as $\lambda^\alpha = (0, \sqrt[4]{2})$ and $\mu^\alpha = (\sqrt[4]{2}, 0)$. These twistors will allow us to construct good and bad fields for specific helicities. Namely, using the decomposition of the Dirac quark field in chiral representation

$$\Psi = \begin{pmatrix} \psi_\alpha \\ \bar\chi^{\dot\alpha} \end{pmatrix}, \tag{3.12}$$

one can introduce their good and bad components as follows

$$\psi_+ = \langle \lambda\, \psi \rangle, \qquad \bar\psi_+ = [\bar\psi \bar\lambda], \qquad \psi_- = \langle \mu\, \psi \rangle, \qquad \bar\psi_- = [\bar\psi \bar\mu]. \tag{3.13}$$

Identical relations hold for χ upon the obvious replacement $\psi \to \chi$. Here one introduced the bra and ket notations for undotted and dotted $SL(2)$ indices, $|\lambda\rangle = \lambda_\alpha$, $\langle\lambda| = \lambda^\alpha$ and $|\bar\lambda] = \lambda^{\dot\alpha}$, $[\bar\lambda| = \bar\lambda_{\dot\alpha}$ that allow us to uniformly contract undotted indices from upper-left to lower-right and dotted ones from lower-left to upper right, i.e., $\langle \lambda\, \psi \rangle = \lambda^\alpha \psi_\alpha$ and $[\bar\mu\, \bar\psi] = \bar\mu_{\dot\alpha} \bar\psi^{\dot\alpha}$.

In a similar fashion, the gluon field strength can be decomposed as

$$F_{\mu\nu} \sigma^\mu_{\alpha\dot\alpha} \sigma^\nu_{\beta\dot\beta} = 2\varepsilon_{\dot\alpha\dot\beta} f_{\alpha\beta} - 2\varepsilon_{\alpha\beta} \bar f_{\dot\alpha\dot\beta}, \tag{3.14}$$

in terms of its chiral $f_{\alpha\beta} = \frac{i}{4} \sigma^{\mu\nu}{}_{\alpha\beta} F_{\mu\nu}$ and anti-chiral $\bar f_{\dot\alpha\dot\beta} = \frac{i}{4} \bar\sigma^{\mu\nu}{}_{\dot\alpha\dot\beta} F_{\mu\nu}$ components with the help of the self-dual $\sigma_{\mu\nu} = \frac{i}{2}[\sigma_\mu \bar\sigma_\nu - \bar\sigma_\nu \bar\sigma_\mu]$ and anti-self-dual tensors $\bar\sigma_{\mu\nu} = \frac{i}{2}[\bar\sigma_\mu \sigma_\nu - \bar\sigma_\nu \sigma_\mu]$. The plus and minus fields are found by projections

$$f_{++} = -\langle \lambda | f | \lambda \rangle, \quad f_{+-} = -\langle \lambda | f | \mu \rangle, \quad \bar f_{++} = -[\bar\lambda | \bar f | \bar\lambda], \quad \bar f_{+-} = -[\bar\lambda | \bar f | \bar\mu], \tag{3.15}$$

etc.

Finally, as for any four-vector, the covariant derivatives are decomposed in twistor components as follows

$$D_{++} = \langle \lambda | D | \bar\lambda], \quad D_{+-} = \langle \lambda | D | \bar\mu], \qquad D_{--} = \langle \mu | D | \bar\mu]. \tag{3.16}$$

3.2.3 Bridging Light-Cone and Twistor Projections

The notations introduced in this and preceding sections allow us to establish a dictionary between the light-cone and twistor components. They are summarized by the following set of relations:

$$\psi_+ = \frac{\sqrt[4]{2}}{4}(1+\gamma_5)\gamma^-\gamma^+\Psi, \qquad \psi_- = \frac{\sqrt[4]{2}}{4}(1+\gamma_5)\gamma^+\gamma^-\Psi, \tag{3.17}$$

$$\chi_+ = \frac{\sqrt[4]{2}}{4}\bar{\Psi}(1+\gamma_5)\gamma^+\gamma^-, \qquad \chi_- = -\frac{\sqrt[4]{2}}{4}\bar{\Psi}(1+\gamma_5)\gamma^-\gamma^+, \tag{3.18}$$

for fermions, where $\gamma_5 = \mathrm{diag}(1,-1)$, and

$$\begin{aligned} f_{++} &= \sqrt{2}F^{+\perp}, \\ f^a_{+-} &= -\frac{1}{2\sqrt{2}}\left((\partial^+A^-)^a + (\bar{D}_\perp A_\perp)^a - (D_\perp \bar{A}_\perp)^a - g f^{abc}\bar{A}^b_\perp A^c_\perp\right), \end{aligned} \tag{3.19}$$

for gluons and, finally, covariant derivatives,

$$D_{-+} = \bar{D}_{+-} = 2\bar{D}_\perp, \qquad D_{+-} = \bar{D}_{-+} = 2D_\perp, \tag{3.20}$$

$$D_{++} = \bar{D}_{++} = 2D^+, \qquad D_{--} = \bar{D}_{--} = 2D^-. \tag{3.21}$$

Making use if these conversion formulas, one can adopt the basis introduce in Ref. [80], on the one hand, and use the momentum-space technique of Ref. [74] that makes the calculation more concise while using conventional four-component notations for Lorentz vectors and Dirac matrices.

3.2.4 $SL(2)$ Invariance and Basis Primary Fields

Though massless QCD is not a conformal theory at the quantum-mechanical level since it induces a scale due to dimensional transmutation, the classical Lagrangian of the theory does enjoy $SO(4,2)$ invariance. The one-loop evolution equations is analyzed here inherit the latter since the symmetry-breaking graphs do not make their appearance till two-loop

order. Since the light-cone operators (3.1) involve fields localized on a light ray, the full conformal algebra reduces to its collinear conformal $SL(2)$ subalgebra that acts only on the minus projections $z_k^- \equiv z_k$ of the Minkowski space-time coordinates z_k^μ. The differential representation of generators acting on the space spanned by the composite operators (3.1) reads

$$S^+ = \sum_{n=1}^{N} (z_n^2 \partial_{z_n} + 2 j_n z_n)\,, \qquad S^- = -\sum_{n=1}^{N} \partial_{z_n}\,, \qquad S^0 = \sum_{n=1}^{N} (z_n \partial_{z_n} + j_n)\,. \tag{3.22}$$

The irreducible representations are characterized by the value of the conformal spin $j_n = (d_n + s_n)/2$ determined by the canonical dimension d_n and light-cone spin s_n of the constituent fields X_n. These generators commute with the generator of helicity introduced in Eq. (3.8) as well as twist $E = \sum_{n=1}^{N} d_n - s_n$, see, e.g., [81, 82].

The field projections introduced in the previous section transform covariantly under $SL(2)$ transformations and can be organized into "multiplets" of the same twist. Namely, the good Φ_+ and bad Φ_- chiral fields

$$\Phi_+ = \{\psi_+, \chi_+, f_{++}\}\,, \qquad \Phi_- = \{\psi_-, \chi_-, f_{+-}\}\,, \tag{3.23}$$

as well as their conjugate anti-chiral analogues $\bar{\Phi}_\pm = \Phi_\pm^*$, possess twist $E = 1$ and $E = 2$, respectively.

Since covariant derivatives D_{++}, $D_{\pm\mp}$, and D_{--} carry twist zero, one and two, respectively, they can be used to generate additional high-twist "single-particle" fields by acting on $\Phi_\pm$. Obviously, one can ignore D_{++} since they just induce an infinitesimal shift along the light cone. The D_{--} derivatives acting on Φ_+ will produce a twist-three constituent, which when accompanied by another good field component, will form a twist-four operator. However, this operator can be safely dropped from the basis thanks to QCD equations of motion. Next, the transverse derivatives $D_{\pm\mp}$ can act either on good or bad fields. However, one can consider only their action on the former, since one can always

move derivatives from bad to good fields in a twist-four operator of the type $\Phi_+ D_{\pm\mp}\Phi_-$. Moreover, since it is desirable to deal with conformal primary fields as individual building blocks, as they obey simple $SL(2)$ transformations (3.22) and thus yield evolution equations with manifest conformal symmetry, one can reduce in half, as advocated in Ref. [80], the basis of good fields with transverse covariant derivatives acting on them. This is achieved by eliminating the ones with non-covariant transformation properties. The net result is that one introduces instead conformal primaries $D_{--}\Phi_+$ which can be safely neglected as alluded to above. This procedure allows us to trade $D_{-+}\Phi_+$, posing "bad" $SL(2)$ transformation properties, in favor of the primary $D_{+-}\Phi_+$. Finally, two transverse derivatives acting on Φ_+ can again be reduced to the irrelevant primary $D_{--}\Phi_+$. This concludes the recapitulation of the reasoning behind the choice of the twist-one X_+ and twist-two X_- primaries

$$X_+ = \{\Phi_+, \bar{\Phi}_+\}\,, \qquad X_- = \{\Phi_-, \bar{\Phi}_-, D_{+-}\Phi_+, D_{-+}\bar{\Phi}_+\}\,, \tag{3.24}$$

which build up the operator basis at twist four. The latter is thus spanned by quasipartonic and nonquasipartonic operators (that read schematically)

$$\mathbb{O}_4 = X_+X_+X_+X_+\,, \qquad \mathbb{O}_3 = X_-X_+X_+\,, \tag{3.25}$$

respectively.

3.3 Evolution Equations

The twist-four light-ray operators (3.25) mix under renormalization. Their mixing matrix admits perturbative expansion in strong coupling $\alpha_s = g^2/(4\pi)$. The goal of our analysis is to calculate the leading term of the series, namely,

$$\frac{d}{d\ln\mu}\begin{pmatrix}\mathbb{O}_3\\ \mathbb{O}_4\end{pmatrix} = -\frac{\alpha_s}{2\pi}\begin{pmatrix}\mathbb{H}^{(3\to3)} & \mathbb{H}^{(3\to4)}\\ 0 & \mathbb{H}^{(4\to4)}\end{pmatrix}\begin{pmatrix}\mathbb{O}_3\\ \mathbb{O}_4\end{pmatrix} + O(\alpha_s^2)\,. \tag{3.26}$$

Notice that the mixing matrix takes a triangular form (to all orders in coupling) since the quasipartonic operators form an autonomous set under renormalization-group evolution. Here the transition kernels are some integral operators that shift fields on the light-cone towards each other. Their form is highly contained by conformal symmetry and was the subject of a recent analysis [78]. The distinguished feature of nonquasipartonic operators is that they can change the number of fields upon evolution. Thus, while $\mathbb{H}^{(N\to N)}$ for $N=3,4$ is merely given by the sum of pairwise transition kernels,

$$\mathbb{H}^{(N\to N)}=\sum_{j<k}\mathbb{H}^{(2\to 2)}_{jk} \tag{3.27}$$

the kernel $\mathbb{H}^{(3\to 4)}$ involves both two-to-two and two-to-three transitions

$$\mathbb{H}^{(3\to 4)}=\sum_{j<k}\left(\mathbb{H}^{(2\to 2)}_{jk}+\mathbb{H}^{(2\to 3)}_{jk}\right), \tag{3.28}$$

the latter existing whenever there is a bad field involved in a two-particle block, i.e., either j or k label belongs to a bad field.

Extracting the color structures from these transitions

$$\mathbb{H}^{(2\to 2)}_{12}[X_1^{I_1}(z_1)X_2^{I_2}(z_2)]=\sum_c\sum_{J_1J_2}[C_c]^{J_1J_2}_{I_1I_2}\mathbb{H}_c[X_1^{J_1}X_2^{J_2}](z_1,z_2), \tag{3.29}$$

$$\mathbb{H}^{(2\to 3)}_{12}[X_1^{I_1}(z_1)X_2^{I_2}(z_2)]=\sum_c\sum_{J_1J_2J_3}[C_c]^{J_1J_2J_3}_{I_1I_2}\mathbb{H}_c[X_1^{J_1}X_2^{J_2}X_3^{J_3}](z_1,z_2), \tag{3.30}$$

the reduced integral operators $\mathbb{H}_c$ for two- and three-particle transitions are defined by their H-kernels are given by

$$[\mathbb{H}_c\mathbb{O}](z_1,z_2)=z_{12}^{\sigma}\int_0^1 d\alpha_1 d\alpha_2\, H_c(\alpha_1,\alpha_2)\mathbb{O}(\bar\alpha_1 z_1+\alpha_1 z_2,\bar\alpha_2 z_2+\alpha_2 z_1), \tag{3.31}$$

$$[\mathbb{H}_c\mathbb{O}](z_1,z_2)=z_{12}^{\sigma}\int_0^1 d\alpha_1 d\alpha_2 d\alpha_3\, H_c(\alpha_1,\alpha_2,\alpha_3)\mathbb{O}(\bar\alpha_1 z_1+\alpha_1 z_2,\bar\alpha_2 z_2+\alpha_2 z_1,\bar\alpha_3 z_2+\alpha_3 z_1), \tag{3.32}$$

where σ is a positive/negative integer reflecting the mismatch in the field dimension in a given operator transition. The manifest $SL(2)$ covariance on conformal primaries building

up the composite operators, and the fact that one-loop transitions do not receive contributions from counter-terms that break conformal invariance, implies the commutativity of the kernels with the generators of the algebra

$$[S^{\pm,0},\mathbb{H}]=0\,, \tag{3.33}$$

and thus impose severe constraints on the form of the kernels.

3.3.1 Renormalization in Momentum Space

Though the conformal symmetry is more explicit in the coordinate space, the actual calculations of one-loop graphs determining the mixing matrix are far more straightforward and elementary in the reciprocal momentum space. As it was pointed out in the introduction, a technique to perform this analysis is available for quasipartonic operators from Ref. [71]. Presently generalizes to nonquasipartonic operators as well. The formalism relies heavily on the light-cone gauge, where the gluon propagator takes the form

$$G^{ab}_{\mu\nu}(k)=\frac{(-i)d_{\mu\nu}(k)}{k^2+i0}\,,\qquad d_{\mu\nu}(k)=g_{\mu\nu}-\frac{k^\mu n^\nu+k^\nu n^\mu}{k^+}\,. \tag{3.34}$$

As one can see, the integration over the loop momentum k decomposed in Sudakov variables $k^\mu=k^+\bar{n}^\mu+k^-n^\mu+k^\mu_\perp$,

$$\int\frac{d^4k}{(2\pi)^4}=\int_{-\infty}^{\infty}\frac{dk^+}{2\pi}\int_{-\infty}^{\infty}\frac{dk^-}{2\pi}\int_{-\mu}^{\mu}\frac{d^2k_\perp}{(2\pi)^2}\,, \tag{3.35}$$

will potentially produce divergences in the longitudinal variable k^+ due to an extra pole in the propagator, in addition to the conventional ultraviolet singularities regularized by a cut-off μ in the transverse momentum. The former arise due to incomplete gauge fixing by the condition (3.4) that allows one for light-cone time-independent residual transformations. To complete gauge fixing, one has to impose a condition on how to go around the $1/k^+$ singularity. This will not be a pressing issue for the current study since one focuses on kinematics away from the phase space boundaries where these have to be treated

properly. Let us point out however, that the advanced/retarded and symmetric boundary conditions on the gauge potential on the light-cone infinity impose $\pm i0$ and principal value prescription [25], while the condition consistent with the equal-time quantization yields the Mandelstam-Leibbrandt prescription [83].

Thus, one converts the light-ray operators to the momentum fraction space

$$\mathcal{O}(x_1,\ldots,x_N) = \int \prod_{n=1}^{N} \frac{d^4k_n}{(2\pi)^4} \delta(k_n^+ - x_n)\, \mathcal{O}(k_1,\ldots,k_N)\,. \tag{3.36}$$

by means of the Fourier transform

$$\mathcal{O}(k_1,\ldots,k_N) = \int \prod_{n=1}^{N} d^4z_n \mathrm{e}^{ik_n\cdot z_n}\, \mathbb{O}(z_1,\ldots,z_N)\,. \tag{3.37}$$

Then, the evolution kernels arise from the N to M-particle transition amplitude,

$$\begin{aligned}\mathcal{O}(x_1,\ldots,x_N) = &\int \prod_{m=1}^{M} dy_m \int \prod_{m=1}^{M} \frac{d^4p_m}{(2\pi)^4} \delta(p_m^+ - y_m)\mathcal{O}(p_1,\ldots,p_M) \\ &\times \int \prod_{n=1}^{N} \frac{d^4k_n}{(2\pi)^4} \delta(k_n^+ - x_n)\mathcal{G}(k_1,\ldots,k_n|p_1,\ldots,p_M)\,,\end{aligned} \tag{3.38}$$

where $\mathcal{G}(k_1,\ldots,k_n|p_1,\ldots,p_M)$ is a sum of corresponding Feynman graphs. Extraction of the leading logarithmic divergence from the momentum integrals results in the sought momentum-space evolution equation,

$$\mathcal{O}(x_1,\ldots,x_N) = -\frac{\alpha_s}{2\pi} \ln\mu\, [\mathcal{K}^{(N\to M)}\mathcal{O}](x_1,\ldots,x_N)\,, \tag{3.39}$$

where integral kernel in the momentum representation is

$$[\mathcal{K}^{(N\to M)}\mathcal{O}](x_1,\ldots,x_N) = \int [\mathcal{D}^M y]_N K(x_1,\ldots,x_N|y_1,\ldots,y_M)\mathcal{O}(y_1,\ldots,y_M)\,, \tag{3.40}$$

with a notation introduced for the measure

$$[\mathcal{D}^M y]_N \equiv \prod_{m=1}^{M} dy_m \delta\left(\sum_{m=1}^{M} y_m - \sum_{n=1}^{N} y_n\right). \tag{3.41}$$

The $N-1$ momentum integrals in (3.38) are eliminated by means of four-momentum conserving delta functions stemming from Feynman rules, leaving us with a single four-dimensional loop-momentum integration measure (3.35). The extraction of $1/k_\perp^2$ contribution in the integrand can be easily achieved by rescaling the k^- component of the loop momentum by introducing a new variable

$$\beta = 2k^-/k_\perp^2\,, \tag{3.42}$$

where $k_\perp$ is the transverse loop momentum. The k^+ integral is removed by making use of the momentum fraction delta functions in Eq. (3.38), while the rescaled k^--integrals are evaluated in terms of the generalized step-functions [71, 85]

$$\vartheta^k_{\alpha_1,\ldots,\alpha_n}(x_1,\ldots,x_n) = \int_{-\infty}^{\infty}\frac{d\beta}{2\pi i}\beta^k\prod_{\ell=1}^{n}(x_\ell\beta-1+i0)^{-\alpha_\ell}\,. \tag{3.43}$$

These can be reduced to the simplest one, $\vartheta^0_{11}(x_1,x_2)=[\theta(x_1)-\theta(x_2)]/(x_1-x_2)$, making use of a set of known relations [71, 85]. So the advantage of this formalism is that there are no actual integrals to perform, and the procedure of computing the evolution kernels is reduced to straightforward but tedious algebraic manipulations with Dirac and Lorentz structures.

So all one needs for the calculation is Fourier transforms of the conformal primary fields defining composite operators. When cast in four-dimensional light-cone notations, they read

$$\Phi_+ \overset{\text{FT}}{\to} \Phi_+ = \left\{\tfrac{1}{4}(1+\gamma_5)\gamma^-\gamma^+\Psi, \tfrac{1}{4}(1-\gamma_5)\gamma^-\gamma^+\Psi, -\tfrac{i}{2}k^+A_\perp\right\}, \tag{3.44}$$

$$\bar{D}_{-+}\Phi_+ \overset{\text{FT}}{\to} -i\sqrt{2}\,(k_\perp + gA_\perp)\,\Phi_+\,, \tag{3.45}$$

$$\begin{aligned}\Phi_- \overset{\text{FT}}{\to} \Phi_- = \Big\{&\tfrac{1}{4}(1+\gamma_5)\gamma^+\gamma^-\Psi, \tfrac{1}{4}(1-\gamma_5)\gamma^+\gamma^-\Psi,\\ &-\tfrac{i}{2}k^+A^- + \tfrac{i}{2}(k_\perp\bar{A}_\perp - \bar{k}_\perp A_\perp) - \tfrac{i}{4}g[\bar{A}_\perp, A_\perp]\Big\}.\end{aligned} \tag{3.46}$$

The results for the antichiral fields $\bar{\Phi}$ are obtained from above by complex conjugation.

3.3.2 From Coordinate to Momentum Space

It is straightforward to relate evolution kernels in coordinate and momentum space by a Fourier transformation. For two-to-two transitions, one immediately finds

$$K(x_1,x_2|y_1,y_2) = (-i\partial_{x_1})^\sigma \int_0^1 d\alpha_1 d\alpha_2 H(\alpha_1,\alpha_2)\delta(x_1-\bar{\alpha}_1 y_1-\alpha_2 y_2)\,, \tag{3.47}$$

which are subject to the momentum-fraction conservation condition $x_1+x_2=y_1+y_2$. Analogously, for two-to-three transitions, one finds

$$\begin{aligned} &K(x_1,x_2|y_1,y_2,y_3) \\ &\qquad = (-i\partial_{x_1})^\sigma \int_0^1 d\alpha_1 d\alpha_2 d\alpha_3 H(\alpha_1,\alpha_2,\alpha_3)\delta(x_1-\bar{\alpha}_1 y_1-\alpha_2 y_2-\alpha_3 y_3)\,, \end{aligned} \tag{3.48}$$

where one assumes that $x_1+x_2=y_1+y_2+y_3$. Having results in one representation, one can easily obtain the other making use of the following two elementary operations

$$\int_0^1 d\alpha f(\alpha)\delta(x-\alpha y) = f\left(\frac{x}{y}\right)\vartheta_{11}^0(x,x-y)\,, \tag{3.49}$$

$$\begin{aligned} \int_0^1 d\alpha\,\bar{\alpha}^n \vartheta_{11}^0(x_1-y_1\bar{\alpha},x_1-\eta\bar{\alpha}) = \frac{1}{n}\Bigg\{ &\left[1-\left(\frac{x_1}{\eta}\right)^n\right]\vartheta_{11}^0(x_1-y_1,-x_2) \\ &-\frac{y_1}{y_2}\left[\left(\frac{x_1}{\eta}\right)^n-\left(\frac{x_1}{y_1}\right)^n\right]\vartheta_{11}^0(x_1-y_1,x_1)\Bigg\}\,, \end{aligned} \tag{3.50}$$

where $\eta = x_1+x_2=y_1+y_2$ implies momentum conservation. Finally, the coordinate kernels possess integrable end-point singularties that have to be regularized in the course of the Fourier transform. We found the cut-off regularization to be the simplest one to handle the emerging divergences

$$\int_\varepsilon^1 \frac{d\alpha}{\alpha}\theta(x-y\alpha) = \left[\ln\left(\frac{x}{y}\right)-\ln\varepsilon\right]\theta(x)-\ln\left(\frac{x}{y}\right)\theta(x-y)\,, \tag{3.51}$$

$$\int_\varepsilon^1 \frac{d\alpha}{\alpha^2}\theta(x-y\alpha) = \left(\frac{1}{\varepsilon}-\frac{y}{x}\right)\theta(x)+\left(\frac{y}{x}-1\right)\theta(x-y)\,. \tag{3.52}$$

At the end of the calculation, all singular terms cancel in the limit $\varepsilon\to 0$, rendering the total result regular. We provide an example of explicit transformation in Appendix B.2.2.

3.3.3 Conformal Symmetry in Momentum Space

Since conformal invariance played a crucial role for the coordinate-space calculations [78], let us analyze its consequences in momentum space. To this end, following the same reasoning leading to the expression of Eqs 3.48 and taking care of the ordering of z and ∂_z, one observes the following identifications between the light-ray coordinates and the momentum fractions,

$$z_n \xrightarrow{FT} -i\partial_{x_n}, \qquad \partial_{z_n} \xrightarrow{FT} ix_n, . \tag{3.53}$$

where x_n is the reciprocal momentum to the coordinate z_n. Thus the conformal generators shown in Eq. (3.22) can be rewritten in momentum space as

$$\widetilde{S}^{+}\mathcal{O}(x_1,\ldots,x_N) = i\sum_{n=1}^{N}\left(\partial_{x_n}^2 x_n - 2j_n\partial_{x_i}\right)\mathcal{O}(x_1,\ldots,x_N)\,, \tag{3.54}$$

$$\widetilde{S}^{0}\mathcal{O}(x_1,\ldots,x_N) = -\sum_{i=1}^{n}\left(\partial_{x_n}x_n - j_n\right)\mathcal{O}(x_1,\ldots,x_N)\,, \tag{3.55}$$

$$\widetilde{S}^{-}\mathcal{O}(x_1,\ldots,x_N) = -i\sum_{n=1}^{n} x_n\mathcal{O}(x_1,\ldots,x_N)\,. \tag{3.56}$$

Imposing the condition of commutativity

$$[\mathcal{K},\tilde{S}^{\pm,0}]\mathcal{O}(x_1,\ldots x_N) = 0\,, \tag{3.57}$$

one finds that the evolution kernels obey the following differential equations (away from kinematical boundaries)

$$\begin{aligned}\left(\sum_{m=1}^{M}\left(y_m\partial_{y_m}^2 + 2j_m\partial_{y_m}\right) - \sum_{n=1}^{N-1}\left(\partial_{x_n}^2 x_n - 2j_n\partial_{x_n}\right)\right)\\ \times K(x_1,\ldots,\left(\sum_{m=1}^{M} y_m - \sum_{n=1}^{N-1} x_n\right)|y_1,\ldots,y_M) = 0\,,\\ \left(\sum_{m=1}^{M}\left(y_m\partial_{y_m} + j_m\right) + \sum_{n=1}^{N-1}\left(\partial_{x_n}x_n - j_n\right) - j_N\right)\end{aligned} \tag{3.58}$$

$$\times K(x_1,\ldots,\Big(\sum_{m=1}^{M} y_m-\sum_{n=1}^{N-1} x_n\Big)|y_1,\ldots,y_M)=0\,, \tag{3.59}$$

for S^+ and S^0, respectively. In arriving at the expressions of Eqs. (3.58) and (3.59), one has made use of the momentum-conserving Dirac delta function factorized from (3.40). Since essentially there are only $M+N-1$ independent variables in the game, one is required to rewrite one of the variables as a linear combination of the rest before differentiation. Above one chose to eliminate x_N. Finally, S^- simply yields the momentum fraction conservation condition which is trivially obeyed due to an overall delta function (3.41) that accompanies the transition kernel,

$$\sum_{m=1}^{M} y_m-\sum_{n=1}^{N} x_n=0\,, \tag{3.60}$$

Since one is interested in two-to-two and two-to-three transitions in this work, the expressions in Eqs. 3.58 and 3.59 simplify to

$$\Big[y_1\partial_{y_1}+y_2\partial_{y_2}+j_{1'}+j_{2'}+\partial_{x_1}x_1-(j_1+j_2)\Big]K(x_1,y_1+y_2-x_1;y_1,y_2)=0 \tag{3.61}$$

$$\Big[y_1\partial^2_{y_1}+y_2\partial^2_{y_2}+2j_{1'}\partial_{y_1}+2j_{2'}\partial_{y_2}-\partial^2_{x_1}x_1+2j_1\partial_{x_1}\Big]K(x_1,y_1+y_2-x_1;y_1,y_2)=0 \tag{3.62}$$

where one uses j_n and $j_{n'}$ to refer to the conformal spins of the incoming and outgoing particles, respectively. Similarly, for three-particle transitions, one gets

$$\Big[\sum_{i=1}^{3}\Big(y_i\partial_{y_i}+j_{i'}\Big)+\partial_{x_1}x_1-(j_1+j_2)\Big]K(x_1,\sum_{i=1}^{3}y_i-x_1;y_1,y_2,y_3)=0\,, \tag{3.63}$$

$$\Big[\sum_{i=1}^{3}\Big(y_i\partial^2_{y_i}+2j_{i'}\partial_{y_i}\Big)-\partial^2_{x_1}x_1+2j_1\partial_{x_1}\Big]K(x_1,\sum_{i=1}^{3}y_i-x_1;y_1,y_2,y_3)=0\,. \tag{3.64}$$

3.4 One-Loop Kernels

In this section one reports on our findings of all nonsinglet transition kernels. The latter will be quoted away from kinematical boundaries, i.e., when some of the momentum fractions (or their sums) could coincide. This will be sufficient to compare our results with

the Fourier transform of the light-ray evolution kernel derived in Ref. [78] by dropping all contact, i.e., delta-function, terms emerging from the latter. Of course, one can keep track of the latter as well and reproduce them from the momentum-fraction formalism by properly incorporating QCD field renormalization (as well as certain contact terms stemming from vertex graphs) into the game. Since the light-cone gauge explicitly breaks Lorentz symmetry, the good and bad components receive different renormalization constants, as can be immediately seen from the quark and gluon propagators [74, 84]

$$\mathcal{P}(k) = Z_1^{(q)}(k)\frac{\not{k}}{k^2+i0}Z_2^{(q)}(k)\,, \qquad G_{\mu\nu}(k) = Z_{\mu\rho}^{(g)}(k)\frac{d^{\rho\sigma}(k)}{k^2+i0}Z_{\sigma\nu}^{(g)}(k)\,, \tag{3.65}$$

computed to one-loop accuracy. Here the Z-factors become momentum-fraction dependent (contrary to covariant gauges) due to assumed principal value prescription for the $1/k_+$-pole in the gluon density matrix,

$$Z_1^{(q)}(k) = \sqrt{1-\Sigma_1}\left(1-(\Sigma_2(k)-\Sigma_1)\frac{\not{k}\gamma^+}{k^+}\right), \tag{3.66}$$

$$Z_2^{(q)}(k) = \sqrt{1-\Sigma_1}\left(1-(\Sigma_2(k)-\Sigma_1)\frac{\gamma^+\not{k}}{k^+}\right), \tag{3.67}$$

$$Z_{\mu\rho}^{(g)}(k) = \sqrt{1+\Pi_1(k)}\left(g_{\mu\rho}-\frac{1}{2}\Pi_2(k)\frac{k_\mu n_\rho + k_\rho n_\mu}{k^+}\right), \tag{3.68}$$

where

$$\Sigma_1 = \frac{\alpha_s C_F}{2\pi}\ln\mu\,, \qquad \Sigma_2(k) = \frac{\alpha_s C_F}{2\pi}\ln\mu\int dq^+\frac{k^+}{k^+-q^+}\vartheta_{11}^0(q^+,q^+-k^+)\,, \tag{3.69}$$

and

$$\Pi_1(k) = \frac{\alpha_s}{\pi}\ln\mu\left[C_A\int dq^+\frac{[(q^+)^2-q^+k^++(k^+)^2]^2}{q^+(q^+-k^+)(k^+)^2}\vartheta_{11}^0(q^+,q^+-k^+)-\frac{n_f}{3}\right], \tag{3.70}$$

$$\begin{aligned}\Pi_2(k) = {}& \frac{\alpha_s}{2\pi}C_A\ln\mu \\ & \times\int dq^+\frac{5q^+(q^+-k^+)(k^+)^2+6(q^+)^2(q^+-k^+)^2+2(k^+)^4}{q^+(q^+-k^+)(k^+)^2}\vartheta_{11}^0(q^+,q^+-k^+)\,,\end{aligned} \tag{3.71}$$

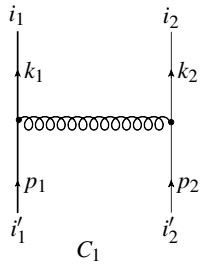

Figure 3.1: Feynman diagram determining the two-to-two transition of quark fields studied in Sec. 3.4.1.

for quark and gluon, respectively. Their contribution to the renormalization of the operator blocks reads

$$\Gamma_{\mu_1\ldots\mu_n} \to Z_2^{(q)}\Gamma_{\mu_1\ldots\mu_n}Z_1^{(q)}Z_{\mu_1\nu_1}^{(g)}\ldots Z_{\mu_n\nu_n}^{(g)}, \tag{3.72}$$

where $\Gamma_{\mu_1\ldots\mu_n}$ is the Dirac-Lorentz tensor defining the composite operator in question. The collinearly divergent integrals entering Σ's and Π's regulate the end-point singularities in the momentum-fraction kernels, promoting them to conventional plus-distributions that become integrable over the entire range of momentum fractions [86].

3.4.1 Two-to-Two Transitions: Quasipartonic Operators

To make our expressions more compact, one introduces a set color structures with open indices that show up in our expressions,

$$\begin{aligned}
&[C_1]^{i_1 i_2}_{i_1' i_2'} = (t^a)_{i_1 i_1'}(t^a)_{i_2 i_2'}, \qquad [C_2]^{ai}_{a'i'} = f^{aa'c}(t^c)_{ii'}, \qquad [C_3]^{ai}_{a'i'} = (t^{a'}t^a)_{ii'}\\
&[C_4]^{i_1 i_2}_{i_1' i_2'} = (t^a)_{i_1 i_2}(t^a)_{i_1' i_2'}, \qquad [\tilde{C}_4]^{i_1 i_2}_{i_1' i_2'} = (t^a)_{i_1 i_2}(\bar{t}^a)_{i_1' i_2'}, \qquad [C_5]^{i_1 i_2}_{ab} = (t^a t^b)_{i_1 i_2},\\
&[C_6]^{i_1 i_2}_{ab} = (t^b t^a)_{i_1 i_2}, \qquad [C_7]^{ab}_{a'b'} = f^{aa'c}f^{bb'c}, \qquad [C_8]^{ab}_{a'b'} = f^{a'bc}f^{ab'c}.
\end{aligned} \tag{3.73}$$

where f^{abc} is the $SU(N)$ structure constants, while t^a and $\bar{t}^a$ are the $SU(N)$ and $SU(\bar{N})$ generators in the fundamental representation and its conjugate, respectively.

The first set of operators under investigation is written as,

$$\mathcal{O}^{i_1 i_2}(x_1,x_2) = \{\psi_+^{i_1}\psi_+^{i_2},\, \psi_+^{i_1}\chi_+^{i_2},\, \bar{\psi}_+^{i_1}\bar{\psi}_+^{i_2},\, \bar{\psi}_+^{i_1}\bar{\chi}_+^{i_2},\, \chi_+^{i_1}\chi_+^{i_2},\, \bar{\chi}_+^{i_1}\bar{\chi}_+^{i_2}\}(x_1,x_2)$$

In this quark-quark sector the fields have open fundamental color indices i_1 and i_2. The operator renormalization kernel acts on them as follows:

$$[\mathcal{K}\mathcal{O}]^{i_1 i_2}(x_1,x_2) = [C_1]^{i_1 i_2}_{i_1' i_2'} \int [\mathcal{D}^2 y]_2 K(x_1,x_2|y_1,y_2)\mathcal{O}^{i_1' i_2'}(y_1,y_2), \tag{3.74}$$

and its explicit expression arises from the graph shown in Fig. 3.1. It is given by

$$K(x_1,x_2|y_1,y_2) = -2\frac{x_1+x_2}{x_1-y_1}\vartheta^0_{111}(x_1,x_1-y_1,-x_2) - \frac{4x_2}{x_1-y_1}\vartheta^0_{11}(x_1-y_1,-x_2). \tag{3.75}$$

$$\mathcal{O}^{i_1 i_2}(x_1,x_2) = \{\psi_+^{i_1}\bar{\chi}_+^{i_2},\, \bar{\psi}_+^{i_1}\chi_+^{i_2},\, \psi_+^{i_1}\bar{\psi}_+^{i_2},\, \bar{\chi}_+^{i_1}\chi_+^{i_2}\}(x_1,x_2)$$

For the nonsinglet sector, the Feynman diagram responsible for the evolution is determined by the very same one-gluon exchange in Fig. 3.1, so that

$$[\mathcal{K}\mathcal{O}]^{i_1 i_2}(x_1,x_2) = [C_1]^{i_1 i_2}_{i_1' i_2'} \int [\mathcal{D}^2 y]_2 K(x_1,x_2|y_1,y_2)\mathcal{O}^{i_1' i_2'}(y_1,y_2)\,, \tag{3.76}$$

where

$$K(x_1,x_2|y_1,y_2) = -\frac{4x_2}{x_1-y_1}\vartheta^0_{11}(x_1-y_1,-x_2) - \frac{x_2+y_1}{x_1-y_1}\vartheta^0_{111}(x_1,x_1-y_1,-x_2)\,. \tag{3.77}$$

For the quark-antiquark operators of the same flavor $\Phi^{i_1}(x_1)\Phi^{i_2}(x_2)$
$= \{\psi_+^{i_1}(x_1)\bar{\psi}_+^{i_2}(x_2),\, \bar{\chi}_+^{i_1}(x_1)\chi_+^{i_2}(x_2)\}$, there are two extra transitions, corresponding to annihilation channels. Although one does not focus on the flavor-singlet quark operators and the operators built up solely by gluon fields, one does provide corresponding results for the $2 \to 2$ evolution kernels in Appendix B.2.

Next consider the evolution kernels of quark-gluon fields,

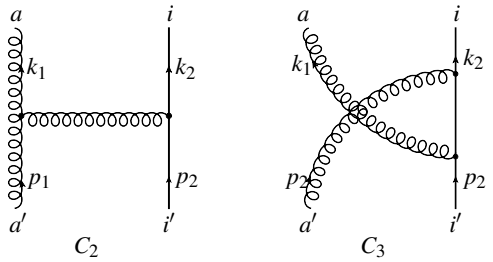

Figure 3.2: Feynman diagrams of two-to-two transition of quasipartonic gluon-quark fields in Sec. (3.4.1).

$$\mathcal{O}^{ai}(x_1,x_2) = \{f^a_{++}\psi^i_+, f^a_{++}\chi^i_+, \bar{f}^a_{++}\bar{\psi}^i_+, \bar{f}^a_{++}\bar{\chi}^i_+\}(x_1,x_2)$$

For the quark-gluon operator blocks, the renormalization opens up more than one color channel,

$$[\mathcal{K}\mathcal{O}]^{ai}(x_1,x_2) = -\int [\mathcal{D}^2 y]_2 \left\{[C_2]^{ai}_{a'i'}K_1 + [C_3]^{ai}_{a'i'}K_2\right\}(x_1,x_2|y_1,y_2)\mathcal{O}^{a'i'}(y_1,y_2)\,, \quad (3.78)$$

with corresponding transition kernels calculated from the graphs shown in Fig. 3.2 being

$$K_1(x_1,x_2;y_1,y_2) = \frac{x_1}{y_1}\frac{2x_1}{x_1-y_1}\vartheta^0_{11}(x_1,x_1-y_1) - \frac{2x_2}{x_1-y_1}\vartheta^0_{11}(x_1-y_1,-x_2)\,, \quad (3.79)$$

$$K_2(x_1,y_1;y_1,y_2) = \frac{2x_2}{y_1}\vartheta^0_{11}(x_1-y_2,-x_2)\,. \quad (3.80)$$

Last but not least, the evolution kernels for antiquark-gluon operators are

$$\mathcal{O}^{ai}(x_1,x_2) = \{f^a_{++}\bar{\psi}^i_+, f^a_{++}\bar{\chi}^i_+, \bar{f}^a_{++}\psi^i_+, \bar{f}^a_{++}\chi^i_+\}(x_1,x_2)$$

Similar results are obtained by replacing the quark and an antiquark field,

$$[\mathcal{K}\mathcal{O}]^{ai}(x_1,x_2) = -\int [\mathcal{D}^2 y]_2 \left\{[C_2]^{ai}_{a'i'}K_1 + [C_3]^{ai}_{a'i'}K_2\right\}(x_1,x_2|y_1,y_2)\mathcal{O}^{a'i'}(y_1,y_2)\,, \quad (3.81)$$

with

$$K_1(x_1,x_2|y_1,y_2) = \frac{2x_1x_2\vartheta^0_{11}(x_1,-x_2)}{y_1(x_1+x_2)} - \frac{2(x_1x_2+y_1^2)\vartheta^0_{111}(x_1,x_1-y_1,-x_2)}{(x_1-y_1)y_1}$$

$$-\frac{2x_2(x_1+y_1)\vartheta_{11}^0(x_1-y_1,-x_2)}{(x_1-y_1)y_1}\,, \tag{3.82}$$

$$K_2(x_1,x_2|y_1,y_2)=-2\frac{x_1-y_2}{y_1}\vartheta_{111}^0(x_1,x_1-y_2,-x_2)+\frac{2x_1x_2}{y_1(x_1+x_2)}\vartheta_{11}^0(x_1,-x_2)\,. \tag{3.83}$$

The Feynman graphs involved in the analysis differ from those in Fig. 3.2 only by the orientation of one of the quark lines.

All of these expressions agree with well-known particle transitions for quasipartonic operators [71, 74, 72, 76, 78].

3.4.2 Two-to-Two Transitions: Non-Quasipartonic Operators

Now, one turns to the analysis of non-quasipartonic operators. According to the adopted basis (3.25), the new two-particle blocks that one has to address contain a bad field component accompanied by a good one, namely

$$\begin{aligned}&\Phi_+(z_1)\otimes\Phi_-(z_2)\,, \qquad \Phi_-(z_1)\otimes\Phi_+(z_2)\\ &\Phi_+(z_1)\otimes D_{-+}\Phi_+(z_2)\,, \qquad D_{-+}\Phi_+(z_1)\otimes\Phi_+(z_2)\,.\end{aligned} \tag{3.84}$$

Quark-Quark Transitions

To start with, one considers the quark-quark transitions first. To this end, one introduces non-quasipartonic two-particle operators built up from primary fields and arranged as doublets since they mix under renormalization group evolution,

$$\mathcal{O}_+^{ij}=\left\{\begin{pmatrix}\psi_-^i\psi_+^j\\ \psi_+^i\psi_-^j\end{pmatrix},\begin{pmatrix}\psi_-^i\chi_+^j\\ \psi_+^i\chi_-^j\end{pmatrix},\begin{pmatrix}\chi_-^i\psi_+^j\\ \chi_+^i\psi_-^j\end{pmatrix},\begin{pmatrix}\chi_-^i\chi_+^j\\ \chi_+^i\chi_-^j\end{pmatrix}\right\}, \tag{3.85}$$

$$\mathcal{O}_-^{ij}=\left\{\begin{pmatrix}\psi_+^i\bar{D}_{-+}\psi_+^j\\ \bar{D}_{-+}\psi_+^i\psi_+^j\end{pmatrix},\begin{pmatrix}\psi_+^i\bar{D}_{-+}\chi_+^j\\ \bar{D}_{-+}\psi_+^i\chi_+^j\end{pmatrix},\begin{pmatrix}\chi_+^i\bar{D}_{-+}\psi_+^j\\ \bar{D}_{-+}\chi_+^i\psi_+^j\end{pmatrix},\begin{pmatrix}\chi_+^i\bar{D}_{-+}\chi_+^j\\ \bar{D}_{-+}\chi_+^i\chi_+^j\end{pmatrix}\right\}. \tag{3.86}$$

The Feynman diagram responsible for the mixing addressed in this section is the same one as in Fig. 3.1. We elaborate on an example of a specific transition in great detail in

Appendix B.1, to demonstrate the inner workings of the formalism. As a result, one finds

$$[\mathcal{K}\mathcal{O}_+]^{ij}(x_1,x_2) = -[C_1]^{ij}_{i'j'}\int[\mathcal{D}^2y]_2 K(x_1,x_2|y_1,y_2)\mathcal{O}_+^{i'j'}(y_1,y_2)\,, \tag{3.87}$$

where the two-by-two mixing matrix

$$K = \begin{pmatrix} K_{11} & K_{12} \\ K_{21} & K_{22} \end{pmatrix} \tag{3.88}$$

possesses the elements

$$K_{11}(x_1,x_2;y_1,y_2) = \frac{2y_1}{x_1-y_1}\vartheta^0_{11}(x_1,x_1-y_1) - \frac{2x_2}{x_1-y_1}\vartheta^0_{11}(x_1-y_1,-x_2)\,, \tag{3.89}$$

$$K_{12}(x_1,x_2,y_1,y_2) = 2\vartheta^0_{11}(x_1,x_1-y_1)\,, \tag{3.90}$$

$$K_{21}(x_1,x_2;y_1,y_2) = 2\vartheta^0_{11}(x_1-y_1,-x_2)\,, \tag{3.91}$$

$$K_{22}(x_1,x_2;y_1,y_2) = \frac{2x_1}{x_1-y_1}\vartheta^0_{11}(x_1,x_1-y_1) - \frac{2y_2}{x_1-y_1}\vartheta^0_{11}(x_1-y_1,-x_2)\,. \tag{3.92}$$

For $\mathcal{O}_-^{ij}$ operator sets, one similarly gets

$$[\mathcal{K}\mathcal{O}_-]^{ij}(x_1,x_2) = -[C_1]^{i_1i_2}_{i'_1i'_2}\int[\mathcal{D}^2y]_2 K(x_1,x_2|y_1,y_2)\mathcal{O}_-^{i'j'}(y_1,y_2)\,, \tag{3.93}$$

where

$$\begin{aligned} K_{11}(x_1,x_2;y_1,y_2) &= \frac{4x_2\vartheta^0_{11}(x_1-y_1,-x_2)}{x_2-y_2} + \frac{2(x_1+x_2)\vartheta^0_{111}(x_1,x_1-y_1,-x_2)}{x_2-y_2} \\ &\quad + \frac{4x_2\vartheta^0_{12}(x_1-y_1,-x_2)}{x_2-y_2} + \frac{2(x_1+x_2)\vartheta^0_{112}(x_1,x_1-y_1,-x_2)}{x_2-y_2}\,, \end{aligned} \tag{3.94}$$

$$\begin{aligned} K_{12}(x_1,x_2;y_1,y_2) &= 2\frac{(y_1+y_2)(\vartheta^0_{112}(x_1,x_1-y_1,-x_2)+\vartheta^0_{121}(x_1,x_1-y_1,-x_2))}{x_2-y_2} \\ &\quad + \frac{2(x_1+y_1+y_2)\vartheta^0_{111}(x_1,x_1-y_1,-x_2)}{x_2-y_2} + \frac{4x_2\vartheta^0_{11}(x_1-y_1,-x_2)}{x_2-y_2} \\ &\quad + \frac{4x_2(\vartheta^0_{12}(x_1-y_1,-x_2)+\vartheta^0_{21}(x_1-y_1,-x_2))}{x_2-y_2}\,, \end{aligned} \tag{3.95}$$

$$\begin{aligned} K_{21}(x_1,x_2;y_1,y_2) &= \frac{2(y_1+y_2)\vartheta^0_{112}(x_1,x_1-y_1,-x_2)}{x_1-y_1} + \frac{2x_1\vartheta^0_{111}(x_1,x_1-y_1,-x_2)}{x_1-y_1} \\ &\quad + \frac{4x_2\vartheta^0_{12}(x_1-y_1,-x_2)}{x_1-y_1}\,, \end{aligned} \tag{3.96}$$

$$K_{22}(x_1,x_2;y_1,y_2) = \frac{2(y_1+y_2)(\vartheta^0_{112}(x_1,x_1-y_1,-x_2)+\vartheta^0_{121}(x_1,x_1-y_1,-x_2))}{y_2-x_2} + \frac{4x_2(\vartheta^0_{12}(x_1-y_1,-x_2)+\vartheta^0_{21}(x_1-y_1,-x_2))}{y_2-x_2} + \frac{2x_1\vartheta^0_{111}(x_1,x_1-y_1,-x_2)}{y_2-x_2}. \tag{3.97}$$

This concludes our discussion of non-singlet operators. In Appendix B.2.2, one also provides transitions into gluonic operators involved in this class when it is generalized to the singlet channel as well.

Quark-Antiquark Transitions

Next, one introduces doublets of quark-antiquark fields,

$$\mathcal{O}^{ij} = \left\{ \begin{pmatrix} \psi^i_- \bar\psi^j_+ \\ \psi^i_+ \frac{1}{2} D_{-+} \bar\psi^j_+ \end{pmatrix}, \begin{pmatrix} \psi^i_- \bar\chi^j_+ \\ \psi^i_+ \frac{1}{2} D_{-+} \bar\chi^j_+ \end{pmatrix}, \begin{pmatrix} \chi^i_- \bar\psi^j_+ \\ \chi^i_+ \frac{1}{2} D_{-+} \bar\psi^j_+ \end{pmatrix}, \begin{pmatrix} \chi^i_- \bar\chi^j_+ \\ \chi^i_+ \frac{1}{2} D_{-+} \bar\chi^j_+ \end{pmatrix} \right\}, \tag{3.98}$$

where one assumes that the two-particle blocks possess different flavor such that they do not undergo annihilation transitions into gluon fields. Then the evolution equation can be written as

$$[\mathcal{K}\mathcal{O}]^{ij}(x_1,x_2) = -[C_1]^{ij}_{i'j'} \int [\mathcal{D}^2 y]_2 K(x_1,x_2|y_1,y_2)\mathcal{O}^{i'j'}(y_1,y_2). \tag{3.99}$$

with the elements of the evolution matrix given by

$$K_{11} = \frac{2x_1y_1(y_1+x_2)\vartheta^0_{11}(x_1,x_1-y_1)}{(y_1+y_2)^2(y_2-x_2)} + \frac{2y_2\vartheta^0_{11}(x_1,-x_2)}{x_1-y_1} + \frac{2\left(y_2^2(y_1+y_2)+y_1x_2(y_1+2y_2)+y_2x_2^2\right)\vartheta^0_{11}(x_1-y_1,-x_2)}{(y_1+y_2)^2(x_2-y_2)}, \tag{3.100}$$

$$K_{12} = \frac{2x_1(y_1+x_2)\vartheta^0_{11}(x_1,x_1-y_1)}{(y_1+y_2)^2(x_2-y_2)} + \frac{2\vartheta^0_{11}(x_1,-x_2)}{x_1-y_1} - \frac{2\left(y_2^2(y_1+y_2)+x_2^2(y_1+2y_2)-y_2x_2(y_1+2y_2)\right)\vartheta^0_{11}(x_1-y_1,-x_2)}{y_2(y_1+y_2)^2(y_2-x_2)}, \tag{3.101}$$

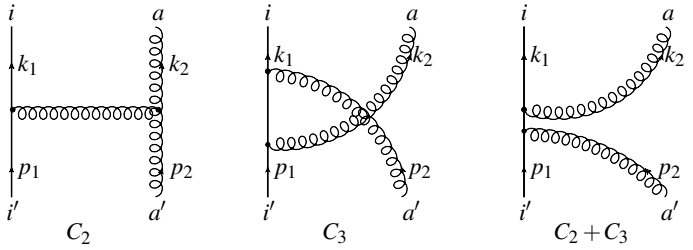

Figure 3.3: Feynman diagrams corresponding to two-to-two transition of non-quasipartonic quark-gluon blocks in Sect. (3.4.2).

$$K_{21} = \frac{2x_1^2 y_1 (y_1+x_2)\vartheta_{11}^0(x_1,x_1-y_1)}{(y_1+y_2)^2(x_2-y_2)} - \frac{2x_1(x_1-2y_1)\vartheta_{11}^0(x_1,-x_2)}{x_1-y_1}$$
$$+ \frac{2y_2\left(x_1^3 - x_1^2(2y_1+y_2) + x_1(y_1+y_2)^2 - y_1(y_1+y_2)^2\right)\vartheta_{11}^0(x_1-y_1,-x_2)}{(y_1+y_2)^2(y_2-x_2)}, \quad (3.102)$$

$$K_{22} = \frac{2x_1^2(y_1+x_2)\vartheta_{11}^0(x_1,x_1-y_1)}{(y_1+y_2)^2(x_2-y_2)} - \frac{2x_1(2y_1+x_2)\vartheta_{11}^0(x_1,-x_2)}{y_1(x_2-y_2)}$$
$$+ \frac{2}{y_1y_2(y_1+y_2)^2(y_2-x_2)}\left\{x_1^2\left(2y_1^3+6y_1^2y_2+4y_1y_2^2+y_2^3\right) - x_1^3y_1(y_1+2y_2)\right.$$
$$\left. - x_1(y_1+y_2)^4 - y_1y_2^2(y_1+y_2)^2\right\}\vartheta_{11}^0(x_1-y_1,-x_2). \quad (3.103)$$

Quark-Gluon Transitions

For the operators involving one quark and one gluon field, one introduces the following two-vectors:

$$\mathcal{O}_+^{ia} = \left\{ \begin{pmatrix} \psi_-^i f_{++}^a \\ \psi_+^i f_{+-}^a \end{pmatrix}, \begin{pmatrix} \chi_-^i f_{++}^a \\ \chi_+^i f_{+-}^a \end{pmatrix} \right\}, \quad (3.104)$$

$$\mathcal{O}_-^{ia} = \left\{ \begin{pmatrix} \psi_+^i \left[\bar{D}_{-+} f_{++}\right]^a \\ \left[D_{-+}\psi_+\right]^i f_{++}^a \end{pmatrix}, \begin{pmatrix} \chi_+^i \left[\bar{D}_{-+} f_{++}\right]^a \\ \left[D_{-+}\chi_+\right]^i f_{++}^a \end{pmatrix} \right\}. \quad (3.105)$$

Then, calculating Feynman diagrams responsible for their one-loop renormalization exhibited in Fig. 3.3, one deduces that, as in the quasipartonic case, there are two color-flow channels that induce the transitions

$$[\mathcal{K}\mathcal{O}_+]^{ia}(x_1,x_2) = -\int [\mathcal{D}^2 y]_2 \Big\{ [C_2]_{a'i'}^{ai} K(x_1,x_2|y_1,y_2)$$

$$- [C_3]^{ai}_{a'i'} \widetilde{K}(x_1,x_2|y_1,y_2)\Big\} \mathcal{O}_+^{i'a'}(y_1,y_2)\,, \tag{3.106}$$

where the elements of the kernels K_{ij} and $\widetilde{K}_{ij}$ admit the form

$$\begin{aligned}
K_{11} &= \frac{y_1(2y_2^2(y_1+y_2)^2 - y_2(y_1+y_2)(3y_1+2y_2)x_2)\vartheta^0_{11}(x_1,x_1-y_1)}{y_2^2(y_1+y_2)^2(y_2-x_2)} \\
&+ \frac{x_2((y_1+y_2)(3y_1+2y_2)+(y_1+2y_2)x_2)\vartheta^0_{11}(x_1-y_1,-x_2)}{(y_1+y_2)^2(x_2-y_2)} \\
&+ \frac{x_2((2y_1^2+y_1y_2-2y_2^2)x_2 - 3y_1y_2(y_1+y_2))\vartheta^0_{11}(x_1,-x_2)}{y_2^2(y_1+y_2)(x_2-y_2)} \\
&+ \frac{y_1^2x_2^2(2y_1+3y_2)\vartheta^0_{11}(x_1,x_1-y_1)}{y_2^2(y_1+y_2)^2(y_2-x_2)} + \frac{2x_2\vartheta^0_{11}(x_1,-x_2)}{y_2}\,,
\end{aligned} \tag{3.107}$$

$$\begin{aligned}
K_{12} &= \frac{2x_1(y_2(y_1+y_2)+y_1x_2)\vartheta^0_{11}(x_1,x_1-y_1)}{(y_1+y_2)^2(y_2-x_2)} \\
&+ \frac{2x_2(x_2-2(y_1+y_2))\vartheta^0_{11}(x_1,-x_2)}{(y_1+y_2)(y_2-x_2)} \\
&+ \frac{2y_2x_2(x_2-2(y_1+y_2))\vartheta^0_{11}(x_1-y_1,-x_2)}{(y_1+y_2)^2(x_2-y_2)}\,,
\end{aligned} \tag{3.108}$$

$$\begin{aligned}
K_{21} &= -\frac{x_1^2y_1\vartheta^0_{11}(x_1,x_1-y_1)}{y_2(x_1-y_1)(y_1+y_2)} + \frac{x_1^2\vartheta^0_{11}(x_1,-x_2)}{y_2(x_1-y_1)} \\
&- \frac{\left(x_2^2(2y_1+3y_2) - 4y_2x_2(y_1+y_2) + y_2(y_1+y_2)^2\right)\vartheta^0_{11}(x_1-y_1,-x_2)}{y_2(y_1+y_2)(y_2-x_2)}\,,
\end{aligned} \tag{3.109}$$

$$\begin{aligned}
K_{22} &= -\frac{\left(x_1^2y_2 + 2x_1\left(y_2^2-y_1^2\right) + 2y_1(y_1+y_2)^2\right)\vartheta^0_{11}(x_1-y_1,-x_2)}{y_1(x_1-y_1)(y_1+y_2)} \\
&- \frac{x_1^2\vartheta^0_{11}(x_1,x_1-y_1)}{(x_1-y_1)(y_1+y_2)} + \frac{x_1(x_1+2(y_1+y_2))\vartheta(x_1,-x_2)}{y_1(x_1-y_1)}\,,
\end{aligned} \tag{3.110}$$

$$\widetilde{K}_{11} = \frac{2x_2\vartheta^0_{11}(x_1,-x_2)}{y_2} + \frac{2y_1\vartheta^0_{111}(x_1,x_1-y_2,-x_2)}{y_2}\,, \tag{3.111}$$

$$\widetilde{K}_{12} = 2\vartheta^0_{12}(x_1,x_1-y_2) - \frac{2y_1\vartheta^0_{111}(x_1,x_1-y_2,-x_2)}{y_2} - \frac{2x_2\vartheta^0_{11}(x_1,-x_2)}{y_2}\,, \tag{3.112}$$

$$\widetilde{K}_{21} = \frac{2x_1(y_1\vartheta^1_{111}(x_1,x_1-y_2,-x_2) - \vartheta^0_{11}(x_1,-x_2)}{y_2}\,, \tag{3.113}$$

$$\widetilde{K}_{22} = 0\,. \tag{3.114}$$

Similarly for the operators in the $\mathcal{O}_-$ group, one gets

$$[\mathcal{K}\,\mathcal{O}_-]^{ia}(x_1,x_2) = -\int [\mathcal{D}^2y]_2 \Big\{ [C_2]^{ai}_{a'i'} K(x_1,x_2|y_1,y_2)$$

$$+[C_3]^{ai}_{a'i'}\widetilde{K}(x_1,x_2|y_1,y_2)\Big\}\mathcal{O}^{i'a'}_{-}(y_1,y_2)\,, \tag{3.115}$$

with

$$K_{11}=-2\frac{x_1^2\vartheta^0_{11}(x_1,x_1-y_1)}{(x_1-y_1)(y_1+y_2)}+2\frac{x_1(x_1+y_1+y_2)\vartheta^0_{11}(x_1,-x_2)}{y_1(x_1-y_1)}$$
$$-2\frac{\left(2y_2^3(y_1+y_2)^2-3y_2^3x_2(y_1+y_2)+y_1x_2^3(y_1+y_2)+y_2^3x_2^2\right)\vartheta^0_{11}(x_1-y_1,-x_2)}{y_1y_2^2(y_1+y_2)(y_2-x_2)}\,, \tag{3.116}$$

$$K_{12}=\frac{2x_1(y_1(y_1+y_2)-x_1y_2)\vartheta^0_{11}(x_1,-x_2)}{(x_1-y_1)y_1^2}-\frac{2x_1^2\vartheta^0_{11}(x_1,x_1-y_1)}{(x_1-y_1)(y_1+y_2)}$$
$$+\frac{2x_1y_2(x_1y_2-y_1(y_1+y_2))\vartheta^0_{11}(x_1-y_1,-x_2)}{(x_1-y_1)y_1^2(y_1+y_2)}\,, \tag{3.117}$$

$$K_{21}=\frac{2x_1^2\vartheta^0_{11}(x_1,x_1-y_1)}{(x_1-y_1)(y_1+y_2)}-\frac{2x_1^2\vartheta^0_{11}(x_1,-x_2)}{y_1(x_1-y_1)}$$
$$+\frac{2(x_2^3y_1(y_1+y_2)+(x_1^2-x_2^2)y_2^3-x_2^2y_2(y_1^2+y_1y_2-y_2^2))\vartheta^0_{11}(x_1-y_1,-x_2)}{y_1y_2^2(y_1+y_2)(y_2-x_2)}\,, \tag{3.118}$$

$$K_{22}=\frac{2x_1^2y_2\vartheta^0_{11}(x_1,-x_2)}{y_1^2(x_1-y_1)}+\frac{2x_1^2\vartheta^0_{11}(x_1,x_1-y_1)}{(x_1-y_1)(y_1+y_2)}$$
$$-\frac{2\left(x_2^2\left(y_1^3+y_1^2y_2+y_2^3\right)-2y_2^3x_2(y_1+y_2)+y_2^3(y_1+y_2)^2\right)\vartheta(x_1-y_1,-x_2)}{y_1^2y_2(y_1+y_2)(y_2-x_2)}\,, \tag{3.119}$$

$$\widetilde{K}_{11}=2\frac{x_1(\vartheta^0_{11}(x_1,x_1-y_2)+\vartheta^0_{12}(x_1,x_1-y_2))}{y_2}\,, \tag{3.120}$$

$$\widetilde{K}_{12}=\frac{2x_1\vartheta^0_{11}(x_1,x_1-y_2)}{y_2}\,, \tag{3.121}$$

$$\widetilde{K}_{21}=-\frac{2x_1\vartheta^0_{12}(x_1,x_1-y_2)}{y_2}\,, \tag{3.122}$$

$$\widetilde{K}_{22}=0\,. \tag{3.123}$$

Having studied the operators generated by primary fields with the same chiralities, one now turns our attention to the cases where the operators are built up by fields of opposite chiralities, namely,

$$\mathcal{O}^{ia}=\left\{\begin{pmatrix}\psi^i_-\bar{f}^a_{++}\\ \psi^i_+\frac{1}{2}D_{-+}\bar{f}^a_{++}\end{pmatrix},\begin{pmatrix}\chi^i_-\bar{f}^a_{++}\\ \chi^i_+\frac{1}{2}D_{-+}\bar{f}^a_{++}\end{pmatrix}\right\}. \tag{3.124}$$

Their one-loop evolution equation is driven by

$$[\mathcal{K}\,\mathcal{O}]^{ia}(x_1,x_2) = -\int [\mathcal{D}^2 y]_2 \Big\{ [C_2]^{ai}_{a'i'} K(x_1,x_2|y_1,y_2) \\ - [C_3]^{ai}_{a'i'} \widetilde{K}(x_1,x_2|y_1,y_2) \Big\} \mathcal{O}^{i'a'}(y_1,y_2)\,, \tag{3.125}$$

and the transition kernels involved read,

$$\begin{aligned}
K_{11} &= \frac{2\left(y_1 x_2^3 + y_2(y_1+y_2)^3 - y_1 x_2^2(y_1+2y_2)\right)\vartheta_{11}^0(x_1,-x_2)}{y_2(y_1+y_2)^2(y_2-x_2)} \\
&\quad - \frac{2\left(y_2^2(y_1+y_2)^2 + y_1 x_2^2(y_1+y_2) + y_2 x_2^3\right)\vartheta_{11}^0(x_1-y_1,-x_2)}{y_2(y_1+y_2)^2(y_2-x_2)} \\
&\quad + \frac{2x_1 x_2^2 y_1 \vartheta_{11}^0(x_1,x_1-y_1)}{y_2(x_1-y_1)(y_1+y_2)^2}\,, \qquad (3.126)\\
K_{12} &= \frac{2x_2^2(x_1+y_2)\vartheta_{11}^0(x_1,-x_2)}{y_2(x_1-y_1)(y_1+y_2)^2} - \frac{2x_1 x_2^2 \vartheta_{11}^0(x_1,x_1-y_1)}{y_2(x_1-y_1)(y_1+y_2)^2} \\
&\quad + \frac{2x_2^2(x_1(y_1+2y_2)-(y_1+y_2)^2)\vartheta_{11}^0(x_1-y_1,-x_2)}{y_2^2(x_1-y_1)(y_1+y_2)^2}\,, \qquad (3.127)\\
K_{21} &= \frac{2x_1^2 y_1\left(y_1 y_2 + x_2^2\right)\vartheta_{11}^0(x_1,x_1-y_1)}{y_2(y_1+y_2)^2(y_2-x_2)} \\
&\quad - \frac{2x_1\left(x_2^2\left(y_1^2+3y_1y_2+y_2^2\right) + y_2(y_1-y_2)(y_1+y_2)^2 - y_1 x_2^3\right)\vartheta_{11}^0(x_1,-x_2)}{y_2(y_1+y_2)^2(y_2-x_2)} \\
&\quad + \frac{2\left(x_1^4 - 2x_1^3(y_1+y_2) + x_1^2\left(y_1^2+3y_1y_2+y_2^2\right)\right)\vartheta_{11}^0(x_1-y_1,-x_2)}{(y_1+y_2)^2(y_2-x_2)} \\
&\quad + \frac{2(y_1-x_1)y_2\vartheta_{11}^0(x_1-y_1,-x_2)}{(y_2-x_2)}\,, \qquad (3.128)\\
K_{22} &= \frac{2x_1\left(x_2^2\left(y_1^2+3y_1y_2+y_2^2\right) + 2y_1y_2(y_1+y_2)^2 - y_1x_2^3\right)\vartheta_{11}^0(x_1,-x_2)}{y_1y_2(y_1+y_2)^2(y_2-x_2)} \\
&\quad + \frac{2x_1^2\left(y_1y_2+x_2^2\right)\vartheta_{11}^0(x_1,x_1-y_1)}{y_2(y_1+y_2)^2(x_2-y_2)} + \frac{2}{y_1y_2^2(y_1+y_2)^2(y_2-x_2)}\Big\{2y_1y_2^3x_2(y_1+y_2) \\
&\quad - x_2^3(y_1+y_2)\left(y_1^2+2y_1y_2-y_2^2\right) - y_2^2x_2^2\left(y_1^2+3y_1y_2+y_2^2\right) - y_1x_2^4(y_1+2y_2) \\
&\quad - 2y_1y_2^3(y_1+y_2)^2\Big\}\vartheta_{11}^0(x_1-y_1,-x_2)\,, \qquad (3.129)\\
\widetilde{K}_{11} &= \frac{2x_1^2y_1^2\vartheta_{11}^0(x_1-y_2,-x_2)}{y_2^2(y_1+y_2)^2} - \frac{2\left(x_1^2y_1(y_1+y_2)+y_2^2x_2^2\right)\vartheta_{11}^0(x_1,-x_2)}{y_2^2(y_1+y_2)^2} \\
&\quad + \frac{2x_1^2y_1\vartheta_{11}^0(x_1,x_1-y_2)}{y_2(y_1+y_2)^2}\,, \qquad (3.130)
\end{aligned}$$

$$
\begin{aligned}
\widetilde{K}_{12} = & -2\frac{x_1^2\vartheta_{11}^0(x_1,x_1-y_2)}{y_2(y_1+y_2)^2} \\
& + \frac{2\left(x_2^2\left(y_1^2+y_1y_2+y_2^2\right)-2y_1^2x_2(y_1+y_2)\right)\vartheta_{11}^0(x_1-y_2,-x_2)}{y_2^3(y_1+y_2)^2} \\
& + \frac{2y_1(y_1-y_2)\vartheta_{11}^0(x_1-y_2,-x_2)}{y_2^3} \\
& + \frac{2\left(2y_1x_2(y_1+y_2)^2-x_2^2\left(y_1^2+2y_1y_2+2y_2^2\right)\right)\vartheta_{11}^0(x_1,-x_2)}{y_2^3(y_1+y_2)^2} \\
& - \frac{2(y_1-y_2)(y_1+y_2)\vartheta_{11}^0(x_1,-x_2)}{y_2^3}, \qquad (3.131) \\
\widetilde{K}_{21} = & \frac{2(x_1-y_2)\left((2y_1-x_2)\vartheta_{111}^0(x_1,x_1-y_2,-x_2)+y_1\vartheta_{112}^0(x_1,x_1-y_2,-x_2)\right)}{y_2} \\
& + \frac{2x_1y_1x_2^2\vartheta_{11}^0(x_1,-x_2)}{y_2(y_1+y_2)^2}, \qquad (3.132) \\
\widetilde{K}_{22} = & \frac{2(x_1-y_2)\left(x_1^2\left(y_1^2+y_1y_2+y_2^2\right)\right)\vartheta_{11}^0(x_1-y_2,-x_2)}{y_2^3(y_1+y_2)^2} \\
& - \frac{2y_2(x_1-y_2)(2y_1+y_2-2x_2)\vartheta_{11}^0(x_1-y_2,-x_2)}{y_2^3} \\
& - \frac{2x_1\left(x_1^2\left(y_1^2+2y_1y_2+2y_2^2\right)-x_1y_2(y_1+y_2)(3y_1+5y_2)\right)\vartheta_{11}^0(x_1,-x_2)}{y_2^3(y_1+y_2)^2} \\
& + \frac{2x_1^2(y_2-x_1)\vartheta_{11}^0(x_1,x_1-y_2)}{y_2(y_1+y_2)^2} - \frac{6x_1\vartheta_{11}^0(x_1,-x_2)}{y_2}. \qquad (3.133)
\end{aligned}
$$

Antiquark-Gluon Transitions

For antiquark-gluon blocks, one introduces the doublets

$$
\mathcal{O}^{ai} = \left\{ \begin{pmatrix} f_{+-}^a\bar{\psi}_+^i \\ f_{++}^a\frac{1}{2}D_{-+}\bar{\psi}_+^i \end{pmatrix}, \begin{pmatrix} f_{+-}^a\bar{\chi}_+^i \\ f_{++}^a\frac{1}{2}D_{-+}\bar{\chi}_+^i \end{pmatrix} \right\}, \qquad (3.134)
$$

whose transitions

$$
\begin{aligned}
[\mathcal{K}\,\mathcal{O}]^{ai}(x_1,x_2) = -\int[\mathcal{D}^2y]_2\Big\{ & [C_2]_{a'i'}^{ai}K(x_1,x_2|y_1,y_2) \\
& + [C_3]_{a'i'}^{ai}\widetilde{K}(x_1,x_2|y_1,y_2)\Big\}\mathcal{O}^{a'i'}(y_1,y_2), \qquad (3.135)
\end{aligned}
$$

are determined by computing Feynman diagrams in Fig. 3.4 and yield

$$
\begin{aligned}
K_{11} &= \frac{2x_1\left(x_1(y_1+y_2)^2-x_1^2y_1+y_1\left(y_1^2+y_1y_2+y_2^2\right)\right)\vartheta_{11}^0(x_1,x_1-y_1)}{y_1(y_1+y_2)^2(y_2-x_2)}\\
&+\frac{2x_1\left(x_1^2y_1(y_1-y_2)+x_1\left(3y_1^2y_2-2y_1^3+4y_1y_2^2+y_2^3\right)\right)\vartheta_{11}^0(x_1,-x_2)}{y_1^2(y_1+y_2)^2(x_2-y_2)}\\
&+\frac{2x_1(y_1-2y_2)\vartheta_{11}^0(x_1,-x_2)}{(y_1+y_2)(x_2-y_2)}\\
&+\frac{2\left(x_1^2(y_1+y_2)^3-x_1^3y_1y_2-x_1y_1^2\left(y_1^2+2y_1y_2+2y_2^2\right)\right)\vartheta_{11}^0(x_1-y_1,-x_2)}{y_1^2(y_1+y_2)^2(y_2-x_2)}\\
&-\frac{2y_2\vartheta_{11}^0(x_1-y_1,-x_2)}{(y_2-x_2)}, \qquad (3.136)\\
K_{12} &= \frac{2x_1\left(x_1(2y_1+y_2)(3y_1+y_2)-2x_1^2y_1-3y_1^2(y_1+y_2)\right)\vartheta_{11}^0(x_1,-x_2)}{y_1^2(y_1+y_2)^2(x_2-y_2)}\\
&+\frac{2x_1\left(y_2^2\left(y_1^2+3y_1y_2+y_2^2\right)-x_2\left(y_2^3-y_1^2y_2\right)\right)\vartheta_{11}^0(x_1-y_1,-x_2)}{y_1^2y_2(y_1+y_2)^2(y_2-x_2)}\\
&-\frac{2x_1x_2^2(y_1+2y_2)\vartheta_{11}^0(x_1-y_1,-x_2)}{y_1y_2(y_1+y_2)^2(y_2-x_2)}+\frac{2x_1\left(x_1^2+y_1y_2\right)\vartheta_{11}^0(x_1,x_1-y_1)}{y_1(x_1-y_1)(y_1+y_2)^2}, \qquad (3.137)\\
K_{21} &= \frac{2x_1^2\left(x_1(y_1+y_2)-x_1^2+y_1^2\right)\vartheta_{11}^0(x_1,x_1-y_1)}{(y_1+y_2)^2(y_2-x_2)}\\
&+\frac{2x_1^2\left(y_2^2(x_2-y_1)+y_2x_2(y_1-x_2)+y_1(y_1+x_2)^2\right)\vartheta_{11}^0(x_1,-x_2)}{y_1(y_1+y_2)^2(x_2-y_2)}\\
&-\frac{2y_2\left(x_1^3(y_1+y_2)-x_1^4+x_1^2y_1^2+y_1(y_1+y_2)^2(x_2-y_2)\right)\vartheta_{11}^0(x_1-y_1,-x_2)}{y_1(y_1+y_2)^2(x_2-y_2)}, \qquad (3.138)\\
K_{22} &= \frac{2x_1^2\left(y_1^2+x_1x_2\right)\vartheta_{11}^0(x_1,x_1-y_1)}{y_1(y_1+y_2)^2(x_2-y_2)}-\frac{2}{y_1^2y_2(y_1+y_2)^2(y_2-x_2)}\\
&\quad\times\Big\{x_1^2\left(y_2^2\left(6y_1^2+6y_1y_2+y_2^2\right)-4y_1y_2^2x_2+y_1x_2^2(y_1+2y_2)\right)\\
&\quad-x_1^3y_2^2(5y_1+y_2)+y_1^2y_2^2(y_1+y_2)^2\Big\}\vartheta_{11}^0(x_1-y_1,-x_2)\\
&+\frac{2(x_1^2\left(x_2\left(3y_1^2+2y_1y_2+y_2^2\right)+2y_1^2(y_1+y_2)+2y_1x_2^2\right)\vartheta_{11}^0(x_1,-x_2)}{y_1^2(y_1+y_2)^2(y_2-x_2)}, \qquad (3.139)\\
\widetilde{K}_{11} &= \frac{2x_1(x_1(y_1+3y_2)-2y_2(y_1+y_2))\vartheta_{11}^0(x_1,-x_2)}{y_2(y_1+y_2)^2}-\frac{2x_1^2\vartheta_{11}^0(x_1,x_1-y_2)}{(y_1+y_2)^2}\\
&-\frac{2x_1^2y_1\vartheta_{11}^0(x_1-y_2,-x_2)}{y_2(y_1+y_2)^2}, \qquad (3.140)\\
\widetilde{K}_{12} &= \frac{2x_1^2\vartheta_{11}^0(x_1,x_1-y_2)}{y_1(y_1+y_2)^2}+\frac{2x_1(x_1(y_1^2-y_2^2)-2x_2y_1y_2)\vartheta_{11}^0(x_1,-x_2)}{y_1y_2^2(y_1+y_2)^2} \qquad (3.141)
\end{aligned}
$$

$$
\begin{aligned}
&- \frac{2\left(x_2^2\left(y_1^2+y_1y_2+y_2^2\right)-2y_1^2x_2(y_1+y_2)\right)\vartheta_{11}^0(x_1-y_2,-x_2)}{y_1y_2^2(y_1+y_2)^2} \\
&- \frac{2(y_1-y_2)\vartheta_{11}^0(x_1-y_2,-x_2)}{y_2^2}, \qquad (3.142)\\
\widetilde{K}_{21} &= 2\frac{(x_1-y_2)((x_2-2y_1)\vartheta_{111}^0(x_1,x_1-y_2,-x_2)-y_1\vartheta_{112}^0(x_1,x_1-y_2,-x_2))}{y_1} \\
&+ \frac{2x_1x_2^2(y_1-y_2)\vartheta_{11}^0(x_1,-x_2)}{y_1(y_1+y_2)^2}, \qquad (3.143)\\
\widetilde{K}_{22} &= \frac{2x_1^2(y_2-x_1)\left(y_1^2+y_1y_2+y_2^2\right)\vartheta_{11}^0(x_1-y_2,-x_2)}{y_1y_2^2(y_1+y_2)^2} \\
&- \frac{2(y_2-x_1)(2y_1+y_2-2x_2)\vartheta_{11}^0(x_1-y_2,-x_2)}{y_1y_2} \\
&+ \frac{2x_1^2\left(y_1^3-x_2\left(y_1^2+2y_1y_2-y_2^2\right)-y_1y_2^2\right)\vartheta_{11}^0(x_1,-x_2)}{y_1y_2^2(y_1+y_2)^2} \\
&+ \frac{2x_1^2(x_1-y_2)\vartheta_{11}^0(x_1,x_1-y_2)}{y_1(y_1+y_2)^2}. \qquad (3.144)
\end{aligned}
$$

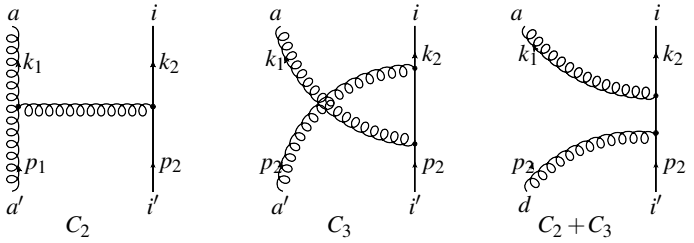

Figure 3.4: Feynman diagrams corresponding to two-to-two transitions of nonquasipartonic antiquark-gluon operator blocks in Sec. 3.4.2.

This concludes our analysis of non-singlet two-to-two transitions of nonquasipartonic operators. They agree with corresponding findings in [74], the last paper of Ref. [72] and [78], after the Fourier transformations. For a partial result in the singlet channel, one refers the reader to Appendix B.2.

3.4.3 Two-to-Three Transitions: Non-Quasipartonic Operators

Finally, one comes to the analysis of particle number-changing transitions. This is the most elaborate sector of twist-four operators. Apart from a proliferation of Feynman graphs,

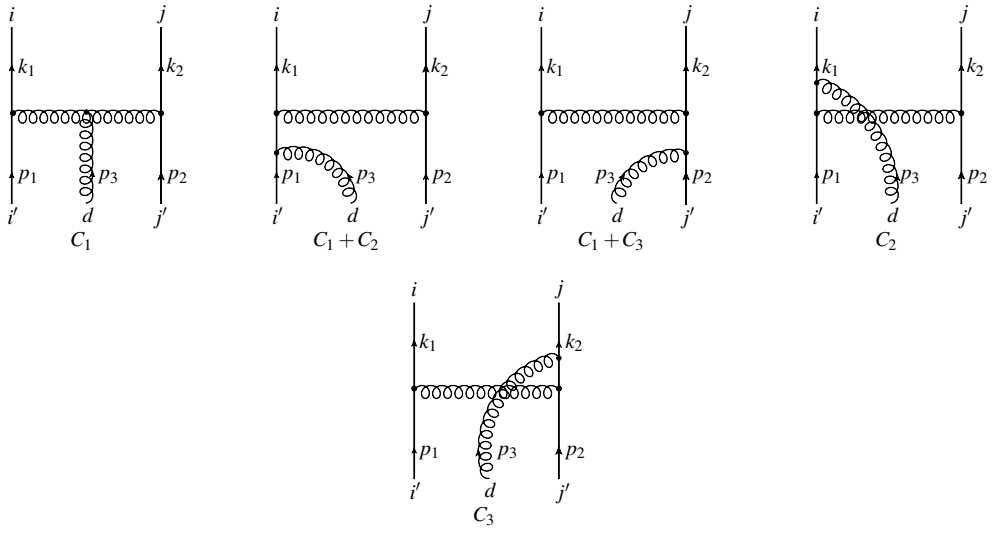

Figure 3.5: Feynman diagrams responsible for the evolution kernels of $\psi_-^i(x_1)\psi_+^j(x_2) \to \psi_+^{i'}(y_1)\psi_+^{j'}(y_2)\bar{f}_{++}^a(y_3)$ in Sec. 3.4.3 and $\bar{\psi}_+(x_1)\psi_-(x_1) \to \bar{\psi}^{i'}(y_1)\psi_+^{j'}\bar{f}_{++}^d(y_3)$ in Sec. 3.4.3. C_c's are the color structures defined in Eq. (3.147).

there are also subtle effects related to transitions induced by the use of QCD equations of motion. We provide for the latter a diagrammatic representation that puts it on the same footing as the rest of the calculation, and thus reduces the procedure to tedious algebraic manipulations. An example exhibiting the formalism is worked out in Appendix B.4.

First consider the quark-quark bad-good and good-good operators with a transverse derivative, respectively,

$$\psi_-\psi_+ \text{ and } \tfrac{1}{2}D_{-+}\bar{\psi}_+\bar{\psi}_+$$

$$\mathcal{O}^{ij}(x_1,x_2) = \psi_-^i(x_1)\psi_+^j(x_2)\,, \qquad \mathcal{O}^{ij}(x_1,x_2) = \tfrac{1}{2}D_{-+}\psi_+^i(x_1)\psi_+^j(x_2)\,, \tag{3.145}$$

mixing with the following three-particle operator constructed from good field components

$$\mathcal{O}^{ija}(y_1,y_2,y_3) = g\sqrt{2}\psi_+^i(y_1)\psi_+^j(y_2)\bar{f}_{++}^a(y_3)\,. \tag{3.146}$$

In both cases, there are three nontrivial color-flow channels

$$[C_1]_{i'j'd}^{ij} = f^{dbc}t_{ii'}^b t_{jj'}^c, \qquad [C_2]_{i'j'd}^{ij} = i(t^d t^b)_{ii'}t_{jj'}^b, \qquad [C_3]_{i'j'd}^{ij} = it_{ii'}^b(t^d t^b)_{jj'}\,, \tag{3.147}$$

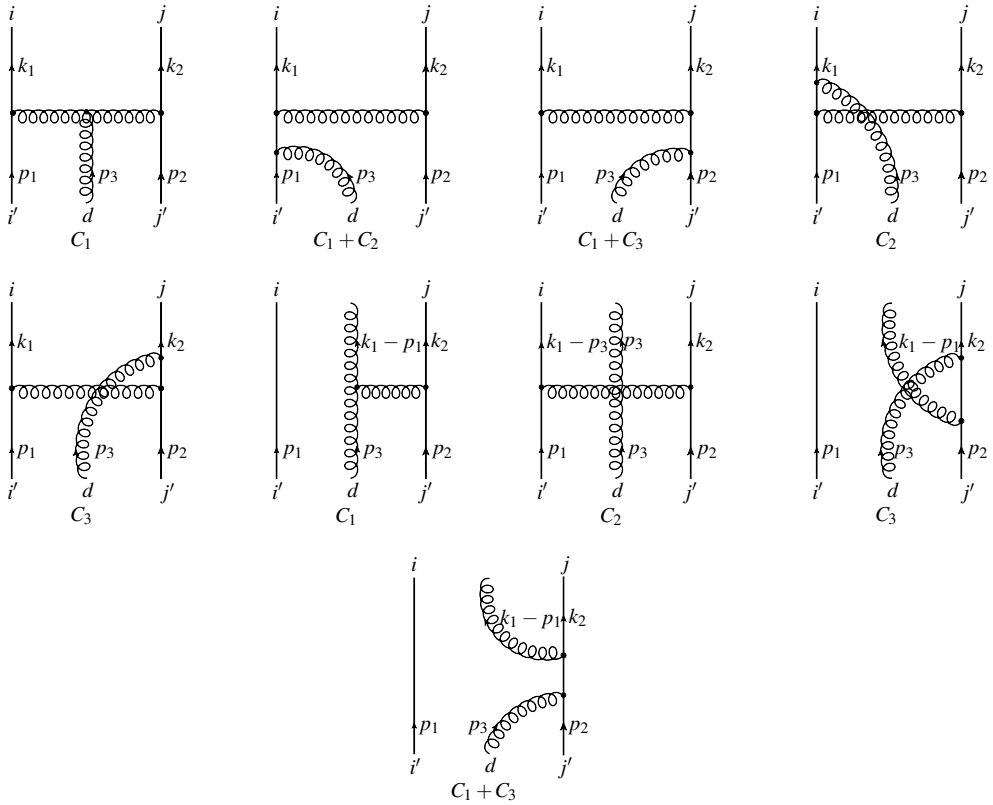

Figure 3.6: Feynman diagrams defining the evolution kernels for transitions $D_{-+}\bar{\psi}^i_+(x_1)\bar{\psi}^j_+(x_2) \to \psi^{i'}_+(y_1)\psi^{j'}_+(y_2)\bar{f}^a_{++}(y_3)$ in Sec. 3.4.3 and $D_{-+}\bar{\psi}^i_+(x_1)\psi^j_+(x_1) \to \bar{\psi}^{i'}(y_1)\psi^{j'}_+\bar{f}^d_{++}(y_3)$ in Sec. 3.4.3, where C_c are the color structures defined in Eq. (3.147). The last four diagrams correspond to the contribution of the gauge field in the covariant derivative D_{-+}.

such that the evolution equation takes the form

$$[\mathcal{K}\mathcal{O}]^{ij}(x_1,x_2) = \int [\mathcal{D}^3 y]_2 \sum_{c=1}^{3} [C_c]^{ij}_{i'j'a} K_c(x_1,x_2|y_1,y_2,y_3)\mathcal{O}^{i'j'a}(y_1,y_2,y_3)\,. \tag{3.148}$$

First, for the $\mathcal{O}^{ij}(z_1,z_2) = \psi^i_-(z_1)\psi^j_+(z_2)$ case, the evolution kernels computed from the diagrams in Fig. 3.5 read

$$K_1 = \frac{\theta(x_1)}{y_1(y_1+y_3)^2} - \frac{\theta(x_1-y_1)}{y_1 y_3^2} + \frac{(y_1+2y_3)\theta(x_1-y_1-y_3)}{y_3^2(y_1+y_3)^2}\,, \tag{3.149}$$

$$K_2 = \frac{y_3(y_1+y_3)-x_1(y_1+2y_3)\theta(x_1)}{y_3^2(y_1+y_3)^2(y_1+y_3-x_1)} + \frac{(x_1-y_3)\theta(x_1-y_3)}{y_1 y_3^2(y_1+y_3-x_1)} + \frac{\theta(x_1-y_1-y_3)}{y_1(y_1+y_3)^2}\,, \tag{3.150}$$

$$K_3 = 0\,, \tag{3.151}$$

while for $\mathcal{O}^{ij}(x_1,x_2)=\frac{1}{2}D_{-+}\psi^i_+(x_1)\psi^j_+(x_2)$ they are

$$\begin{aligned}K_1 &= \left[\frac{y_2-x_2}{y_2y_3^2}+\frac{y_1(y_1+y_3)-x_1(y_1+2y_3)}{(y_1+y_3)^2y_3^2}-\frac{1}{y_3^2}\right]\theta(y_2-x_2)\\ &+\left[\frac{1}{y_3^2}-\frac{(x_1-y_1)^2}{y_1(x_2-y_2)y_3^2}+\frac{y_3(y_2+y_3)-x_1(y_2+2y_3)+y_1(y_2+2y_3)}{(y_2+y_3)^2y_3^2}\right]\theta(x_1-y_1)\\ &+\frac{x_2\theta(x_1-y_1-y_2-y_3)}{y_2(y_2+y_3)^2}+\frac{x_1^2\theta(x_1)}{y_1(y_1+y_3)^2(x_2-y_2)}\,, \qquad (3.152)\\ K_2 &= \frac{x_1^2(y_1+2y_3)\theta(x_1)}{y_3^2(y_1+y_3)^2(x_2-y_2)}+\frac{(y_3^2-x_1^2)\theta(x_1-y_3)}{y_1y_3^2(y_1+y_3-x_1)}-\frac{(x_1+y_1+y_3)\theta(y_2-x_2)}{y_1(y_1+y_3)^2}\,, \qquad (3.153)\\ K_3 &= -\frac{x_2\theta(x_1-y_1)}{y_2(y_2+y_3)^2}+\frac{x_2\theta(x_1-y_1-y_2)}{y_2y_3^2}-\frac{x_2(y_2+2y_3)\theta(-x_2)}{y_3^2(y_2+y_3)^2}\,. \qquad (3.154)\end{aligned}$$

Making use of the differential operators introduced in section 3.3.3, it is straightforward to verify that these kernels are all conformally invariant.

Next, the good-good quark-gluon operators with transverse derivatives is addressed:

$$\tfrac{1}{2}D_{-+}\bar\psi_+\bar f_{++} \text{ and } \bar\psi_+\tfrac{1}{2}D_{-+}\bar f_{++}$$

$$\mathcal{O}^{ia}(x_1,x_2)=\tfrac{1}{2}D_{-+}\bar\psi^i_+(x_1)\bar f^a_{++}(x_2)\,, \qquad \mathcal{O}^{ia}(x_1,x_2)=\tfrac{1}{2}\bar\psi^i_+(x_1)D_{-+}\bar f^a_{++}(x_2) \qquad (3.155)$$

evolving into

$$\mathcal{O}^{iad}=g\sqrt{2}\bar\psi^i_+(y_1)\bar f^a_{++}(y_2)\bar f^d_{++}(y_3)\,. \qquad (3.156)$$

Their one-loop evolution equation,

$$[\mathcal{K}\mathcal{O}]^{ia}(x_1,x_2)=\int[\mathcal{D}^3y]_2\sum_{c=1}^{6}[C_c]^{ia}_{i'a'd}K_c(x_1,x_2|y_1,y_2,y_3)\mathcal{O}^{a'i'd}(y_1,y_2,y_3)\,, \qquad (3.157)$$

develops six independent color structures:

$$\begin{aligned}[C_1]^{ia}_{i'a'd} &= -i(t^c)_{ii'}f^{cde}f^{aa'e}\,, & [C_2]^{ia}_{i'a'd} &= -(t^dt^e)_{ii'}f^{aa'e}\,,\\ [C_3]^{ia}_{ia'd'} &= -i(t^c)_{ii'}f^{ade}f^{ca'e}\,, & [C_4]^{ia}_{ia'd} &= i(t^dt^{a'}t^a)_{ii'}\,,\\ [C_5]^{ia}_{i'a'd} &= i(t^{a'}t^dt^a)_{ii'}\,, & [C_6]^{ia}_{i'a'd} &= i(t^{a'}t^at^d)_{ii'}\,. \qquad (3.158)\end{aligned}$$

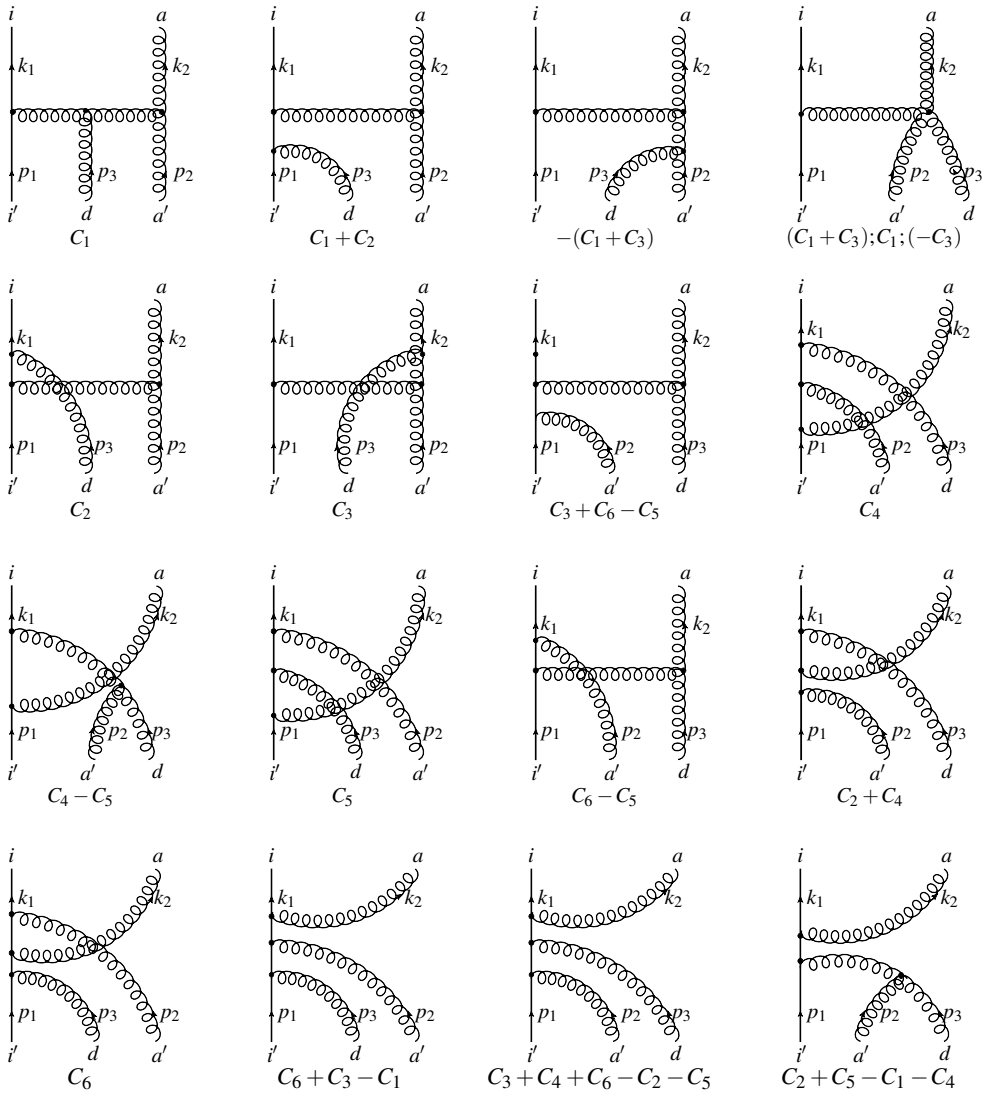

Figure 3.7: Feynman diagrams that induce the transitions in Sec. 3.4.3. For the operators in Sec. 3.4.3 and operator $\frac{1}{2}D_{-+}\bar{\psi}f_{++}$ in Sec. 3.4.3, these diagrams correspond to the flat derivative $\bar{\partial}_\perp$ residing in the covariant derivative D_{-+}, while for the operator $\bar{\psi}_+ f_{+-}$ in Sec. 3.4.3, they account for the contribution of $\partial^+ A^-, \bar{\partial}_\perp A_\perp$ and $\bar{\partial}_\perp \bar{A}_\perp$ originating from Eq. (3.19).

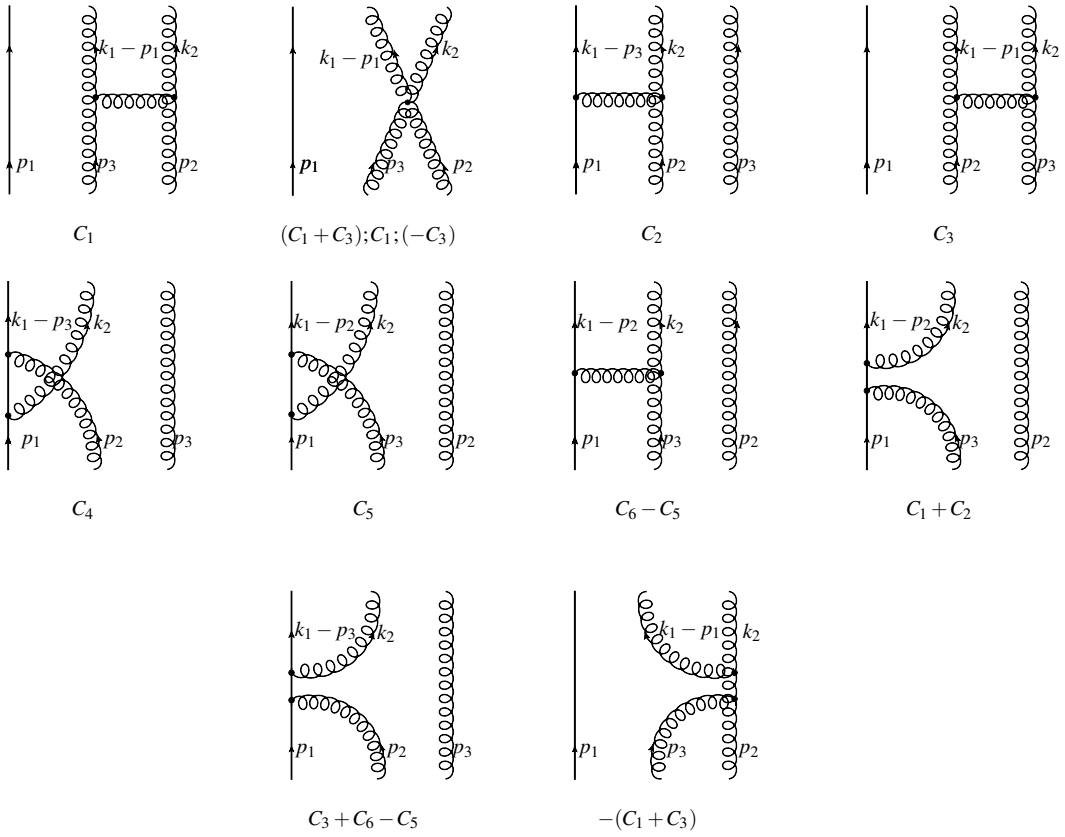

Figure 3.8: Feynman diagrams corresponding to the contributions of the gauge fields nested inside the covariant derivatives for the transitions of $\frac{1}{2}D_{-+}\bar{\psi}^i_+ \bar{f}^a_{++} \to \bar{\psi}^i_+ \bar{f}^a_{++} \bar{f}^d_{++}$ and $\frac{1}{2}D_{-+}\bar{\psi}^i_+ f^a_{++} \to \bar{\psi}^i_+ f^a_{++} \bar{f}^d_{++}$ in Secs. 3.4.3 and 3.4.3 respectively.

Translating the evolution kernels of the operator transitions into the following relevant Feynman diagrams:

The computation of the diagrams in Figs. 3.7 and 3.8 yields for the $\frac{1}{2}D_{-+}\bar{\psi}^i_+(x_1)\bar{f}^a_{++}(x_2)$ operator:

$$
\begin{aligned}
K_1 = {} & \frac{x_1^2\theta(x_1)}{y_1(y_1+y_3)^2(x_2-y_2)} + \frac{x_2^2(3y_2+y_3)\theta(-x_2)}{y_2^2(y_2+y_3)^3} \\
& + \frac{1}{y_1y_3^2(x_2-y_2)(y_2+y_3)^3}\Big\{x_2^3y_1(y_2+3y_3) - x_2^2\big(y_1y_2(y_2+3y_3)+(y_2+y_3)^3\big) \\
& \qquad + 2x_2(y_2+y_3)^4 - (y_2+y_3)^5\Big\}\theta(x_1-y_1) \\
& + \frac{1}{y_2^2y_3^2(y_1+y_3)^2}\Big\{y_2^2x_2(y_1+2y_3) + y_2^2(2y_3(y_2+y_3) - (y_1(y_2+2y_3))) \\
& \qquad - x_2^2(y_1+y_3)^2\Big\}\theta(y_2-x_2)\,, \qquad (3.159)
\end{aligned}
$$

$$
K_2 = \frac{x_1^2(y_1+2y_3)\theta(x_1)}{y_3^2(y_1+y_3)^2(y_2-x_2)} - \frac{(x_1^2-y_3^2)\theta(x_1-y_3)}{y_1y_3^2(x_2-y_2)} - \frac{(x_1+y_1+y_3)\theta(y_2-x_2)}{y_1(y_1+y_3)^2}\,, \qquad (3.160)
$$

$$
\begin{aligned}
K_3 = {} & \frac{x_1^2\theta(x_1)}{y_1(y_1+y_2)^2(y_3-x_2)} - \frac{x_2^2(y_2+3y_3)\theta(-x_2)}{y_3^2(y_2+y_3)^3} \\
& + \frac{1}{y_1y_2^2(y_2+y_3)^3(x_2-y_3)}\Big\{x_2^2\left(y_3^2(y_1+3y_2)+3y_2y_3(y_1+y_2)+y_2^3+y_3^3\right) \\
& - y_1x_2^3(3y_2+y_3) - 2x_2(y_2+y_3)^4 + (y_2+y_3)^5\Big\}\theta(x_1-y_1) \\
& + \frac{\left(y_3^2(x_1(y_1+2y_2)-y_1(y_1+y_2)) + x_2^2(y_1+y_2)^2\right)\theta(y_3-x_2)}{y_2^2y_3^2(y_1+y_2)^2}\,, \qquad (3.161)
\end{aligned}
$$

$$
\begin{aligned}
K_4 = {} & \frac{x_1^2(y_2+3y_3)\theta(x_1)}{y_3^2(y_2+y_3)^3} + \frac{\left(x_1^2(3y_2+y_3)-(y_2+y_3)^3\right)\theta(y_1-x_2)}{y_2^2(y_2+y_3)^3} \\
& + \frac{\left(y_3^2-x_1^2\right)\theta(x_1-y_3)}{y_2^2y_3^2}\,, \qquad (3.162)
\end{aligned}
$$

$$
\begin{aligned}
K_5 = {} & \frac{x_1^2}{2y_2^2}\Big\{\frac{y_1+2y_2}{(y_1+y_2)^2(x_2-y_3)} - \frac{2y_2}{(y_2+y_3)^3} - \frac{1}{(y_2+y_3)^2}\Big\}\theta(x_1) \\
& + \frac{\left((y_2+y_3)^3 - x_1^2(y_2+3y_3)\right)\theta(y_1-x_2)}{2y_3^2(y_2+y_3)^3} \\
& - \frac{(x_1+y_1+y_2)\theta(y_3-x_2)}{2y_1(y_1+y_2)^2} + \frac{(x_1^2-y_2^2)(y_1x_2-y_3(y_1+y_3))\theta(x_1-y_2)}{2y_1y_2^2y_3^2(x_2-y_3)}\,, \qquad (3.163)
\end{aligned}
$$

$$
K_6 = \frac{x_1^2(y_1+2y_2)\theta(x_1)}{2y_2^2(y_1+y_2)^2(y_3-x_2)} + \frac{(x_1^2-y_2^2)\theta(x_1-y_2)}{2y_1y_2^2(x_2-y_3)} + \frac{(x_1+y_1+y_2)\theta(y_3-x_2)}{2y_1(y_1+y_2)^2}\,. \qquad (3.164)
$$

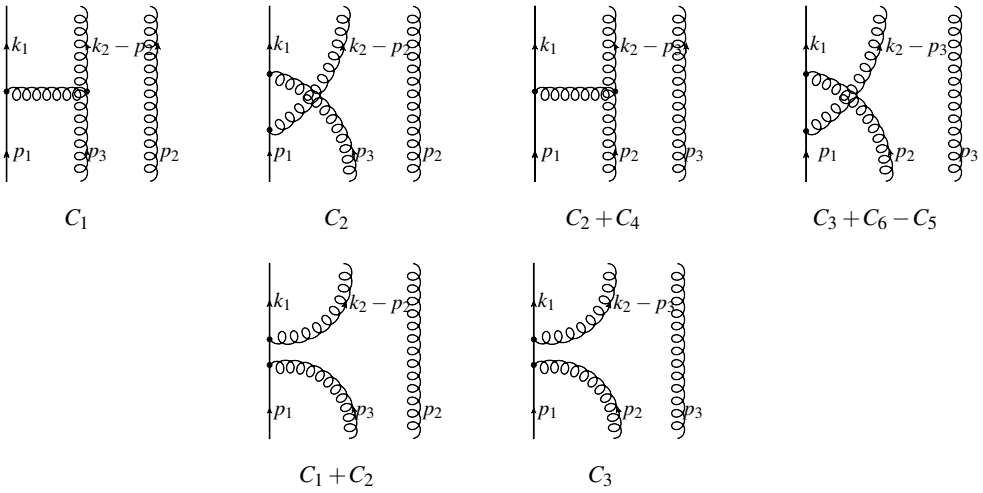

Figure 3.9: Additional Feynman diagrams contributing to the transition $\frac{1}{2}D_{-+}\bar{\psi}^i_+(x_1)\bar{f}^a_{++}(x_2) \to \bar{\psi}^{i'}_+(y_1)\bar{f}^{a'}_{++}(y_2)\bar{f}^d_{++}(y_3)$ in Sec. 3.4.3.

While for the $\bar{\psi}^i_+(z_1)\frac{1}{2}D_{-+}\bar{f}^a_{++}(z_2)$, the contributing graphs are shown in Figs. 3.7 and 3.9 and their computation gives,

$$
\begin{aligned}
K_1 = {} & \frac{x_1\theta(x_1)}{y_1(y_1+y_3)^2} - \frac{1}{y_1y_3^2(y_2+y_3)^3}\Big\{y_1x_2^2(y_2+3y_3) - x_2(y_2+y_3)\big((y_2+y_3)^2 \\
& - y_1(y_2+3y_3)\big) + (y_2+y_3)^2\left(y_1(y_3-y_2)+(y_2+y_3)^2\right)\Big\}\theta(x_1-y_1) \\
& + \frac{1}{y_2^2y_3^2(x_1-y_1)(y_1+y_3)^2}\Big\{y_2^2x_2^2(y_1+2y_3) - x_2^3(y_1+y_3)^2 \\
& + y_2^2\big(y_1^2(y_3-y_2)+y_1\left(y_2^2+3y_3^2\right)+2y_3\left(y_2^2+y_2y_3+y_3^2\right)\big) \\
& - y_2^2x_2\big(2y_1(y_2-y_3)-2y_1^2+y_3(4y_2+y_3)\big)\Big\}\theta(y_2-x_2) \\
& + \frac{x_2^3(3y_2+y_3)\theta(-x_2)}{y_2^2(x_1-y_1)(y_2+y_3)^3}\,, \qquad (3.165)
\end{aligned}
$$

$$
K_2 = \frac{x_1(y_1+2y_3)\theta(x_1)}{y_3^2(y_1+y_3)^2} - \frac{x_1\theta(x_1-y_3)}{y_1y_3^2} + \frac{x_1\theta(y_2-x_2)}{y_1(y_1+y_3)^2}\,, \qquad (3.166)
$$

$$
\begin{aligned}
K_3 = {} & -\frac{x_1\theta(x_1)}{y_1(y_1+y_2)^2} + \frac{1}{y_1y_2^2(y_2+y_3)^3}\Big\{-x_2(y_2+y_3)\left((y_2+y_3)^2 - y_1(3y_2+y_3)\right) \\
& + y_1x_2^2(3y_2+y_3) + (y_2+y_3)^2\left(y_1(y_2-y_3)+(y_2+y_3)^2\right)\Big\}\theta(x_1-y_1) \\
& + \frac{1}{y_2^2y_3^2(x_1-y_1)(y_1+y_2)^2}\Big\{(y_1+y_2)^2(x_2-y_3)^3 - x_1y_3^2(x_1-y_1)(y_1+2y_2) \\
& + 3y_3(y_1+y_2)^2(x_2-y_3)^2\Big\}\theta(y_3-x_2) - \frac{x_2^3(y_2+3y_3)\theta(-x_2)}{y_3^2(x_1-y_1)(y_2+y_3)^3}\,, \qquad (3.167)
\end{aligned}
$$

$$K_4 = \frac{x_1(x_2-y_1)(y_2+3y_3)\theta(x_1)}{y_3^2(y_2+y_3)^3} + \frac{x_1(y_1-x_2)\theta(x_1-y_3)}{y_2^2 y_3^2} + \frac{x_1(y_1-x_2)(3y_2+y_3)\theta(y_1-x_2)}{y_2^2(y_2+y_3)^3}\,, \tag{3.168}$$

$$K_5 = \frac{x_1}{y_2^2(y_1+y_2)^2(y_2+y_3)^3}\Big\{x_1(y_1+y_2)^2(3y_2+y_3) - (y_2+y_3)\Big[y_3\left(y_1^2-3y_2^2\right) + y_2\left(3y_1^2+5y_1y_2+y_2^2\right) - y_3^2(y_1+2y_2)\Big]\Big\}\theta(x_1) + \frac{x_1\theta(y_3-x_2)}{y_1(y_1+y_2)^2} + \frac{x_1(y_1-x_2)(y_2+3y_3)\theta(y_1-x_2)}{y_3^2(y_2+y_3)^3} + \frac{x_1}{y_2^2}\left\{\frac{x_2-y_1}{y_3^2} - \frac{1}{y_1}\right\}\theta(x_1-y_2)\,, \tag{3.169}$$

$$K_6 = -\frac{x_1(y_1+2y_2)\theta(x_1)}{y_2^2(y_1+y_2)^2} + \frac{x_1\theta(x_1-y_2)}{y_1y_2^2} - \frac{x_1\theta(y_3-x_2)}{y_1(y_1+y_2)^2}\,. \tag{3.170}$$

One of the consistency checks on the above kernels is their conformal invariance: they are annihilated by the differential operators in Eqs. (3.63) and (3.64). Yet, they when Fourier transformed to the coordinate space, they look superficially different from the corresponding results obtained using the conformal technique [78]. This is obvious from the fact that the C_6 channel is absent in the latter analysis, and what is more disconcerting is that the Fourier transform of the light-ray kernels in Ref. [78] for the transitions given in Eq. (3.157) develops logarithmic dependence on the momentum fraction variables. From the momentum-space technique that is employed is this work, it is obvious that logarithms simply cannot emerge at one loop merely because one does not have enough integrations to generate them in the first place. This disparity between the two results is actually an agreement in disguise. To observe it, one has to use the symmetry of the operators involved in the transition. Namely, the three-particle operator $\mathcal{O}^{iad}$ defined in Eq. (3.156) is symmetric under the interchange of the gluon fields, i.e., simultaneous exchange $a \leftrightarrow d$ and $y_2 \leftrightarrow y_3$. This procedure eliminates the logarithms from the coordinate-space analysis. To get a complete agreement, one can redistribute the color structure $[C_6]^{ia}_{ia'd}$ and its corresponding kernel K_6 into other channels. The final expressions do coincide. To be more explicit, one inverse-Fourier transforms the results to the coordinate space, and lists results

in Appendix B.5.1 since it gives a simplified form of the corresponding light-ray transition kernels.

Now consider operator group,

$$\bar{f}_{++}\psi_{-} \text{ and } \tfrac{1}{2}D_{-+}\bar{f}_{++}\psi_{+}$$

For the transitions of

$$\mathcal{O}^{ai}(x_1,x_2)=\bar{f}^{a}_{++}(x_1)\psi^{i}_{-}(x_2)\,,\qquad \mathcal{O}^{ai}(x_1,x_2)=\tfrac{1}{2}D_{-+}\bar{f}^{a}_{++}(x_1)\psi^{i}_{+}(x_2)\,, \tag{3.171}$$

to

$$\mathcal{O}^{aid}=g\sqrt{2}\bar{f}^{a}_{++}(y_1)\psi^{i}_{+}(y_2)\bar{f}^{d}_{++}(y_3)\,, \tag{3.172}$$

one finds

$$[\mathcal{K}\,\mathcal{O}]^{ai}(x_1,x_2)=\int[\mathcal{D}^3y]_2\sum_{c=1}^{6}[C_c]^{ai}_{a'i'd}K_c(x_1,x_2|y_1,y_2,y_3)\mathcal{O}^{a'i'd}(y_1,y_2,y_3)\,, \tag{3.173}$$

where the color structures are determined by the following tensors

$$\begin{aligned}
&[C_1]^{ai}_{a'i'd}=-i(t^c)_{ii'}f^{cde}f^{aa'e}\,, && [C_2]^{ia}_{ia'd'}=-i(t^c)_{ii'}f^{ade}f^{ca'e}\,,\\
&[C_3]^{ia}_{i'a'd}=-(t^dt^e)_{ii'}f^{aa'e}\,, && [C_4]^{ia}_{ia'd}=i(t^dt^{a'}t^a)_{ii'}\,,\\
&[C_5]^{ia}_{i'a'd}=i(t^{a'}t^dt^a)_{ii'}\,, && [C_6]^{ia}_{i'a'd}=i(t^{a'}t^at^d)_{ii'}\,.
\end{aligned} \tag{3.174}$$

For the $\mathcal{O}^{ai}(x_1,x_2)=\bar{f}^{a}_{++}(x_1)\psi^{i}_{-}(x_2)$ case, the Feynman diagrams responsible for the one-loop evolution are presented in Fig. 3.10, and produce the following contributions

$$\begin{aligned}
K_1=&-\frac{x_1^2\left(8y_1^3+9y_1^2(y_2+2y_3)+3y_1(y_2+2y_3)^2+y_3(y_2+y_3)(y_2+2y_3)\right)\theta(x_1)}{y_1^2(y_1+y_3)^3(x_1+x_2)^3}\\
&+\frac{x_1^2(y_2+2y_3)\theta(x_1-y_1)}{y_1^2y_3^2(y_2+y_3)^2}-\frac{x_1^2(y_1+3y_3)\theta(y_2-x_2)}{y_2y_3^2(y_1+y_3)^3}\\
&+\frac{x_1^2(y_1+3(y_2+y_3))\theta(-x_2)}{y_2(y_2+y_3)^2(x_1+x_2)^3}\,,
\end{aligned} \tag{3.175}$$

$$K_2 = \frac{x_1^2\left(9y_3^2(2y_1+y_2)+3y_3(2y_1+y_2)^2+y_1(y_1+y_2)(2y_1+y_2)+8y_3^3\right)\theta(x_1)}{y_3^2(y_1+y_3)^3(x_1+x_2)^3}$$
$$-\frac{x_1^2(2y_1+y_2)\theta(x_1-y_3)}{y_1^2y_3^2(y_1+y_2)^2}+\frac{x_1^2(3y_1+y_3)\theta(y_2-x_2)}{y_1^2y_2(y_1+y_3)^3}$$
$$-\frac{x_1^2(3(y_1+y_2)+y_3)\theta(-x_2)}{y_2(y_1+y_2)^2(x_1+x_2)^3}, \tag{3.176}$$

$$K_3 = \frac{x_1^2\left(4y_1^2+y_1(5y_2+2y_3)+y_2(y_2+y_3)\right)\theta(x_1)}{y_1^2(y_1+y_2)^2(x_1+x_2)^3}-\frac{x_1^2\theta(x_1-y_1)}{y_1^2y_2(y_2+y_3)^2}$$
$$+\frac{(y_3-x_2)\left(x_1^2+x_1y_2+y_2(y_1+y_2)\right)\theta(y_3-x_2)}{y_2y_3^2(x_1-y_1)(y_1+y_2)^2}$$
$$+\frac{1}{y_3^2(x_1-y_1)(y_2+y_3)^2(y_1+y_2+y_3)^3}\Big\{x_1^2y_1(y_1(y_2+2y_3)$$
$$+(y_2+y_3)^2(x_1+x_2)^3-x_1^3(y_1(y_2+2y_3)+(y_2+y_3)(y_2+4y_3))$$
$$+(y_2+y_3)(y_2+4y_3))\Big\}\theta(-x_2), \tag{3.177}$$

$$K_4 = \frac{x_1^2(3(y_1+y_2)+y_3)\theta(x_1)}{y_2(y_1+y_2)^2(y_1+y_2+y_3)^3}-\frac{(x_1-y_2)^2(3y_1+y_3)\theta(x_1-y_2)}{y_1^2y_2(y_1+y_3)^3}$$
$$+\frac{(x_2-y_3)(y_2(y_1+y_2)-x_1(2y_1+y_2))\theta(y_3-x_2)}{y_1^2y_3^2(y_1+y_2)^2}$$
$$-\frac{1}{y_3^2(y_1+y_3)^3(y_1+y_2+y_3)^3}\Big\{x_1^2\big(9y_3^2(2y_1+y_2)+3y_3(2y_1+y_2)^2+8y_3^3$$
$$+y_1(y_1+y_2)(2y_1+y_2)\big)-2x_1(y_1+3y_3)(x_1+x_2)^3$$
$$+y_2(y_1+3y_3)(x_1+x_2)^3\Big\}\theta(-x_2), \tag{3.178}$$

$$K_5 = \frac{x_1^2\left(y_1+y_2+3y_3\right)\theta(x_1)}{y_2y_3^2(x_1+x_2)^3}-\frac{(x_1-y_2)^2(y_1+3y_3)\theta(x_1-y_2)}{y_2y_3^2(y_1+y_3)^3}-\frac{x_1^2\theta(x_1-y_3)}{y_2y_3^2(y_1+y_2)^2}$$
$$+\frac{(x_2-y_1)\left(x_1^2-x_1y_2+y_2y_3\right)\theta(y_1-x_2)}{y_1^2y_2y_3^2(y_3-x_1)}$$
$$+\frac{1}{y_1^2y_3(x_1+x_2)^3}\Big\{\frac{x_2(x_1-y_2)(x_1+x_2)^2}{y_1+y_3}+\frac{y_1(x_1+x_2)}{(x_1-y_3)(y_1+y_2)^2}$$
$$\times\Big[x_1^2(y_3(y_1+y_2+x_2)+2x_2(y_1+y_2))+x_1y_3(y_1+y_2)(2x_2-y_1-y_2)$$
$$+y_3x_2^2(y_1+y_2)\Big]-\frac{(x_1+x_2)^2\left(x_1^3-x_1^2(y_2+y_3)+y_3(x_1y_1-x_2y_2)\right)}{(x_1-y_3)(y_1+y_2)}$$
$$-\frac{y_1(x_1-y_2)(x_1+x_2)(y_1-y_3)\left((x_1+x_2)^2-x_1(2y_1+y_2+2y_3)\right)}{(y_1+y_3)^3}\Big\}\theta(-x_2)$$

$$+\frac{x_1y_1x_2(y_3-y_1)}{y_1+y_3}-x_1y_1x_2\,, \tag{3.179}$$

$$\begin{aligned}
K_6 = &-\frac{x_1^2(y_1(y_2+2y_3)+(y_2+y_3)(y_2+4y_3))\theta(x_1)}{y_3^2(y_2+y_3)^2(x_1+x_2)^3}+\frac{x_1^2\theta(x_1-y_3)}{y_2y_3^2(y_1+y_2)^2}\\
&+\frac{(x_2-y_1)\left(x_1^2+x_1y_2+y_2(y_2+y_3)\right)\theta(y_1-x_2)}{y_1^2y_2(x_1-y_3)(y_2+y_3)^2}\\
&+\frac{1}{y_1^2(x_1-y_3)(y_1+y_2)^2(x_1+x_2)^3}\Big\{x_1^3\left(4y_1^2+y_1(5y_2+2y_3)+y_2(y_2+y_3)\right)\\
&-x_1^2y_3\left(4y_1^2+y_1(5y_2+2y_3)+y_2(y_2+y_3)\right)\\
&-(y_1+y_2)^2(x_1+x_2)^3\Big\}\theta(-x_2)\,.
\end{aligned} \tag{3.180}$$

For the $\mathcal{O}^{ai}(x_1,x_2)=\frac{1}{2}D_{-+}\bar{f}^a_{++}(x_1)\psi^i_+(x_2)$ operator, the Feynman graphs describing its transition into $\bar{f}^{a'}_{++}(z_1)\psi^{i'}_+(z_2)\bar{f}^d_{++}(z_3)$ are shown in Figs. 3.10 and 3.11, such that

$$\begin{aligned}
K_1 = &\frac{x_1^3}{y_1^2(y_1+y_3)^3(x_2-y_2)(x_1+x_2)^3}\Big\{x_2\Big[8y_1^3+9y_1^2(y_2+2y_3)+3y_1(y_2+2y_3)^2\\
&+y_3(y_2+y_3)(y_2+2y_3)\Big]+(y_1+y_3)^3(3y_1+y_2+y_3)\Big\}\theta(x_1)\\
&+\frac{1}{y_1^2y_3^2(y_2+y_3)^2(x_2-y_2)}\Big\{-x_1^3\left(y_1(y_2+2y_3)+y_2^2+3y_2y_3+3y_3^2\right)\\
&+x_1^4(y_2+2y_3)-3x_1^2y_1^2(y_2+2y_3)+x_1y_1^2\left(5y_1(y_2+2y_3)+2y_2^2+7y_2y_3+8y_3^2\right)\\
&-y_1^2\left(2y_1^2(y_2+2y_3)+y_1\left(y_2^2+4y_2y_3+5y_3^2\right)-y_3(y_2+y_3)^2\right)\Big\}\theta(x_1-y_1)\\
&-\frac{1}{y_2y_3^2(y_1+y_3)^3}\Big\{x_1^2y_2(y_1+3y_3)-x_1^3(y_1+3y_3)\\
&+x_1(y_1+y_3)\left(3y_1^2+y_1(y_2+6y_3)+3y_3(y_2+y_3)\right)\\
&-(y_1+y_3)^2\left(2y_1^2+y_1(y_2+2y_3)-y_2y_3\right)\Big\}\theta(y_2-x_2)\\
&+\frac{x_2\left(x_1^2(y_1+3(y_2+y_3))+x_1(x_1+x_2)(y_1+3(y_2+y_3))\right)\theta(-x_2)}{y_2(y_2+y_3)^2(x_1+x_2)^3}\\
&-\frac{2x_2y_1\theta(-x_2)}{y_2(y_2+y_3)^2(x_1+x_2)}\,,
\end{aligned} \tag{3.181}$$

$$\begin{aligned}
K_2 = &\frac{x_1^3}{y_3^2(y_1+y_3)^3(y_2-x_2)(x_1+x_2)^3}\Big\{x_2\big(9y_3^2(2y_1+y_2)+3y_3(2y_1+y_2)^2\\
&+y_1(y_1+y_2)(2y_1+y_2)+8y_3^3\big)+(y_1+y_3)^3(y_1+y_2+3y_3)\Big\}\theta(x_1)
\end{aligned}$$

$$
\begin{aligned}
&+\frac{1}{y_1^2y_3^2(y_1+y_2)^2(x_2-y_2)}\Big\{x_1^3\big(y_1^2+x_2(2y_1+y_2)\big)+y_3^2\big(3x_1^2(2y_1+y_2)\\
&\quad -x_1\left(8y_1^2+7y_1y_2+2y_2^2\right)-y_1(y_1+y_2)^2\big)-y_3^3\big(5x_1(2y_1+y_2)\\
&\qquad -5y_1^2-4y_1y_2-y_2^2\big)+2y_3^4(2y_1+y_2)\Big\}\theta(x_1-y_3)\\
&+\frac{1}{y_1^2y_2(y_1+y_3)^3}\Big\{x_1(y_1+y_3)\big(y_3(6y_1+y_2)+3y_1(y_1+y_2)+3y_3^2\big)\\
&\quad +x_1^2y_2(3y_1+y_3)-x_1^3(3y_1+y_3)\\
&\quad (y_1+y_3)^2\big(y_3(y_2+2y_3)-y_1(y_2-2y_3)\big)\Big\}\theta(y_2-x_2)\\
&-\frac{x_2\big(x_1^2(3(y_1+y_2)+y_3)+x_1(x_1+x_2)(3(y_1+y_2)+y_3)\big)}{y_2(y_1+y_2)^2(x_1+x_2)^3}\theta(-x_2)\\
&+\frac{2x_2y_3}{y_2(y_1+y_2)^2(x_1+x_2)}\theta(-x_2)\,,
\end{aligned}
\tag{3.182}
$$

$$
\begin{aligned}
K_3=&\frac{x_1^3\left(4y_1^2+y_1(5y_2+2y_3)+y_2(y_2+y_3)\right)\theta(x_1)}{y_1^2(y_1+y_2)^2(x_1+x_2)^3}\\
&-\frac{(x_1-y_1)^2(x_1+2y_1)\theta(x_1-y_1)}{y_1^2y_2(y_2+y_3)^2}\\
&+\frac{(x_2-y_3)^2(x_1+2(y_1+y_2))\theta(y_3-x_2)}{y_2y_3^2(y_1+y_2)^2}\\
&-\frac{1}{y_3^2(y_2+y_3)^2(x_1+x_2)^3}\Big\{x_1^3\big(y_1(y_2+2y_3)+(y_2+y_3)(y_2+4y_3)\big)\\
&\quad -3x_1(y_2+2y_3)(x_1+x_2)^3+2(x_1+x_2)^3\big(y_1(y_2+2y_3)+(y_2+y_3)^2\big)\Big\}\theta(-x_2)\,,
\end{aligned}
\tag{3.183}
$$

$$
\begin{aligned}
K_4=&-\frac{x_1^3(3(y_1+y_2)+y_3)\theta(x_1)}{y_2(y_1+y_2)^2(x_1+x_2)^3}+\frac{(x_1-y_2)^3(3y_1+y_3)\theta(x_1-y_2)}{y_1^2y_2(y_1+y_3)^3}\\
&-\frac{(x_2-y_3)^2\left(2x_1y_1+x_1y_2+y_1^2-y_2^2\right)\theta(y_3-x_2)}{y_1^2y_3^2(y_1+y_2)^2}\\
&+\frac{x_2}{y_3^2(y_1+y_3)^3(y_1+y_2+y_3)^3}\Big\{3x_2(y_1+y_3)\big(3y_3(2y_1+y_2)+y_1(y_1+y_2)\\
&\qquad +5y_3^2\big)(x_1+x_2)-x_2^2\big(9y_3^2(2y_1+y_2)+3y_3(2y_1+y_2)^2\\
&\qquad +y_1(y_1+y_2)(2y_1+y_2)+8y_3^3\big)-6y_3(y_1+y_3)^2(x_1+x_2)^2\Big\}\theta(-x_2)\,,
\end{aligned}
\tag{3.184}
$$

$$
K_5=-\frac{x_1^3\left(y_1+y_2+3y_3\right)\theta(x_1)}{y_2y_3^2(x_1+x_2)^3}+\frac{(x_1-y_2)^3(y_1+3y_3)\theta(x_1-y_2)}{y_2y_3^2(y_1+y_3)^3}
$$

$$
\begin{aligned}
&+\frac{(x_1-y_3)^2(x_1+2y_3)\theta(x_1-y_3)}{y_2y_3^2(y_1+y_2)^2}-\frac{(x_1-y_2+2y_3)\,(x_2-y_1)^2\,\theta(y_1-x_2)}{y_1^2y_2y_3^2}\\
&+\frac{1}{y_1^2y_3}\Bigg\{\frac{2x_1^3y_1^2}{y_2(x_1+x_2)^3}-\frac{x_1^3y_1^2}{y_2(x_1+x_2)(y_1+y_2)^2}-\frac{x_1^3y_1^2}{y_2(x_1+x_2)^2(y_1+y_2)}\\
&\quad-\frac{2y_1^2(x_1-y_2)^3}{y_2(y_1+y_3)^3}+\frac{3y_3\left((y_1+y_2)^2-x_1(2y_1+y_2)\right)}{(y_1+y_2)^2}+\frac{(x_1-y_2)^3}{y_2(y_1+y_3)}\\
&\quad+\frac{y_1(x_1-y_2)^3}{y_2(y_1+y_3)^2}+\frac{2y_3^2(2y_1+y_2)}{(y_1+y_2)^2}\Bigg\}\theta(-x_2)\,,
\end{aligned}
\tag{3.185}
$$

$$
\begin{aligned}
K_6=&\frac{x_1^3(y_1(y_2+2y_3)+(y_2+y_3)(y_2+4y_3))\theta(x_1)}{y_3^2(y_2+y_3)^2(x_1+x_2)^3}\\
&-\frac{(x_1-y_3)^2(x_1+2y_3)\theta(x_1-y_3)}{y_2y_3^2(y_1+y_2)^2}\\
&+\frac{(x_2-y_1)^2(x_1+2(y_2+y_3))\theta(y_1-x_2)}{y_1^2y_2(y_2+y_3)^2}\\
&-\frac{x_2}{y_1^2(y_1+y_2)^2(x_1+x_2)^3}\Big\{x_2^2\big(4y_1^2+y_1(5y_2+2y_3)\\
&\quad+y_2(y_2+y_3)\big)-3x_2\left(4y_1^2+y_1(5y_2+2y_3)+y_2(y_2+y_3)\right)(x_1+x_2)\\
&\quad+6y_1(y_1+y_2)(x_1+x_2)^2\Big\}\theta(-x_2)\,.
\end{aligned}
\tag{3.186}
$$

In this transition channel, one encounters the same logarithmic conundrum as in the channel discussed in the previous Sec. 3.4.3 after Fourier transforming corresponding kernels derived in Ref. [78]. Yet again making use of the symmetry under $a \leftrightarrow d$, $y_1 \leftrightarrow y_3$, one manages to get rid of all logarithmic terms, and the resulting expression completely agree with our Feynman diagrammatic results. All our results here are conformally invariant as expected. The inverse-Fourier transformed kernels are provided in Appendix B.5.2 for comparison with Ref. [78].

Now the following operators are considered under one-loop renormalization,

$$f_{+-}\psi_{+} \text{ and } f_{++}\psi_{-}$$

The two-particle blocks

$$\mathcal{O}^{ai}(x_1,x_2) = f^a_{+-}(x_1)\psi^i_{+}(x_2)\,, \qquad \mathcal{O}^{ai}(x_1,x_2) = f^a_{++}(x_1)\psi^i_{-}(x_2)\,, \tag{3.187}$$

undergo a transition to the following three-field operator

$$\mathcal{O}^{aid} = g\sqrt{2} f^a_{++}(y_1)\psi^i_{+}(y_2)\bar{f}^d_{++}(y_3)\,, \tag{3.188}$$

according to

$$[\mathcal{K}\mathcal{O}]^{ai}(x_1,x_2) = \int [\mathcal{D}^3 y]_2 \sum_{c=1}^{6} [C_c]^{ai}_{a'i'd} K_c(x_1,x_2|y_1,y_2,y_3)\mathcal{O}^{a'i'd}(y_1,y_2,y_3)\,, \tag{3.189}$$

where the decomposition runs over the color structures given in Eq. (3.158).

The evolution kernels for the two cases $\mathcal{O}^{ai}(x_1,x_2) = f^a_{+-}(x_1)\psi^i_{+}(x_2)$ and $\mathcal{O}^{ai}(x_1,x_2) = f^a_{++}(x_1)\psi^i_{-}(x_2)$ read

$$K_1 = \frac{x_1(3y_1+y_3)\theta(x_1)}{y_1^2(y_1+y_3)^3} - \frac{x_1\theta(x_1-y_1)}{y_1^2 y_3^2} + \frac{x_1(y_1+3y_3)\theta(x_1-y_1-y_3)}{y_3^2(y_1+y_3)^3}\,, \tag{3.190}$$

$$K_2 = \frac{x_1(x_1(y_1+3y_3)-2y_3(y_1+y_3))\theta(x_1)}{(x_1-y_1-y_3)y_3^2(y_1+y_3)^3} - \frac{(x_1-y_3)^2\theta(x_1-y_3)}{y_1^2 y_3^2(x_1-y_1-y_3)} - \frac{((y_1+y_3)^2 - x_1(3y_1+y_3))\theta(x_1-y_1-y_3)}{y_1^2(y_1+y_3)^3}\,, \tag{3.191}$$

$$K_3 = 0\,, \tag{3.192}$$

$$K_4 = 0\,, \tag{3.193}$$

$$K_5 = 0\,, \tag{3.194}$$

$$K_6 = 0 \tag{3.195}$$

and

$$K_1 = \frac{(y_2+2y_3)\theta(x_1-y_1)}{y_3^2(y_2+y_3)^2} - \frac{\theta(x_1-y_1-y_3)}{y_2 y_3^2} + \frac{\theta(-x_2)}{y_2(y_2+y_3)^2}\,, \tag{3.196}$$

$$K_2 = 0\,, \tag{3.197}$$

$$K_3 = -\frac{\theta(x_1-y_1)}{y_2(y_2+y_3)^2} + \frac{\left(1-\dfrac{y_2}{x_1-y_1}\right)\theta(x_1-y_1-y_2)}{y_2 y_3^2} - \frac{\left(y_2+2y_3-\dfrac{(y_2+y_3)^2}{x_1-y_1}\right)\theta(-x_2)}{y_3^2(y_2+y_3)^2}\,, \tag{3.198}$$

$$K_4 = \frac{(x_1(3y_1+y_3)-y_1(y_1+3y_2)-y_3(y_1+y_2))\theta(x_1)}{y_1^2(y_1+y_3)^3} + \frac{(x_2-y_3)\theta(y_3-x_2)}{y_1^2 y_3^2} + \frac{((y_3-x_2)(y_1+3y_3)-2y_3^2)\theta(-x_2)}{y_3^2(y_1+y_3)^3}\,, \tag{3.199}$$

$$K_5 = \frac{(x_1(y_1+3y_3)-y_1(y_2+y_3)-y_3(3y_2+y_3))\theta(x_1-y_2)}{y_3^2(y_1+y_3)^3} + \frac{(x_2-y_1)\theta(y_1-x_2)}{y_1^2 y_3^2} - \frac{(2y_1^2-x_1(3y_1+y_3)+3y_1(y_2+y_3)+y_3(y_2+y_3))\theta(-x_2)}{y_1^2(y_1+y_3)^3}\,, \tag{3.200}$$

$$K_6 = 0\,, \tag{3.201}$$

respectively. The first set comes from Fig. 3.10, while the second one from both Figs. 3.10 and 3.11. This time one found an exact agreement with the findings of Ref. [78] without further implementation of symmetry properties. This can be easily explained by the fact that the operators in this case lack the "field exchanging" symmetries. As a result, no redundancies in the evolution kernels are allowed to be left over. By taking the heavy quark limit, one also reproduced the results reported in Ref. [87].

Next, the following transitions are considered:

$$\bar{\psi}_+ f_{+-} \text{ and } \tfrac{1}{2} D_{-+} \bar{\psi}_+ f_{++}$$

$$\mathcal{O}^{ia}(x_1,x_2) = \bar{\psi}_+^i(x_1) f_{+-}^a(x_2)\,, \qquad \mathcal{O}^{ia}(x_1,x_2) = \tfrac{1}{2} D_{-+} \bar{\psi}_+^i(x_1) f_{++}^a(x_2)\,, \tag{3.202}$$

to

$$\mathcal{O}^{iad} = g\sqrt{2}\,\bar{\psi}_+^i(y_1) f_{++}^a(y_2) \bar{f}_{++}^d(y_3)\,. \tag{3.203}$$

It is described by

$$[\mathcal{K}\,\mathcal{O}]^{ia}(x_1,x_2)=\int[\mathcal{D}^3y]_2\sum_{c=1}^{6}[C_n]^{ia}_{a'i'd}K_c(x_1,x_2|y_1,y_2,y_3)\mathcal{O}^{a'i'd}(y_1,y_2,y_3)\,, \tag{3.204}$$

with the color structures given in Eq. (3.158).

For $\mathcal{O}^{ia}(x_1,x_2)=\bar{\psi}^i_+(x_1)f^a_{+-}(x_2)$ the kernels are

$$\begin{aligned}
K_1 =& -\frac{x_1x_2(3y_1+y_2+3y_3)\theta(x_1)}{y_1(y_1+y_3)^2(x_1+x_2)^3}+\frac{x_1x_2(y_2+3y_3)\theta(x_1-y_1)}{y_1y_3^2(y_2+y_3)^3}\\
&+\frac{x_1x_2\big(y_1^2(3y_2+y_3)+3y_1(y_2+y_3)(3y_2+y_3)+2(y_2+y_3)^2(4y_2+y_3)\big)\theta(-x_2)}{y_2^2(x_1+x_2)^3(y_2+y_3)^3}\\
&-\frac{x_1x_2(y_1+2y_3)\theta(y_2-x_2)}{y_2^2y_3^2(y_1+y_3)^2}\,,
\end{aligned} \tag{3.205}$$

$$\begin{aligned}
K_2 =& -\frac{x_1x_2\big(y_1^2+2y_3(y_2+2y_3)+y_1(y_2+5y_3)\big)\theta(x_1)}{y_3^2(y_1+y_3)^2(x_1+x_2)^3}+\frac{x_1x_2\theta(x_1-y_3)}{y_1y_3^2(y_1+y_2)^2}\\
&+\frac{x_1x_2\big(y_1^2+2y_2(2y_2+y_3)+y_1(5y_2+y_3)\big)\theta(-x_2)}{y_2^2(y_1+y_2)^2(x_1+x_2)^3}-\frac{x_1x_2\theta(y_2-x_2)}{y_1^2y_2^2(y_1+y_3)^2}\,,
\end{aligned} \tag{3.206}$$

$$\begin{aligned}
K_3 =& \frac{x_1\big(2(x_1+x_2)(y_1+y_2)-x_1(3(y_1+y_2)+y_3)\big)\theta(x_1)}{y_1(y_1+y_2)^2(x_1+x_2)^3}\\
&-\frac{x_1\big(2y_2(y_2+y_3)-x_1(3y_2+y_3)+y_1(3y_2+y_3)\big)\theta(x_1-y_1)}{y_1y_2^2(y_2+y_3)^3}\\
&-\frac{(x_2-y_3)^2\big(y_2^2+x_1(y_1+2y_2)\big)\theta(y_3-x_2)}{y_2^2y_3^2(x_1-y_1)(y_1+y_2)^2}+\frac{1}{y_3^2(y_2+y_3)^3}\Big\{\frac{(y_2+y_3)^3}{x_1-y_1}\\
&+\frac{x_1^2\big(y_1^2(y_2+3y_3)+3y_1(y_2+y_3)(y_2+3y_3)+2(y_2+y_3)^2(y_2+4y_3)\big)}{(x_1+x_2)^3}\\
&-\frac{x_1\big(y_1^2(y_2+3y_3)+3(y_2+y_3)^2(y_2+3y_3)\big)}{(x_1+x_2)^2}\\
&+\frac{2x_1y_1(y_2+y_3)(2y_2+5y_3)\big)}{(x_1+x_2)^2}\Big\}\theta(-x_2)\,,
\end{aligned} \tag{3.207}$$

$$\begin{aligned}
K_4 =& \frac{x_1}{y_3^2(x_1+x_2)^3(y_2+y_3)^3}\Big\{x_1\big(y_1^2(y_2+3y_3)+3y_1(y_2+y_3)(y_2+3y_3)\\
&+2(y_2+y_3)^2(y_2+4y_3)\big)-(x_1+x_2)(y_2+y_3)\big(y_1(y_2+3y_3)\\
&+(y_2+y_3)(y_2+5y_3)\big)\Big\}\theta(x_1)\\
&-\frac{x_1\big(x_1(y_1+2y_2)-y_1(y_2+y_3)-y_2(y_2+2y_3)\big)\theta(x_1-y_3)}{y_2^2y_3^2(y_1+y_2)^2}
\end{aligned}$$

$$
\begin{aligned}
&-\frac{x_1(x_2-y_1)(3y_2+y_3)\theta(y_1-x_2)}{y_1y_2^2(y_2+y_3)^3}+\frac{x_1x_2(3(y_1+y_2)+y_3)\theta(-x_2)}{y_1(y_1+y_2)^2(x_1+x_2)^3}, \qquad (3.208)\\
K_5=&\frac{x_1}{y_3^2}\Big\{\frac{2x_1y_2}{y_1(y_2+y_3)^3}-\frac{2y_2(y_1+y_2)+x_1(y_1+2y_2)}{y_2^2(y_1+y_2)^2}-\frac{3x_1+2y_2}{y_1(y_2+y_3)^2}\\
&+\frac{4}{y_1(y_2+y_3)}-\frac{2x_1(y_1+y_2)}{y_1(x_1+x_2)^3}+\frac{3x_1+2(y_1+y_2)}{y_1(x_1+x_2)^2}-\frac{4}{y_1(x_1+x_2)}\Big\}\theta(x_1)\\
&-\frac{(x_1-y_2)^2\theta(x_1-y_2)}{y_1y_2^2y_3^2}+\frac{(x_2-y_3)^2\theta(y_3-x_2)}{y_1(y_1+y_2)^2y_3^2}\\
&-\frac{\big((x_1+x_2)^3-2x_1(x_1+x_2)(y_1+y_2+2y_3)+x_1^2(y_1+y_2+3y_3)\big)\theta(-x_2)}{y_1y_3^2(x_1+x_2)^3}\\
&+\frac{(y_1-x_2)\big(x_1(y_2+3y_3)-(y_2+y_3)^2\big)\theta(y_1-x_2)}{y_1y_3^2(y_2+y_3)^3}, \qquad (3.209)\\
K_6=&\frac{x_1\big(2y_2(x_1+x_2)(y_1+y_2)-x_1(y_1^2+2y_2(2y_2+y_3)+y_1(5y_2+y_3))\big)\theta(x_1)}{y_2^2(y_1+y_2)^2(x_1+x_2)^3}\\
&+\frac{(x_1-y_2)^2\theta(x_1-y_2)}{y_1y_2^2(y_1+y_3)^2}-\frac{(x_2-y_3)^2\theta(y_3-x_2)}{y_1y_3^2(y_1+y_2)^2}\\
&+\frac{x_2\big((x_1+x_2)^2(y_1+2y_3)-x_1(y_1^2+2y_3(y_2+2y_3)+y_1(y_2+5y_3))\big)\theta(-x_2)}{y_3^2(x_1+x_2)^3(y_1+y_2)^2}, \qquad (3.210)
\end{aligned}
$$

while for $\mathcal{O}^{ia}(z_1,z_2)=\frac{1}{2}D_{-+}\bar{\psi}^i_+(z_1)f^a_{++}(z_2)$ they are found to be

$$
\begin{aligned}
K_1=&\frac{x_1^2}{y_1(y_1+y_3)^2}\Big\{\frac{1}{x_2-y_2}+\frac{2x_1y_2-3(x_1+x_2)(x_1+y_2)+5(x_1+x_2)^2}{(x_1+x_2)^3}\Big\}\theta(x_1)\\
&+\frac{1}{y_3^2}\Big\{1-\frac{(x_1-y_1)^2}{y_1(x_2-y_2)(y_2+y_3)^3}\big(y_2(x_2-y_3)^2+y_3(x_2-y_3)(3y_1+5y_2-3x_1)\\
&+2y_3^2(4y_1+5y_2-4x_1)+6y_3^3\big)\Big\}\theta(x_1-y_1)\\
&+\frac{1}{y_2^2y_3^2(y_1+y_3)^2}\Big\{(y_1+y_3)\big(y_1^3-y_2^2y_3+2y_1^2(y_2+y_3)+y_1y_3(2y_2+y_3)\big)\\
&-x_1^3(y_1+2y_3)-x_1(x_1+x_2)\big(3y_1^2+2y_3(y_2+y_3)+y_1(y_2+5y_3)\big)\\
&+x_1^2\big(3y_1^2+4y_3(y_2+y_3)+y_1(2y_2+7y_3)\big)\Big\}\theta(y_2-x_2)\\
&+\frac{x_2^2}{y_2^2(y_2+y_3)^3(x_1+x_2)^3}\Big\{x_1\big(y_1^2(3y_2+y_3)+3y_1(y_2+y_3)(3y_2+y_3)\\
&\quad+2(4y_2+y_3)(y_2+y_3)^2\big)\\
&-y_1(x_1+x_2)\big(y_1(3y_2+y_3)+(y_2+y_3)(4y_2+y_3)\big)\Big\}\theta(-x_2), \qquad (3.211)
\end{aligned}
$$

$$
\begin{aligned}
K_2 &= \frac{x_1^2}{y_3^2(y_1+y_3)^2}\Big\{9+\frac{2x_1-y_1}{x_2-y_2}-\frac{2x_1y_2(y_1+y_2)}{(x_1+x_2)^3}-\frac{4x_1+5y_1+10y_2}{x_1+x_2}\\
&\quad+\frac{3(y_2(y_1+y_2)+x_1(y_1+2y_2))}{(x_1+x_2)^3}\Big\}\theta(x_1)\\
&\quad-\frac{x_1^2-y_3^2}{y_1y_3^2(y_1+y_2)^2(x_2-y_2)}\Big\{x_1^2+3y_1^2+(y_2+y_3)^2+y_1(4y_2+3y_3)\\
&\quad-x_1\big(3y_1+2(y_2+y_3)\big)\Big\}\theta(x_1-y_3)-\frac{x_2^2(x_1+y_1+y_3)\theta(y_2-x_2)}{y_1y_2^2(y_1+y_3)^2}\\
&\quad+\frac{x_2^2}{y_2^2(y_1+y_2)^2(x_1+x_2)^3}\Big\{x_1\big(y_1^2+2y_2(2y_2+y_3)+y_1(5y_2+y_3)\big)\\
&\quad+(x_1+x_2)\big(y_1^2+y_1(4y_2+y_3)+y_2(3y_2+2y_3)\big)\Big\}\theta(-x_2)\,, \qquad (3.212)\\
K_3 &= \frac{x_1^2\big(x_1(3(y_1+y_2)+y_3)-3(x_1+x_2)(y_1+y_2)\big)\theta(x_1)}{y_1(y_1+y_2)^2(x_1+x_2)^3}\\
&\quad-\frac{(x_1-y_1)^2}{y_1y_2^2(y_2+y_3)^3}\Big\{x_1(3y_2+y_3)-3y_2(y_2+y_3)-y_1(3y_2+y_3)\Big\}\theta(x_1-y_1)\\
&\quad+\frac{(y_3-x_2)^3(y_1+2y_2)\theta(y_3-x_2)}{y_2^2y_3^2(y_1+y_2)^2}\\
&\quad+\frac{x_2^2}{y_3^2(y_2+y_3)^3(x_1+x_2)^3}\Big\{(x_1+x_2)\big(2(y_2+y_3)^3+3y_1(y_2+y_3)(y_2+2y_3)\\
&\qquad+y_1^2(y_2+3y_3)\big)-x_1\big(y_1^2(y_2+3y_3)+3y_1(y_2+y_3)(y_2+3y_3)\\
&\qquad+2(y_2+y_3)^2(y_2+4y_3)\big)\Big\}\theta(-x_2)\,, \qquad (3.213)\\
K_4 &= \frac{x_1^2}{y_3^2(y_2+y_3)^3(x_1+x_2)^3}\Big\{(x_1+x_2)(y_2+y_3)\big(2(y_2+y_3)(y_2+4y_3)\\
&\qquad+y_1(2y_2+5y_3)\big)-x_1\big(y_1^2(y_2+3y_3)+3y_1(y_2+y_3)(y_2+3y_3)\\
&\qquad+2(y_2+y_3)^2(y_2+4y_3)\big)\Big\}\theta(x_1)\\
&\quad+\frac{x_1^2-y_3^2}{y_2^2(y_1+y_2)^2y_3^2}\Big\{x_1(y_1+2y_2)-2y_2(y_2+y_3)-y_1(2y_2+y_3)\Big\}\theta(x_1-y_3)\\
&\quad-\frac{(x_2-y_1)^2\big((y_2+y_3)(2y_2+y_3)+x_1(3y_2+y_3)\big)\theta(y_1-x_2)}{y_1y_2^2(y_2+y_3)^3}\\
&\quad+\frac{x_2^2\big((x_1+x_2)(2(y_1+y_2)+y_3)+x_1(3(y_1+y_2)+y_3)\big)\theta(-x_2)}{y_1(y_1+y_2)^2(x_1+x_2)^3}\,, \qquad (3.214)\\
K_5 &= \frac{x_1^2}{y_3^2}\Big\{\frac{3y_2(y_1+y_2)-x_1(y_1+2y_2)}{y_2^2(y_1+y_2)^2}-\frac{2x_1y_2}{y_1(y_1+y_3)^3}+\frac{3(x_1+y_2)}{y_1(y_2+y_3)^2}
\end{aligned}
$$

$$
\begin{aligned}
&\quad - \frac{6}{y_1(y_2+y_3)} + \frac{2x_1(y_1+y_2)}{y_1(x_1+x_2)^3} - \frac{3(x_1+y_1+y_2)}{y_1(x_1+x_2)^2} + \frac{6}{y_1(x_1+x_2)} \Big\} \theta(x_1) \\
&+ \frac{(x_1-y_2)^3\theta(x_1-y_2)}{y_1y_2^2y_3^2} + \frac{(x_2-y_3)^3\theta(y_3-x_2)}{y_1y_3^2(y_1+y_2)^2} \\
&+ \frac{(x_2-y_1)^2\big(y_2(y_2+y_3)-x_1(y_2+3y_3)\big)\theta(y_1-x_2)}{y_1y_3^2(y_2+y_3)^3} \\
&- \frac{x_2^2\big((x_1+x_2)(y_1+y_2)-x_1(y_1+y_2+3y_3)\big)\theta(-x_2)}{y_1y_3^2(x_1+x_2)^3}, \qquad (3.215)
\end{aligned}
$$

$$
\begin{aligned}
K_6 = &\frac{x_1^2\big(x_1(y_1^2+2y_2(2y_2+y_3)+y_1(5y_2+y_3)-3y_2(x_1+x_2)(y_1+y_2))\big)\theta(x_1)}{y_2^2(y_1+y_2)^2(x_1+x_2)^3} \\
&- \frac{(x_1-y_2)^3\theta(x_1-y_2)}{y_1y_2^2(y_1+y_3)^2} - \frac{(x_2-y_3)^3\theta(y_3-x_2)}{y_1y_3^2(y_1+y_2)^2} \\
&+ \frac{x_2^2}{y_3^2(y_1+y_3)^2(x_1+x_2)^3}\Big\{(x_1+x_2)\big((y_1+2y_3)(y_1+y_2)+y_3^2\big) \\
&- x_1\big(y_1^2+2y_3(y_2+2y_3)+y_1(y_2+5y_3)\big)\Big\}\theta(-x_2)\,. \qquad (3.216)
\end{aligned}
$$

Here one again finds complete agreement with Ref. [78].

Finally, one compute the one-loop renormalization of operators

$$\bar{\psi}_+\psi_- \text{ and } \tfrac{1}{2}D_{-+}\bar{\psi}_+\psi_+$$

i.e., transitions from

$$\mathcal{O}^{ij}(x_1,x_2) = \bar{\psi}_+^i(x_1)\psi_-^j(x_2)\,, \qquad \mathcal{O}^{ij}(x_1,x_2) = \tfrac{1}{2}D_{-+}\bar{\psi}_+^i(x_1)\psi_+^j(x_2)\,, \qquad (3.217)$$

into

$$\mathcal{O}^{ijd} = g\sqrt{2}\bar{\psi}_+^i(y_1)\psi_+^j(y_2)\bar{f}_{++}^d(y_3)\,. \qquad (3.218)$$

This sector is determined by

$$[\mathcal{K}\mathcal{O}]^{ij}(x_1,x_2) = \int [\mathcal{D}^3y]_2 \sum_{c=1}^{3} [C_c]^{ij}_{a'i'd} K_c(x_1,x_2|y_1,y_2,y_3)\mathcal{O}^{i'j'd}(y_1,y_2,y_3)\,, \qquad (3.219)$$

expanded over three color structures given in Eq. (3.147), with explicit results for $\mathcal{O}^{ij}(x_1,x_2) = \bar{\psi}^i_+(x_1)\psi^j_-(x_2)$ and $\mathcal{O}^{ij}(z_1,z_2) = \frac{1}{2}D_{-+}\bar{\psi}^i_+(z_1)\psi^j_+(z_2)$ cases being

$$
\begin{aligned}
K_1 &= \frac{x_1(2y_1+y_2+2y_3)\theta(x_1)}{y_1(x_1+x_2)^2(y_1+y_3)^2} - \frac{x_1(y_2+2y_3)\theta(x_1-y_1)}{y_1y_3^2(y_2+y_3)^2} \\
&\quad + \frac{x_1(y_1+2y_3)\theta(y_2-x_2)}{y_2y_3^2(y_1+y_3)^2} - \frac{x_1\big(y_1+2(y_2+y_3)\big)\theta(-x_2)}{y_2(x_1+x_2)^2(y_2+y_3)^2}\,, \qquad (3.220)\\
K_2 &= \frac{x_1\big(y_1(y_1+y_2)+2y_3(2y_1+y_2)+3y_3^2\big)\theta(x_1)}{y_3^2(x_1+x_2)^2(y_1+y_3)^2} - \frac{x_1\theta(x_1-y_3)}{y_1y_3^2(y_1+y_2)} \\
&\quad + \frac{x_1\theta(y_2-x_2)}{y_1y_2(y_1+y_3)^2} - \frac{x_1\theta(-x_2)}{y_2(y_1+y_2)(x_1+x_2)^2}\,, \qquad (3.221)\\
K_3 &= \frac{x_1\theta(x_1)}{y_1(y_1+y_2)(x_1+x_2)^2} - \frac{x_1\theta(x_1-y_1)}{y_1y_2(y_2+y_3)^2} + \frac{(y_3-x_2)(x_1+y_2)\theta(y_3-x_2)}{y_2y_3^2(x_1-y_1)(y_1+y_2)} \\
&\quad + \frac{1}{y_3^2(x_1-y_1)(x_1+x_2)^2(y_2+y_3)^2}\Big\{(x_1+x_2)^2(y_2+y_3)^2 - x_1^2\big(y_1(y_2+2y_3) \\
&\quad + (y_2+y_3)(y_2+3y_3)\big) + x_1y_1\big(y_1(y_2+2y_3)+(y_2+y_3)(y_2+3y_3)\big)\Big\}\theta(-x_2)\,, \qquad (3.222)
\end{aligned}
$$

and

$$
\begin{aligned}
K_1 &= \frac{x_1^2\big(3y_1(y_1+y_2)+y_2^2+3y_3(2y_1+y_2+y_3)-x_1(2y_1+y_2+2y_3)\big)\theta(x_1)}{y_1(x_2-y_2)(y_1+y_3)^2(x_1+x_2)^2} \\
&\quad - \frac{1}{y_3^2}\Big\{\frac{(x_1-y_1)^2\big(y_2(y_1+y_2)+y_3(2y_1+3y_2)+3y_3^2-x_1(y_2+2y_3)\big)}{y_1(x_2-y_2)(y_2+y_3)^2} \\
&\quad - 1\Big\}\theta(x_1-y_1) - \frac{1}{y_3^2}\Big\{1-\frac{x_2\big(y_1(y_1+y_3)-x_1(y_1+2y_3)\big)}{y_2(y_1+y_3)^2}\Big\}\theta(y_2-x_2) \\
&\quad - \frac{x_2\big(y_1(x_1+x_2)-x_1(y_1+2(y_2+y_3))\big)\theta(-x_2)}{y_2(x_1+x_2)^2(y_2+y_3)^2}\,, \qquad (3.223)\\
K_2 &= \frac{x_1^2}{y_3^2(y_1+y_3)^2}\Big\{\frac{y_1+2y_3}{x_2-y_2} + \frac{y_1(y_1+y_2)+2y_3(2y_1+y_2)+3y_3^2}{(x_1+x_2)^2}\Big\}\theta(x_1) \\
&\quad - \frac{(x_2+y_1)(x_1^2-y_3^2)\theta(x_1-y_3)}{y_1y_3^2(x_2-y_2)(y_1+y_2)} - \frac{x_2(x_1+y_1+y_3)\theta(y_2-x_2)}{y_1y_2(y_1+y_3)^2} \\
&\quad + \frac{x_2(2x_1+x_2)\theta(-x_2)}{y_2(y_1+y_2)(x_1+x_2)^2}\,, \qquad (3.224)\\
K_3 &= \frac{x_1^2\theta(x_1)}{y_1(y_1+y_2)(x_1+x_2)^2} - \frac{(x_1-y_1)^2\theta(x_1-y_1)}{y_1y_2(y_2+y_3)^2} + \frac{(x_2-y_3)^2\theta(y_3-x_2)}{y_2y_3^2(y_1+y_2)} \\
&\quad - \frac{x_2}{y_3^2(x_1+x_2)^2(y_2+y_3)^2}\Big\{(x_1+x_2)\big((y_2+y_3)^2+y_1(y_2+2y_3)\big)
\end{aligned}
$$

$$-x_1\big(y_1(y_2+2y_3)+(y_2+y_3)(y_2+3y_3)\big)\Big\}\theta(-x_2)\,, \tag{3.225}$$

respectively. Again, when Fourier transformed to the coordinate space, one found complete agreement with the conformally approach of Ref. [78]. This completes our study of flavor-nonsinglet transitions.

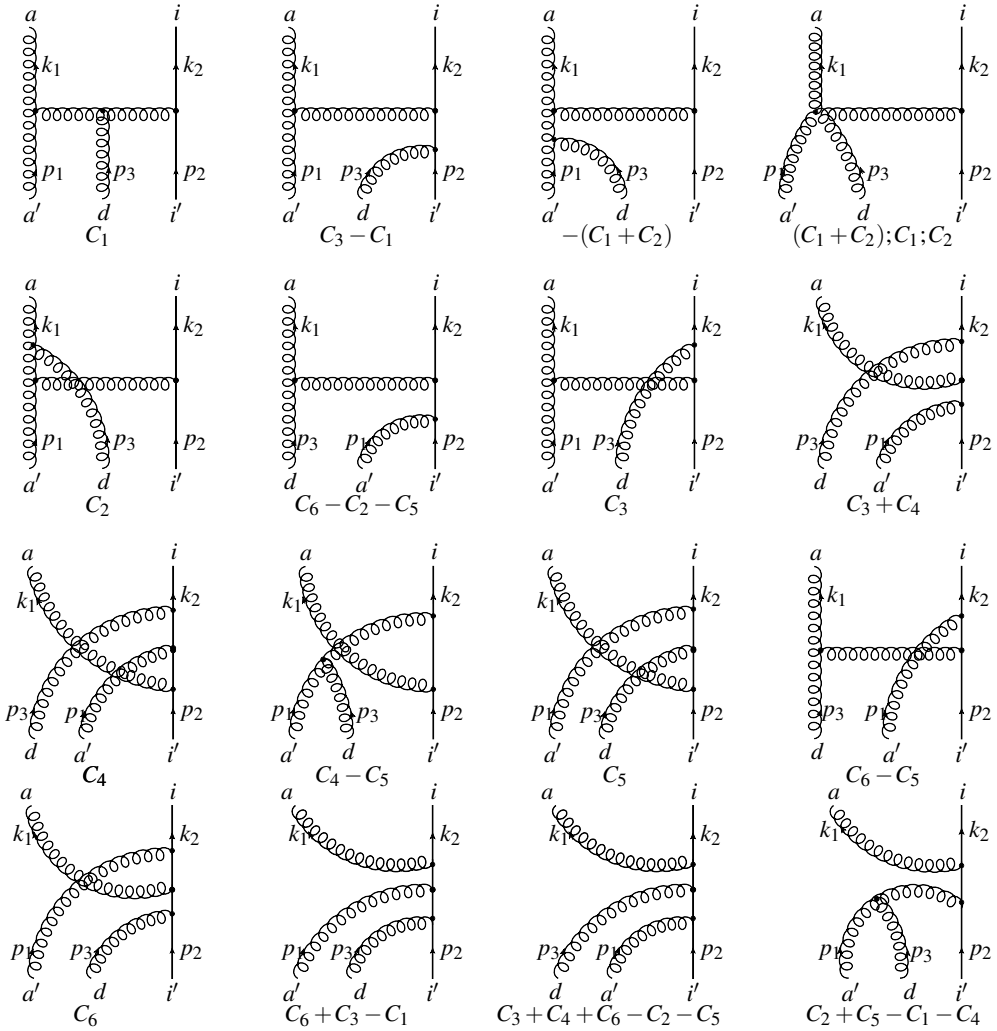

Figure 3.10: Feynman diagrams defining the evolution kernels in Secs. 3.4.3 and 3.4.3.

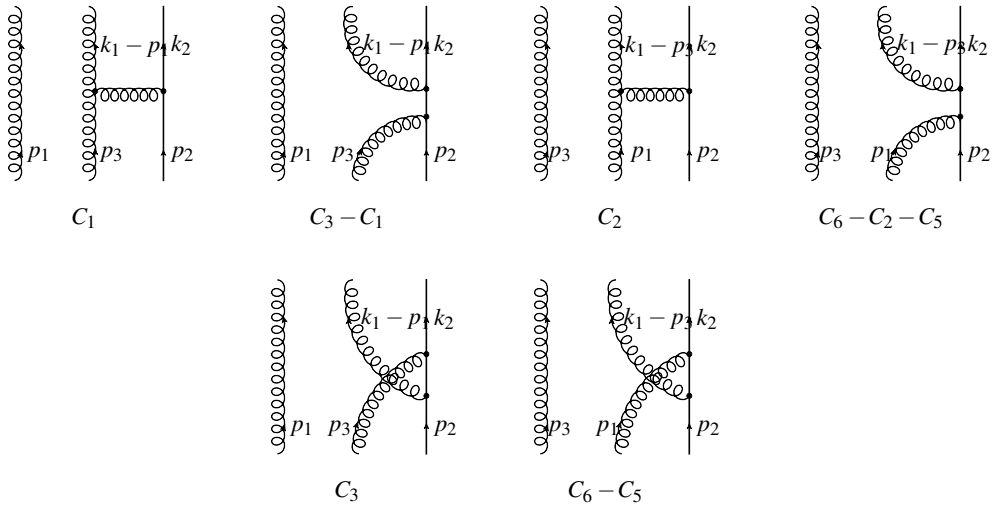

Figure 3.11: Graphs producing the contribution of gluon fields in the covariant derivative D_{-+}, as for the case of $\frac{1}{2}D_{-+}\bar{f}_{++}\psi_{-}$ in Sec. 3.4.3, or in the form of $\bar{A}_{\perp}A_{\perp}$ for the case of $f_{+-}\psi$ in Sec. 3.4.3.

CHAPTER 4

SUMMARY AND OUTLOOK

4.1 Summary

In the introduction it was argued that, in order to have a better understanding of the nucleon spin content, the generalized parton distribution functions unifying different aspects of nucleon observables proved to be an excellent framework to work with.

The second chapter developed a unified framework for virtual Compton scattering that uses helicity Compton form factors for the analysis of different regimes of the processes, interpolating between deeply virtual and quasi-real. The main ingredients of the consideration include: a clear separation between the leptonic and hadronic components via computation of helicity amplitudes in the target rest frame and an exact reconstruction of the kinematical tensor decomposition for the hadronic Compton amplitude. The target rest frame is special since the entire dependence on the azimuthal angle of the photon-nucleon scattering plane is encoded in the leptonic part of the cross section that was calculated exactly, overcoming the limitation of the scheme from Ref. [36] adopted previously for the analysis of electroproduction. Since partial results for the hadronic helicity amplitudes with unpolarized and longitudinally polarized targets were available before, one complemented them with the ones for the transversally polarized nucleon as well. We also incorporated the double photon helicity-flip amplitudes, induced by the gluon-transversity GPDs, into the analysis. To relate the helicity CFFs with the conventional ones emerging in the OPE analysis of the Compton amplitude, one introduced an exact Lorentz decomposition for the latter that is free from kinematical singularities, and computed the relations exactly.

One also explored the low-energy limit of Compton scattering and relation of the CFFs to the generalized polarizabilities in the center-of-mass frame. Along the way, ex-

pressions of the helicity form factors in terms of the structure functions of the VCS amplitude introduced by Tarrach were derived, as well as defined their low-energy expansion. The formulae set allows one to provide in a rather straightforward manner the low-energy expansion of the cross section for all possible polarization options in terms of generalized polarizabilities, in an analytic form. This may, as in the DVCS case, provide a useful guideline for further experimental measurements. This analysis suggests a complementary approach to the low-energy limit: instead of relying on a low-energy expansion in order to extract generalized polarizabilities, where a subtraction procedure (yielding its own ambiguities) is needed to extract genuine information about nucleon deformation, one may adopt the known scheme used in DVCS kinematics and seek a complete measurement of CFFs at low final-state photon energies.

In the third chapter, one generalized the formalism suggested by Bukhvostov-Frolov-Lipatov-Kuraev for renormalization of quasipartonic operators to include nonquasipartonic operators as well. The advantage of the method is that at one-loop order, the procedure is purely algebraic, requiring straightforward though quite tedious manipulations with the Dirac and Lorentz structure of Feynman graphs. In this chapter, one focused on the evolution equations for non-singlet twist-four operators. Their basis consists of four-particle quasipartonic and three-particle good-good-bad light-cone operators. While the former were studied at length in existing literature, the latter were addressed here starting from Feynman graphs, providing an explicit brute-force calculation of these evolution kernels. The main ingredients for these transitions are good-bad two-to-two and two-to-three components. A crucial role in both cases is played by proper use of QCD equations of motion, which induce extra contribution that are required for proper closure of evolutions equations. Since the basis of twist-four operators is built from conformal primary fields, the resulting evolution kernels should obey a very stringent consistency constraint of being conformally invariant. This was explicitly confirmed by the analysis.

One also performed a Fourier transform from momentum to coordinate space and back and checked the relevant evolution kernels against the only available earlier results for nonquasipartonic operators that were derived for light-ray operators making use of conformal symmetry and the dynamical part of the Poincaré algebra. One observed agreement in all cases, and also provided a simplified form of light-ray kernels in certain channels that made use of the exchange symmetry of the operators involved.

4.2 Outlook

In the future, the constructions and calculations introduced in this thesis can be implemented into the analysis of deep inelastic scattering experiments of a new generation dedicated to the study of nucleon structure [89, 90, 91]. The formalism presented in Chapter 2 is implemented in existing CFF/GPD fitting codes for deeply-virtual kinematics [57, 58]. This is required for an unbiased random variable map of an (almost) complete DVCS measurement by the HERMES collaboration [59, 60, 61, 62], providing 34 asymmetries in 12 kinematical bins, into the space of CFFs. Another advantage of such a tool is that one can easily switch between various "parton-to-hadron" conventions, which will allow for a precise numerical cross check with other existing software packages, which are adopted for GPD model predictions [63, 64]. In addition, the kinematical power-suppressed corrections from Ref. [65, 49, 50] can be conveniently taken into account relying on our formalism, thereby, avoiding a recalculation of the leptoproduction cross section.

It is also possible to extend the study introduced in Chapter 3 by computing the full contributions of one-loop twist-four operators in the non-singlet sector, using techniques developed within the present thesis in a straightforward manner. These results [65, 78] provide QCD background information for the study of GPDs, as well as precision measurements of the next generation dedicated to the exploration of New Physics. One may

also wish to study the two-loop effects of the non-quasipartonic operators, in which case the conformal symmetry is no long respected and inputs from Feynman diagram calculations are necessary. These studies have the potential to provide new insights into strong interactions. One may also proceed to calculate the corrections of the twist-4 operators to the nucleon structure functions in deep-inelastic scattering as a next step. One should keep in mind, however, this analysis is expected to be much more complicated, as a result of the vast numbers of evolution kernels still uncalculated. Another direction is to explore the possibility of constructing twist-4 2-to-3 kernels from 2-to-2 kernels already known in the literature as it was pointed out in Refs. [80, 88].

REFERENCES

[1] R. Frisch, O. Stern, Z. Phys. **85**: 416 (1933). doi:10.1007/bf01330773.

[2] I. Esterman, O. Stern, Z. Phys. **85**: 1724 (1933). doi:10.1007/bf01330774.

[3] I. Esterman, O. Stern, Physical Review **45**: 761(A109) (1934).

[4] I. I. Rabi, J. M. Kellogg, J. R. Zacharias, Physical Review **46**: 157163 (1934). doi:10.1103/physrev.46.157.

[5] I. I. Rabi, J. M. Kellogg, J. R. Zacharias, Physical Review **46**: 163165 (1934). doi:10.1103/physrev.46.163.

[6] R. Hofstadter, R. W. McAllister Phys. Rev. **98**, 217 (1955);
R. Hofstadter Rev. Mod. Phys. **28**, 214 (1956).

[7] M. R. Yearian, R. Hofstadter, Phys. Rev. **110**, 552 (1958).

[8] M. Gell-Mann, Physics Letters **8** (3): 214215 (1964);
G. Zweig,CERN Report No.8182/TH.401 (1964);
G. Zweig,CERN Report No.8419/TH.412 (1964).

[9] R. P. Feynman, "The Behavior of Hadron Collisions at Extreme Energies" High Energy Collisions: Third International Conference at Stony Brook, N.Y. Gordon & Breach. pp. 237249 (1969);
J. Bjorken, E. Paschos, Physical Review **185** (5): 19751982 (1969).

[10] J. Ashman; EMC Collaboration, Physics Letters B **206** (2): 364 (1988);
J. T. Londergan, "Nucleon Resonances and Quark Structure". International Journal of Modern Physics E **18** (56): 1135. arXiv:0907.3431.

[11] HERMES Collaboration (A. Airapetian, et al.), Phys.Lett. B **666** (2008) 446-450 arXiv:0803.2993.

[12] R. L. Jaffe, A. V. Manohar, Nucl. Phys. B **337**, 509 (1990).

[13] X. -D. Ji, Phys. Rev. Lett. **78**, 610 (1997) [hep-ph/9603249].

[14] X. -D. Ji, Phys. Rev. D **55** (1997) 7114 [hep-ph/9609381].
P. Hoodbhoy, X. -D.'Ji, W. Lu, Phys. Rev. D **59** (1998) 014013 [hep-ph/9804337].

[15] A. V. Radyushkin, Phys. Lett. B **380** (1996) 417; Phys. Rev. D **56** (1997) 5524.

[16] D. Muller, D. Robaschik, B. Geyer, F. M. Dittes, J. Horejsi, Fortsch. Phys. **42** (1994) 101.

[17] M. Guidal, Progress in Particle and Nuclear Physics **61** (2008) 89105.

[18] M. Diehl, Phys. Rept. **388**:41-277,2003.

[19] A.V. Belitsky and A.V. Radyushkin, Phys. Rept. **418**, 1 (2005), hep-ph/0504030.

[20] M. E. Peskin, D. V. Schroeder, "An Introduction to Quantum Field Theory",1995. Addison-Wesley.

[21] E. D. Bloom; et al., Physical Review Letters **23** (16) (1969): 930934.
M. Breidenbach; et al.,Physical Review Letters **23** (16) (1969): 935939.

[22] X. Ji, J. Osborne, Phys. Rev. D**58** (1998) 094018 [hep-ph/9801260].

[23] J. C. Collins, L. Frankfurt, M. Strikman, Phys. Rev. D **56** (1997) 2982.

[24] C.G. Callan, D.J. Gross, Phys. Rev. Lett. **22** (1968) 156.

[25] A.V. Belitsky, X. Ji, F. Yuan, "Final state interactions and gauge invariant parton distributions," Nucl. Phys. B **656** (2003) 165 [hep-ph/0208038].

[26] M. Diehl, Eur. Phys. J. C 19 (2001) 485.

[27] X. Ji, J. Phys. G **24** (1998) 1181.

[28] X. Ji, Phys. Rev. **D 55**, 7114 (1997), hep-ph/9609381.

[29] P. Hoodbhoy, X. Ji, Phys. Rev. D **58** (1998) 054006.

[30] A.V. Belitsky and D. Müller, Phys. Lett. **B 486**, 369 (2000), hep-ph/0005028.

[31] S. J. Brodsky, H. C. Pauli, S. S. Pinsky, Phys. Rept. **301** (1998) 299.

[32] S. Boffi, B. Pasquini, Riv. Nuovo Cim.**30**: 387,(2007) arXiv:0711.2625v2.

[33] X. -D. Ji, Phys. Rev. D**58**, 056003 (1998), hep-ph/9710290.

[34] S. J. Brodsky, D. S. Hwang, B. -Q. Ma, I. Schmidt, Nucl. Phys. B **593**, 311 (2001), hep-th/0003082.,

[35] Andrei V. Belitsky, Dieter Müller, Yao Ji, Nucl.Phys. B**878** (2014) 214-268, arXiv:1309.0769.

[36] A.V. Belitsky, D. Müller, and A. Kirchner, Nucl. Phys. **B 629**, 323 (2002), hep-ph/0112108.

[37] D. Drechsel, B. Pasquini, and M. Vanderhaeghen, Phys. Rept. **378**, 99 (2003), hep-ph/0212124.

[38] P.A. Guichon, G. Liu, and A.W. Thomas, Nucl. Phys. **A 591**, 606 (1995), nucl-th/9605031.

[39] D. Drechsel, G. Knochlein, A.Y. Korchin, A. Metz, and S. Scherer, Phys. Rev. **C 57**, 941 (1998), nucl-th/9704064.

[40] G.P. Lepage and S.J. Brodsky, Phys. Rev. **D 22**, 2157 (1980).

[41] A.V. Radyushkin, Phys. Rev. **D 58**, 114008 (1998), hep-ph/9803316.

[42] D. Müller, D. Robaschik, B. Geyer, F.-M. Dittes, and J. Hořejši, Fortschr. Phys. **42**, 101 (1994), hep-ph/9812448.

[43] A.V. Radyushkin, Phys. Lett. **B 380**, 417 (1996), hep-ph/9604317.

[44] A.V. Belitsky and D. Müller, Phys. Rev. **D 82**, 074010 (2010), arXiv:1005.5209 [hep-ph].

[45] R. Tarrach, Nuovo Cim. **A 28**, 409 (1975).

[46] A.V. Belitsky and D. Müller, Phys. Rev. **D 79**, 014017 (2009), arXiv:0809.2890 [hep-ph].

[47] M. Diehl, T. Gousset, B. Pire, and J.P. Ralston, Phys. Lett. **B 411**, 193 (1997), hep-ph/9706344.

[48] C. Itzykson and J. Zuber, *Quantum Field Theory* (McGraw-Hill, New York, 1980).

[49] V.M. Braun and A.N. Manashov, JHEP **01**, 085 (2012), arXiv:1111.6765 [hep-ph]; Phys. Rev. Lett. **107**, 202001 (2011), arXiv:1108.2394 [hep-ph].

[50] V.M. Braun, A.N. Manashov, and B. Pirnay, Phys. Rev. **D 86**, 014003 (2012), arXiv:1205.3332 [hep-ph]; (2012), arXiv:1209.2559 [hep-ph].

[51] M. Diehl, Eur. Phys. J. **C 19**, 485 (2001), hep-ph/0101335.

[52] R.E. Prange, Phys. Rev. **110**, 240 (1958).

[53] A.C. Hearn and E. Leader, Phys. Rev. **126**, 789 (1962).

[54] L. Mankiewicz, G. Piller, E. Stein, M. Vänttinen, and T. Weigl, Phys. Lett. **B 425**, 186 (1998), hep-ph/9712251.

[55] F. Low, Phys. Rev. **96**, 1428 (1954).

[56] A. Siegert, Phys. Rev. **52**, 787 (1937).

[57] K. Kumerički, D. Müller, and K. Passek-Kumerički, Nucl. Phys. **B 794**, 244 (2008), hep-ph/0703179.

[58] K. Kumerički and D. Müller, Nucl. Phys. **B 841**, 1 (2010), arXiv:0904.0458 [hep-ph].

[59] HERMES, A. Airapetian *et al.*, JHEP **06**, 066 (2008), arXiv:0802.2499 [hep-ex].

[60] HERMES, A. Airapetian *et al.*, JHEP **06**, 019 (2010), arXiv:1004.0177 [hep-ex].

[61] The HERMES, A. Airapetian *et al.*, Phys. Lett. **B 704**, 15 (2011), arXiv:1106.2990 [hep-ex].

[62] HERMES, A. Airapetian *et al.*, JHEP **1207**, 032 (2012), arXiv:1203.6287 [hep-ex].

[63] M. Vanderhaeghen, P.A. Guichon, and M. Guidal, Phys. Rev. Lett. **80**, 5064 (1998).

[64] P. Kroll, H. Moutarde, and F. Sabatie, Eur. Phys. J. **C 73**, 2278 (2013), arXiv:1210.6975 [hep-ph].

[65] Yao Ji, A. V. Belitsky, Nucl.Phys. B**896** (2015) 493-554, arXiv:1405.2828.

[66] R.P. Feynman, "Photon Hadron Interactions," (W.A. Benjamin, New York), 1971.

[67] E.V. Shuryak, A.I. Vainshtein, "Theory of power corrections to deep inelastic scattering in quantum chromodynamics. 1. Q^2 effects," Nucl. Phys. B **199** (1982) 451; "Theory of power corrections to deep inelastic scattering in quantum chromodynamics. 2. Q^4 effects: polarized target," Nucl. Phys. B **201** (1982) 141;
R.L. Jaffe, M. Soldate, "Twist four in electroproduction: canonical operators and coefficient functions," Phys. Rev. D **26** (1982) 49;
R.K. Ellis, W. Furmanski, R. Petronzio, "Power corrections to the parton model in QCD," Nucl. Phys. B **207** (1982) 1; "Unraveling higher twists," Nucl. Phys. B **212** (1983) 29;
I.I. Balitsky, V.M. Braun, "Evolution equations for QCD string operators," Nucl. Phys. B **311** (1989) 541;
J.-W. Qiu, "Twist four contributions to the parton structure functions," Phys. Rev. D **42** (1990) 30.

[68] T. Hobbs, W. Melnitchouk, "Finite-Q^2 corrections to parity-violating DIS," Phys. Rev. D **77** (2008) 114023 [arXiv:0801.4791 [hep-ph]].
S. Mantry, M.J. Ramsey-Musolf, G.F. Sacco, "Examination of higher-order twist contributions in parity-violating deep-inelastic electron-deuteron scattering," Phys. Rev. C **82** (2010) 065205 [arXiv:1004.3307 [hep-ph]].
A.V. Belitsky, A.N. Manashov, A. Schäfer, "Twist-four corrections to parity-violating electron-deuteron scattering," Phys. Rev. D **84** (2011) 014010 [arXiv:1104.0511 [hep-ph]].

[69] S.A. Gottlieb, "Contribution of twist four operators to deep inelastic scattering," Nucl. Phys. B **139** (1978) 125;
S. Wada, "Analysis of twist four two quark process by the renormalization mixing," Nucl. Phys. B **202** (1982) 201;
M. Okawa, "Higher twist effects in asymptotically free gauge theories: the anomalous dimensions of four quark operators," Nucl. Phys. B **172** (1980) 481; "Higher twist effects in asymptotically free gauge theories," Nucl. Phys. B **187** (1981) 71;
A.Yu. Morozov, "Calculation Of One Loop Anomalous Dimensions By Means Of The Background Field Method," ITEP-190-1983; ITEP-191-1983; "Matrix of mixing of scalar and vector mesons of dimension $d \leq 8$ in QCD," Sov. J. Nucl. Phys. **40** (1984) 505;

[70] M.J. Glatzmaier, S. Mantry, M.J. Ramsey-Musolf, "Higher twist in electroproduction: Flavor nonsinglet QCD evolution," Phys. Rev. C **88** (2013) 2, 025202 [arXiv:1208.2998 [hep-ph]].

[71] A.P. Bukhvostov, G.V. Frolov, L.N. Lipatov, E.A. Kuraev, "Evolution equations for quasi-partonic operators," Nucl. Phys. B **258** (1985) 601.

[72] A. Ali, V.M. Braun, G. Hiller, "Asymptotic solutions of the evolution equation for the polarized nucleon structure function $g_2(x,Q^2)$," Phys. Lett. B **266** (1991) 117;
J. Kodaira, Y. Yasui, K. Tanaka, T. Uematsu, "QCD corrections to the nucleon's spin structure function $g_2(x,Q^2)$," Phys. Lett. B **387** (1996) 855 [hep-ph/9603377];
B. Geyer, D. Müller, D. Robaschik, "Evolution kernels of twist-three light ray operators in polarized deep inelastic scattering," Nucl. Phys. Proc. Suppl. **51C** (1996) 106 [hep-ph/9606320];
Y. Koike, K. Tanaka, "Q^2 evolution of nucleon's chiral odd twist-three structure function: $h_L(x,Q^2)$," Phys. Rev. D **51** (1995) 6125 [hep-ph/9412310];
Y. Koike, N. Nishiyama, "Q^2 evolution of chiral odd twist-three distribution $e(x,Q^2)$," Phys. Rev. D **55** (1997) 3068 [hep-ph/9609207];
I.I. Balitsky, V.M. Braun, Y. Koike, K. Tanaka, "Q^2 evolution of chiral odd twist-three distributions $h_L(x,Q^2)$ and $e(x,Q^2)$ in the large-N_c limit," Phys. Rev. Lett. **77** (1996) 3078 [hep-ph/9605439];
D. Müller, "Calculation of higher twist evolution kernels for polarized deep inelastic scattering," Phys. Lett. B **407** (1997) 314 [hep-ph/9701338];
A.V. Belitsky, "Leading order analysis of the twist-three space-like and time-like cut vertices in QCD," hep-ph/9703432.
A.V. Belitsky, D. Müller, "Scale dependence of the chiral odd twist-three distributions $h_L(x)$ and $e(x)$," Nucl. Phys. B **503** (1997) 279 [hep-ph/9702354];

[73] Z.-B. Kang, J.-W. Qiu, "Evolution of twist-3 multi-parton correlation functions relevant to single transverse-spin asymmetry," Phys. Rev. D **79** (2009) 016003 [arXiv:0811.3101 [hep-ph]];
W. Vogelsang, F. Yuan, "Next-to-leading order calculation of the single transverse spin asymmetry in the Drell-Yan process," Phys. Rev. D **79** (2009) 094010 [arXiv:0904.0410 [hep-ph]];
V.M. Braun, A.N. Manashov, B. Pirnay, "Scale dependence of twist-three contributions to single spin asymmetries," Phys. Rev. D **80** (2009) 114002 [arXiv:0909.3410 [hep-ph]].

[74] A.P. Bukhvostov, E.A. Kuraev, L.N. Lipatov, "Evolution equations for higher twist operators," Sov. J. Nucl. Phys. **38** (1983) 263; "Deep inelastic scattering on a polarized target in Abelian gauge theory," Sov. J. Nucl. Phys. **39** (1984) 121; "Deep inelastic electron scattering by a polarized target in Quantum Chromodynamics," Sov. Phys. JETP **60** (1984) 22

[75] V.M. Braun, S.E. Derkachov, A.N. Manashov, "Integrability of three particle evolution equations in QCD," Phys. Rev. Lett. **81** (1998) 2020 [hep-ph/9805225];
V.M. Braun, S.E. Derkachov, G.P. Korchemsky, A.N. Manashov, "Baryon distribution amplitudes in QCD," Nucl. Phys. B **553** (1999) 355 [hep-ph/9902375];
S.E. Derkachov, G.P. Korchemsky, A.N. Manashov, "Evolution equations for quark gluon distributions in multicolor QCD and open spin chains," Nucl. Phys. B **566** (2000) 203 [hep-ph/9909539];
V.M. Braun, G.P. Korchemsky, A.N. Manashov, "Evolution equation for the structure function $g_2(x,Q^2)$," Nucl. Phys. B **603**, 69 (2001) [hep-ph/0102313].

[76] A.V. Belitsky, "Fine structure of spectrum of twist-three operators in QCD," Phys. Lett. B **453** (1999) 59 [hep-ph/9902361]; "Integrability and WKB solution of twist-three evolution equations," Nucl. Phys. B **558** (1999) 259 [hep-ph/9903512]; "Renormalization of twist-three operators and integrable lattice models," Nucl. Phys. B **574** (2000) 407 [hep-ph/9907420].

[77] A.P. Bukhvostov, G.V. Frolov , "Anomalous dimensions of quasipartonics twist-four operators," Yad. Fiz. **45** (1987) 1136.

[78] V.M. Braun, A.N. Manashov, J. Rohrwild, "Renormalization of twist-four operators in QCD," Nucl. Phys. B **826** (2010) 235 [arXiv:0908.1684 [hep-ph]].

[79] A.V. Belitsky, S.E. Derkachov, G.P. Korchemsky , A.N. Manashov, "Superconformal operators in Yang-Mills theories on the light-cone," Nucl. Phys. B **708** (2005) 115 [hep-th/0409120].

[80] V.M. Braun, A.N. Manashov, J. Rohrwild, "Baryon operators of higher twist in QCD and nucleon distribution amplitudes," Nucl. Phys. B **807** (2009) 89 [arXiv:0806.2531 [hep-ph]].

[81] V.M. Braun, G.P. Korchemsky, D. Müller, "The Uses of conformal symmetry in QCD," Prog. Part. Nucl. Phys. **51** (2003) 311 [hep-ph/0306057].

[82] A.V. Belitsky, V.M. Braun, A.S. Gorsky, G.P. Korchemsky, "Integrability in QCD and beyond," Int. J. Mod. Phys. A **19** (2004) 4715 [hep-th/0407232].

[83] A. Bassetto, G. Nardelli, R. Soldati "Yang-Mills theories in algebraic non-covariant gauges: canonical quantization and renormalization", (World Scientific, Singapore), 1991.

[84] A.V. Belitsky, E.A. Kuraev, "Evolution of chiral odd spin independent fracture functions in Quantum Chromodynamics," Nucl. Phys. B **499** (1997) 301 [hep-ph/9612256].

[85] A.V. Belitsky, A.V. Radyushkin, "Unraveling hadron structure with generalized parton distributions," Phys. Rept. **418** (2005) 1 [hep-ph/0504030].

[86] G. Altarelli, G. Parisi, "Asymptotic freedom in parton language," Nucl. Phys. B **126** (1977) 298.

[87] M. Knodlseder, N. Offen, "Renormalisation of heavy-light light ray operators," JHEP **1110** (2011) 069 [arXiv:1105.4569 [hep-ph]].

[88] J. H. Rohrwild, "Renormalization and applications of baryon distribution amplitudes in QCD," PhD thesis (2009).

[89] A. Sandacz, (Compass Collaboration), Poceedings of CIPANP 2015 conference, arXiv:1509.07732.

[90] V. Kubarovsky, (CLAS Collaboration), Jlab Report JLAB-PHY-15-2011, arXiv:1601.04367.

[91] A. Bacchetta, et al., DESY-15-253, IPPP/15/76, arXiv:1601.01499.

[92] Yao Ji, A. V. Belitsky, Int. J. Mod. Phys. Conf. Ser. **37** (2015) 1560051 arXiv:1410.5805.

APPENDIX A

DEEPLY VIRTUAL COMPTON SCATTERING

A.1 Kinematical Decomposition in Target Rest Frame

Let us first quote particles' momenta involved in scattering in the rest frame of the target. The components of the corresponding four-vectors read

$$p_1 = (M,0,0,0)\,, \quad q_1 = \frac{\mathcal{Q}}{\varepsilon}\left(1,0,0,-\sqrt{1+\varepsilon^2}\right)\,, \quad k = \frac{\mathcal{Q}}{y\varepsilon}\left(1,\sin\theta_l,0,\cos\theta_l\right)\,, \tag{A.1}$$

with the lepton scattering angle being

$$\cos\theta_l = -\frac{1+\frac{y\varepsilon^2}{2}}{\sqrt{1+\varepsilon^2}}\,, \qquad \sin\theta_l = \frac{\varepsilon\sqrt{1-y-\frac{y^2\varepsilon^2}{4}}}{\sqrt{1+\varepsilon^2}}\,. \tag{A.2}$$

The outgoing momenta are parameterized in terms of the scattering angles in the hadronic plane, see Fig. 2.1,

$$q_2 = \frac{\mathcal{Q}^2 + x_{\rm B} t}{2M x_{\rm B}}\left(1,\cos\varphi_\gamma\sin\theta_\gamma,\sin\varphi_\gamma\sin\theta_\gamma,\cos\theta_\gamma\right)\,, \tag{A.3}$$

$$p_2 = \left(M - \frac{t}{2M}, \sqrt{-t+\frac{t^2}{4M^2}}\cos\phi\sin\theta_p\,, \right.$$
$$\left. \sqrt{-t+\frac{t^2}{4M^2}}\sin\phi\sin\theta_p, \sqrt{-t+\frac{t^2}{4M^2}}\cos\theta_p\right)\,, \tag{A.4}$$

where the polar angles read in terms of the kinematical variables of the phase space

$$\cos\theta_\gamma = -\frac{1+\frac{\varepsilon^2}{2}\frac{\mathcal{Q}^2+t}{\mathcal{Q}^2+x_{\rm B}t}}{\sqrt{1+\varepsilon^2}}\,, \qquad \cos\theta_p = -\frac{\varepsilon^2(\mathcal{Q}^2-t)-2x_{\rm B}t}{4x_{\rm B}M\sqrt{1+\varepsilon^2}\sqrt{-t+\frac{t^2}{4M^2}}}\,. \tag{A.5}$$

The azimuthal angle of the photon φ_γ is related to the one of the outgoing hadron ϕ via $\varphi_\gamma = \phi + \pi$.

The photon polarization vectors (2.6), (2.7) can be kinematically decomposed in term of those involved in the virtual Compton scattering process as follows:

$$\varepsilon_1^\mu(0) = -\frac{1}{\mathcal{Q}\sqrt{1+\varepsilon^2}}\,q_1^\mu - \frac{2x_{\rm B}}{\mathcal{Q}\sqrt{1+\varepsilon^2}}\,p_1^\mu \tag{A.6}$$

$$\varepsilon_1^\mu(\pm1) = \frac{\sqrt{1+\varepsilon^2}}{\sqrt{2}\widetilde{K}}\left[\Delta^\mu - \frac{\varepsilon^2\left(\mathcal{Q}^2-t\right)-2x_{\rm B}t}{2\mathcal{Q}^2\left(1+\varepsilon^2\right)}q_1^\mu + x_{\rm B}\frac{\mathcal{Q}^2-t+2x_{\rm B}t}{\mathcal{Q}^2\left(1+\varepsilon^2\right)}p_1^\mu\right] \mp \frac{x_{\rm B}}{\sqrt{2}\widetilde{K}}\frac{i\varepsilon_{pq\Delta}{}^\mu}{\mathcal{Q}^2}, \tag{A.7}$$

$$\varepsilon_2^\mu(\pm1) = \frac{1+\frac{\varepsilon^2}{2}\frac{\mathcal{Q}^2+t}{\mathcal{Q}^2+x_{\rm B}t}}{\sqrt{2}\widetilde{K}}\left[\Delta^\mu - \frac{\varepsilon^2\left(\mathcal{Q}^2-t\right)-2x_{\rm B}t}{2\mathcal{Q}^2\left(1+\varepsilon^2\right)}q_1^\mu + x_{\rm B}\frac{\mathcal{Q}^2-t+2x_{\rm B}t}{\mathcal{Q}^2\left(1+\varepsilon^2\right)}p_1^\mu\right] + \frac{\widetilde{K}}{\sqrt{2}\left(1+\varepsilon^2\right)\left(\mathcal{Q}^2+x_{\rm B}t\right)}\left[\varepsilon^2 q_1^\mu - 2\,x_{\rm B}\,p_1^\mu\right] \mp \frac{x_{\rm B}}{\sqrt{2}\widetilde{K}}\frac{i\varepsilon_{pq\Delta}{}^\mu}{\mathcal{Q}^2}, \tag{A.8}$$

where $\widetilde{K}$ is defined in Eq. (2.8). Analogously one finds for the nucleon polarization vector (2.31)

$$S_{\rm L}^\mu = \frac{1}{\sqrt{1+\varepsilon^2}}\left[\frac{1}{M}\,p_1^\mu - \frac{\varepsilon}{\mathcal{Q}}\,q_1^\mu\right], \tag{A.9}$$

$$S_{\rm T}^\mu = \frac{\sqrt{1+\varepsilon^2}}{\widetilde{K}}\left[\Delta^\mu - \frac{\varepsilon^2\left(\mathcal{Q}^2-t\right)-2x_{\rm B}t}{2\mathcal{Q}^2\left(1+\varepsilon^2\right)}\,q_1^\mu + x_{\rm B}\frac{\mathcal{Q}^2-t+2x_{\rm B}t}{\mathcal{Q}^2\left(1+\varepsilon^2\right)}\,p_1^\mu\right]\cos(\varphi) - \frac{x_{\rm B}}{i\widetilde{K}}\frac{i\varepsilon_{pq\Delta}{}^\mu}{\mathcal{Q}^2}\sin(\varphi)\,. \tag{A.10}$$

The photon polarization vectors (A.6)–(A.8) remain well defined in the whole physical region including the phase-space boundary $t = t_{\rm min}$ where $\widetilde{K}$ vanishes.

The following useful relation is added that was used multiple times in simplification of analytical results

$$\frac{\widetilde{K}^2}{\mathcal{Q}^2} = -\left(1+\frac{t}{\mathcal{Q}^2}\right)^2\frac{\varepsilon^2}{4} - (1-x_{\rm B})\left(1+\frac{x_{\rm B}t}{\mathcal{Q}^2}\right)\frac{t}{\mathcal{Q}^2}\,. \tag{A.11}$$

A.2 Fourier Harmonics of the Leptonic Tensor

Let us present explicit expressions for the Fourier coefficients entering the leptonic part of the interference term (2.56), see Sect. 2.2.3. As in Ref. [36], one uses the following shorthand notation

$$K = \sqrt{1-y-\frac{\varepsilon^2}{4}y^2}\,\frac{\widetilde{K}}{\mathcal{Q}}\,,$$

where t' is

$$t' = t - t_{\min}\,.$$

A.2.1 Unpolarized and Transversally Polarized TP− *Target*

The angular coefficients for unpolarized target and the transversally polarized TP− part are given by the expressions

$$\begin{aligned} &C_{ab}(n)\,,\, C^V_{ab}(n)\,,\, C^A_{ab}(n)\,, \qquad \text{for} \quad n \in \{0,1,2,3\}\,,\\ &S_{ab}(n)\,,\, S^V_{ab}(n)\,,\, S^A_{ab}(n)\,, \qquad \text{for} \quad n \in \{1,2\}\,. \end{aligned}$$

Note that these coefficients are identical with $C_{ab}^{\text{unp},\cdots}(n)$ and $S_{ab}^{\text{unp},,\cdots}(n)/\lambda$ of Ref. [44] and that the third odd harmonics, i.e.,

$$S_{ab}(n=3) = S^V_{ab}(n=3) = S^A_{ab}(n=3) = 0\,,$$

and the following third even harmonics in longitudinal helicity flip CFFs

$$C_{0b}(n=3) = C^V_{0b}(n=3) = C^A_{0b}(n=3) = 0$$

vanish and will be not listed.

- Conserved photon-helicity coefficients:

$$\begin{aligned} C_{++}(n=0) = -\frac{4(2-y)\left(1+\sqrt{1+\varepsilon^2}\right)}{(1+\varepsilon^2)^2}\Bigg\{ &\frac{\widetilde{K}^2}{\mathcal{Q}^2}\frac{(2-y)^2}{\sqrt{1+\varepsilon^2}} + \frac{t}{\mathcal{Q}^2}\left(1-y-\frac{\varepsilon^2}{4}y^2\right)\\ &\times(2-x_{\rm B})\left(1+\frac{2x_{\rm B}\left(2-x_{\rm B}+\frac{\sqrt{1+\varepsilon^2}-1}{2}+\frac{\varepsilon^2}{2x_{\rm B}}\right)\frac{t}{\mathcal{Q}^2}+\varepsilon^2}{(2-x_{\rm B})(1+\sqrt{1+\varepsilon^2})}\right)\Bigg\}\,, \end{aligned} \tag{A.12}$$

$$C^V_{++}(n=0) = \frac{8(2-y)}{(1+\varepsilon^2)^2}\frac{x_{\rm B}t}{\mathcal{Q}^2}\left\{\frac{(2-y)^2\widetilde{K}^2}{\sqrt{1+\varepsilon^2}\mathcal{Q}^2} + \left(1-y-\frac{\varepsilon^2}{4}y^2\right)\frac{1+\sqrt{1+\varepsilon^2}}{2}\right.$$

$$\times \left(1+\frac{t}{\mathcal{Q}^2}\right)\left(1+\frac{\sqrt{1+\varepsilon^2}-1+2x_{\rm B}}{1+\sqrt{1+\varepsilon^2}}\frac{t}{\mathcal{Q}^2}\right)\Bigg\},$$

$$C^A_{++}(n=0)=\frac{8(2-y)}{(1+\varepsilon^2)^2}\frac{t}{\mathcal{Q}^2}\Bigg\{\frac{(2-y)^2\widetilde{K}^2}{\sqrt{1+\varepsilon^2}\mathcal{Q}^2}\frac{1+\sqrt{1+\varepsilon^2}-2x_{\rm B}}{2}-\left(1-y-\frac{\varepsilon^2}{4}y^2\right)$$
$$\times\left[\frac{2\widetilde{K}^2}{\mathcal{Q}^2}-\frac{1+\sqrt{1+\varepsilon^2}}{2}\left(\left(\sqrt{1+\varepsilon^2}-1+x_{\rm B}\frac{3+\sqrt{1+\varepsilon^2}-2x_{\rm B}}{1+\sqrt{1+\varepsilon^2}}\right)\right.\right.$$
$$\left.\left.+1+\sqrt{1+\varepsilon^2}-x_{\rm B}\frac{t}{\mathcal{Q}^2}\right)\right]\Bigg\},$$

$$C_{++}(n=1)=\frac{-16K\left(1-y-\frac{\varepsilon^2}{4}y^2\right)}{(1+\varepsilon^2)^{5/2}}\Bigg\{\left(1+(1-x_{\rm B})\frac{\sqrt{\varepsilon^2+1}-1}{2x_{\rm B}}+\frac{\varepsilon^2}{4x_{\rm B}}\right)\frac{x_{\rm B}t}{\mathcal{Q}^2}$$
$$-\frac{3\varepsilon^2}{4}\Bigg\}-4K\left(2-2y+y^2+\frac{\varepsilon^2}{2}y^2\right)\frac{1+\sqrt{1+\varepsilon^2}-\varepsilon^2}{(1+\varepsilon^2)^{5/2}}$$
$$\times\quad\left\{1-(1-3x_{\rm B})\frac{t}{\mathcal{Q}^2}+\frac{1-\sqrt{1+\varepsilon^2}+3\varepsilon^2}{1+\sqrt{1+\varepsilon^2}-\varepsilon^2}\frac{x_{\rm B}t}{\mathcal{Q}^2}\right\},$$

$$C^V_{++}(n=1)=\frac{16K}{(1+\varepsilon^2)^{5/2}}\frac{x_{\rm B}t}{\mathcal{Q}^2}\Bigg\{(2-y)^2\left(1-(1-2x_{\rm B})\frac{t}{\mathcal{Q}^2}\right)$$
$$+\left(1-y-\frac{\varepsilon^2}{4}y^2\right)\frac{1+\sqrt{1+\varepsilon^2}-2x_{\rm B}}{2}\frac{t'}{\mathcal{Q}^2}\Bigg\},$$

$$C^A_{++}(n=1)=\frac{-16K}{(1+\varepsilon^2)^2}\frac{t}{\mathcal{Q}^2}\Bigg\{\left(1-y-\frac{\varepsilon^2}{4}y^2\right)\left(1-(1-2x_{\rm B})\frac{t}{\mathcal{Q}^2}\right.$$
$$\left.+\frac{4x_{\rm B}(1-x_{\rm B})+\varepsilon^2}{4\sqrt{1+\varepsilon^2}}\frac{t'}{\mathcal{Q}^2}\right)-(2-y)^2\left(1-\frac{x_{\rm B}}{2}\right.$$
$$\left.+\frac{1+\sqrt{1+\varepsilon^2}-2x_{\rm B}}{4}\left(1-\frac{t}{\mathcal{Q}^2}\right)+\frac{4x_{\rm B}(1-x_{\rm B})+\varepsilon^2}{2\sqrt{1+\varepsilon^2}}\frac{t'}{\mathcal{Q}^2}\right)\Bigg\},$$

$$C_{++}(n=2)=\frac{8(2-y)\left(1-y-\frac{\varepsilon^2}{4}y^2\right)}{(1+\varepsilon^2)^2}\Bigg\{\frac{2\varepsilon^2}{\sqrt{1+\ \varepsilon^2}(1+\sqrt{1+\varepsilon^2})}\frac{\widetilde{K}^2}{\mathcal{Q}^2}$$
$$+\frac{x_{\rm B}tt'}{\mathcal{Q}^4}\left(1-x_{\rm B}-\frac{\sqrt{1+\varepsilon^2}-1}{2}+\frac{\varepsilon^2}{2x_{\rm B}}\right)\Bigg\},$$

$$C^V_{++}(n=2) = \frac{8(2-y)\left(1-y-\frac{\varepsilon^2}{4}y^2\right)}{(1+\varepsilon^2)^2}\frac{x_{\rm B}t}{\mathcal{Q}^2}\left\{\frac{4\widetilde{K}^2}{\sqrt{1+\varepsilon^2}\mathcal{Q}^2} + \frac{1+\sqrt{1+\varepsilon^2}-2x_{\rm B}}{2}\left(1+\frac{t}{\mathcal{Q}^2}\right)\frac{t'}{\mathcal{Q}^2}\right\},$$

$$C^A_{++}(n=2) = \frac{4(2-y)\left(1-y-\frac{\varepsilon^2}{4}y^2\right)}{(1+\varepsilon^2)^2}\frac{t}{\mathcal{Q}^2}\left\{\frac{4(1-2x_{\rm B})\widetilde{K}^2}{\sqrt{1+\varepsilon^2}\mathcal{Q}^2} - \left(3-\sqrt{1+\varepsilon^2}-2x_{\rm B}+\frac{\varepsilon^2}{x_{\rm B}}\right)\frac{x_{\rm B}t'}{\mathcal{Q}^2}\right\},$$

$$C_{++}(n=3) = -8K\left(1-y-\frac{\varepsilon^2}{4}y^2\right)\frac{\sqrt{1+\varepsilon^2}-1}{(1+\varepsilon^2)^{5/2}}\left\{(1-x_{\rm B})\frac{t}{\mathcal{Q}^2} + \frac{\sqrt{1+\varepsilon^2}-1}{2}\left(1+\frac{t}{\mathcal{Q}^2}\right)\right\},$$

$$C^V_{++}(n=3) = -\frac{8K\left(1-y-\frac{\varepsilon^2}{4}y^2\right)}{(1+\varepsilon^2)^{5/2}}\frac{x_{\rm B}t}{\mathcal{Q}^2}\left\{\sqrt{1+\varepsilon^2}-1 + \left(1+\sqrt{1+\varepsilon^2}-2x_{\rm B}\right)\frac{t}{\mathcal{Q}^2}\right\},$$

$$C^A_{++}(n=3) = \frac{16K\left(1-y-\frac{\varepsilon^2}{4}y^2\right)}{(1+\varepsilon^2)^{5/2}}\frac{t\,t'}{\mathcal{Q}^4}\left\{x_{\rm B}(1-x_{\rm B})+\frac{\varepsilon^2}{4}\right\},$$

$$S_{++}(n=1) = \frac{8K(2-y)y}{1+\varepsilon^2}\left\{1+\frac{1-x_{\rm B}+\frac{\sqrt{1+\varepsilon^2}-1}{2}}{1+\varepsilon^2}\frac{t'}{\mathcal{Q}^2}\right\},$$

$$S^V_{++}(n=1) = -\frac{8K(2-y)y}{(1+\varepsilon^2)^2}\frac{x_{\rm B}t}{\mathcal{Q}^2}\left\{\sqrt{1+\varepsilon^2}-1+\left(1+\sqrt{1+\varepsilon^2}-2x_{\rm B}\right)\frac{t}{\mathcal{Q}^2}\right\},$$

$$S^A_{++}(n=1) = \frac{8K(2-y)y}{(1+\varepsilon^2)}\frac{t}{\mathcal{Q}^2}\left\{1-(1-2x_{\rm B})\frac{1+\sqrt{1+\varepsilon^2}-2x_{\rm B}}{2(1+\varepsilon^2)}\frac{t'}{\mathcal{Q}^2}\right\}$$

$$S_{++}(n=2) = -\frac{4\left(1-y-\frac{\varepsilon^2}{4}y^2\right)y}{(1+\varepsilon^2)^{3/2}}\left(1+\sqrt{1+\varepsilon^2}-2x_{\rm B}\right) \times\frac{t'}{\mathcal{Q}^2}\left\{\frac{\varepsilon^2-x_{\rm B}(\sqrt{1+\varepsilon^2}-1)}{1+\sqrt{\varepsilon^2+1}-2x_{\rm B}}-\frac{2x_{\rm B}+\varepsilon^2}{2\sqrt{1+\varepsilon^2}}\frac{t'}{\mathcal{Q}^2}\right\},$$

$$S^V_{++}(n=2) = -\frac{4\left(1-y-\frac{\varepsilon^2}{4}y^2\right)y}{(1+\varepsilon^2)^2}\frac{x_{\rm B}t}{\mathcal{Q}^2} \times\left(1-(1-2x_{\rm B})\frac{t}{\mathcal{Q}^2}\right)\left\{\sqrt{1+\varepsilon^2}-1+\left(1+\sqrt{1+\varepsilon^2}-2x_{\rm B}\right)\frac{t}{\mathcal{Q}^2}\right\},$$

$$S^A_{++}(n=2) = -\frac{8\left(1-y-\frac{\varepsilon^2}{4}y^2\right)y}{(1+\varepsilon^2)^2}\frac{t\,t'}{\mathcal{Q}^4}\left(1-\frac{x_{\rm B}}{2}+\frac{3\varepsilon^2}{4}\right) \times\left(1+\sqrt{1+\varepsilon^2}-2x_{\rm B}\right)\left(1+\frac{4(1-x_{\rm B})x_{\rm B}+\varepsilon^2}{4-2x_{\rm B}+3\varepsilon^2}\frac{t}{\mathcal{Q}^2}\right).$$

- Longitudinal-transverse coefficients:

$$C_{0+}(n=0) = \frac{12\sqrt{2}K(2-y)\sqrt{1-y-\frac{\varepsilon^2}{4}y^2}}{(1+\varepsilon^2)^{5/2}}\left\{\varepsilon^2+\frac{2-6x_{\rm B}-\varepsilon^2}{3}\frac{t}{\mathcal{Q}^2}\right\}, \tag{A.13}$$

$$C^V_{0+}(n=0) = \frac{24\sqrt{2}K(2-y)\sqrt{1-y-\frac{\varepsilon^2}{4}y^2}}{(1+\varepsilon^2)^{5/2}}\frac{x_{\rm B}t}{\mathcal{Q}^2}\left\{1-(1-2x_{\rm B})\frac{t}{\mathcal{Q}^2}\right\},$$

$$C^A_{0+}(n=0) = \frac{4\sqrt{2}K(2-y)\sqrt{1-y-\frac{\varepsilon^2}{4}y^2}}{(1+\varepsilon^2)^{5/2}}\frac{t}{\mathcal{Q}^2}(8-6x_{\rm B}+5\varepsilon^2) \times\left\{1-\frac{t}{\mathcal{Q}^2}\frac{2-12x_{\rm B}(1-x_{\rm B})-\varepsilon^2}{8-6x_{\rm B}+5\varepsilon^2}\right\},$$

$$C_{0+}(n=1) = \frac{8\sqrt{2}\sqrt{1-y-\frac{\varepsilon^2}{4}y^2}}{(1+\varepsilon^2)^2}\left\{(2-y)^2\frac{t'}{\mathcal{Q}^2}\left(1-x_{\rm B}+\frac{(1-x_{\rm B})x_{\rm B}+\frac{\varepsilon^2}{4}}{\sqrt{1+\varepsilon^2}}\frac{t'}{\mathcal{Q}^2}\right)\right.$$
$$\left.+\frac{1-y-\frac{\varepsilon^2}{4}y^2}{\sqrt{1+\varepsilon^2}}\left(1-(1-2x_{\rm B})\frac{t}{\mathcal{Q}^2}\right)\left(\varepsilon^2-2\left(1+\frac{\varepsilon^2}{2x_{\rm B}}\right)\frac{x_{\rm B}t}{\mathcal{Q}^2}\right)\right\},$$

$$C^V_{0+}(n=1) = \frac{16\sqrt{2}\sqrt{1-y-\frac{\varepsilon^2}{4}y^2}}{(1+\varepsilon^2)^{5/2}}\frac{x_{\rm B}t}{\mathcal{Q}^2}\left\{\left(1-(1-2x_{\rm B})\frac{t}{\mathcal{Q}^2}\right)^2\left(1-y-\frac{\varepsilon^2}{4}y^2\right)\right.$$
$$\left.+\frac{\widetilde{K}^2(2-y)^2}{\mathcal{Q}^2}\right\},$$

$$C^A_{0+}(n=1) = \frac{8\sqrt{2}\sqrt{1-y-\frac{\varepsilon^2}{4}y^2}}{(1+\varepsilon^2)^{5/2}}\frac{t}{\mathcal{Q}^2}\left\{\frac{\widetilde{K}^2}{\mathcal{Q}^2}(1-2x_{\rm B})(2-y)^2 + \left(1-(1-2x_{\rm B})\frac{t}{\mathcal{Q}^2}\right)\left(1-y-\frac{\varepsilon^2}{4}y^2\right)\left(4-2x_{\rm B}+3\varepsilon^2 + \frac{t}{\mathcal{Q}^2}(4x_{\rm B}(1-x_{\rm B})+\varepsilon^2)\right)\right\},$$

$$C_{0+}(n=2) = -\frac{8\sqrt{2}K(2-y)\sqrt{1-y-\frac{\varepsilon^2}{4}y^2}}{(1+\varepsilon^2)^{5/2}}\left(1+\frac{\varepsilon^2}{2}\right)\left\{1+\frac{1+\frac{\varepsilon^2}{2x_{\rm B}}}{1+\frac{\varepsilon^2}{2}}\frac{x_{\rm B}t}{\mathcal{Q}^2}\right\},$$

$$C^V_{0+}(n=2) = \frac{8\sqrt{2}K(2-y)\sqrt{1-y-\frac{\varepsilon^2}{4}y^2}}{(1+\varepsilon^2)^{5/2}}\frac{x_{\rm B}t}{\mathcal{Q}^2}\left(1-(1-2x_{\rm B})\frac{t}{\mathcal{Q}^2}\right),$$

$$C^A_{0+}(n=2) = \frac{8\sqrt{2}K(2-y)\sqrt{1-y-\frac{\varepsilon^2}{4}y^2}}{(1+\varepsilon^2)^{2}}\frac{t}{\mathcal{Q}^2}\left\{\frac{t'}{2\mathcal{Q}^2}\frac{4x_{\rm B}(1-x_{\rm B})+\varepsilon^2}{\sqrt{1+\varepsilon^2}} + 1-x_{\rm B}\right\},$$

$$S_{0+}(n=1) = \frac{8\sqrt{2}(2-y)y\sqrt{1-y-\frac{\varepsilon^2}{4}y^2}}{(1+\varepsilon^2)^{2}}\frac{\widetilde{K}^2}{\mathcal{Q}^2},$$

$$S^V_{0+}(n=1) = \frac{4\sqrt{2}y(2-y)\sqrt{1-y-\frac{\varepsilon^2}{4}y^2}}{(1+\varepsilon^2)^{2}}\frac{x_{\rm B}t}{\mathcal{Q}^2}\left\{4(1-x_{\rm B})\frac{t}{\mathcal{Q}^2}\left(1+\frac{x_{\rm B}t}{\mathcal{Q}^2}\right) + \varepsilon^2\left(1+\frac{t}{\mathcal{Q}^2}\right)^2\right\},$$

$$S^A_{0+}(n=1) = -\frac{8\sqrt{2}y(2-y)(1-2x_{\rm B})\sqrt{1-y-\frac{\varepsilon^2}{4}y^2}}{(1+\varepsilon^2)^{2}}\frac{t\widetilde{K}^2}{\mathcal{Q}^4},$$

$$S_{0+}(n=2) = \frac{8\sqrt{2}Ky\sqrt{1-y-\frac{\varepsilon^2}{4}y^2}}{(1+\varepsilon^2)^{2}}\left(1+\frac{\varepsilon^2}{2}\right)\left\{1+\frac{1+\frac{\varepsilon^2}{2x_{\rm B}}}{1+\frac{\varepsilon^2}{2}}\frac{x_{\rm B}t}{\mathcal{Q}^2}\right\},$$

$$S^V_{0+}(n=2) = -\frac{8\sqrt{2}Ky\sqrt{1-y-\frac{\varepsilon^2}{4}y^2}}{(1+\varepsilon^2)^{2}}\frac{x_{\rm B}t}{\mathcal{Q}^2}\left\{1-(1-2x_{\rm B})\frac{t}{\mathcal{Q}^2}\right\},$$

$$S^A_{0+}(n=2) = -\frac{2\sqrt{2}Ky\sqrt{1-y-\frac{\varepsilon^2}{4}y^2}}{(1+\varepsilon^2)^2}\frac{t}{\mathcal{Q}^2}\Bigg(4-4x_{\rm B}+2\varepsilon^2 + \frac{2t}{\mathcal{Q}^2}(4x_{\rm B}(1-x_{\rm B})+\varepsilon^2)\Bigg),$$

- Transverse-transverse helicity-flip coefficients:

$$C_{-+}(n=0) = \frac{8(2-y)}{(1+\varepsilon^2)^{3/2}}\Bigg\{(2-y)^2\frac{\sqrt{1+\varepsilon^2}-1}{2(1+\varepsilon^2)}\frac{\widetilde{K}^2}{\mathcal{Q}^2} + \frac{1-y-\frac{\varepsilon^2}{4}y^2}{\sqrt{1+\varepsilon^2}}\left(1-x_{\rm B}-\frac{\sqrt{1+\varepsilon^2}-1}{2}+\frac{\varepsilon^2}{2x_{\rm B}}\right)\frac{x_{\rm B}t\,t'}{\mathcal{Q}^4}\Bigg\}, \tag{A.14}$$

$$C^V_{-+}(n=0) = \frac{4(2-y)}{(1+\varepsilon^2)^{5/2}}\frac{x_{\rm B}t}{\mathcal{Q}^2}\Bigg\{\frac{2\widetilde{K}^2}{\mathcal{Q}^2}\left(2-2y+y^2+\frac{\varepsilon^2}{2}y^2\right)-\left(1-(1-2x_{\rm B})\frac{t}{\mathcal{Q}^2}\right) \times\left(1-y-\frac{\varepsilon^2}{4}y^2\right)\left(\sqrt{1+\varepsilon^2}-1+\left(\sqrt{1+\varepsilon^2}+1-2x_{\rm B}\right)\frac{t}{\mathcal{Q}^2}\right)\Bigg\}.$$

$$C^A_{-+}(n=0) = \frac{4(2-y)}{(1+\varepsilon^2)^2}\frac{t}{\mathcal{Q}^2}\Bigg\{\frac{t'}{\mathcal{Q}^2}\left(1-y-\frac{\varepsilon^2}{4}y^2\right)\left(2x_{\rm B}^2-\varepsilon^2-3x_{\rm B}+x_{\rm B}\sqrt{1+\varepsilon^2}\right) + \frac{\widetilde{K}^2}{\mathcal{Q}^2\sqrt{1+\varepsilon^2}}\left(4-2x_{\rm B}(2-y)^2-4y+y^2-y^2(1+\varepsilon^2)^{3/2}\right)\Bigg\},$$

$$C_{-+}(n=1) = \frac{8K}{(1+\varepsilon^2)^{3/2}}\Bigg\{(2-y)^2\frac{2-\sqrt{1+\varepsilon^2}}{1+\varepsilon^2} \times\left(\frac{\sqrt{1+\varepsilon^2}-1+\varepsilon^2}{2\left(2-\sqrt{1+\varepsilon^2}\right)}\left(1-\frac{t}{\mathcal{Q}^2}\right)-\frac{x_{\rm B}t}{\mathcal{Q}^2}\right) + 2\frac{1-y-\frac{\varepsilon^2}{4}y^2}{\sqrt{1+\varepsilon^2}}\left(\frac{1-\sqrt{1+\varepsilon^2}+\frac{\varepsilon^2}{2}}{2\sqrt{1+\varepsilon^2}}+\frac{t}{\mathcal{Q}^2}\left(1-\frac{3x_{\rm B}}{2}+\frac{x_{\rm B}+\frac{\varepsilon^2}{2}}{2\sqrt{1+\varepsilon^2}}\right)\right)\Bigg\},$$

$$C^V_{-+}(n=1) = \frac{8K}{(1+\varepsilon^2)^{5/2}}\frac{x_{\rm B}t}{\mathcal{Q}^2}\Bigg\{2\left(1-(1-2x_{\rm B})\frac{t}{\mathcal{Q}^2}\right)\left(2-2y+y^2+\frac{\varepsilon^2}{2}y^2\right) + \left(1-y-\frac{\varepsilon^2}{4}y^2\right)\left(3-\sqrt{1+\varepsilon^2}-\left(3(1-2x_{\rm B})+\sqrt{1+\varepsilon^2}\right)\frac{t}{\mathcal{Q}^2}\right)\Bigg\},$$

$$C^{A}_{-+}(n=1) = \frac{4K}{(1+\varepsilon^2)^{5/2}}\frac{t}{\mathcal{Q}^2}\Bigg\{\left(2-2y+y^2+\frac{\varepsilon^2}{2}y^2\right)$$
$$\times\Bigg(5-4x_{\rm B}+3\varepsilon^2-\sqrt{1+\varepsilon^2}-\frac{t}{\mathcal{Q}^2}\big(1-\varepsilon^2-\sqrt{1+\varepsilon^2}$$
$$-2x_{\rm B}(4-4x_{\rm B}-\sqrt{1+\varepsilon^2})\big)\Bigg)+\left(1-y-\frac{\varepsilon^2}{4}y^2\right)$$
$$\times\Bigg(8+5\varepsilon^2-6x_{\rm B}+2x_{\rm B}\sqrt{1+\varepsilon^2}$$
$$-\frac{t}{\mathcal{Q}^2}\left(2-\varepsilon^2+2\sqrt{1+\varepsilon^2}-4x_{\rm B}(3-3x_{\rm B}+\sqrt{1+\varepsilon^2})\right)\Bigg)\Bigg\},$$

$$C_{-+}(n=2) = 4(2-y)\left(1-y-\frac{\varepsilon^2}{4}y^2\right)\frac{1+\sqrt{1+\varepsilon^2}}{(1+\varepsilon^2)^{5/2}}\Bigg\{(2-3x_{\rm B})\frac{t}{\mathcal{Q}^2}$$
$$+\left(1-2x_{\rm B}+\frac{2(1-x_{\rm B})}{1+\sqrt{1+\varepsilon^2}}\right)\frac{x_{\rm B}t^2}{\mathcal{Q}^4}$$
$$+\left(1+\frac{\sqrt{1+\varepsilon^2}+x_{\rm B}+(1-x_{\rm B})\frac{t}{\mathcal{Q}^2}}{1+\sqrt{1+\varepsilon^2}}\frac{t}{\mathcal{Q}^2}\right)\varepsilon^2\Bigg\},$$

$$C^{V}_{-+}(n=2) = \frac{4(2-y)\left(1-y-\frac{\varepsilon^2}{4}y^2\right)}{(1+\varepsilon^2)^{5/2}}\frac{x_{\rm B}t}{\mathcal{Q}^2}\Bigg\{4\frac{\widetilde{K}^2}{\mathcal{Q}^2}+1+\sqrt{1+\varepsilon^2}$$
$$+\frac{t}{\mathcal{Q}^2}\left((1-2x_{\rm B})\left(1-2x_{\rm B}-\sqrt{1+\varepsilon^2}\right)\frac{t}{\mathcal{Q}^2}-2+4x_{\rm B}+2x_{\rm B}\sqrt{1+\varepsilon^2}\right)\Bigg\},$$

$$C^{A}_{-+}(n=2) = \frac{16(2-y)\left(1-y-\frac{\varepsilon^2}{4}y^2\right)}{(1+\varepsilon^2)^{3/2}}\frac{t}{\mathcal{Q}^2}\Bigg\{\frac{\widetilde{K}^2}{\mathcal{Q}^2}\frac{1-2x_{\rm B}}{1+\varepsilon^2}$$
$$-\frac{1-x_{\rm B}}{4x_{\rm B}(1-x_{\rm B})+\varepsilon^2}\left(2x_{\rm B}^2-\varepsilon^2-3x_{\rm B}-x_{\rm B}\sqrt{1+\varepsilon^2}\right)$$
$$-\frac{t'}{\mathcal{Q}^2}\frac{2x_{\rm B}^2-\varepsilon^2-3x_{\rm B}-x_{\rm B}\sqrt{1+\varepsilon^2}}{4\sqrt{1+\varepsilon^2}}\Bigg\},$$

$$C_{-+}(n=3) = -8K\left(1-y-\frac{\varepsilon^2}{4}y^2\right)\frac{1+\sqrt{1+\varepsilon^2}+\frac{\varepsilon^2}{2}}{(1+\varepsilon^2)^{5/2}}$$
$$\times\left\{1+\frac{1+\sqrt{1+\varepsilon^2}+\frac{\varepsilon^2}{2x_{\rm B}}}{1+\sqrt{1+\varepsilon^2}+\frac{\varepsilon^2}{2}}\frac{x_{\rm B}t}{\mathcal{Q}^2}\right\},$$

$$C^V_{-+}(n=3) = \frac{8K\left(1-y-\frac{\varepsilon^2}{4}y^2\right)}{(1+\varepsilon^2)^{5/2}}\frac{x_{\rm B}t}{\mathcal{Q}^2}\left(1+\sqrt{1+\varepsilon^2}\right) \times\left\{1-\frac{t}{\mathcal{Q}^2}\frac{1-2x_{\rm B}-\sqrt{1+\varepsilon^2}}{1+\sqrt{1+\varepsilon^2}}\right\},$$

$$C^A_{-+}(n=3) = \frac{16K\left(1-y-\frac{\varepsilon^2}{4}y^2\right)}{(1+\varepsilon^2)^2}\frac{t}{\mathcal{Q}^2}\left\{1-x_{\rm B}+\frac{t'}{\mathcal{Q}^2}\frac{4x_{\rm B}(1-x_{\rm B})+\varepsilon^2}{4\sqrt{1+\varepsilon^2}}\right\},$$

$$S_{-+}(n=1) = \frac{4K(2-y)y}{(1+\varepsilon^2)^2}\left\{1-\sqrt{1+\varepsilon^2}+2\varepsilon^2-2\left(1+\frac{\sqrt{1+\varepsilon^2}-1}{2x_{\rm B}}\right)\frac{x_{\rm B}t}{\mathcal{Q}^2}\right\},$$

$$S^V_{-+}(n=1) = \frac{8Ky(2-y)}{(1+\varepsilon^2)^2}\frac{x_{\rm B}t}{\mathcal{Q}^2}\left(1+\sqrt{1+\varepsilon^2}\right)\left\{1-\frac{t}{\mathcal{Q}^2}\frac{1-2x_{\rm B}-\sqrt{1+\varepsilon^2}}{1+\sqrt{1+\varepsilon^2}}\right\},$$

$$S^A_{-+}(n=1) = \frac{4Ky(2-y)}{(1+\varepsilon^2)^2}\frac{t}{\mathcal{Q}^2}\Bigg\{3+2\varepsilon^2 + \sqrt{1+\varepsilon^2}-2x_{\rm B}-2x_{\rm B}\sqrt{1+\varepsilon^2}-\frac{t}{\mathcal{Q}^2}(1-2x_{\rm B})\left(1-2x_{\rm B}-\sqrt{1+\varepsilon^2}\right)\Bigg\},$$

$$S_{-+}(n=2) = 2y\left(1-y-\frac{\varepsilon^2}{4}y^2\right)\frac{1+\sqrt{1+\varepsilon^2}}{(1+\varepsilon^2)^2}\left(\varepsilon^2-2\left(1+\frac{\varepsilon^2}{2x_{\rm B}}\right)\frac{x_{\rm B}t}{\mathcal{Q}^2}\right) \times\left\{1+\frac{\sqrt{1+\varepsilon^2}-1+2x_{\rm B}}{1+\sqrt{1+\varepsilon^2}}\frac{t}{\mathcal{Q}^2}\right\},$$

$$S^V_{-+}(n=2) = \frac{4y\left(1-y-\frac{\varepsilon^2}{4}y^2\right)}{(1+\varepsilon^2)^2}\frac{x_{\rm B}t}{\mathcal{Q}^2} \times\left(1+\sqrt{1+\varepsilon^2}\right)\left(1-(1-2x_{\rm B})\frac{t}{\mathcal{Q}^2}\right)\left\{1-\frac{t}{\mathcal{Q}^2}\frac{1-2x_{\rm B}-\sqrt{1+\varepsilon^2}}{1+\sqrt{1+\varepsilon^2}}\right\},$$

$$S^A_{-+}(n=2) = \frac{2y\left(1-y-\frac{\varepsilon^2}{4}y^2\right)}{(1+\varepsilon^2)^2}\frac{t}{\mathcal{Q}^2}\left(4-2x_{\rm B}+3\varepsilon^2+\frac{t}{\mathcal{Q}^2}\left(4x_{\rm B}(1-x_{\rm B})+\varepsilon^2\right)\right) \times\left(1+\sqrt{1+\varepsilon^2}-\frac{t}{\mathcal{Q}^2}\left(1-2x_{\rm B}-\sqrt{1+\varepsilon^2}\right)\right).$$

A.2.2 Longitudinally and Transversally Polarized TP+ *Target*

The angular coefficients for longitudinally and transversally polarized TP+ parts are determined by the expressions

$$\delta C_{ab}(n)\,,\ \delta C^{V}_{ab}(n)\,,\ \delta C^{A}_{ab}(n)\,, \qquad \text{for} \quad n\in\{0,1,2\}\,,$$
$$\delta S_{ab}(n)\,,\ \delta S^{V}_{ab}(n)\,,\ \delta S^{A}_{ab}(n)\,, \qquad \text{for} \quad n\in\{1,2,3\}\,.$$

Note again, as in the previous section, these coefficients are identical with $C^{\mathrm{LP},\cdots}_{ab}(n)/\lambda\Lambda$ and $S^{\mathrm{LP},,\cdots}_{ab}(n)/\Lambda$ of Ref. [44] and that the third even harmonics, i.e.,

$$\delta C_{ab}(n=3)=\delta C^{V}_{ab}(n=3)=\delta C^{A}_{ab}(n=3)=0,$$

and the following third odd harmonics in longitudinal helicity flip CFFs

$$\delta S_{0b}(n=3)=\delta S^{V}_{0b}(n=3)=\delta S^{A}_{0b}(n=3)=0$$

vanish and thus will not be presented below.

- Conserved photon-helicity coefficients:

$$\begin{aligned}\delta C_{++}(n=0) = &-\frac{4y\left(1+\sqrt{1+\varepsilon^2}\right)}{(1+\varepsilon^2)^{5/2}}\left\{(2-y)^2\frac{\widetilde{K}^2}{\mathcal{Q}^2}+\left(1-y-\frac{\varepsilon^2}{4}y^2\right)\right.\\ &\left.\times\left(\frac{x_{\mathrm{B}}t}{\mathcal{Q}^2}-\left(1-\frac{t}{\mathcal{Q}^2}\right)\frac{\varepsilon^2}{2}\right)\left(1+\frac{\sqrt{1+\varepsilon^2}-1+2x_{\mathrm{B}}}{1+\sqrt{1+\varepsilon^2}}\frac{t}{\mathcal{Q}^2}\right)\right\},\end{aligned} \tag{A.15}$$

$$\begin{aligned}\delta C^{V}_{++}(n=0) = &\frac{4y\left(1+\sqrt{1+\varepsilon^2}\right)}{(1+\varepsilon^2)^{5/2}}\frac{t}{\mathcal{Q}^2}\left\{(2-y)^2\,\frac{1+\sqrt{1+\varepsilon^2}-2x_{\mathrm{B}}}{1+\sqrt{1+\varepsilon^2}}\,\frac{\widetilde{K}^2}{\mathcal{Q}^2}\right.\\ &\left.+\left(1-y-\frac{\varepsilon^2}{4}y^2\right)\left(2-x_{\mathrm{B}}+\frac{3\varepsilon^2}{2}\right)\left(1+\frac{4(1-x_{\mathrm{B}})x_{\mathrm{B}}+\varepsilon^2}{4-2x_{\mathrm{B}}+3\varepsilon^2}\frac{t}{\mathcal{Q}^2}\right)\right.\end{aligned}$$

$$\times\left(1+\frac{\sqrt{1+\varepsilon^2}-1+2x_{\rm B}}{1+\sqrt{1+\varepsilon^2}}\frac{t}{\mathcal{Q}^2}\right)\Bigg\},$$

$$\delta C^A_{++}(n=0)=\frac{4y}{(1+\varepsilon^2)^{5/2}}\frac{x_{\rm B}t}{\mathcal{Q}^2}\Bigg\{2(2-y)^2\frac{\widetilde{K}^2}{\mathcal{Q}^2}+\left(1-y-\frac{\varepsilon^2}{4}y^2\right)(1+\sqrt{1+\varepsilon^2})$$
$$\times\left(1-(1-2x_{\rm B})\frac{t}{\mathcal{Q}^2}\right)\left(1+\frac{\sqrt{1+\varepsilon^2}-1+2x_{\rm B}}{1+\sqrt{1+\varepsilon^2}}\frac{t}{\mathcal{Q}^2}\right)\Bigg\},$$

$$\delta C_{++}(n=1)=-\frac{4Ky(2-y)}{(1+\varepsilon^2)^{5/2}}(1+\sqrt{1+\varepsilon^2}-\varepsilon^2)$$
$$\times\left\{1-\left(1-2x_{\rm B}\frac{2+\sqrt{1+\varepsilon^2}}{1+\sqrt{1+\varepsilon^2}-\varepsilon^2}\right)\frac{t}{\mathcal{Q}^2}\right\},$$

$$\delta C^V_{++}(n=1)=\frac{8K(2-y)y}{(1+\varepsilon^2)^2}\left(\sqrt{1+\varepsilon^2}+2(1-x_{\rm B})\right)\frac{t}{\mathcal{Q}^2}$$
$$\times\left\{1-\frac{1+\frac{1-\varepsilon^2}{\sqrt{1+\varepsilon^2}}-2x_{\rm B}\left(1+\frac{4(1-x_{\rm B})}{\sqrt{1+\varepsilon^2}}\right)}{2\left(\sqrt{1+\varepsilon^2}+2(1-x_{\rm B})\right)}\frac{t'}{\mathcal{Q}^2}\right\},$$

$$\delta C^A_{++}(n=1)=\frac{16K(2-y)y}{(1+\varepsilon^2)^{5/2}}\frac{x_{\rm B}t}{\mathcal{Q}^2}\left(1-(1-2x_{\rm B})\frac{t}{\mathcal{Q}^2}\right),$$

$$\delta C_{++}(n=2)=-\frac{4y\left(1-y-\frac{\varepsilon^2}{4}y^2\right)}{(1+\varepsilon^2)^{5/2}}\left(\frac{x_{\rm B}t}{\mathcal{Q}^2}-\left(1-\frac{t}{\mathcal{Q}^2}\right)\frac{\varepsilon^2}{2}\right)$$
$$\times\left\{1-\sqrt{1+\varepsilon^2}-\left(1+\sqrt{1+\varepsilon^2}-2x_{\rm B}\right)\frac{t}{\mathcal{Q}^2}\right\},$$

$$\delta C^V_{++}(n=2)=-\frac{2y\left(1-y-\frac{\varepsilon^2}{4}y^2\right)}{(1+\varepsilon^2)^{5/2}}\left(4-2x_{\rm B}+3\varepsilon^2\right)\frac{t}{\mathcal{Q}^2}\left(1+\frac{4(1-x_{\rm B})x_{\rm B}+\varepsilon^2}{4-2x_{\rm B}+3\varepsilon^2}\frac{t}{\mathcal{Q}^2}\right)$$
$$\times\left\{\sqrt{1+\varepsilon^2}-1+\left(1+\sqrt{1+\varepsilon^2}-2x_{\rm B}\right)\frac{t}{\mathcal{Q}^2}\right\},$$

$$\delta C^A_{++}(n=2)=\frac{4y\left(1-y-\frac{\varepsilon^2}{4}y^2\right)}{(1+\varepsilon^2)^{5/2}}\frac{x_{\rm B}t}{\mathcal{Q}^2}\left(1-(1-2x_{\rm B})\frac{t}{\mathcal{Q}^2}\right)$$
$$\times\left\{1-\sqrt{1+\varepsilon^2}-\left(1+\sqrt{1+\varepsilon^2}-2x_{\rm B}\right)\ \frac{t}{\mathcal{Q}^2}\right\},$$

$$\delta S_{++}(n=1) = \frac{4K\left(2-2y+y^2+\frac{\varepsilon^2}{2}y^2\right)}{(1+\varepsilon^2)^3}(1+\sqrt{1+\varepsilon^2})$$
$$\times\left\{2\sqrt{1+\varepsilon^2}-1+\frac{1+\sqrt{1+\varepsilon^2}-2x_{\rm B}}{1+\sqrt{1+\varepsilon^2}}\frac{t}{\mathcal{Q}^2}\right\}$$
$$+\frac{8K\left(1-y-\frac{\varepsilon^2}{4}y^2\right)}{(1+\varepsilon^2)^3}\left\{\left(1-\sqrt{1+\varepsilon^2}-\frac{\varepsilon^2}{2}-x_{\rm B}\left(3-\sqrt{1+\varepsilon^2}\right)\right)\frac{t}{\mathcal{Q}^2}\right.$$
$$\left.+\frac{3\varepsilon^2}{2}\right\},$$

$$\delta S^V_{++}(n=1) = \frac{8K\left(2-2y+y^2+\frac{\varepsilon^2}{2}y^2\right)}{(1+\varepsilon^2)^2}\frac{t}{\mathcal{Q}^2}$$
$$\times\left\{1-\frac{(1-2x_{\rm B})\left(1+\sqrt{1+\varepsilon^2}-2x_{\rm B}\right)}{2(1+\varepsilon^2)}\frac{t'}{\mathcal{Q}^2}\right\}$$
$$+\frac{32K\left(1-y-\frac{\varepsilon^2}{4}y^2\right)}{(1+\varepsilon^2)^3}\left(1-\frac{3+\sqrt{1+\varepsilon^2}}{4}x_{\rm B}+\frac{5\varepsilon^2}{8}\right)\frac{t}{\mathcal{Q}^2}$$
$$\times\left\{1-\frac{1-\sqrt{1+\varepsilon^2}-\frac{\varepsilon^2}{2}-2x_{\rm B}\left(3(1-x_{\rm B})-\sqrt{1+\varepsilon^2}\right)}{4-x_{\rm B}\left(\sqrt{1+\varepsilon^2}+3\right)+\frac{5\varepsilon^2}{2}}\frac{t}{\mathcal{Q}^2}\right\},$$

$$\delta S^A_{++}(n=1) = -\frac{8K\left(2-2y+y^2+\frac{\varepsilon^2}{2}y^2\right)}{(1+\varepsilon^2)^3}\frac{x_{\rm B}t}{\mathcal{Q}^2}$$
$$\times\left\{\sqrt{1+\varepsilon^2}-1+(1+\sqrt{1+\varepsilon^2}-2x_{\rm B})\frac{t}{\mathcal{Q}^2}\right\}$$
$$+\frac{8K\left(1-y-\frac{\varepsilon^2}{4}y^2\right)}{(1+\varepsilon^2)^3}(3+\sqrt{1+\varepsilon^2})\frac{x_{\rm B}t}{\mathcal{Q}^2}$$
$$\times\left\{1-\frac{3-\sqrt{1+\varepsilon^2}-6x_{\rm B}}{3+\sqrt{1+\varepsilon^2}}\frac{t}{\mathcal{Q}^2}\right\},$$

$$\delta S_{++}(n=2) = -\frac{4(2-y)\left(1-y-\frac{\varepsilon^2}{4}y^2\right)}{(1+\varepsilon^2)^{5/2}}$$
$$\times\left\{\frac{4\widetilde{K}^2}{\sqrt{1+\varepsilon^2}\mathcal{Q}^2}+(1+\sqrt{1+\varepsilon^2}-2x_{\rm B})\left(1+\sqrt{1+\varepsilon^2}+\frac{x_{\rm B}t}{\mathcal{Q}^2}\right)\frac{t'}{\mathcal{Q}^2}\right\},$$

$$\delta S^{V}_{++}(n=2) = \frac{4(2-y)\left(1-y-\frac{\varepsilon^2}{4}y^2\right)}{(1+\varepsilon^2)^{5/2}}\frac{t}{\mathcal{Q}^2}$$
$$\times\left\{\frac{4(1-2x_{\rm B})\widetilde{K}^2}{\sqrt{1+\varepsilon^2}\mathcal{Q}^2}-\left(3-\sqrt{1+\varepsilon^2}-2x_{\rm B}+\frac{\varepsilon^2}{x_{\rm B}}\right)\frac{x_{\rm B}t'}{\mathcal{Q}^2}\right\},$$

$$\delta S^{A}_{++}(n=2) = \frac{4(2-y)\left(1-y-\frac{\varepsilon^2}{4}y^2\right)}{(1+\varepsilon^2)^{3}}\frac{x_{\rm B}t}{\mathcal{Q}^2}$$
$$\times\left\{\frac{4\widetilde{K}^2}{\mathcal{Q}^2}-\left(1+\sqrt{1+\varepsilon^2}-2x_{\rm B}\right)\left(1-\frac{(1-2x_{\rm B})t}{\mathcal{Q}^2}\right)\frac{t'}{\mathcal{Q}^2}\right\},$$

$$\delta S_{++}(n=3) = -\frac{4K\left(1-y-\frac{\varepsilon^2}{4}y^2\right)}{(1+\varepsilon^2)^{3}}\frac{1+\sqrt{1+\varepsilon^2}-2x_{\rm B}}{1+\sqrt{1+\varepsilon^2}}\frac{\varepsilon^2 t'}{\mathcal{Q}^2},$$

$$\delta S^{V}_{++}(n=3) = \frac{4K\left(1-y-\frac{\varepsilon^2}{4}y^2\right)}{(1+\varepsilon^2)^{3}}\left(4(1-x_{\rm B})x_{\rm B}+\varepsilon^2\right)\frac{t\,t'}{\mathcal{Q}^4},$$

$$\delta S^{A}_{++}(n=3) = -\frac{8K\left(1-y-\frac{\varepsilon^2}{4}y^2\right)}{(1+\varepsilon^2)^{3}}\left(1+\sqrt{1+\varepsilon^2}-2x_{\rm B}\right)\frac{x_{\rm B}t\,t'}{\mathcal{Q}^4}.$$

- Photon helicity-flip amplitudes by one unit:

$$\delta C_{0+}(n=0) = \frac{8\sqrt{2}K(1-x_{\rm B})y\sqrt{1-y-\frac{\varepsilon^2}{4}y^2}}{(1+\varepsilon^2)^2}\frac{t}{\mathcal{Q}^2}, \tag{A.16}$$

$$\delta C^{V}_{0+}(n=0) = \frac{8\sqrt{2}Ky\sqrt{1-y-\frac{\varepsilon^2}{4}y^2}}{(1+\varepsilon^2)^2}\frac{t}{\mathcal{Q}^2}\left(x_{\rm B}-\frac{t}{\mathcal{Q}^2}(1-2x_{\rm B})\right),$$

$$\delta C^{A}_{0+}(n=0) = -\frac{8\sqrt{2}Ky\sqrt{1-y-\frac{\varepsilon^2}{4}\,y^2}}{(1+\varepsilon^2)^2}\frac{x_{\rm B}t}{\mathcal{Q}^2}\left(1+\frac{t}{\mathcal{Q}^2}\right),$$

$$\delta C_{0+}(n=1) = -\frac{8\sqrt{2}y(2-y)\sqrt{1-y-\frac{\varepsilon^2}{4}y^2}}{(1+\varepsilon^2)^2}\frac{\widetilde{K}^2}{\mathcal{Q}^2},$$

$$\delta C^{V}_{0+}(n=1) = \frac{8\sqrt{2}y(2-y)\sqrt{1-y-\frac{\varepsilon^2}{4}y^2}}{(1+\varepsilon^2)^2}\frac{t\widetilde{K}^2}{\mathcal{Q}^4},$$

$$\delta C_{0+}^{A}(n=1)=0\,,$$

$$\delta C_{0+}(n=2)=-\frac{8\sqrt{2}Ky\sqrt{1-y-\frac{\varepsilon^2}{4}y^2}}{(1+\varepsilon^2)^2}\left(1+\frac{x_{\rm B}t}{\mathcal{Q}^2}\right),$$

$$\delta C_{0+}^{V}(n=2)=\frac{8\sqrt{2}Ky(1-x_{\rm B})\sqrt{1-y-\frac{\varepsilon^2}{4}y^2}}{(1+\varepsilon^2)^2}\frac{t}{\mathcal{Q}^2},$$

$$\delta C_{0+}^{A}(n=2)=\frac{8\sqrt{2}Ky\sqrt{1-y-\frac{\varepsilon^2}{4}\,y^2}}{(1+\varepsilon^2)^2}\frac{x_{\rm B}t}{\mathcal{Q}^2}\left(1+\frac{t}{\mathcal{Q}^2}\right),$$

$$\begin{aligned}\delta S_{0+}(n=1)=\frac{8\sqrt{2}\sqrt{1-y-\frac{\varepsilon^2}{4}y^2}}{(1+\varepsilon^2)^{5/2}}\Bigg\{&\frac{\widetilde{K}^2}{\mathcal{Q}^2}(2-y)^2\\&+\left(1+\frac{t}{\mathcal{Q}^2}\right)\left(1-y-\frac{\varepsilon^2}{4}y^2\right)\left(2\frac{x_{\rm B}t}{\mathcal{Q}^2}-\left(1-\frac{t}{\mathcal{Q}^2}\right)\varepsilon^2\right)\Bigg\},\end{aligned}$$

$$\begin{aligned}\delta S_{0+}^{V}(n=1)=-\frac{8\sqrt{2}\sqrt{1-y-\frac{\varepsilon^2}{4}y^2}}{(1+\varepsilon^2)^{5/2}}\frac{t}{\mathcal{Q}^2}\Bigg\{&\frac{\widetilde{K}^2}{\mathcal{Q}^2}(2-y)^2\\&+\left(1+\frac{t}{\mathcal{Q}^2}\right)\left(1-y-\frac{\varepsilon^2}{4}y^2\right)\Bigg(4-2x_{\rm B}+3\varepsilon^2\\&\qquad+\frac{t}{\mathcal{Q}^2}(4x_{\rm B}(1-x_{\rm B})+\varepsilon^2)\Bigg)\Bigg\},\end{aligned}$$

$$\delta S_{0+}^{A}(n=1)=-\frac{16\sqrt{2}\left(1-y-\frac{\varepsilon^2}{4}y^2\right)^{3/2}}{(1+\varepsilon^2)^{5/2}}\frac{x_{\rm B}t}{\mathcal{Q}^2}\left(1+\frac{t}{\mathcal{Q}^2}\right)\left(1-(1-2x_{\rm B})\frac{t}{\mathcal{Q}^2}\right),$$

$$\delta S_{0+}(n=2)=\frac{8\sqrt{2}K(2-y)\sqrt{1-y-\frac{\varepsilon^2}{4}y^2}}{(1+\varepsilon^2)^{5/2}}\left(1+\frac{x_{\rm B}t}{\mathcal{Q}^2}\right),$$

$$\delta S_{0+}^{V}(n=2)=-\frac{8\sqrt{2}K(2-y)(1-x_{\rm B})\sqrt{1-y-\frac{\varepsilon^2}{4}y^2}}{(1+\varepsilon^2)^{5/2}}\frac{t}{\mathcal{Q}^2},$$

$$\delta S_{0+}^{A}(n=2)=-\frac{8\sqrt{2}K(2-y)\sqrt{1-y-\frac{\varepsilon^2}{4}y^2}}{(1+\varepsilon^2)^{5/2}}\frac{x_{\rm B}t}{\mathcal{Q}^2}\left(1+\frac{t}{\mathcal{Q}^2}\right).$$

- Photon helicity-flip amplitudes by two units:

$$\delta C_{-+}(n=0) = \frac{4y}{(1+\varepsilon^2)^{5/2}}\left\{\frac{\widetilde{K}^2}{\mathcal{Q}^2}(2-y)^2\left(1-\sqrt{1+\varepsilon^2}\right)+\frac{1}{2}\left(1-y-\frac{\varepsilon^2}{4}y^2\right)\right.$$
$$\times\left(2\frac{x_{\rm B}t}{\mathcal{Q}^2}-\left(1-\frac{t}{\mathcal{Q}^2}\right)\varepsilon^2\right)\left(1-\sqrt{1+\ \varepsilon^2}\right.$$
$$\left.\left.-\frac{t}{\mathcal{Q}^2}\left(1-2x_{\rm B}+\sqrt{1+\varepsilon^2}\right)\right)\right\}, \qquad \text{(A.17)}$$

$$\delta C^V_{-+}(n=0) = \frac{2y}{(1+\varepsilon^2)^{5/2}}\frac{t}{\mathcal{Q}^2}\left\{(4-2x_{\rm B}+3\varepsilon^2)\left(1-y-\frac{\varepsilon^2}{4}y^2\right)\right.$$
$$\times\left(1+\frac{t}{\mathcal{Q}^2}\frac{4x_{\rm B}(1-x_{\rm B})+\varepsilon^2}{4-2x_{\rm B}+3\varepsilon^2}\right)\left(\sqrt{1+\varepsilon^2}-1\right.$$
$$\left.+\frac{t}{\mathcal{Q}^2}\left(1-2x_{\rm B}+\sqrt{1+\ \varepsilon^2}\right)\right)$$
$$\left.+2(2-y)^2(\sqrt{1+\varepsilon^2}-1+2x_{\rm B})\ \frac{\widetilde{K}^2}{\mathcal{Q}^2}\right\},$$

$$\delta C^A_{-+}(n=0) = \frac{4x_{\rm B}y}{(1+\varepsilon^2)^{5/2}}\frac{t}{\mathcal{Q}^2}\left\{2(2-y)^2\left((1-x_{\rm B})\frac{t}{\mathcal{Q}^2}\left(1+\frac{x_{\rm B}t}{\mathcal{Q}^2}\right)\right.\right.$$
$$\left.+\left(1+\frac{t}{\mathcal{Q}^2}\right)^2\frac{\varepsilon^2}{4}\right)$$
$$-\left(1-y-\frac{\varepsilon^2}{4}y^2\right)\left(1-(1-2x_{\rm B})\frac{t}{\mathcal{Q}^2}\right)$$
$$\left.\times\left(1-\sqrt{1+\varepsilon^2}-\frac{t}{\mathcal{Q}^2}(1+\sqrt{1+\varepsilon^2}-2x_{\rm B})\right)\right\},$$

$$\delta C_{-+}(n=1) = \frac{4Ky(2-y)}{(1+\varepsilon^2)^{5/2}}\left\{1-\varepsilon^2-\sqrt{1+\varepsilon^2}\right.$$
$$\left.-\frac{t}{\mathcal{Q}^2}\left(1-\varepsilon^2-\sqrt{1+\varepsilon^2}-2x_{\rm B}\left(2-\sqrt{1+\varepsilon^2}\right)\right)\right\},$$

$$\delta C^V_{-+}(n=1) = -\frac{4Ky(2-y)}{(1+\varepsilon^2)^{5/2}}\frac{t}{\mathcal{Q}^2}\left\{5-4x_{\rm B}+3\varepsilon^2-\sqrt{1+\varepsilon^2}\right.$$

$$- \frac{t}{\mathcal{Q}^2}\left(1-\varepsilon^2-\sqrt{1+\varepsilon^2}-2x_{\rm B}(4-4x_{\rm B}-\sqrt{1+\varepsilon^2})\right)\Bigg\},$$

$$\delta C^A_{-+}(n=1) = -\frac{16Kx_{\rm B}y(2-y)}{(1+\varepsilon^2)^{5/2}}\frac{t}{\mathcal{Q}^2}\left(1-(1-2x_{\rm B})\frac{t}{\mathcal{Q}^2}\right),$$

$$\delta C_{-+}(n=2) = -\frac{2y\left(1-y-\frac{\varepsilon^2}{4}y^2\right)}{(1+\varepsilon^2)^{5/2}}\Bigg\{\varepsilon^2\left(1+\sqrt{1+\varepsilon^2}\right)$$
$$-2\frac{t}{\mathcal{Q}^2}\left((1-x_{\rm B})\varepsilon^2+x_{\rm B}\left(1+\sqrt{1+\varepsilon^2}\right)\right)$$
$$+\frac{t^2}{\mathcal{Q}^4}(2x_{\rm B}+\varepsilon^2)\left(1-2x_{\rm B}-\sqrt{1+\varepsilon^2}\right)\Bigg\},$$

$$\delta C^V_{-+}(n=2) = -\frac{2y\left(1-y-\frac{\varepsilon^2}{4}y^2\right)}{(1+\varepsilon^2)^{5/2}}\left(1+\sqrt{1+\varepsilon^2}-\frac{t}{\mathcal{Q}^2}(1-\sqrt{1+\varepsilon^2}-2x_{\rm B})\right)$$
$$\times\frac{t}{\mathcal{Q}^2}\left(4-2x_{\rm B}+3\varepsilon^2+\frac{t}{\mathcal{Q}^2}(4x_{\rm B}(1-x_{\rm B})+\varepsilon^2)\right),$$

$$\delta C^A_{-+}(n=2) = -\frac{4x_{\rm B}y\left(1-y-\frac{\varepsilon^2}{4}y^2\right)}{(1+\varepsilon^2)^{5/2}}$$
$$\times\frac{t}{\mathcal{Q}^2}\left(1-(1-2x_{\rm B})\frac{t}{\mathcal{Q}^2}\right)\left\{1+\sqrt{1+\varepsilon^2}-\frac{t}{\mathcal{Q}^2}\left(1-\sqrt{1+\varepsilon^2}-2x_{\rm B}\right)\right\},$$

$$\delta S_{-+}(n=1) = -\frac{4K}{(1+\varepsilon^2)^3}\Bigg\{(2-y)^2\Bigg(1+2\varepsilon^2-\sqrt{1+\varepsilon^2}$$
$$+\frac{t}{\mathcal{Q}^2}\left(1-2x_{\rm B}-\sqrt{1+\varepsilon^2}\right)\Bigg)$$
$$-\left(1-y-\frac{\varepsilon^2}{4}y^2\right)\Bigg(2+\varepsilon^2-2\sqrt{1+\varepsilon^2}$$
$$+\frac{t}{\mathcal{Q}^2}\left(\varepsilon^2-4\sqrt{1+\varepsilon^2}+2x_{\rm B}(1+\sqrt{1+\varepsilon^2})\right)\Bigg)\Bigg\},$$

$$\delta S^V_{-+}(n=1) = -\frac{4K}{(1+\varepsilon^2)^3}\frac{t}{\mathcal{Q}^2}\Bigg\{\left(2-2y+y^2+\frac{\varepsilon^2}{2}y^2\right)$$
$$\times\Bigg(3+2\varepsilon^2+\sqrt{1+\varepsilon^2}-2x_{\rm B}(1+\sqrt{1+\ \varepsilon^2})$$
$$-\frac{t}{\mathcal{Q}^2}(1-2x_{\rm B})(1-2x_{\rm B}-\sqrt{1+\varepsilon^2})\Bigg)$$

$$+\left(1-y-\frac{\varepsilon^2}{4}y^2\right)\left(8+5\varepsilon^2-2x_{\rm B}(3-\sqrt{1+\varepsilon^2})\right.$$
$$\left.\left.-\frac{t}{\mathcal{Q}^2}\left(2-\varepsilon^2+2\sqrt{1+\varepsilon^2}-12x_{\rm B}(1-x_{\rm B})-4x_{\rm B}\sqrt{1+\varepsilon^2}\right)\right)\right\},$$

$$\delta S^A_{-+}(n=1)=-\frac{8K\left(2-2y+y^2+\frac{\varepsilon^2}{2}y^2\right)}{(1+\varepsilon^2)^3}(1+\sqrt{1+\varepsilon^2})\frac{x_{\rm B}t}{\mathcal{Q}^2}$$
$$\times\left(1-\frac{t}{\mathcal{Q}^2}\frac{1-\sqrt{1+\varepsilon^2}-2x_{\rm B}}{1+\sqrt{1+\varepsilon^2}}\right)$$
$$-\frac{8K\left(1-y-\frac{\varepsilon^2}{4}y^2\right)}{(1+\varepsilon^2)^3}\frac{x_{\rm B}t}{\mathcal{Q}^2}\left\{3-\sqrt{1+\varepsilon^2}-\frac{t}{\mathcal{Q}^2}\left(3+\sqrt{1+\varepsilon^2}-6x_{\rm B}\right)\right\},$$

$$\delta S_{-+}(n=2)=-\frac{4(2-y)\left(1-y-\frac{\varepsilon^2}{4}y^2\right)}{(1+\varepsilon^2)^3}\left\{\frac{t^2}{\mathcal{Q}^4}\Big(\varepsilon^2-2x_{\rm B}^2(2+\sqrt{1+\varepsilon^2})\right.$$
$$+x_{\rm B}(3-\varepsilon^2+\sqrt{1+\varepsilon^2})\Big)+\varepsilon^2\left(1+\sqrt{1+\varepsilon^2}\right)$$
$$\left.+\frac{t}{\mathcal{Q}^2}\left(2+2\sqrt{1+\varepsilon^2}+\varepsilon^2\sqrt{1+\varepsilon^2}-x_{\rm B}\left(3-\varepsilon^2+3\sqrt{1+\varepsilon^2}\right)\right)\right\},$$

$$\delta S^V_{-+}(n=2)=-\frac{4(2-y)\left(1-y-\frac{\varepsilon^2}{4}y^2\right)}{(1+\varepsilon^2)^{5/2}}\frac{t}{\mathcal{Q}^2}\left\{(2-x_{\rm B})(1+\sqrt{1+\varepsilon^2})\right.$$
$$\left.+\varepsilon^2+\frac{4\widetilde{K}^2(1-2x_{\rm B})}{\mathcal{Q}^2\sqrt{1+\varepsilon^2}}+\frac{t}{\mathcal{Q}^2}\left(\varepsilon^2+x_{\rm B}(3-2x_{\rm B}+\sqrt{1+\varepsilon^2})\right)\right\},$$

$$\delta S^A_{-+}(n=2)=-\frac{4(2-y)\left(1-y-\frac{\varepsilon^2}{4}y^2\right)}{(1+\varepsilon^2)^3}\frac{x_{\rm B}t}{\mathcal{Q}^2}\left\{1+4\frac{\widetilde{K}^2}{\mathcal{Q}^2}\right.$$
$$+\sqrt{1+\varepsilon^2}-2\frac{t}{\mathcal{Q}^2}\left(1-2x_{\rm B}-x_{\rm B}\sqrt{1+\varepsilon^2}\right)$$
$$\left.+\frac{t^2}{\mathcal{Q}^4}(1-2x_{\rm B})\left(1-2x_{\rm B}-\sqrt{1+\varepsilon^2}\right)\right\},$$

$$\delta S_{-+}(n=3)=\frac{4K\left(1-y-\frac{\varepsilon^2}{4}y^2\right)}{(1+\varepsilon^2)^3}\left\{2+\varepsilon^2+2\sqrt{1+\varepsilon^2}\right.$$
$$\left.+\frac{t}{\mathcal{Q}^2}\left(\varepsilon^2+2x_{\rm B}(1+\sqrt{1+\varepsilon^2})\right)\right\},$$

$$\delta S^V_{-+}(n=3) = -\frac{4K\left(1-y-\frac{\varepsilon^2}{4}y^2\right)}{(1+\varepsilon^2)^{5/2}}\frac{t}{\mathcal{Q}^2}\left\{4-4x_{\rm B}+\frac{t'}{\mathcal{Q}^2}\frac{4x_{\rm B}(1-x_{\rm B})+\varepsilon^2}{\sqrt{1+\varepsilon^2}}\right\},$$

$$\delta S^A_{-+}(n=3) = -\frac{8K\left(1-y-\frac{\varepsilon^2}{4}y^2\right)}{(1+\varepsilon^2)^{3}}\frac{x_{\rm B}t}{\mathcal{Q}^2}\left\{1+\sqrt{1+\varepsilon^2}\right.$$
$$\left.-\frac{t}{\mathcal{Q}^2}\left(1-2x_{\rm B}-\sqrt{1+\varepsilon^2}\right)\right\}.$$

A.3 Helicity Amplitudes from Tarrach Tensor

Let us establish a relation of the Compton tensor parametrization introduced in Eq. (2.130) in terms of CFFs and the one by Tarrach [45] (also quoted in [39]) that is used as a starting point for the low-energy expansion relevant for generalized polarizabilities. The Tarrach's tensor is written as a linear superposition of independent tensor structures $\rho_{\mu\nu}$ accompanied by f functions encoding the structural information about the nucleon,

$$\varepsilon_\mu(a)T_{\mu\nu}\varepsilon'^*_\nu(b) = \sum_{k=1}^{12} f_k\,\bar{u}_2 R^{(k)}_{ab} u_1 \qquad \text{with} \qquad R^{(k)}_{ab} = \varepsilon_\mu(a)\rho^{\mu\nu}_k\varepsilon'^*_\nu(b)\,. \tag{A.18}$$

Now one computes the helicity amplitudes for all polarization states of the photons and express the result in terms of the Dirac structures used in the parametrization of helicity CFFs in Eqs. (2.14) and (2.15) multiplied by the functions of the kinematical invariants. Comparing Eqs. (2.5) and (2.13)–(2.15) with what one finds below, one can establish relation formulas of CFFs and f's. In the following one presents an overcomplete set of 3×12 relations from which an interesting reader can express helicity dependent CFFs in terms of f's or reverse.

- (1,1) helicity amplitude:

$$R^{(1)}_{++} = \frac{(\not{q}\mathcal{Q}\varepsilon - i\sigma_{q\Delta}x_{\rm B})\left((1-2x_{\rm B})t-\mathcal{Q}^2-\left(t+\mathcal{Q}^2\right)\sqrt{1+\varepsilon^2}\right)}{2\left(tx_{\rm B}+(2-x_{\rm B})\mathcal{Q}^2\right)\sqrt{1+\varepsilon^2}} \tag{A.19}$$

$$R^{(2)}_{++} = (\not{q}\,\mathcal{Q}\varepsilon - i\sigma_{q\Delta}x_{\rm B})\left\{\frac{tx_{\rm B}+(2-x_{\rm B})\mathcal{Q}^2}{4x_{\rm B}^2} - \frac{t^2(1-2x_{\rm B})+2t(2-x_{\rm B})\mathcal{Q}^2-\mathcal{Q}^4}{4\left(tx_{\rm B}+(2-x_{\rm B})\mathcal{Q}^2\right)\sqrt{1+\varepsilon^2}}\right.$$
$$\left. + \frac{\mathcal{Q}^2\left(2tx_{\rm B}+t(1-x_{\rm B})\varepsilon^2+(1-x_{\rm B})\mathcal{Q}^2\left(2+\varepsilon^2\right)\right)}{2x_{\rm B}^2\left(tx_{\rm B}+(2-x_{\rm B})\mathcal{Q}^2\right)\sqrt{1+\varepsilon^2}}\right\} \tag{A.20}$$

$$R^{(3)}_{++} = \frac{(\not{q}\mathcal{Q}\varepsilon - i\sigma_{q\Delta}x_{\rm B})\mathcal{Q}^2}{2x_{\rm B}}\left\{\frac{\mathcal{Q}^2\left(2-x_{\rm B}+\varepsilon^2\right)+t\left((3-2x_{\rm B})x_{\rm B}+\varepsilon^2\right)}{\left(tx_{\rm B}+(2-x_{\rm B})\mathcal{Q}^2\right)\sqrt{1+\varepsilon^2}}+1\right\} \tag{A.21}$$

$$R^{(4)}_{++} = i\sigma_{q\Delta}\frac{(1-x_{\rm B})\mathcal{Q}\varepsilon}{x_{\rm B}\sqrt{1+\varepsilon^2}} - \not{q}\,\gamma^5\frac{\left(tx_{\rm B}+(2-x_{\rm B})\mathcal{Q}^2\right)\left(1+\sqrt{1+\varepsilon^2}\right)}{2x_{\rm B}\sqrt{1+\varepsilon^2}}$$
$$- \gamma^5\frac{M\left(tx_{\rm B}+(2-x_{\rm B})\mathcal{Q}^2\right)\left(1-2x_{\rm B}-\sqrt{1+\varepsilon^2}\right)}{2x_{\rm B}\sqrt{1+\varepsilon^2}} - \not{q}\,\frac{t(1-x_{\rm B})}{\sqrt{1+\varepsilon^2}} \tag{A.22}$$

$$R^{(5)}_{++} = \not{q}\,\frac{tx_{\rm B}}{4\sqrt{1+\varepsilon^2}} - i\sigma_{q\Delta}\frac{\mathcal{Q}\varepsilon}{4\sqrt{1+\varepsilon^2}} + \not{q}\,\gamma^5\frac{tx_{\rm B}+\mathcal{Q}^2\left(1+\sqrt{1+\varepsilon^2}\right)}{4\sqrt{1+\varepsilon^2}}$$
$$+ \gamma^5\frac{M\mathcal{Q}^2\left(1-x_{\rm B}-\sqrt{1+\varepsilon^2}\right)}{4\sqrt{1+\varepsilon^2}}, \tag{A.23}$$

$$R^{(6)}_{++} = -\not{q}\,\frac{\mathcal{Q}\left(t^2(2-3x_{\rm B})+(2-x_{\rm B})\mathcal{Q}^4\right)\varepsilon}{2\left(tx_{\rm B}+(2-x_{\rm B})\mathcal{Q}^2\right)\sqrt{1+\varepsilon^2}}$$
$$- i\sigma_{q\Delta}\mathcal{Q}^2\frac{(2-x_{\rm B})\mathcal{Q}^2\left(2(1-x_{\rm B})+\varepsilon^2\right)+tx_{\rm B}\left(4-2(3-x_{\rm B})x_{\rm B}+\varepsilon^2\right)}{x_{\rm B}\left(tx_{\rm B}+(2-x_{\rm B})\mathcal{Q}^2\right)\sqrt{1+\varepsilon^2}}$$
$$- \not{q}\,\gamma^5\left\{M\left(t-\mathcal{Q}^2\right)+\frac{M(1-x_{\rm B})\left(t+\mathcal{Q}^2\right)}{\sqrt{1+\varepsilon^2}}\right\}$$
$$- \gamma^5\left\{\frac{\left(tx_{\rm B}+(2-x_{\rm B})\mathcal{Q}^2\right)^2+\mathcal{Q}^2\left(t+3\mathcal{Q}^2\right)\varepsilon^2}{4x_{\rm B}^2} - \frac{M^2(1-x_{\rm B})\left(t+\mathcal{Q}^2\right)}{\sqrt{1+\varepsilon^2}}\right.$$
$$\left. - \frac{\left(tx_{\rm B}+(2-x_{\rm B})\mathcal{Q}^2\right)\left(tx_{\rm B}(1-2x_{\rm B})+(2-3x_{\rm B})\mathcal{Q}^2\right)}{4x_{\rm B}^2\sqrt{1+\varepsilon^2}}\right\} \tag{A.24}$$

$$R^{(7)}_{++} = \not{q}\frac{tx_{\rm B}}{4\sqrt{1+\varepsilon^2}} - i\sigma_{q\Delta}\frac{\mathcal{Q}\varepsilon}{4\sqrt{1+\varepsilon^2}} + \not{q}\gamma^5\frac{t}{4}\left\{\frac{1-x_{\rm B}}{\sqrt{1+\varepsilon^2}}-1\right\}$$
$$+ \gamma^5\frac{M\mathcal{Q}^2}{4}\left\{\frac{1-x_{\rm B}}{\sqrt{1+\varepsilon^2}}-1\right\} \tag{A.25}$$

$$R^{(8)}_{++} = \not{q}\frac{x_{\rm B}\mathcal{Q}\left(t+\mathcal{Q}^2\right)^2\varepsilon}{4\left(tx_{\rm B}+(2-x_{\rm B})\mathcal{Q}^2\right)\sqrt{1+\varepsilon^2}} + i\sigma_{q\Delta}\frac{(1-x_{\rm B})\mathcal{Q}^2\left(tx_{\rm B}+\mathcal{Q}^2\right)}{\left(tx_{\rm B}+(2-x_{\rm B})\mathcal{Q}^2\right)\sqrt{1+\varepsilon^2}}$$

$$+\gamma^5\frac{\mathcal{Q}^2}{8x_{\rm B}}\left\{tx_{\rm B}+(2-x_{\rm B})\,\mathcal{Q}^2-\frac{t(1-2x_{\rm B})x_{\rm B}+(2-3x_{\rm B})\,\mathcal{Q}^2}{\sqrt{1+\varepsilon^2}}\right\}$$
$$+\not{q}\gamma^5\frac{\mathcal{Q}\left(t+\mathcal{Q}^2\right)\varepsilon}{4\sqrt{1+\varepsilon^2}} \tag{A.26}$$

$$\begin{aligned}R^{(9)}_{++}=&\not{q}\mathcal{Q}\varepsilon\frac{t^2x_{\rm B}+4t(1-x_{\rm B})\,\mathcal{Q}^2-x_{\rm B}\,\mathcal{Q}^4}{4\left(tx_{\rm B}+(2-x_{\rm B})\,\mathcal{Q}^2\right)\sqrt{1+\varepsilon^2}}\\&-i\sigma_{q\Delta}\mathcal{Q}^2\left\{\frac{(1-x_{\rm B})\left(tx_{\rm B}+\mathcal{Q}^2\right)}{\left(tx_{\rm B}+(2-x_{\rm B})\,\mathcal{Q}^2\right)\sqrt{1+\varepsilon^2}}+\frac{\varepsilon^2}{2x_{\rm B}\sqrt{1+\varepsilon^2}}\right\}\\&-\not{q}\gamma^5\left\{\frac{M\left(t-\mathcal{Q}^2\right)}{2}-\frac{M(1-x_{\rm B})\left(t+\mathcal{Q}^2\right)}{2\sqrt{1+\varepsilon^2}}\right\}\\&-\gamma^5\mathcal{Q}^2\left\{\frac{(1-x_{\rm B})\left(4(1-x_{\rm B})\left(tx_{\rm B}+\mathcal{Q}^2\right)+\left(t+\mathcal{Q}^2\right)\varepsilon^2\right)}{8x_{\rm B}^2\sqrt{1+\varepsilon^2}}\right.\\&\qquad\left.+\frac{(4(1-x_{\rm B})\left(tx_{\rm B}+\mathcal{Q}^2\right)+\left(t+3\mathcal{Q}^2\right)\varepsilon^2}{8x_{\rm B}^2}\right\}\end{aligned} \tag{A.27}$$

$$\begin{aligned}R^{(10)}_{++}=&\not{q}\frac{x_{\rm B}\mathcal{Q}\left(t+\mathcal{Q}^2\right)\varepsilon}{\left(tx_{\rm B}+(2-x_{\rm B})\,\mathcal{Q}^2\right)\sqrt{1+\varepsilon^2}}\\&+\frac{\gamma^5}{2}\left\{t+\frac{(2-x_{\rm B})\,\mathcal{Q}^2}{x_{\rm B}}-\frac{t(1-2x_{\rm B})x_{\rm B}+\mathcal{Q}^2\left(2-3x_{\rm B}+\varepsilon^2\right)}{x_{\rm B}\sqrt{1+\varepsilon^2}}\right\}\\&+i\sigma_{q\Delta}\left\{\frac{t(1-2x_{\rm B})x_{\rm B}+(2-3x_{\rm B})\,\mathcal{Q}^2}{\left(tx_{\rm B}+(2-x_{\rm B})\,\mathcal{Q}^2\right)\sqrt{1+\varepsilon^2}}-1\right\}+\not{q}\gamma^5\frac{\mathcal{Q}\varepsilon}{\sqrt{1+\varepsilon^2}}\end{aligned} \tag{A.28}$$

$$\begin{aligned}R^{(11)}_{++}=&\not{q}\,\frac{tx_{\rm B}}{\sqrt{1+\varepsilon^2}}-i\sigma_{q\Delta}\frac{\mathcal{Q}\varepsilon}{\sqrt{1+\varepsilon^2}}+\not{q}\,\gamma^5\frac{tx_{\rm B}+\mathcal{Q}^2\left(1+\sqrt{1+\varepsilon^2}\right)}{\sqrt{1+\varepsilon^2}}\\&+\gamma^5\mathcal{Q}\varepsilon\frac{t\left(1-2x_{\rm B}-\sqrt{1+\varepsilon^2}\right)-\mathcal{Q}^2\left(x_{\rm B}+2\sqrt{1+\varepsilon^2}\right)}{2x_{\rm B}\sqrt{1+\varepsilon^2}}\end{aligned} \tag{A.29}$$

$$\begin{aligned}R^{(12)}_{++}=&\not{q}\,\frac{x_{\rm B}\mathcal{Q}\left(t+\mathcal{Q}^2\right)^2\varepsilon}{4\left(tx_{\rm B}+(2-x_{\rm B})\,\mathcal{Q}^2\right)\sqrt{1+\varepsilon^2}}+\not{q}\,\gamma^5\frac{\mathcal{Q}\left(t+\mathcal{Q}^2\right)\varepsilon}{4\sqrt{1+\varepsilon^2}}\\&-\gamma^5\frac{\mathcal{Q}^2}{8}\left\{t+\mathcal{Q}^2+\frac{\mathcal{Q}^2\left(4-3x_{\rm B}+\varepsilon^2\right)+t\left((3-2x_{\rm B})x_{\rm B}+\varepsilon^2\right)}{\sqrt{1+\varepsilon^2}}\right\}\\&+i\sigma_{q\Delta}\frac{(1-x_{\rm B})\,\mathcal{Q}^2\left(tx_{\rm B}+\mathcal{Q}^2\right)}{\left(tx_{\rm B}+(2-x_{\rm B})\,\mathcal{Q}^2\right)\sqrt{1+\varepsilon^2}}.\end{aligned} \tag{A.30}$$

- (0,1) helicity amplitude:

$$R_{0+}^{(1)} = \frac{\sqrt{2}(\not{q}\mathcal{Q}\varepsilon - i\sigma_{q\Delta}x_{\rm B})\widetilde{K}\mathcal{Q}}{(tx_{\rm B}+(2-x_{\rm B})\mathcal{Q}^2)\sqrt{1+\varepsilon^2}} \tag{A.31}$$

$$R_{0+}^{(2)} = -\frac{(\not{q}\mathcal{Q}\varepsilon - i\sigma_{q\Delta}x_{\rm B})\widetilde{K}\mathcal{Q}\left(tx_{\rm B}^2 - \mathcal{Q}^2\left((2-x_{\rm B})x_{\rm B}+2\varepsilon^2\right)\right)}{\sqrt{2}x_{\rm B}^2\left(tx_{\rm B}+(2-x_{\rm B})\mathcal{Q}^2\right)\sqrt{1+\varepsilon^2}} \tag{A.32}$$

$$R_{0+}^{(3)} = -\frac{\sqrt{2}(\not{q}\mathcal{Q}\varepsilon - i\sigma_{q\Delta}x_{\rm B})\widetilde{K}(1-x_{\rm B})\mathcal{Q}^3}{x_{\rm B}\left(tx_{\rm B}+(2-x_{\rm B})\mathcal{Q}^2\right)\sqrt{1+\varepsilon^2}} \tag{A.33}$$

$$\begin{aligned}
R_{0+}^{(4)} = {} & (\not{q}\, tx_{\rm B} - i\sigma_{q\Delta}\mathcal{Q}\varepsilon)\frac{\mathcal{Q}^2\left(2-x_{\rm B}+\varepsilon^2\right)+t\left((3-2x_{\rm B})x_{\rm B}+\varepsilon^2\right)}{\sqrt{2}\widetilde{K}x_{\rm B}\mathcal{Q}\sqrt{1+\varepsilon^2}} \\
& + \not{q}\,\gamma^5\frac{\sqrt{2}\widetilde{K}\left(tx_{\rm B}+(2-x_{\rm B})\mathcal{Q}^2\right)}{x_{\rm B}\mathcal{Q}\sqrt{1+\varepsilon^2}} \\
& + (\not{q}\,\gamma^5 t + \gamma^5 M\mathcal{Q}^2) \\
& \quad \times \frac{\varepsilon\left(tx_{\rm B}+(2-x_{\rm B})\mathcal{Q}^2\right)\left(t\left(4(1-x_{\rm B})x_{\rm B}+\varepsilon^2\right)+\mathcal{Q}^2\left(4-2x_{\rm B}+3\varepsilon^2\right)\right)}{4\sqrt{2}M\widetilde{K}x_{\rm B}^2\mathcal{Q}^2\sqrt{1+\varepsilon^2}}
\end{aligned} \tag{A.34}$$

$$\begin{aligned}
R_{0+}^{(5)} = {} & (\not{q}\, tx_{\rm B} - i\sigma_{q\Delta}\mathcal{Q}\varepsilon)\frac{t(1-2x_{\rm B})-\mathcal{Q}^2}{4\sqrt{2}\widetilde{K}\mathcal{Q}\sqrt{1+\varepsilon^2}} - \not{q}\,\gamma^5\frac{\widetilde{K}\mathcal{Q}}{\sqrt{2}\sqrt{1+\varepsilon^2}} \\
& - (\not{q}\,\gamma^5 t + \gamma^5 M\mathcal{Q}^2)\frac{\mathcal{Q}^2\left(2-x_{\rm B}+\varepsilon^2\right)+t\left((3-2x_{\rm B})x_{\rm B}+\varepsilon^2\right)}{4\sqrt{2}\widetilde{K}\mathcal{Q}\sqrt{1+\varepsilon^2}}
\end{aligned} \tag{A.35}$$

$$\begin{aligned}
R_{0+}^{(6)} = {} & -\not{q}\,\frac{\sqrt{2}\widetilde{K}\mathcal{Q}^2\left((2-x_{\rm B})\mathcal{Q}^2+t\left(x_{\rm B}(5-2x_{\rm B})+2\varepsilon^2\right)\right)}{(tx_{\rm B}+(2-x_{\rm B})\mathcal{Q}^2)\,\varepsilon\sqrt{1+\varepsilon^2}} \\
& - (\not{q}\, tx_{\rm B} - i\sigma_{q\Delta}\mathcal{Q}\varepsilon)\left\{\frac{\sqrt{2}t(1-x_{\rm B})\left(2(2-x_{\rm B})\left(tx_{\rm B}+\mathcal{Q}^2\right)+\left(t+\mathcal{Q}^2\right)\varepsilon^2\right)}{\widetilde{K}\varepsilon\left(tx_{\rm B}+(2-x_{\rm B})\mathcal{Q}^2\right)\sqrt{1+\varepsilon^2}}\right. \\
& \qquad \left. + \frac{2(1-x_{\rm B})\left(tx_{\rm B}+\mathcal{Q}^2\right)+\left(t+\mathcal{Q}^2\right)\varepsilon^2}{\sqrt{2}\widetilde{K}x_{\rm B}\varepsilon\sqrt{1+\varepsilon^2}}\right\} \\
& - \not{q}\,\gamma^5\frac{\sqrt{2}\widetilde{K}\left(t^2x_{\rm B}^2+\mathcal{Q}^4\left(2-x_{\rm B}+\varepsilon^2\right)+t\mathcal{Q}^2\left((3-x_{\rm B})x_{\rm B}+\varepsilon^2\right)\right)}{x_{\rm B}\mathcal{Q}^2\varepsilon\sqrt{1+\varepsilon^2}} \\
& + (\not{q}\,\gamma^5 t + \gamma^5 M\mathcal{Q}^2)\left\{\frac{\widetilde{K}\mathcal{Q}\varepsilon^2}{\sqrt{2}Mx_{\rm B}^2\sqrt{1+\varepsilon^2}} - (tx_{\rm B}+(2-x_{\rm B})\mathcal{Q})\right. \\
& \qquad \times\left[\frac{(1-x_{\rm B})\left(tx_{\rm B}+\mathcal{Q}^2\right)^2}{\sqrt{2}M\widetilde{K}x_{\rm B}^2\mathcal{Q}^3\sqrt{1+\varepsilon^2}}\right. \\
& \qquad\qquad \left.\left. + \frac{\left(t^2x_{\rm B}+t(1+2x_{\rm B})\mathcal{Q}^2+(3-x_{\rm B})\mathcal{Q}^4\right)\varepsilon^2}{4\sqrt{2}M\widetilde{K}x_{\rm B}^2\mathcal{Q}^3\sqrt{1+\varepsilon^2}}\right]\right\}
\end{aligned} \tag{A.36}$$

$$
\begin{aligned}
R_{0+}^{(7)} =& (\not{q}\, t x_{\rm B} - i\sigma_{q\Delta}\mathcal{Q}\varepsilon)\frac{t(1-2x_{\rm B})-\mathcal{Q}^2}{4\sqrt{2}\widetilde{K}\mathcal{Q}\sqrt{1+\varepsilon^2}} \\
&- \left(\not{q}\,\gamma^5 t + \gamma^5 M\mathcal{Q}^2\right)\frac{\mathcal{Q}^2\left(2-x_{\rm B}+\varepsilon^2\right)+t\left((3-2x_{\rm B})x_{\rm B}+\varepsilon^2\right)}{4\sqrt{2}\widetilde{K}\mathcal{Q}\sqrt{1+\varepsilon^2}}
\end{aligned}
\tag{A.37}
$$

$$
\begin{aligned}
R_{0+}^{(8)} =& -\not{q}\,\frac{\widetilde{K}x_{\rm B}\mathcal{Q}^2\left(t(1-2x_{\rm B})-\mathcal{Q}^2\right)}{\sqrt{2}\left(tx_{\rm B}+(2-x_{\rm B})\mathcal{Q}^2\right)\varepsilon\sqrt{1+\varepsilon^2}} + \not{q}\,\gamma^5\frac{\widetilde{K}\left(tx_{\rm B}+\mathcal{Q}^2\right)}{\sqrt{2}\varepsilon\sqrt{1+\varepsilon^2}} \\
&- (\not{q}\, t x_{\rm B} - i\sigma_{q\Delta}\mathcal{Q}\varepsilon)\frac{(1-x_{\rm B})\left(tx_{\rm B}+\mathcal{Q}^2\right)\left(t(1-2x_{\rm B})-\mathcal{Q}^2\right)}{\sqrt{2}\widetilde{K}\varepsilon\left(tx_{\rm B}+(2-x_{\rm B})\mathcal{Q}^2\right)\sqrt{1+\varepsilon^2}} \\
&+ (\not{q}\,\gamma^5 t + \gamma^5 M\mathcal{Q}^2)\frac{4(1-x_{\rm B})\left(tx_{\rm B}+\mathcal{Q}^2\right)^2+\left(t+\mathcal{Q}^2\right)\left(tx_{\rm B}+(2-x_{\rm B})\mathcal{Q}^2\right)\varepsilon^2}{8\sqrt{2}M\widetilde{K}x_{\rm B}\mathcal{Q}\sqrt{1+\varepsilon^2}}
\end{aligned}
\tag{A.38}
$$

$$
\begin{aligned}
R_{0+}^{(9)} =& \not{q}\,\widetilde{K}\mathcal{Q}^2\frac{tx_{\rm B}(1-2x_{\rm B})-\mathcal{Q}^2\left(x_{\rm B}-2\left(1+\varepsilon^2\right)\right)}{\sqrt{2}\left(tx_{\rm B}+(2-x_{\rm B})\mathcal{Q}^2\right)\varepsilon\sqrt{1+\varepsilon^2}} \\
&+ (\not{q}\, t x_{\rm B} - i\sigma_{q\Delta}\mathcal{Q}\varepsilon)\left\{\frac{2(1-x_{\rm B})\left(tx_{\rm B}+\mathcal{Q}^2\right)+\left(t+\mathcal{Q}^2\right)\varepsilon^2}{2\sqrt{2}\widetilde{K}x_{\rm B}\varepsilon\sqrt{1+\varepsilon^2}}\right. \\
&\qquad\left. - \frac{\left(tx_{\rm B}+\mathcal{Q}^2\right)\left(2t(1-x_{\rm B})x_{\rm B}+\left(t+\mathcal{Q}^2\right)\varepsilon^2\right)}{\sqrt{2}\widetilde{K}\varepsilon\left(tx_{\rm B}+(2-x_{\rm B})\mathcal{Q}^2\right)\sqrt{1+\varepsilon^2}}\right\} \\
&+ \not{q}\,\gamma^5\frac{\widetilde{K}\left(\mathcal{Q}^2\left(2-x_{\rm B}+\varepsilon^2\right)+t\left((3-2x_{\rm B})x_{\rm B}+\varepsilon^2\right)\right)}{\sqrt{2}x_{\rm B}\varepsilon\sqrt{1+\varepsilon^2}} \\
&+ (\not{q}\,\gamma^5 t + \gamma^5 M\mathcal{Q}^2)\frac{4(1-x_{\rm B})\left(tx_{\rm B}+\mathcal{Q}^2\right)+\left(t+\mathcal{Q}^2\right)\varepsilon^2}{8\sqrt{2}M\widetilde{K}x_{\rm B}^2\mathcal{Q}\sqrt{1+\varepsilon^2}}\left\{\mathcal{Q}^2\left(2-x_{\rm B}+\varepsilon^2\right)\right. \\
&\qquad\left. + t\left(x_{\rm B}(3-2x_{\rm B})+\varepsilon^2\right)\right\}
\end{aligned}
\tag{A.39}
$$

$$
\begin{aligned}
R_{0+}^{(10)} =& \not{q}\,\frac{2\sqrt{2}\widetilde{K}x_{\rm B}\left(tx_{\rm B}+\mathcal{Q}^2\right)}{\left(tx_{\rm B}+(2-x_{\rm B})\mathcal{Q}^2\right)\varepsilon\sqrt{1+\varepsilon^2}} + \not{q}\,\gamma^5\frac{2\sqrt{2}\widetilde{K}\left(tx_{\rm B}+\mathcal{Q}^2\right)}{\mathcal{Q}^2\varepsilon\sqrt{1+\varepsilon^2}} \\
&+ (\not{q}\, t x_{\rm B} - i\sigma_{q\Delta}\mathcal{Q}\varepsilon) \\
&\qquad\times\left\{\frac{2\sqrt{2}(1-x_{\rm B})\left(tx_{\rm B}+\mathcal{Q}^2\right)^2}{\widetilde{K}\mathcal{Q}^2\varepsilon\left(tx_{\rm B}+(2-x_{\rm B})\mathcal{Q}^2\right)\sqrt{1+\varepsilon^2}}+\frac{\left(t+\mathcal{Q}^2\right)\varepsilon}{\sqrt{2}\widetilde{K}\mathcal{Q}^2\sqrt{1+\varepsilon^2}}\right\} \\
&+ (\not{q}\,\gamma^5 t + \gamma^5 M\mathcal{Q}^2) \\
&\quad\times\frac{4(1-x_{\rm B})\left(tx_{\rm B}+\mathcal{Q}^2\right)^2+\left(t^2x_{\rm B}+t(1+2x_{\rm B})\mathcal{Q}^2+(3-x_{\rm B})\mathcal{Q}^4\right)\varepsilon^2}{2\sqrt{2}M\widetilde{K}x_{\rm B}\mathcal{Q}^3\sqrt{1+\varepsilon^2}}
\end{aligned}
\tag{A.40}
$$

$$R_{0+}^{(11)} = (\not{q}\, t x_{\rm B} - i\sigma_{q\Delta}\mathcal{Q}\varepsilon)\frac{t(1-2x_{\rm B})-\mathcal{Q}^2}{\sqrt{2}\widetilde{K}\mathcal{Q}\sqrt{1+\varepsilon^2}} - \not{q}\,\gamma^5\frac{2\sqrt{2}\widetilde{K}\left(t+\mathcal{Q}^2\right)}{\mathcal{Q}\sqrt{1+\varepsilon^2}}$$
$$-(\not{q}\,\gamma^5 t+\gamma^5 M\mathcal{Q}^2)\varepsilon\left\{\frac{2\mathcal{Q}^2\left(2t+\mathcal{Q}^2\right)+\left(t+\mathcal{Q}^2\right)\left(t+2\mathcal{Q}^2\right)\varepsilon^2}{2\sqrt{2}M\widetilde{K}x_{\rm B}\mathcal{Q}^2\sqrt{1+\varepsilon^2}}\right.$$
$$\left.-\frac{t x_{\rm B}\left(2t+\mathcal{Q}^2\right)}{\sqrt{2}M\widetilde{K}\mathcal{Q}^2\sqrt{1+\varepsilon^2}}+\frac{4t^2-t\mathcal{Q}^2-\mathcal{Q}^4}{2\sqrt{2}M\widetilde{K}\mathcal{Q}^2\sqrt{1+\varepsilon^2}}\right\} \tag{A.41}$$

$$R_{0+}^{(12)} = -\not{q}\,\frac{\widetilde{K}\mathcal{Q}^2\left(t(1-2x_{\rm B})x_{\rm B}+\mathcal{Q}^2\left(2-x_{\rm B}+2\varepsilon^2\right)\right)}{\sqrt{2}\left(t x_{\rm B}+(2-x_{\rm B})\mathcal{Q}^2\right)\varepsilon\sqrt{1+\varepsilon^2}} - (\not{q}\, t x_{\rm B} - i\sigma_{q\Delta}\mathcal{Q}\varepsilon)$$
$$\times\frac{(1-x_{\rm B})\left(t x_{\rm B}+\mathcal{Q}^2\right)\left(t(1-2x_{\rm B})x_{\rm B}+\mathcal{Q}^2\left(2-x_{\rm B}+2\varepsilon^2\right)\right)}{\sqrt{2}\widetilde{K}x_{\rm B}\varepsilon\left(t x_{\rm B}+(2-x_{\rm B})\mathcal{Q}^2\right)\sqrt{1+\varepsilon^2}}$$
$$-\not{q}\,\gamma^5\widetilde{K}\frac{t(1-x_{\rm B})x_{\rm B}-\mathcal{Q}^2\left(x_{\rm B}-2\left(1+\varepsilon^2\right)\right)}{\sqrt{2}x_{\rm B}\varepsilon\sqrt{1+\varepsilon^2}}$$
$$-(\not{q}\,\gamma^5 t+\gamma^5 M\mathcal{Q}^2)\left\{\frac{t^2x_{\rm B}^2}{2\sqrt{2}M\widetilde{K}\mathcal{Q}\sqrt{1+\varepsilon^2}}+\frac{\mathcal{Q}\sqrt{1+\varepsilon^2}\left(t\varepsilon^2+\mathcal{Q}^2\left(4+\varepsilon^2\right)\right)}{4\sqrt{2}M\widetilde{K}x_{\rm B}^2}\right.$$
$$+\frac{t^2\left(4-\varepsilon^2\right)+\mathcal{Q}^4\left(4+\varepsilon^2\right)-4t\mathcal{Q}^2\left(5+2\varepsilon^2\right)}{8\sqrt{2}M\widetilde{K}\mathcal{Q}\sqrt{1+\varepsilon^2}}$$
$$\left.+\frac{\left(t-\mathcal{Q}^2\right)\left(t\left(\varepsilon^2-8x_{\rm B}^2\right)+3\mathcal{Q}^2\left(4+3\varepsilon^2\right)\right)}{8\sqrt{2}M\widetilde{K}x_{\rm B}\mathcal{Q}\sqrt{1+\varepsilon^2}}\right\} \tag{A.42}$$

- (-1,1) helicity amplitude:

$$R_{-+}^{(1)} = (\not{\varepsilon}\,\mathcal{Q} - i\sigma_{q\Delta}x_{\rm B})\frac{t-2tx_{\rm B}-\mathcal{Q}^2+\left(t+\mathcal{Q}^2\right)\sqrt{1+\varepsilon^2}}{2(t x_{\rm B}+(2-x_{\rm B})\mathcal{Q}^2)\sqrt{1+\varepsilon^2}} \tag{A.43}$$

$$R_{-+}^{(2)} = \frac{\not{q}\,\mathcal{Q}\varepsilon - i\sigma_{q\Delta}x_{\rm B}}{2x_{\rm B}^2}\left\{\frac{(1-x_{\rm B})\mathcal{Q}^2\left(t+\mathcal{Q}^2\right)\varepsilon^2}{\left(t x_{\rm B}+(2-x_{\rm B})\mathcal{Q}^2\right)\sqrt{1+\varepsilon^2}}\right.$$
$$\left.-\frac{(t x_{\rm B}+(2-x_{\rm B})\mathcal{Q}^2)(1+\sqrt{1+\varepsilon^2})}{2\sqrt{1+\varepsilon^2}}+\frac{\left(t x_{\rm B}+\mathcal{Q}^2\right)\left(t x_{\rm B}^2+(2-x_{\rm B})^2\mathcal{Q}^2\right)}{\left(t x_{\rm B}+(2-x_{\rm B})\mathcal{Q}^2\right)\sqrt{1+\varepsilon^2}}\right\} \tag{A.44}$$

$$R_{-+}^{(3)} = \frac{(\not{\varepsilon}\,\mathcal{Q} - i\sigma_{q\Delta}x_{\rm B})\mathcal{Q}^2}{2x_{\rm B}}\left\{\frac{\mathcal{Q}^2\left(2-x_{\rm B}+\varepsilon^2\right)+t\left((3-2x_{\rm B})x_{\rm B}+\varepsilon^2\right)}{\left(t x_{\rm B}+(2-x_{\rm B})\mathcal{Q}^2\right)\sqrt{1+\varepsilon^2}}-1\right\} \tag{A.45}$$

$$R_{-+}^{(4)} = i\sigma_{q\Delta}\frac{2M(1-x_{\rm B})}{\sqrt{1+\varepsilon^2}} - \not{q}\,\gamma^5\frac{\left(t x_{\rm B}+(2-x_{\rm B})\mathcal{Q}^2\right)\left(1-\sqrt{1+\varepsilon^2}\right)}{2x_{\rm B}\sqrt{1+\varepsilon^2}}$$

$$- \gamma^5 \frac{M\left(t x_{\rm B} + (2-x_{\rm B})\mathcal{Q}^2\right)\left(1-2x_{\rm B}+\sqrt{1+\varepsilon^2}\right)}{2x_{\rm B}\sqrt{1+\varepsilon^2}} - \not{q}\,\frac{t(1-x_{\rm B})}{\sqrt{1+\varepsilon^2}} \tag{A.46}$$

$$\begin{aligned} R^{(5)}_{-+} =& \not{q}\,\frac{t x_{\rm B}}{4\sqrt{1+\varepsilon^2}} - i\sigma_{q\Delta}\frac{\mathcal{Q}\varepsilon}{4\sqrt{1+\varepsilon^2}} + \not{q}\,\gamma^5\frac{t x_{\rm B} + \mathcal{Q}^2\left(1-\sqrt{1+\varepsilon^2}\right)}{4\sqrt{1+\varepsilon^2}} \\ &+ \gamma^5\frac{M\mathcal{Q}^2\left(1-x_{\rm B}+\sqrt{1+\varepsilon^2}\right)}{4\sqrt{1+\varepsilon^2}} \end{aligned} \tag{A.47}$$

$$\begin{aligned} R^{(6)}_{-+} =& -\not{q}\,M x_{\rm B}\frac{t^2(2-3x_{\rm B})+(2-x_{\rm B})\mathcal{Q}^4}{(t x_{\rm B}+(2-x_{\rm B})\mathcal{Q}^2)\sqrt{1+\varepsilon^2}} \\ &- \frac{i\sigma_{q\Delta}}{\sqrt{1+\varepsilon^2}}\left\{4M^2 x_{\rm B} + \frac{2(2-x_{\rm B})(1-x_{\rm B})\mathcal{Q}^2\left(t x_{\rm B}+\mathcal{Q}^2\right)}{x_{\rm B}\left(t x_{\rm B}+(2-x_{\rm B})\mathcal{Q}^2\right)}\right\} \\ &- \not{q}\,\gamma^5 M\left\{\frac{(1-x_{\rm B})\left(t+\mathcal{Q}^2\right)}{\sqrt{1+\varepsilon^2}} - \left(t-\mathcal{Q}^2\right)\right\} + \gamma^5\left\{\frac{\left(t x_{\rm B}+(2-x_{\rm B})\mathcal{Q}^2\right)^2}{4x_{\rm B}^2}\right. \\ &\quad + M^2\left(t+3\mathcal{Q}^2\right) + \frac{M^2(1-x_{\rm B})\left(t+\mathcal{Q}^2\right)}{\sqrt{1+\varepsilon^2}} \\ &\quad \left. + \frac{\left(t x_{\rm B}+(2-x_{\rm B})\mathcal{Q}^2\right)\left(t x_{\rm B}(1-2x_{\rm B})+(2-3x_{\rm B})\mathcal{Q}^2\right)}{4x_{\rm B}^2\sqrt{1+\varepsilon^2}}\right\} \end{aligned} \tag{A.48}$$

$$R^{(7)}_{-+} = \frac{\not{q}\,t x_{\rm B} - i\sigma_{q\Delta}\mathcal{Q}\varepsilon}{4\sqrt{1+\varepsilon^2}} + \left(\not{q}\,\gamma^5 t + \gamma^5 M\mathcal{Q}^2\right)\frac{1-x_{\rm B}+\sqrt{1+\varepsilon^2}}{4\sqrt{1+\varepsilon^2}} \tag{A.49}$$

$$\begin{aligned} R^{(8)}_{-+} =& \not{q}\,\frac{x_{\rm B}\mathcal{Q}\left(t+\mathcal{Q}^2\right)^2\varepsilon}{4\left(t x_{\rm B}+(2-x_{\rm B})\mathcal{Q}^2\right)\sqrt{1+\varepsilon^2}} + i\sigma_{q\Delta}\frac{(1-x_{\rm B})\mathcal{Q}^2\left(t x_{\rm B}+\mathcal{Q}^2\right)}{\left(t x_{\rm B}+(2-x_{\rm B})\mathcal{Q}^2\right)\sqrt{1+\varepsilon^2}} \\ &- \gamma^5\frac{\mathcal{Q}^2}{8x_{\rm B}}\left\{t x_{\rm B}+(2-x_{\rm B})\mathcal{Q}^2 + \frac{t x_{\rm B}(1-2x_{\rm B})+(2-3x_{\rm B})\mathcal{Q}^2}{\sqrt{1+\varepsilon^2}}\right\} \\ &+ \not{q}\,\gamma^5\frac{\mathcal{Q}\left(t+\mathcal{Q}^2\right)\varepsilon}{4\sqrt{1+\varepsilon^2}} \end{aligned} \tag{A.50}$$

$$\begin{aligned} R^{(9)}_{-+} =& \not{q}\,\frac{\varepsilon\mathcal{Q}\left(t^2 x_{\rm B}+4t(1-x_{\rm B})\mathcal{Q}^2 - x_{\rm B}\mathcal{Q}^4\right)}{4\left(t x_{\rm B}+(2-x_{\rm B})\mathcal{Q}^2\right)\sqrt{1+\varepsilon^2}} \\ &- i\sigma_{q\Delta}\mathcal{Q}^2\frac{2(1-x_{\rm B})x_{\rm B}\left(t x_{\rm B}+\mathcal{Q}^2\right)+\left(t x_{\rm B}+(2-x_{\rm B})\mathcal{Q}^2\right)\varepsilon^2}{2x_{\rm B}\left(t x_{\rm B}+(2-x_{\rm B})\mathcal{Q}^2\right)\sqrt{1+\varepsilon^2}} \\ &+ \not{q}\,\gamma^5\frac{M}{2}\left\{t-\mathcal{Q}^2+\frac{(1-x_{\rm B})(t+\mathcal{Q}^2)}{\sqrt{1+\varepsilon^2}}\right\} \end{aligned}$$

$$
\begin{aligned}
&- \gamma^5 \frac{\mathcal{Q}^2}{8x_{\rm B}^2} \Bigg\{ \frac{(1-x_{\rm B})\left(4(1-x_{\rm B})\left(tx_{\rm B}+\mathcal{Q}^2\right)+\left(t+\mathcal{Q}^2\right)\varepsilon^2\right)}{\sqrt{1+\varepsilon^2}} \\
&\qquad - \left(4(1-x_{\rm B})\left(tx_{\rm B}+\mathcal{Q}^2\right)+\left(t+3\mathcal{Q}^2\right)\varepsilon^2\right) \Bigg\}
\end{aligned} \tag{A.51}
$$

$$
\begin{aligned}
R_{-+}^{(10)} =& \not{q}\, \frac{x_{\rm B}\mathcal{Q}\left(t+\mathcal{Q}^2\right)\varepsilon}{\left(tx_{\rm B}+(2-x_{\rm B})\mathcal{Q}^2\right)\sqrt{1+\varepsilon^2}} + i\sigma_{q\Delta}\left\{1+\frac{t(1-2x_{\rm B})x_{\rm B}+(2-3x_{\rm B})\mathcal{Q}^2}{\left(tx_{\rm B}+(2-x_{\rm B})\mathcal{Q}^2\right)\sqrt{1+\varepsilon^2}}\right\} \\
&+ \not{q}\,\gamma^5 \frac{\mathcal{Q}\varepsilon}{\sqrt{1+\varepsilon^2}} - \frac{\gamma^5}{2}\left\{t+\frac{(2-x_{\rm B})\mathcal{Q}^2}{x_{\rm B}}+\frac{t(1-2x_{\rm B})x_{\rm B}+\mathcal{Q}^2\left(2-3x_{\rm B}+\varepsilon^2\right)}{x_{\rm B}\sqrt{1+\varepsilon^2}}\right\}
\end{aligned} \tag{A.52}
$$

$$
\begin{aligned}
R_{-+}^{(11)} =& \not{q}\, \frac{tx_{\rm B}}{\sqrt{1+\varepsilon^2}} - i\sigma_{q\Delta}\frac{\mathcal{Q}\varepsilon}{\sqrt{1+\varepsilon^2}} + \not{q}\,\gamma^5 \frac{tx_{\rm B}+\mathcal{Q}^2\left(1-\sqrt{1+\varepsilon^2}\right)}{\sqrt{1+\varepsilon^2}} \\
&+ \gamma^5 M\left\{t+2\mathcal{Q}^2+\frac{t-2tx_{\rm B}-x_{\rm B}\mathcal{Q}^2}{\sqrt{1+\varepsilon^2}}\right\}
\end{aligned} \tag{A.53}
$$

$$
\begin{aligned}
R_{-+}^{(12)} =& \not{q}\, \frac{x_{\rm B}\mathcal{Q}\left(t+\mathcal{Q}^2\right)^2\varepsilon}{4\left(tx_{\rm B}+(2-x_{\rm B})\mathcal{Q}^2\right)\sqrt{1+\varepsilon^2}} + i\sigma_{q\Delta}\frac{(1-x_{\rm B})\mathcal{Q}^2\left(tx_{\rm B}+\mathcal{Q}^2\right)}{\left(tx_{\rm B}+(2-x_{\rm B})\mathcal{Q}^2\right)\sqrt{1+\varepsilon^2}} \\
&+ \gamma^5\frac{\mathcal{Q}^2}{8}\left\{t+\mathcal{Q}^2-\frac{\mathcal{Q}^2\left(4-3x_{\rm B}+\varepsilon^2\right)+t\left((3-2x_{\rm B})x_{\rm B}+\varepsilon^2\right)}{x_{\rm B}\sqrt{1+\varepsilon^2}}\right\} \\
&+ \not{q}\,\gamma^5\frac{\mathcal{Q}\left(t+\mathcal{Q}^2\right)\varepsilon}{4\sqrt{1+\varepsilon^2}}\,.
\end{aligned} \tag{A.54}
$$

A.4 Low Energy Expansion: CFFs and Tarrach fs

For the low energy expansion one adopts the momenta in the center-of-mass frame as defined in Ref. [39]:

$$
q_1 = (\sqrt{\omega'^2+M^2}+\omega'-\sqrt{\bar{q}^2+M^2},0,0,\bar{q}) \tag{A.55}
$$

$$
q_2 = (\omega',\omega'\sin\vartheta,0,\omega'\cos\vartheta) \tag{A.56}
$$

$$
\begin{aligned}
p_1 &= \left(\sqrt{\bar{q}^2+M^2},0,0,-\bar{q}\right), \\
p_2 &= (\sqrt{\omega'^2+M^2},-\omega'\sin\vartheta,0,-\omega'\cos\vartheta)\,.
\end{aligned} \tag{A.57}
$$

A.4.1 Low Energy Expansions as Functions of f_i

Here one quotes our results for the leading term in the low-energy expansion for the helicity CFFs in terms of Tarrach's structure functions (A.18). Only the leading Non-Born contributions are kept here, i.e., linear in ω', and neglect all subleading $O(\omega')$ effects.

- (+1,+1) helicity amplitude:

$$\begin{aligned}\mathcal{H}_{++} = \frac{\omega' M}{2\bar{q}}\Big\{ & 4\bar{q}^2(f_{10}+M\bar{q}f_3)+\omega_0\Big[\bar{q}^2\big(4f_{11}+f_5+f_7-4M(f_3-2f_6-f_9)\big) \\ & +8Mf_{10}\Big]-\bar{q}\Big[\omega_0\big(4f_{10}+\omega_0(4f_{11}+f_5+f_7+8Mf_6+4Mf_9)\big) \\ & -2(\bar{q}-\omega_0)(2M\bar{q}f_3-f_1)\Big]\cos\vartheta-2\bar{q}(\bar{q}-\omega_0)f_1\Big\}, \end{aligned} \tag{A.58}$$

$$\begin{aligned}\mathcal{E}_{++} = \frac{\omega' M}{\bar{q}}\Big\{ & \bar{q}\Big[(\bar{q}-\omega_0)f_1-M\bar{q}(4f_{11}+f_5+f_7+8Mf_6+4Mf_9 \\ & +2\bar{q}f_3-2\omega_0 f_3)\Big]-2\Big[\bar{q}(\bar{q}-\omega_0)+2M(\bar{q}+\omega_0)\Big]f_{10}+\bar{q}\Big[(\bar{q}-\omega_0)f_1 \\ & -2\bar{q}(M\bar{q}f_3+f_{10})+\omega_0\big(2f_{10}+M(4f_{11}+f_5+f_7+8Mf_6 \\ & +4Mf_9+2\bar{q}f_3)\big)\Big]\cos\vartheta\Big\}, \end{aligned} \tag{A.59}$$

$$\widetilde{\mathcal{H}}_{++} = \frac{\omega' M(\omega_0\cos\vartheta-\bar{q})}{2}\Big\{4f_{10}+\bar{q}\big(4f_{11}+f_5+f_7+8Mf_6+4Mf_9\big)\Big\}, \tag{A.60}$$

$$\widetilde{\mathcal{E}}_{++} = \frac{\omega' M^2(\omega_0-2M-\bar{q}\cos\vartheta)}{\bar{q}}\Big\{4f_{10}+\bar{q}\big(4f_{11}+f_5+f_7+8Mf_6+4Mf_9\big)\Big\}. \tag{A.61}$$

- (0,+1) helicity amplitude:

$$\mathcal{H}_{0+} = -\frac{\omega'\sqrt{-M\omega_0}}{2q}\Big\{\Big[q\big[4Mq^2f_{12}+\omega_0\big(4f_{10}+\omega_0(4f_{11}+f_5+f_7)\big)\big]\cos\theta$$

$$
\begin{aligned}
&- 2q^2\left[4(M-\omega_0)f_4+\omega_0(4f_{11}+f_5+f_7+4Mf_{12})\right]-4\left(q^2+\omega_0^2\right)f_{10}\Big]\cot\theta\\
&+\frac{q}{\sin\theta}\Big[q^2(4f_{11}-8f_4+f_5+f_7)+4\omega_0(f_{10}+M\omega_0 f_{12})\Big]\\
&+4q\sin\theta\Big[q^2f_4+M\big(f_1+4M^2f_2-2M\omega_0(f_2+2f_6+f_9)\big)\Big]\Big\}, \qquad \text{(A.62)}
\end{aligned}
$$

$$
\begin{aligned}
\mathcal{E}_{0+} = -\frac{\omega' M\sqrt{-M\omega_0}}{q}\Big\{&\Big[2q^2\left(4f_{11}+f_5+f_7\right)-8M\left(f_{10}+2Mf_4-q^2f_{12}\right)\\
&+8\omega_0(f_{10}+3Mf_4)-8\omega_0^2f_4-q\omega_0\cos\theta\left(f_5+f_7\right)\Big]\cot\theta\\
&-\frac{q}{\sin\theta}\Big[8f_{10}-2M\big(4f_{11}-8f_4+f_5+f_7+4Mf_{12}\big)\\
&+\omega_0\big(8f_{11}-8f_4+f_5+f_7+8Mf_{12}\big)\Big]\\
&+2q\sin\theta\Big[2\omega_0\big(f_{11}-f_4+M(f_2+2f_6+f_9)\big)-f_1+2f_{10}+4Mf_4\\
&-4M^2f_2\Big]\Big\}, \qquad \text{(A.63)}
\end{aligned}
$$

$$
\begin{aligned}
\widetilde{\mathcal{H}}_{0+} = -\frac{\omega' M}{2\sqrt{-M\omega_0}}\Big\{&\frac{q^2}{\sin\theta}\Big[4f_{10}+(8M-6\omega_0)f_4+\omega_0(4f_{11}+f_5+f_7+4Mf_{12})\\
&-2\omega_0\cos2\theta f_4\Big]-\Big[q^3\big(4f_{11}-8f_4+f_5+f_7+4Mf_{12}\big)+8q\omega_0f_{10}\\
&-\omega_0\big(q^2(4f_{11}+f_5+f_7+4Mf_{12})+4\omega_0f_{10}\big)\cos\theta\Big]\\
&+q\omega_0^2\big(4f_{11}+f_5+f_7+4Mf_{12}\big)\cot\theta\Big\}, \qquad \text{(A.64)}
\end{aligned}
$$

$$
\begin{aligned}
\widetilde{\mathcal{E}}_{0+} = -\frac{\omega' M^2(q-\omega_0\cos\theta)}{\sin\theta\sqrt{-M\omega_0}}\Big\{&\Big[q^2\big(4f_{11}-4f_4+f_5+f_7+4Mf_{12}\big)+4\omega_0f_{10}\Big]\\
&\times\cos\theta-q\Big[4f_{10}+\big(8M-4\omega_0\big)f_4+\omega_0\big(4f_{11}+f_5+f_7+4Mf_{12}\big)\Big]\Big\}. \qquad \text{(A.65)}
\end{aligned}
$$

- $(-1,+1)$ helicity amplitude:

$$
\mathcal{H}_{-+} = \frac{\omega' M}{2\bar{q}}\Big\{4\left(\bar{q}^2+2M\omega_0\right)f_{10}+\bar{q}^2\Big[\omega_0(4f_{11}+f_5+f_7+8Mf_6+4Mf_9)
$$

$$
\begin{aligned}
&-4M(\bar{q}+\omega_0)f_3\Big]-2\bar{q}(\bar{q}+\omega_0)f_1-\bar{q}\cos\vartheta\Big[\bar{q}^2\big(4f_{11}+f_5+f_7\\
&-4M(f_3-2f_6-f_9)\big)+2M\omega_0(4f_{11}+f_5+f_7+8Mf_6+4Mf_9-2\bar{q}f_3)\\
&+4\omega_0 f_{10}-2(\bar{q}+\omega_0)f_1\Big]\Big\}, \qquad \text{(A.66)}
\end{aligned}
$$

$$
\begin{aligned}
\mathcal{E}_{-+}=\frac{\omega' M}{\bar{q}}\Big\{&2\big(2M(\bar{q}-\omega_0)-\bar{q}(\bar{q}+\omega_0)\big)f_{10}-\bar{q}\Big[M\bar{q}\big(4f_{11}+f_7+4M(2f_6+f_9)\\
&-(\bar{q}+\omega_0)f_1-f_5+2(\bar{q}+\omega_0)f_3\big)\Big]+\bar{q}\Big[M\omega_0(4f_{11}+f_5+f_7\\
&+8Mf_6+4Mf_9-2\bar{q}f_3)-2M\bar{q}^2f_3+(\bar{q}+\omega_0)(2f_{10}-f_1)\Big]\cos\vartheta\Big\}, \qquad \text{(A.67)}
\end{aligned}
$$

$$
\widetilde{\mathcal{H}}_{-+}=\frac{\omega' M}{2}\Big\{\bar{q}\big(4f_{11}+f_5+f_7+8Mf_6+4Mf_9\big)-4f_{10}\Big\}\big(\bar{q}-\omega_0\cos\vartheta\big), \qquad \text{(A.68)}
$$

$$
\widetilde{\mathcal{E}}_{-+}=\frac{\omega' M^2}{\bar{q}}\Big\{\bar{q}\big(4f_{11}+f_5+f_7+8Mf_6+4Mf_9\big)-4f_{10}\Big\}\big(2M-\omega_0+\bar{q}\cos\vartheta\big). \qquad \text{(A.69)}
$$

A.5 Born Term for Compton Scattering off Nucleon

In this Appendix, one lists the results for the computation of the helicity CFFs in the Born approximation using the target rest frame. These will be extracted from Eq. (2.5) where the covariant Compton amplitude is replaced by its Born approximation,

$$
\mathcal{T}_{ab}^{\text{Born}}=(-1)^{a-1}\varepsilon_1^{\mu}(a)\,T_{\mu\nu}^{\text{Born}}\,\varepsilon_2^{\nu *}(b), \qquad \text{(A.61)}
$$

making use of the definitions given in Eqs. (2.13)–(2.15) and (2.136). The r.h.s. can be decomposed into a sum of four terms that differ by the form factor products accompanying them, i.e.,

$$
e_N F_1(-q_1^2), \quad e_N F_2(-q_1^2), \quad \kappa_N F_1(-q_1^2), \quad \text{and} \quad \kappa_N F_2(-q_1^2),
$$

where one sets $e_N = F_1(0)$ and $\kappa_N = F_2(0)$ and use in the following also the nucleon magnetic moment $\mu_N = e_N + \kappa_N$. The following results are found (suppressing superscript

Born)

$$\begin{aligned}\mathcal{H}_{+b} = &-\frac{\left(1+b\sqrt{1+\varepsilon^2}\right)\left(2-x_{\rm B}+\frac{x_{\rm B}t}{Q^2}\right)^2}{4\sqrt{1+\varepsilon^2}(1-x_{\rm B})\left(1+\frac{x_{\rm B}t}{Q^2}\right)}\,e_N F_1 \\ &-b\,\frac{x_{\rm B}^2\left(1+\frac{t}{Q^2}\right)^2}{4(1-x_{\rm B})\left(1+\frac{x_{\rm B}t}{Q^2}\right)}\left[\kappa_N F_1+\mu_N F_2\right] \\ &-\frac{e_N x_{\rm B}^2\left(1+\frac{t}{Q^2}\right)}{2\sqrt{1+\varepsilon^2}\left(1+\frac{x_{\rm B}t}{Q^2}\right)}\left\{\frac{4M^2}{Q^2}F_1-\frac{\left(2-x_{\rm B}+\frac{x_{\rm B}t}{Q^2}\right)\frac{t}{Q^2}\left[F_1+F_2\right]}{\left(1+\frac{t}{Q^2}\right)(1-x_{\rm B})}\right. \\ &\qquad\left.+\frac{x_{\rm B}\left(1+\frac{t}{Q^2}\right)F_2}{2(1-x_{\rm B})}\right\},\end{aligned} \tag{A.62}$$

$$\begin{aligned}\mathcal{E}_{+b} = &-b\left[\kappa_N F_1+\mu_N F_2\right] \\ &-\frac{e_N\varepsilon^2}{2\sqrt{1+\varepsilon^2}}\left\{\frac{2x_{\rm B}F_2}{\varepsilon^2}-\frac{\left(1+\frac{t}{Q^2}\right)F_1}{1+\frac{x_{\rm B}t}{Q^2}}+\frac{\left(2-x_{\rm B}+\frac{x_{\rm B}t}{Q^2}\right)\left[F_1+F_2\right]}{(1-x_{\rm B})\left(1+\frac{x_{\rm B}t}{Q^2}\right)}\right\},\end{aligned} \tag{A.63}$$

$$\begin{aligned}\widetilde{\mathcal{H}}_{+b} = &-\frac{\left(1+b\sqrt{1+\varepsilon^2}\right)x_{\rm B}\left(2-x_{\rm B}+\frac{x_{\rm B}t}{Q^2}\right)}{2\sqrt{1+\varepsilon^2}}\left[\frac{\kappa_N F_2}{\varepsilon^2}+\frac{\left(1-\frac{t}{Q^2}\right)e_N\left[F_1+F_2\right]}{2(1-x_{\rm B})\left(1+\frac{x_{\rm B}t}{Q^2}\right)}\right] \\ &-\frac{x_{\rm B}}{4\sqrt{1+\varepsilon^2}}\,\frac{2-x_{\rm B}+\frac{x_{\rm B}t}{Q^2}}{(1-x_{\rm B})\left(1+\frac{x_{\rm B}t}{Q^2}\right)}\left\{\mu_N\left[(2-x_{\rm B})F_2+\frac{x_{\rm B}t}{Q^2}\left[2F_1+F_2\right]\right]\right. \\ &\qquad\left.+\left(1-\frac{t}{Q^2}\right)\left[\kappa_N F_1-e_N F_2\right]\right\},\end{aligned} \tag{A.64}$$

$$\begin{aligned}\widetilde{\mathcal{E}}_{+b} = &\frac{\left(1+b\sqrt{1+\varepsilon^2}\right)\left(2-x_{\rm B}+\frac{x_{\rm B}t}{Q^2}\right)}{2\sqrt{1+\varepsilon^2}}\left[\frac{\kappa_N\left[2F_1+F_2\right]}{x_{\rm B}}\right. \\ &\left.-\frac{\varepsilon^2\left(3+\frac{t}{Q^2}\right)e_N\left[F_1+F_2\right]}{2x_{\rm B}(1-x_{\rm B})\left(1+\frac{x_{\rm B}t}{Q^2}\right)}\right]-\frac{2-x_{\rm B}+\frac{x_{\rm B}t}{Q^2}}{x_{\rm B}\sqrt{1+\varepsilon^2}}\left\{e_N(1-x_{\rm B})F_2+\kappa_N\left[F_1+F_2\right]\right\} \\ &+\frac{\varepsilon^2\left(2-x_{\rm B}+\frac{x_{\rm B}t}{Q^2}\right)}{4x_{\rm B}\sqrt{1+\varepsilon^2}(1-x_{\rm B})\left(1+\frac{x_{\rm B}t}{Q^2}\right)}\left\{e_N\left(3+\frac{t}{Q^2}\right)\left[F_1+F_2\right]\right.\end{aligned}$$

$$- \mu_N \left(1 + \frac{x_{\rm B} t}{\mathcal{Q}^2}\right) [F_1 + F_2] + \mu_N (1 - x_{\rm B}) \left[\frac{t F_1}{\mathcal{Q}^2} - F_2\right] \Bigg\}, \tag{A.65}$$

$$\mathcal{H}_{0+} = \frac{\sqrt{2}\widetilde{K} x_{\rm B}}{\mathcal{Q}\sqrt{1+\varepsilon^2}}\, e_N \left\{ \frac{2 - x_{\rm B} - \frac{x_{\rm B} t}{\mathcal{Q}^2} + \frac{8 x_{\rm B} M^2}{\mathcal{Q}^2}}{2(1-x_{\rm B})\left(1 + \frac{x_{\rm B} t}{\mathcal{Q}^2}\right)} \left[F_1 - \frac{\mathcal{Q}^2}{4 x_{\rm B} M^2} F_2\right] + \frac{1 - \frac{t}{4M^2}}{1 + \frac{x_{\rm B} t}{\mathcal{Q}^2}} F_2 \right\} - \frac{t\, \mathcal{E}_{0+}}{4M^2}, \tag{A.66}$$

$$\mathcal{E}_{0+} = \frac{(-1)\sqrt{2}\widetilde{K}}{\mathcal{Q}\sqrt{1+\varepsilon^2}} \frac{e_N \left[\varepsilon^2 F_1 - x_{\rm B}^2 F_2\right]}{(1-x_{\rm B})\left(1 + \frac{x_{\rm B} t}{\mathcal{Q}^2}\right)} + \frac{\left(1 + \frac{(1-x_{\rm B})\mathcal{Q}^2}{\mathcal{Q}^2 + x_{\rm B} t}\right)\mathcal{Q}}{\sqrt{2}\widetilde{K}\sqrt{1+\varepsilon^2}} \times \left[1 + \frac{x_{\rm B} t}{\mathcal{Q}^2} + \frac{\varepsilon^2 \left(1 + \frac{t}{\mathcal{Q}^2}\right)}{2}\right] e_N F_2\,, \tag{A.67}$$

$$\widetilde{\mathcal{H}}_{0+} = \frac{\sqrt{2}\widetilde{K} x_{\rm B} \left(2 - x_{\rm B} + \frac{x_{\rm B} t}{\mathcal{Q}^2}\right)}{\mathcal{Q}\sqrt{1+\varepsilon^2}} \left\{ \frac{e_N F_2}{\varepsilon^2} - \frac{\left(1 + \frac{t}{\mathcal{Q}^2}\right)\mu_N \left[F_1 - \frac{\mathcal{Q}^2}{4 x_{\rm B} M^2} F_2\right]}{2(1-x_{\rm B})\left(1 + \frac{x_{\rm B} t}{\mathcal{Q}^2}\right)} \right\} - \frac{t\, \widetilde{\mathcal{E}}_{0+}}{4M^2}, \tag{A.68}$$

$$\widetilde{\mathcal{E}}_{0+} = \frac{(-1)\sqrt{2}\widetilde{K}}{\mathcal{Q}\sqrt{1+\varepsilon^2}} \frac{\left(2 - x_{\rm B} + \frac{x_{\rm B} t}{\mathcal{Q}^2}\right)\frac{4 x_{\rm B} M^2}{\mathcal{Q}^2}}{2(1-x_{\rm B})\left(1 + \frac{x_{\rm B} t}{\mathcal{Q}^2}\right)} \mu_N \left[F_1 - \frac{\mathcal{Q}^2}{4 x_{\rm B} M^2} F_2\right] - \frac{\left(2 - x_{\rm B} + \frac{x_{\rm B} t}{\mathcal{Q}^2}\right)\mathcal{Q}}{2\sqrt{2}\widetilde{K} x_{\rm B}\sqrt{1+\varepsilon^2}} \left[4 - 2x_{\rm B} + 3\varepsilon^2 + \left(4(1-x_{\rm B})x_{\rm B} + \varepsilon^2\right)\frac{t}{\mathcal{Q}^2}\right] e_N F_2\,. \tag{A.69}$$

Notice that in the longitudinal helicity-flip CFFs a spurious kinematical $1/\widetilde{K}$ singularity appears, which cancels, however, in electric-like combinations introduced in Eq. (2.110). Hence, the Born result is well defined for any value of kinematical variables, except for the elastic poles at $s = M^2$ ($x_B = 1$) and $u = M^2$ ($x_B = -\mathcal{Q}^2/t$).

APPENDIX B

RENORMALIZATION OF TWIST FOUR OPERATORS

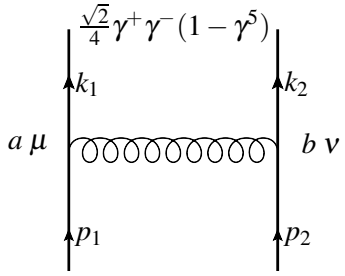

Figure B.1: Feynman Diagram responsible for $\chi_+ \otimes \psi_- \to \chi_+ \otimes \psi_- + \chi_- \otimes \psi_+$ in Eq. (3.85).

B.1 Sample Calculations in Light-Cone Gauge

In this appendix one provides an explicit calculation of the transitions kernel for good-bad two-to-two quark transitions $\chi_+ \otimes \psi_- \to \chi_+ \otimes \psi_- + \chi_- \otimes \psi_+$, shown in Fig. B.1. The operator in question can be written at one loop in the form

$$\mathcal{O}(x_1,x_2) = \int \prod_{i=1}^{2} \frac{d^4p_i}{(2\pi)^4}\frac{d^4k_i}{(2\pi)^4}\delta(k_1^+ - x_1)\delta(k_2^+ - x_1)\delta(p_1^+ - y_1)\delta(p_2^+ - y_2)$$
$$\times \bar{\psi}(p_2)\big\{\mathcal{V}_\nu^b(k_3,p_2,-k_2)i\mathcal{P}(-k_2)\frac{\sqrt{2}}{4}\gamma^+\gamma^-(1+\gamma^5)i\mathcal{P}(k_1)$$
$$\times \mathcal{V}_\mu^a(-k_3,-k_1,p_1)(-i)\Delta_{\mu\nu}^{ab}(k_3)\big\}\psi(p_1)\,,$$

where in the gluon propagator in the light-cone gauge was introduced in Eq. (3.34), while for reader's convenience one provides below expressions for the quark propagator and and the vertex function, respectively,

$$\mathcal{P}(k) = \frac{\not{k}}{k^2+i0}\,, \qquad \mathcal{V}_\mu^a(k_1,k_2,k_3) = igt^a\gamma^\mu(2\pi)^4\delta^4(k_1+k_2+k_3)\,.$$

Denoting the string introduced in curly brackets as $\mathcal{N}/\mathcal{D}$, one can work out the denominator $\mathcal{D}$ stemming from the propagators as $\mathcal{D} = (p_1+p_2-k_1)^2(p_1-k_1)^2k_1^2$. Choosing the loop momentum as $k = k_1$, one expands $\mathcal{D}$ in inverse powers of the transverse momentum $k_\perp$ and find immediately for the leading and first subleasing contributions

$$\frac{1}{\mathcal{D}} = \frac{1}{k_\perp^6}\frac{1}{[k^+\beta-1][(k^+-p_1^+-p_2^+)\beta-1][(k^+-p_1^+)\beta-1]} \tag{B.1}$$

$$\times\left[1-\frac{2(p_1^\perp+p_2^\perp)\cdot k^\perp}{k_\perp^2[(k^+-p_1^+-p_2^+)\beta-1]}-\frac{2p_1^\perp\cdot k^\perp}{k_\perp^2[(k^+-p_1^+)\beta-1]}\right]+O(1/k_\perp^8)\,,$$

We will parametrize the contributions of the first, second and third terms in the square brackets as $\mathcal{A}$, $\mathcal{B}$ and $\mathcal{C}$ contributions, respectively, i.e., $\mathcal{A}-\mathcal{B}-\mathcal{C}$.

To clarity the manipulations involved in the analysis, the numerator

$$\begin{aligned}\mathcal{N}=&-\frac{i\sqrt{2}}{4}g^2t^a\otimes t^a\bar{\psi}(p_2)[\gamma^\nu(\not{k}-\not{p}_1-\not{p}_2)\gamma^+\gamma^-\not{k}\gamma^\mu](1+\gamma^5)\psi(p_1)\\&\times\left(g_{\mu\nu}+\frac{(k-p_1)_\mu n_\nu+(k-p_1)_\nu n_\mu}{(p_1-k)^+}\right),\end{aligned}\tag{B.2}$$

will be calculated term by term. To start with, notice that p_1^- and p_2^- can be automatically neglected in the calculation as they vanish for Fourier transform of light-ray operators that one considers. Let us start with the $g_{\mu\nu}$ piece and denote its contraction with the strong of Dirac matrices in Eq. (B.2) as $\mathcal{I}_1$. Then after Sudakov decomposition of all momenta and little Dirac algebra, one finds after rescaling the k^- momentum component according to Eq. (3.42)

$$\mathcal{I}_1=g_{\mu\nu}\gamma^\nu(\not{k}-\not{p}_1-\not{p}_2)\gamma^+\gamma^-\not{k}\gamma^\mu\simeq 4k_\perp^2[\beta(k^+-p_1^+-p_2^+)-1]\tag{B.3}$$

where one has neglected all terms that do not produce any divergences, i.e., terms scaling as $k_\perp^n$ with $n<2$. Next, one turns to the second $(k-p_1)_\mu n_\nu$ and third $(k-p_1)_\nu n_\mu$ terms. For their contraction with the scare bracket, one finds in a completely analogous manner

$$\begin{aligned}\mathcal{I}_2=&\,\gamma_\nu(\not{k}-\not{p}_1-\not{p}_2)\gamma^+\gamma^-\not{k}\gamma_\mu(k-p_1)^\mu n^\nu\\\simeq&\,2(k^+-p_1^+-p_2^+)[2k^-(k^+-p_1^+)-k_\perp^2]\gamma^+\gamma^--2\beta k_\perp^2(k^+-p_1^+-p_2^+)\gamma^+\not{p}_1^\perp\,,\end{aligned}\tag{B.4}$$

$$\begin{aligned}\mathcal{I}_3=&\,\gamma_\nu(\not{k}-\not{p}_1-\not{p}_2)\gamma^+\gamma^-\not{k}\gamma_\mu(k-p_1)^\nu n^\mu\\\simeq&\,4k_\perp\cdot(p_{1\perp}+p_{2\perp})\not{k}_\perp\gamma^+-2k_\perp^2\not{p}_2\gamma^+-2k_\perp^2[\beta(k^+-p_1^+-p_2^+)-1]\gamma^+\not{k}_\perp\,.\end{aligned}\tag{B.5}$$

Now, combining the above in the integrand, one traces only terms with $1/k_\perp^2$ behavior since these are the only contributions yielding logarithmic divergence. Integrating over the

longitudinal k^+ component with the help of the Dirac delta function in Eq. (B.1)

$$\mathcal{I}_1\mathcal{A} = \frac{1}{8\pi^2}\int_0^{2\pi}\frac{d\varphi}{2\pi}\int\frac{d\beta}{2\pi} \times \int^{\mu^2} dk_\perp^2\, k_\perp^2 \frac{4k_\perp^2[\beta(x_1-p_1^+-p_2^+)-1]}{k_\perp^6[\beta x_1-1][\beta(x_1-p_1^+)-1][\beta(x_1-p_1^+-p_2^+)-1]} = \frac{1}{\pi^2}\ln\mu\int\frac{d\beta}{2\pi}\frac{1}{[\beta x_1-1][\beta(x_1-p_1^+)-1]} = \frac{i}{\pi^2}\ln\mu\,\vartheta_{11}^0(x_1,x_1-p_1^+), \tag{B.6}$$

where in the last step one restored the omitted causal $i0$ prescription in the longitudinal denominators use the defining integral Eq. (B.52) for the generalized step functions. Similarly, one finds

$$\mathcal{I}_2\mathcal{A} = \frac{i}{2\pi^2}\ln\mu\frac{x_1-p_1^+-p_2^+}{p_1^+-x_1}\gamma^+\gamma^-\vartheta_{11}^0(x_1,x_1-p_1^+-p_2^+) - \frac{i}{2\pi^2}\ln\mu\frac{\gamma^+\not{p}_{2\perp}}{p_1^+-x_1}[\vartheta_{11}^0(x_1,x_1-p_1^+)+\vartheta_{111}^0(x_1,x_1-p_1^+,x_1-p_1^+-p_2^+)]. \tag{B.7}$$

To proceed further with other contributions, one computes the following integral first

$$\int_0^{2\pi}\frac{d\varphi}{2\pi}\int^{\mu^2}\frac{dk_\perp^2}{k_\perp^4}p_\perp\cdot k_\perp k_\perp^\alpha = \ln\mu\, p_\perp^\alpha. \tag{B.8}$$

Here one used the fact that the integrand does not have any vectors but $k_\perp$ so that one can immediately calculate the average in the two-dimensional transverse plane $k_\perp^\alpha k_\perp^\beta \to k_\perp^2\delta^{\alpha\beta}/2$. Thus one obtains

$$\mathcal{I}_3\mathcal{A} = -\frac{i}{2\pi^2}\ln\mu\frac{\gamma^+\not{p}_{1\perp}+p_2^+\gamma^-\gamma^+}{p_1^+-x_1}\vartheta_{111}^0(x_1,x_1-p_1^+,x_1-p_1^+-p_2^+) \tag{B.9}$$

$$\mathcal{I}_3\mathcal{B} = \frac{i}{2\pi^2}\ln\mu\frac{\gamma^+(\not{p}_1^\perp+\not{p}_2^\perp)}{p_1^+-x_1}\vartheta_{111}^0(x_1,x_1-p_1^+,x_1-p_1^+-p_2^+) \tag{B.10}$$

$$\mathcal{I}_3\mathcal{C} = \frac{i}{2\pi^2}\ln\mu\frac{\gamma^+\not{p}_1^\perp}{p_1^+-x_1}\vartheta_{12}^0(x_1,x_1-p_1^+). \tag{B.11}$$

Putting all the pieces together, one gets

$$\mathcal{G} = \frac{\alpha_s}{\pi}t^a\otimes t^a\ln\mu\int dy_1dy_2\int\frac{dp_1^-d^2p_{1\perp}}{(2\pi)^4}\int\frac{dp_1^-d^2p_{2\perp}}{(2\pi)^4}\delta(x_1+x_2-y_1-y_2) \times\bar\psi(p_1)\left\{2\vartheta_{11}^0(x_1,x_1-y_1)-\frac{2y_2}{y_1-x_1}\vartheta_{111}^0(x_1,x_1-y_1,-x_2)\right.$$

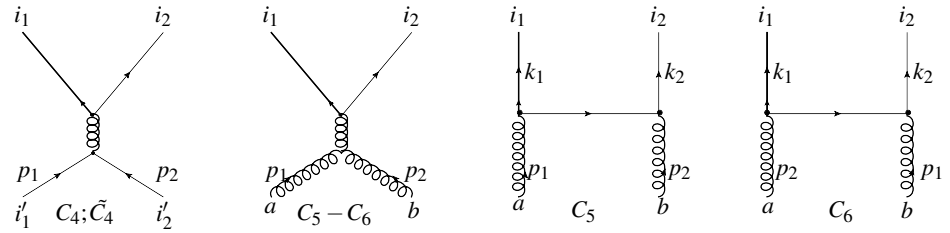

Figure B.2: Two-to-two quark-gluon transitions in Eq. (B.13). The color structures C_c are defined in Eq. (3.73).

$$
\begin{aligned}
&+\gamma^+\gamma^-\left[\frac{y_2}{y_1-x_1}\vartheta^0_{111}(x_1,x_1-y_1,-x_2)-\frac{x_2}{y_1-x_1}\vartheta^0_{11}(x_1,x_1-y_1-y_2)\right]\\
&+\frac{\gamma^+\not{p}_1^{\perp}}{y_1-x_1}[\vartheta^0_{12}(x_1,x_1-y_1)-\vartheta^0_{11}(x_1,x_1-y_1)-\vartheta^0_{111}(x_1,x_1-y_1,-x_2)]\\
&+\frac{\gamma^+\not{p}_2^{\perp}}{y_1-x_1}\vartheta^0_{111}(x_1,x_1-y_1,-x_2)\Bigg\}\frac{\sqrt{2}(1+\gamma_5)}{4}\psi(p_2)\,. \qquad \text{(B.12)}
\end{aligned}
$$

Finally, using equations of motion for the (anti)quark fields, with neglected gluon field since one after the two-to-two transitions only, $(p_2^+\gamma^- + \not{p}_{2\perp})\psi(p_2)=0$ and $\bar{\psi}(p_1)(p_1^+\gamma^- + \not{p}_{1\perp})=0$, one can trade transverse momenta accompanying the good component of the quark to the bad quark fields. This way one arrives at Eqs. (3.89)-(3.92).

B.2 Flavor Singlet $2\to 2$ Transitions

We complement the non-singlet analysis performed in the body of the paper with particle results involving the singlet sector. In all cases one found agreement with corresponding expressions reported in Ref. [78].

B.2.1 Quasi-Partonic Operators

To start with, one presents the quasipartonic quark-antiquark to gluon-gluon kernels and gluon-gluon transitions as well.

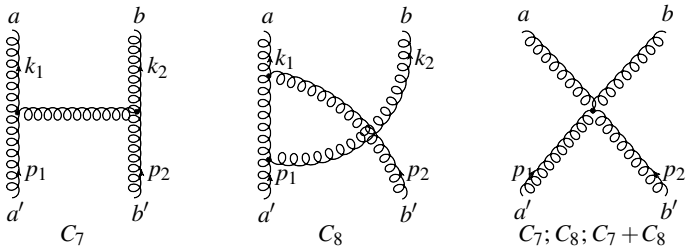

Figure B.3: Two-to-two quasipartonic gluon-gluon transition of Sect. B.2.1. The induced color-flow structure is defined in Eq. (3.73).

$$\mathcal{O}^{i_1 i_2}(x_1,x_2) = \{\psi_+^{i_1}\bar{\chi}_+^{i_2},\, \bar{\psi}_+^{i_1}\chi_+^{i_2},\, \psi_+^{i_1}\bar{\psi}_+^{i_2},\, \bar{\chi}_+^{i_1}\chi_+^{i_2}\}(x_1,x_2)$$

In the singlet sector, the quark-antiquark evolution will produce extra annihilation-type contributions shown by the first two graph in Fig. B.2

$$\begin{aligned}[\mathcal{K}\,\mathcal{O}]^{i_1 i_2}(x_1,x_2) = \ldots - \int [\mathcal{D}^2 y]_2 K_1(x_1,x_2|y_1,y_2) \sum_f \Big\{ [C_4]^{i_1 i_2}_{i_1' i_2'} \bar{\psi}_+^{i_1' f}(y_1)\psi_+^{i_2' f}(y_2) \\ + [\tilde{C}_4]^{i_1 i_2}_{i_1' i_2'} \chi_+^{i_1' f}(y_1)\bar{\chi}_+^{i_2' f}(y_2)\Big\} \\ - i\int [\mathcal{D}y^2]_2 \Big\{ [C_5]^{i_1 i_2}_{ab} K_2 + [C_6]^{i_1 i_2}_{ab} K_3 \Big\}(x_1,x_2|y_1,y_2) f^a_{++}(y_1)\bar{f}^b_{++}(y_2)\,,\end{aligned} \tag{B.13}$$

in addition to already computed transitions, denoted above by ellipses, and given in Eqs. (3.76) and (3.77). The index f runs over all quark flavors. The last line represents transitions into gluons, exhibited by the last two graphs in Fig. (B.2). The color structures are displayed in Eq. (3.73). The transition kernels then read

$$K_1(x_1,x_2;y_1,y_2) = \frac{4x_1x_2\vartheta_{11}^0(x_1,-x_2)}{(x_1+x_2)^2}\,, \tag{B.14}$$

$$\begin{aligned}K_2(x_1,x_2;y_1,y_2) = \frac{2x_2}{y_1y_2}\Big\{ \frac{x_1(y_2-y_1)}{(x_1+x_2)^2}\vartheta_{11}^0(x_1,-x_2) \\ - \vartheta_{111}^0(x_1,x_1-y_1,-x_2) - \vartheta_{11}^0(x_1-y_1,-x_2)\Big\}\,,\end{aligned} \tag{B.15}$$

$$K_3(x_1,x_2;y_1,y_2) = 2\frac{x_1-y_2}{y_1y_2}\vartheta_{111}^0(x_1,x_1-y_2,-x_2) + \frac{2x_1x_2(y_1-y_2)}{y_1y_2(x_1+x_2)^2}\vartheta_{11}^0(x_1,-x_2)\,. \tag{B.16}$$

In the following two subsection, one will list the results of the evolution kernels for the pure gluonic transitions.

$$\mathcal{O}^{ab}(x_1,x_2)=\{f^a_{++}f^b_{++},\bar f^a_{++}\bar f^b_{++}\}(x_1,x_2)$$

For gluon blocks of the same chirality, the nonvanshing Feynman graphs that induce the transition

$$[\mathcal{K}\mathcal{O}]^{ab}(x_1,x_2)=\int(\mathcal{D}^2y)_2\{[C_7]^{ab}_{a'b'}K_1+[C_8]^{ab}_{a'b'}K_2\}(x_1,x_2|y_1,y_2)\mathcal{O}^{a'b'}(y_2,y_2)\,, \quad \text{(B.17)}$$

are given in Fig. B.3 and produce

$$\begin{aligned}K_1(x_1,x_2;y_1,y_2)=&\frac{x_1^3+x_1^2(2x_2-y_1+y_2)-x_2y_1(x_1+2x_2)}{(x_1-y_1)y_1y_2}\vartheta^0_{111}(x_1,x_1-y_1,-x_2)\\&+\frac{x_1x_2(x_1+y_1)(x_2+y_2)}{(x_1-y_1)y_1y_2}\vartheta^1_{111}(x_1,x_1-y_1,-x_2)\\&+\frac{x_1x_2}{y_1y_2}\vartheta^0_{11}(x_1,-x_2)\,,\end{aligned} \quad \text{(B.18)}$$

$$\begin{aligned}K_2(x_1,x_2;y_1,y_2)=&\frac{x_1^3+x_1^2(2x_2-y_2+y_1)-x_2y_2(x_1+2x_2)}{(x_1-y_2)y_1y_2}\vartheta^0_{111}(x_1,x_1-y_2,-x_2)\\&+\frac{x_1x_2(x_1+y_2)(x_2+y_1)}{(x_1-y_2)y_1y_2}\vartheta^1_{111}(x_1,x_1-y_2,-x_2)\\&+\frac{x_1x_2}{y_1y_2}\vartheta^0_{11}(x_1,-x_2)\,.\end{aligned} \quad \text{(B.19)}$$

Here one again observes the "exchange symmetry" elaborated in details in Sects. 3.4.3 and 3.4.3. In the present case, it implies the simultaneous interchange of $a\leftrightarrow b$ and $z_1\leftrightarrow z_2$.

$$\mathcal{O}^{ab}(x_1,x_1)=\{f^a_{++}\bar f^b_{++}\}(x_1,x_2)$$

Finally, the opposite-chirality gluon sector evolves as

$$[\mathcal{K}\mathcal{O}]^{ab}(x_1,x_2)=\int[\mathcal{D}^2y]_2\{[C_7]^{ab}_{a'b'}K_1+[C_8]^{ab}_{a'b'}K_2\}(x_1,x_2|y_1,y_2)\mathcal{O}^{a'b'}(y_2,y_2)\,, \quad \text{(B.20)}$$

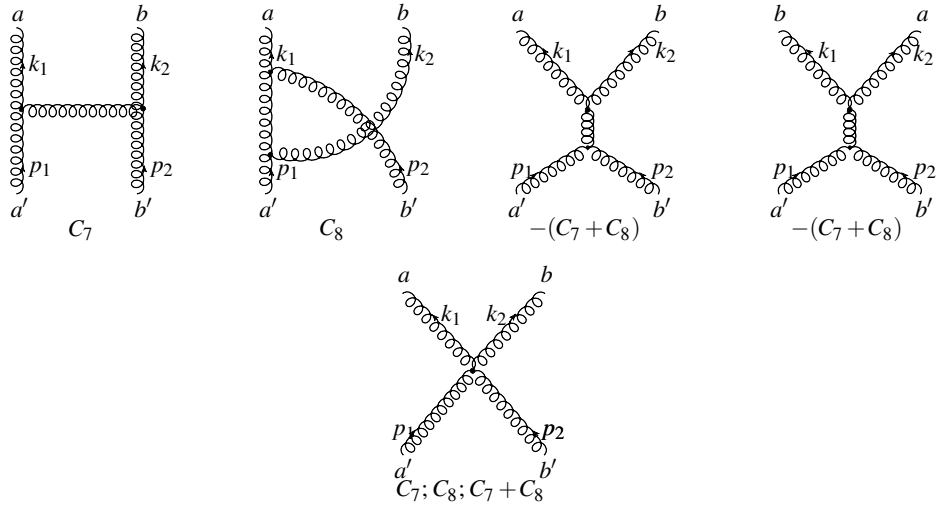

Figure B.4: Two-to-two transition of quasipartonic gluon-gluon fields in sect. B.2.1 where the color structures are define in Eq. (3.73).

according to nontrivial Feynman diagrams in Fig. B.4 with

$$
\begin{aligned}
K_1(x_1,x_2;y_1,y_2) &= \frac{x_1^2x_2+x_1(x_2-2y_1)y_1+2(x_2-y_1)^2y_1}{(y_1-x_1)y_1y_2}\,\vartheta^0_{111}(x_1,x_1-y_1,-x_2)\\
&\quad+\frac{x_1x_2(x_1+2x_2-y_1)(x_1+y_1)}{(x_1-y_1)y_1y_2}\,\vartheta^1_{111}(x_1,x_1-y_1,-x_2)\\
&\quad-\frac{x_1x_2(x_1^2+x_2(3x_2-2y_1)+2x_1(2x_2+y_1))}{(x_1+x_2)^2y_1y_2}\,\vartheta^0_{11}(x_1,-x_2)\,, \qquad \text{(B.21)}\\
K_2(x_1,y_1;y_1,y_2) &= \frac{2(x_1-y_2)^2}{y_1y_2}\,\vartheta^0_{111}(x_1,x_1-y_2,-x_2)\\
&\quad+\frac{2x_1x_2(x_2(x_2-y_1)+x_1(x_2+y_1))}{(x_1+x_2)^2y_1y_2}\,\vartheta^0_{11}(x_1,-x_2)\,. \qquad \text{(B.22)}
\end{aligned}
$$

All other quasipartonic singlet transitions can be found in the literature [71, 74, 76, 78]

B.2.2 Non-Quasipartonic Operators

In this Appendix, one complements non-quasipartonic operators with purely gluonic transitions, thus extending the consideration of Sect. 3.4.2.

Extending the class of non-singlet operators Eq. (3.85) to gluons, one introduces two doublets of gluonic blocks,

$$\mathcal{O}_+^{ab} = \left\{ \begin{pmatrix} f^a_{+-} \otimes f^b_{++} \\ f^a_{++} \otimes f^b_{+-} \end{pmatrix} \right\}, \qquad \mathcal{O}_-^{ab} = \left\{ \begin{pmatrix} f^a_{++} \otimes \bar{D}_{-+} f^b_{++} \\ \bar{D}_{-+} f^a_{++} \otimes f^b_{++} \end{pmatrix} \right\}. \tag{B.23}$$

Then the transition equation can be written as in the quasipartonic case

$$[\mathcal{K}\,\mathcal{O}_+]^{ab}(x_1,x_2) = -[C_7]^{ab}_{a'b'} \int (\mathcal{D}^2 y)_2 K(x_1,x_2|y_1,y_2) \mathcal{O}_+^{a'b'}(y_1,y_2), \tag{B.24}$$

though the kernels are now matrix valued and obviously have different components

$$\begin{aligned} K_{11} = {} & \frac{x_1 x_2 \left(y_1^2 - 2y_1 y_2 - 2y_2^2\right) \vartheta^0_{11}(x_1,-x_2)}{y_1 y_2 (y_1+y_2)(x_2-y_2)} \\ & + \frac{x_1 \left(2x_1 y_2 (y_1+y_2) + y_1^2 x_2\right) \vartheta^0_{11}(x_1,x_1-y_1)}{y_2 (y_1+y_2)^2 (y_2-x_2)} \\ & - \frac{x_2 \left(2y_1 (y_1+y_2)^3 - x_1 \left(2y_1^3 + 5y_1^2 y_2 - 2y_2^3\right)\right) \vartheta^0_{11}(x_1-y_1,-x_2)}{y_1 y_2 (y_1+y_2)^2 (y_2-x_2)}, \end{aligned} \tag{B.25}$$

$$\begin{aligned} K_{12} = {} & \frac{x_1 \left(x_2 y_1^2 + 2x_1 y_2 (y_1+y_2)\right) \vartheta^0_{11}(x_1,x_1-y_1)}{y_1 (x_1-y_1)(y_1+y_2)^2} \\ & - \frac{x_1 x_2 (3y_1+2y_2) \vartheta^0_{11}(x_1,-x_2)}{y_1 (x_1-y_1)(y_1+y_2)} + \frac{x_1 y_2 x_2 (3y_1+2y_2) \vartheta^0_{11}(x_1-y_1,-x_2)}{y_1 (x_1-y_1)(y_1+y_2)^2}, \end{aligned} \tag{B.26}$$

$$\begin{aligned} K_{21} = {} & \frac{x_1 x_2 y_1 (2y_1+3y_2) \vartheta^0_{11}(x_1,x_1-y_1)}{y_2 (y_1+y_2)^2 (x_2-y_2)} - \frac{x_1 x_2 (2y_1+3y_2) \vartheta^0_{11}(x_1,-x_2)}{y_2 (y_1+y_2)(x_2-y_2)} \\ & + \frac{x_2 \left(2y_1^2 x_2 + y_2^2 (y_1-x_2) + 2y_1 y_2 x_2 + y_2^3\right) \vartheta^0_{11}(x_1-y_1,-x_2)}{y_2 (y_1+y_2)^2 (x_2-y_2)}, \end{aligned} \tag{B.27}$$

$$\begin{aligned} K_{22} = {} & \frac{x_1 \left(x_2 \left(2y_1^3 - 5y_1 y_2^2 - 2y_2^3\right) + 2y_2 (y_1+y_2)^3\right) \vartheta^0_{11}(x_1,x_1-y_1)}{y_1 y_2 (y_1+y_2)^2 (y_2-x_2)} \\ & + \frac{x_1 x_2 \left(2y_1 (y_1+y_2) - y_2^2\right) \vartheta^0_{11}(x_1,-x_2)}{y_1 y_2 (y_1+y_2)(x_2-y_2)} \\ & + \frac{x_2 \left(2y_1^2 x_2 + y_2^2 (y_1-x_2) + 2y_1 y_2 x_2 + y_2^3\right) \vartheta^0_{11}(x_1-y_1,-x_2)}{y_1 (y_1+y_2)^2 (x_2-y_2)}. \end{aligned} \tag{B.28}$$

For $\mathcal{O}_-^{ab}$ operator set, one finds

$$[\mathcal{K}\,\mathcal{O}_-]^{ab}(x_1,x_2) = -[C_7]^{ab}_{a'b'} \int (\mathcal{D}^2 y)_2 K(x_1,x_2|y_1,y_2) \mathcal{O}_-^{a'b'}(y_1,y_2), \tag{B.29}$$

where

$$
\begin{aligned}
K_{11} &= \frac{x_2^2\left(2y_1^3x_2+2y_1^2y_2x_2+y_2^3(y_1-2x_2)+y_2^2x_2(x_2-y_1)+y_2^4\right)\vartheta_{11}^0(x_1,-x_2)}{y_1y_2^3(y_1+y_2)(x_2-y_2)}\\
&+\frac{x_2^2\left(-x_2\left(2y_1^2+3y_1y_2+2y_2^2\right)+y_2^2(y_1+y_2)+y_2x_2^2\right)\vartheta_{11}^0(x_1-y_1,-x_2)}{y_1y_2(y_1+y_2)^2(y_2-x_2)}\\
&+\frac{1}{y_1y_2^3(y_1+y_2)^2(y_2-x_2)}\Big\{y_1x_2^3\left(2y_1^3+2y_1^2y_2-y_1y_2^2-2y_2^3\right)\\
&-4y_2^3x_2(y_1+y_2)^3+2y_2^3(y_1+y_2)^4+y_1y_2^2x_2^4\\
&+y_2^3x_2^2(3y_1+2y_2)(y_1+y_2)\Big\}\vartheta_{11}^0(x_1,x_1-y_1), \qquad \text{(B.30)}\\
K_{12} &= \frac{\left(x_1^2y_2+x_1y_1(2y_1+y_2)-2y_1(y_1+y_2)^2\right)\vartheta_{211}^0(x_1,x_1-y_1,-x_2)}{y_1y_2(y_2-x_2)}\\
&-\frac{x_1x_2^2\vartheta_{11}^0(x_1,-x_2)}{y_1y_2(y_1+y_2)}+\frac{x_1(x_1+y_1)(y_2+x_2)\vartheta_{21}^0(x_1,x_1-y_1)}{y_1y_2(x_2-y_2)}\\
&+\frac{2x_2^2\vartheta_{111}^0(x_1,x_1-y_1,-x_2)}{y_2(x_2-y_2)}, \qquad \text{(B.31)}\\
K_{21} &= \frac{2x_1^2\vartheta_{111}^0(x_1,x_1-y_1,-x_2)}{y_1(y_2-x_2)}-\frac{x_1^2x_2\vartheta(x_1,-x_2)}{y_1y_2(y_1+y_2)}\\
&-\frac{\left(y_2x_2(y_1+2y_2)-2y_2(y_1+y_2)^2+y_1x_2^2\right)\vartheta_{112}^0(x_1,x_1-y_1,-x_2)}{y_1y_2(y_2-x_2)}\\
&+\frac{x_2(x_1+y_1)(y_2+x_2)\vartheta_{12}^0(x_1-y_1,-x_2)}{y_1y_2(y_2-x_2)}, \qquad \text{(B.32)}\\
K_{22} &= \frac{x_1^2\left(2y_2\left(y_2(x_1+y_1)+y_1^2\right)-y_1y_2x_2-y_1x_2^2\right)\vartheta_{11}^0(x_1,y_2-x_2)}{y_1y_2(y_1+y_2)^2(y_2-x_2)}\\
&+\frac{x_1^2\left(2x_1y_2^2(y_1+y_2)-y_1^2y_2x_2+y_1^2x_2^2\right)\vartheta_{11}^0(x_1,-x_2)}{y_1^3y_2(y_1+y_2)(y_2-x_2)}\\
&-\frac{1}{y_1^3y_2(y_1+y_2)^2(y_2-x_2)}\Big\{x_1^4y_1^2y_2-x_1^3y_2\left(2y_1^3+y_1^2y_2-2y_1y_2^2-2y_2^3\right)\\
&+x_1^2y_1^3(y_1+y_2)(2y_1+3y_2)-2y_1^3(y_1+y_2)^3(x_1-x_2)\Big\}\vartheta_{11}^0(x_1-y_1,-x_2). \qquad \text{(B.33)}
\end{aligned}
$$

Notice that the graphs defining these transitions are the same as the quasipartonic case.

For opposite-helicity gluon operators, one introduces

$$\mathcal{O}^{ab} = \begin{pmatrix} f^a_{+-} \otimes \bar{f}^b_{++} \\ f^a_{++} \otimes \frac{1}{2} D_{-+} \bar{f}^b_{+-}, \end{pmatrix} \tag{B.34}$$

and focus on the mixing within the group $\mathcal{O}^{ab}$ and disregard transitions into singlet quark opertaors. The transition then reads

$$[\mathcal{K}\,\mathcal{O}]^{ab}(x_1,x_2) = -\int [\mathcal{D}^2 y]_2 \Big\{ [C_7]^{ab}_{a'b'} K(x_1,x_2|y_1,y_2) + [C_8]^{ab}_{a'b'} \widetilde{K}(x_1,x_2|y_1,y_2) \Big\} \mathcal{O}^{a'b'}(y_1,y_2)\,. \tag{B.35}$$

with the matrix elements being

$$\begin{aligned} K_{11} = {} & \frac{x_1}{y_1 y_2 (y_1+y_2)^3 (y_2-x_2)} \Big\{ 2x_2^3 \left(y_1^2 - y_1 y_2 + y_2^2\right) - 3 y_1 x_2^2 \left(y_1^2 + 2 y_1 y_2 - y_2^2\right) \\ & + 4 y_1 y_2 x_2 (y_1+y_2)^2 + y_1 y_2 (y_1+y_2)^3 \Big\} \vartheta^0_{11}(x_1,-x_2) \\ & - \frac{1}{y_1 y_2 (y_1+y_2)^2 (y_2-x_2)} \Big\{ x_2^3 \left(y_1 y_2 - 2 y_1^2 + 2 y_2^2\right) + y_1 x_2^2 \left(2 y_1^2 + 3 y_1 y_2 - y_2^2\right) \\ & + 3 y_1 y_2^2 x_2 (y_1+y_2) + y_1 y_2^2 (y_1+y_2)^2 - 2 y_2 x_2^4 \Big\} \vartheta^0_{11}(x_1-y_1,-x_2) \\ & + \frac{x_1 \left(x_2^2 (3y_1+2y_2) - 2 y_1 y_2 x_2 + y_1 y_2 (y_1+y_2) - 2 x_2^3\right) \vartheta^0_{11}(x_1,x_1-y_1)}{y_2 (y_1+y_2)^2 (y_2-x_2)}, \end{aligned} \tag{B.36}$$

$$\begin{aligned} K_{12} = {} & \frac{\left((y_1+y_2)^2 - 2 y_2 x_2 + x_2^2\right) \vartheta^0_{11}(x_1,-x_2)}{(y_1+y_2)(y_2-x_2)} \\ & - \frac{x_1 \left(x_2^2 (3y_1+2y_2) - 2 y_1 y_2 x_2 + y_1 y_2 (y_1+y_2) - 2 x_2^3\right) \vartheta^0_{11}(x_1,x_1-y_1)}{y_2 (y_1+y_2)^2 (y_2-x_2)} \\ & - \frac{x_1 \left(y_2^3 (y_1+y_2) + 2 x_2^3 (y_1+2y_2) - y_2 x_2^2 (2y_1+y_2) - 2 y_2^3 x_2\right) \vartheta^0_{11}(x_1-y_1,-x_2)}{y_2^2 (y_1+y_2)^2 (y_2-x_2)}, \end{aligned} \tag{B.37}$$

$$K_{21} = \frac{x_1^2 \left(-2 y_1^2 y_2 - x_2^2 (3y_1+2y_2) + y_1 y_2 x_2 + 2 x_2^3\right) \vartheta^0_{11}(x_1,x_1-y_1)}{y_2 (y_1+y_2)^2 (y_2-x_2)}$$

$$+\frac{x_1^2}{y_1y_2(y_1+y_2)^3(y_2-x_2)}\Big\{x_2^2\left(3y_1^3+12y_1^2y_2+5y_1y_2^2+2y_2^3\right)$$
$$-2x_2^3\left(y_1^2-y_1y_2+y_2^2\right)+y_1y_2x_2(y_1-3y_2)(y_1+y_2)$$
$$+2y_1y_2(y_1-y_2)(y_1+y_2)^2\Big\}\vartheta_{11}^0(x_1,-x_2)+\frac{1}{y_1(y_1+y_2)^2(x_2-y_2)}$$
$$\times\Big\{\Big(2x_1^3x_2^2+x_1^2y_1\left(2y_1y_2-y_2x_2+x_2^2\right)$$
$$+2y_1y_2(y_1+y_2)^2(x_2-y_2)\Big)\Big\}\vartheta_{11}^0(x_1-y_1,-x_2)\,, \tag{B.38}$$

$$K_{22}=\frac{x_1^2\left(2x_2^3-2y_1^2y_2-x_2^2(3y_1+2y_2)+y_1y_2x_2\right)\vartheta_{11}^0(x_1,y_2-x_2)}{y_1y_2(y_1+y_2)^2(y_2-x_2)}$$
$$+\frac{x_1^2}{y_1^2y_2(y_1+y_2)^3(y_2-x_2)}\Big\{4y_1^2y_2(y_1+y_2)^2+x_2^2\left(3y_1^3+14y_1^2y_2+7y_1y_2^2+2y_2^3\right)$$
$$-2y_1x_2^3(y_1-2y_2)+y_1y_2x_2(3y_1-y_2)(y_1+y_2)\Big\}\vartheta_{11}^0(x_1,-x_2)$$
$$-\frac{1}{y_1^2y_2^2(y_1+y_2)^2(y_2-x_2)}\Big\{2y_2^5\left(x_1^2+y_1^2\right)+3x_1^2y_1y_2^2(5x_1-7y_1)(x_1-y_1)$$
$$-2x_1^2y_1y_2(2x_1-5y_1)(x_2-y_2)^2+2y_2^4\left(-2x_1^3+5x_1^2y_1+2y_1^3\right)$$
$$+y_2^3\left(2x_1^4-21x_1^3y_1+23x_1^2y_1^2+2y_1^4\right)-2x_1^2y_1^2(x_1-y_1)^3\Big\}\vartheta_{11}^0(x_1-y_1,-x_2)\,, \tag{B.39}$$

$$\widetilde{K}_{11}=\frac{2x_1y_1(x_2-y_1)^2\vartheta_{11}^0(x_1-y_2,-x_2)}{y_2^2(y_1+y_2)^2}+\frac{2x_1(x_1-y_2)^2\vartheta_{11}^0(x_1,x_1-y_2)}{y_2(y_1+y_2)^2}$$
$$-\frac{2x_1\left(x_2^2\left(y_1^2+2y_1y_2+4y_2^2\right)+y_1^2(y_1+y_2)^2-2y_1x_2(y_1+y_2)^2\right)\vartheta_{11}^0(x_1,-x_2)}{y_2^2(y_1+y_2)^3} \tag{B.40}$$

$$\widetilde{K}_{12}=\frac{2(x_2-y_1)^2\left(y_1^2(y_1+y_2)-x_2\left(y_1^2+y_1y_2+y_2^2\right)\right)\vartheta_{11}^0(x_1-y_2,-x_2)}{y_1y_2^3(y_1+y_2)^2}$$
$$-\frac{2x_1}{y_1y_2^3(y_1+y_2)^3}\Big\{y_1^3(y_1+y_2)^2+x_2^2\left(y_1^3+3y_1^2y_2+4y_1y_2^2-y_2^3\right)$$
$$-y_1x_2(y_1+y_2)^2(2y_1+y_2)\Big\}\vartheta_{11}^0(x_1,-x_2)-\frac{2x_1(x_1-y_2)^2\vartheta_{11}^0(x_1,x_1-y_2)}{y_1y_2(y_1+y_2)^2}\,, \tag{B.41}$$

$$\widetilde{K}_{21}=\frac{2x_1x_2^2\left((y_2^2-y_1^2)y_2-x_1(y_1^2-y_1y_2+y_2^2)\right)\vartheta_{11}^0(x_1,-x_2)}{y_1y_2(y_1+y_2)^3}$$
$$-\frac{2(x_1-y_2)^2}{y_1y_2}\Big\{(x_1+y_1-y_2)\vartheta_{111}^0(x_1,x_1-y_2,-x_2)$$
$$+y_1\vartheta_{112}^0(x_1,x_1-y_2,-x_2)\Big\}\,, \tag{B.42}$$

$$\widetilde{K}_{22}=\frac{-2x_1^2}{y_1y_2^3(y_1+y_2)^3}\Big\{y_1^2(y_1-y_2)(y_1+y_2)^2-2x_2\left(y_1^4+2y_1^3y_2-y_1y_2^3\right)$$

$$+x_2^2\left(y_1^3+3y_1^2y_2+4y_1y_2^2-y_2^3\right)\Big\}\vartheta_{11}^0(x_1,-x_2)$$
$$+\frac{2(x_2-y_1)^2}{y_1y_2^3(y_1+y_2)^2}\Big\{x_2^2\left(y_1^2+y_1y_2+y_2^2\right)+y_1(y_1-y_2)(y_1+y_2)^2$$
$$-2y_1^2x_2(y_1+y_2)\Big\}\vartheta_{11}^0(x_1-y_2,-x_2)-\frac{2x_1^2(x_1-y_2)^2\vartheta_{11}^0(x_1,x_1-y_2)}{y_1y_2(y_1+y_2)^2}. \tag{B.43}$$

This concludes the discussion for the two-to-two gluonic transitions in the singlet sector. All the results presented here coincide with the ones given in Ref. [78].

B.3 Fourier Transform

As an example, one starts with a coordinates-space kernel

$$[\mathcal{H}_{12}](z_1,z_2)=z_{12}^2\int_0^1 d\alpha\int_{\bar\alpha}^1 d\beta\,\frac{\bar\alpha\bar\beta}{\alpha}\,\varphi(z_{12}^\alpha,z_2,z_{21}^\beta)\,, \tag{B.44}$$

where $z_{ij}^\alpha=\bar\alpha z_i+\alpha z_j=(1-\alpha)z_i+\alpha z_j$. Then the Fourier transform takes form

$$\begin{aligned}
&K(x_1,x_2|y_1,y_2,y_3)\\
&\quad=\partial_{x_1}^2\int_0^1 d\alpha\int_{\bar\alpha}^1 d\beta\,\frac{\bar\alpha\bar\beta}{\alpha}\,\delta[x_1-\bar\alpha y_1-\beta y_3]\\
&\quad=\partial_{x_1}^2\int_0^1 d\alpha\frac{1}{y_3}\bar\alpha\big(\bar\alpha y_1-x_1+y_3\big)\vartheta_{11}^0(x_1-\bar\alpha(y_1+y_3),x_1-y_3-\bar\alpha y_1)\\
&\quad=\frac{1}{y_3}\partial_{x_1}^2\Bigg\{\Bigg[(x_1-2y_1-y_3)\frac{y_1}{y_3}\left(\frac{x_1-y_1-y_3}{y_1+y_3}-\frac{x_1-y_1-y_3}{y_1}\right)\\
&\quad-\frac{y_1^2}{2y_3}\left(\left(\frac{x_1-y_1-y_3}{y_1+y_3}\right)^2-\left(\frac{x_1-y_1-y_3}{y_1}\right)^2\right)\Bigg]\vartheta_{11}^0(x_1-y_3,x_1-y_1-y_3)\\
&\qquad+\left[\frac{x_1(x_1-2y_1-y_3)}{y_1+y_3}+\frac{y_1}{2}\left(1-\left(\frac{x_1-y_1-y_3}{y_1+y_3}\right)^2\right)\right]\vartheta_{11}^0(x_1,x_1-y_3)\\
&\quad+\frac{x_1-y_1-y_3}{y_3^2}\Bigg[\ln\left(\frac{y_1+y_3-x_1}{y_1}\right)\big(\theta(x_1-y_1-y_3)-\theta(x_1-y_3)\big)\\
&\qquad-\ln\left(\frac{y_1+y_3-x_1}{y_1+y_3}\right)\big(\theta(x_1-y_1-y_3)-\theta(x_1)\big)\Bigg]\Bigg\}\\
&\quad=\frac{x_1(y_1+2y_3)-y_3(y_1+y_3)}{y_3^2(y_1+y_3)^2(x_1-y_1-y_3)}\theta(x_1)-\frac{(x_1-y_3)\theta(x_1-y_3)}{y_1y_3^2(x_1-y_1-y_3)}+\frac{\theta(x_1-y_1-y_3)}{y_1(y_1+y_3)^2}\,,
\end{aligned} \tag{B.45}$$

where one has employed the results in Eq. (3.48). In the last step of differentiation, one has dropped all the terms proportional to the Dirac delta function and its derivatives since one focuses on expressions away from the kinematical boundaries which are sufficient to confront against the light-ray results of Ref. [78]. In principle, it is very straightforward to recover the contact terms as well. In this case, all the calculations follow through as in Eq. (B.45) until the last step of differentiation. Then one gets

$$
\begin{aligned}
K = & \frac{x_1(y_1+2y_3)-y_3(y_1+y_3)}{y_3^2(y_1+y_3)^2(x_1-y_1-y_3)}\theta(x_1) - \frac{(x_1-y_3)\theta(x_1-y_3)}{y_1y_3^2(x_1-y_1-y_3)} + \frac{\theta(x_1-y_1-y_3)}{y_1(y_1+y_3)^2} \\
& + \frac{2\Big[x_1(y_1+2y_3)+(y_1+y_3)^2\ln\left(\frac{x_2-y_2}{y_1+y_3}\right)\Big]\delta(x_1)}{y_3^2(y_1+y_3)^2} \\
& - \frac{2\Big[x_1-y_3+y_1\ln\left(\frac{x_2-y_2}{y_1}\right)\Big]\delta(x_1-y_3)}{y_1y_3^2} \\
& - \frac{2\Big[y_3\big(y_1^2+(x_2+y_1-y_2)y_3\big)+y_1(y_1+y_3)^2\ln\left(\frac{y_1}{y_1y_3}\right)\Big]\delta(y_2-x_2)}{y_1y_3^2(y_1+y_3)^2} \\
& + \frac{\Big[x_1(x_1(y_1+2y_3)-2(y_1+y_3)^2)-2(x_2-y_2)(y_1+y_3)^2\ln\left(\frac{x_2-y_2}{y_1+y_3}\right)\Big]\delta'(x_1)}{2y_3^2(y_1+y_3)^2} \\
& - \frac{\Big[x_2^2-y_1^2-2x_2y_2+y_2^2-2y_1(x_2-y_2)\ln\left(\frac{x_2-y_2}{y_1}\right)\Big]\delta'(x_1-y_3)}{2y_1y_3^2} \\
& + \frac{(x_2-y_2)\Big[y_3(2y_1^2+(x_2+2y_1-y_2)y_3)+2y_1(y_1+y_3)^2\ln\left(\frac{y_1}{y_1+y_3}\right)\Big]\delta'(y_2-x_2)}{2y_1y_3^2(y_1+y_3)^2}\,, \qquad \text{(B.46)}
\end{aligned}
$$

where one invoked the momentum conservation condition $x_1+x_2=y_1+y_2+y_3$ to simplify the expression. The extra delta-function terms can be recovered within the momentum formalism as well by properly taking into account field renormalization as discussed in Sect. 3.4.

B.4 Equation-of-Motion Graphs

In the preceding Appendix B.1 illustrating the good-bad two-to-two transitions, one already had to rely on the use of equations of motion to produce correct evolution kernels.

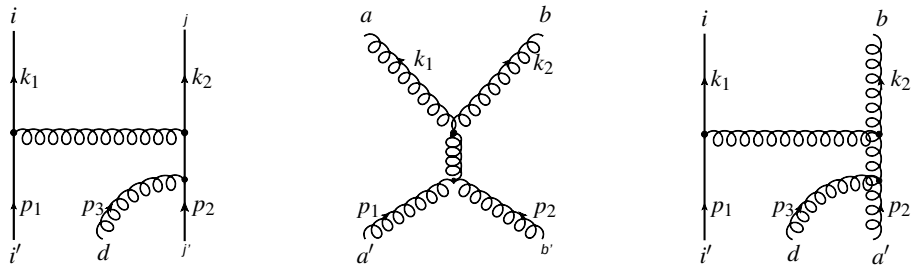

(a) (b) (c)

Figure B.5: Diagrams corresponding to the use of quark and gluon equations of motion in (a) and (b,c), respectively.

one ignored however the effects of the gluon field. In the analysis of the two-to-three transitions, one has to restore this neglected contributions. Here one demonstrates how this can be achieved. Here several nontrivial diagrams from Sect. 3.4.3 etc. are chosen to illustrate the point [92].

B.4.1 Quark Equation of Motion

To start with, let us consider the twist-three sub-block $\psi_-^i(x_1)\psi_+^j(x_2)$ built from bad/good components $\psi_\mp^i$ of the quark field $\psi^i = \psi_+^i + \psi_-^i$ of a twist-four operator and unravel the contribution from the quark equation of motion in the transition channel involving the quasipartonic operator $\psi_-^i(x_1)\psi_+^j(x_2) \to \psi_+^i(y_1)\psi^j(y_2)\bar{f}_{++}^d(y_3)$. This is shown at the diagrammatic level in Fig. B.5 (a) and reads in terms of momentum integrals

$$\mathcal{O}_{ij}(x_1,x_2) = \int \prod_{i=1}^{3} \frac{d^4p_i}{(2\pi)^4}\delta(p_i^+ - y_i) \prod_{j=1}^{2} \frac{d^4k_j}{(2\pi)^4}\delta(k_j^+ - x_j)\bar{\psi}_{i'}(p_1) i\mathcal{V}_\mu^a(p_1,-k_1,-k_3)$$
$$\times i\mathcal{P}(k_1)\Gamma^{-+} i\mathcal{P}(-k_2) i\mathcal{V}_\nu^b(p_2+p_3,-k_2,k_3) i\mathcal{P}(-p_2-p_3) i\mathcal{V}_\rho^c(-p_2-p_3,p_2,p_3)$$
$$\times \psi_{j'}(p_2) A_\perp^{d\rho}(p_3)(-i)\Delta_{\mu\nu}^{ab}(k_3)\,. \tag{B.47}$$

Here the operator Γ^{-+}-matrix, projecting out on appropriate components of four-dimensional Dirac spinors, and the quark-gluon interaction vertex are, respectively,

$$\Gamma^{-+} = \tfrac{1}{2\sqrt{2}}\gamma^-\gamma^+(1+\gamma^5)\,, \qquad \mathcal{V}_\mu^a(k_1,k_2,k_3) = gt^a\gamma^\mu(2\pi)^4\delta^4(k_1+k_2+k_3) \tag{B.48}$$

while the quark and light-cone-gauge gluon propagator read

$$\mathcal{P}(k)=\frac{\not k}{k^2}\,,\qquad \Delta^{ab}_{\mu\nu}(k)=\frac{d_{\mu\nu}(k)}{k^2}\,,\qquad d_{\mu\nu}(k)=g_{\mu\nu}-\frac{k_\mu n_\nu+k^\nu n_\mu}{k_+}\,. \tag{B.49}$$

Denoting the integrand in Eq. (B.47) by $\mathcal{N}/\mathcal{D}$, one can work out the denominator $\mathcal{D}$ originated from the propagators as $\mathcal{D}=k_1^2(p_1-k)^2(p_1+p_2+p_3-k_1)^2(p_2+p_3)^2$. Notice that since all field lines of the quasipartonic quark-gluon operator $\psi^i_+(y_1)\psi^j(y_2)\bar f^d_{++}(y_3)$ are on-shell, one immediately encounters a problem. Namely, the external legs possess collinear momenta $p_i=(p_i^+,0,0_\perp)$ with $p_i^+=y_i$ and thus the propagator $(p_2+p_3)^2$ diverges. To alleviate the problem, one has to properly regularize this. One option is to give a non-vanishing minus component p_i^- to particles' momenta. This was done in the past in Refs.[74]. Presently, one follows a different route and use instead the transverse momentum as a regulator. Choosing the loop momentum as $k=k_1$, one defines $p\equiv p_1+p_2+p_3, q\equiv p_2+p_3$, giving the latter a non-vanishing transverse component while keeping $q^-=p_2^-+p_3^-=0$. This yields a regularized intermediate propagator $q^2=2q^+q^--q_\perp^2=-q_\perp^2$. Expanding the denominator $\mathcal{D}$ in the inverse powers of the loop's transverse momentum $k_\perp$, one finds to the lowest few orders

$$\begin{aligned}\frac{1}{\mathcal{D}}=&\frac{1}{k_\perp^6q_\perp^2}\frac{1}{[k^+\beta-1][(k^+-p_1^+)\beta-1][(k^+-p^+)\beta-1]}\\&\times\left[1-\frac{2p_{1,\perp}\cdot k_\perp}{k_\perp^2[(k^+-p_1^+)\beta-1]}-\frac{2p_{1,\perp}\cdot k_\perp}{k_\perp^2[(k^+-p^+)\beta-1]}\right]+O(1/k_\perp^8)\,.\end{aligned} \tag{B.50}$$

Here one kept only terms that induce logarithmic dependence on the ultraviolet cut-off μ in transverse momentum integrals. These are the renormalization-group logs that one is resumming. In the above equation, one introduced the β-variable as a rescaled minus component of the loop momentum $\beta=2k^-/k_\perp^2$. The Dirac algebra in the numerator

$$\mathcal{N}=-ig^3(t^a)_{ii'}(t^at^d)_{jj'}\bar\psi_{i'}(p_1)[\gamma^\mu\not k\Gamma^{-+}(\not k-\not p)\gamma^\nu\not q\not A^{(d}_\perp]\psi_{j'}(p_2)d_{\mu\nu}(k-p_1)\,, \tag{B.51}$$

can be easily performed by means of Sudakov decomposition of all momenta, loop and external. Working this out and performing momentum integrations, with k^+ momentum

simply eliminated by means of the delta-function constraints, k^- momentum (a.k.a. β) generating generalized step-functions [19]

$$\vartheta^k_{\alpha_1,\ldots,\alpha_n}(x_1,\ldots,x_n)=\int_{-\infty}^{\infty}\frac{d\beta}{2\pi i}\beta^k\prod_{\ell=1}^{n}(x_\ell\beta-1+i0)^{-\alpha_\ell}\,, \tag{B.52}$$

and, finally, the $k_\perp$ one yielding $\ln\mu$ dependence, one immediately arrives at the result

$$\begin{aligned}\mathcal{O}_{ij}(x_1,x_2)=&-\frac{g^3\ln\mu}{16\sqrt{2}\pi^2q_\perp^2}t^a_{ii'}(t^at^d)_{jj'}\\ &\times\int d\mathcal{M}_3\,\bar\psi_{i'}(p_1)\left[\frac{q_\perp^2\gamma^+\not{A}^d_\perp(p_3)\vartheta^0_{111}(x_1,x_1-y_1,-x_2)}{x_1-y_1}+\ldots\right]\psi_{j'}(p_2)\,,\end{aligned} \tag{B.53}$$

where here and below one used the three-particle measure

$$d\mathcal{M}_3\equiv\prod_{i=1}^{3}\frac{dp_i^-d^2p_{i,\perp}}{(2\pi)^4}\delta\left(\sum_{i=1}^{3}y_i-\sum_{j=1}^{2}x_j\right). \tag{B.54}$$

Since Fig. B.5 (a) corresponds to the quark equation of motion

$$\not{p}\psi(p)=-g\int d^4p'\not{A}(p')\psi(p-p')$$

and $\not{q}\not{q}=q^2=-q_\perp^2$, one only needs to keep terms proportional to $q_\perp^2$ thus neglecting everything else denoted by ellipses in the right-hand side of the above equation. Effectively, the use of the quark equation of motion can be understood as a contraction of the fermion propagator $i\mathcal{P}(-q)$ into a point. Thus, one gets the final addendum to the rest of the evolution kernel

$$\begin{aligned}\mathcal{O}_{ij}(x_1,x_2)=&\frac{\sqrt{2}g^3}{32\pi^2}t^a_{ii'}(t^at^d)_{jj'}\ln\mu\\ &\times\int d\mathcal{M}_3\,\frac{\vartheta^0_{111}(x_1,x_1-y_1,-x_2)}{x_1-y_1}\bar\psi_{i'}(p_1)\gamma^+\not{A}^d_\perp(p_3)\psi_{j'}(p_2)\,,\end{aligned} \tag{B.55}$$

where $\gamma^+\not{A}_\perp$ provides the correct Dirac structure for the channel. Only after this contribution is accounted for, the total results coincides with the one available in the literature.

B.4.2 Gluon Equation of Motion

Moving on to the gluon equations of motion, $D_\mu F^{\mu\nu}=gj^\nu$, the same story applies without significant modifications. It becomes more involved though due to Lorentz structures

of contributing diagrams. Since the focus of the study was a nonsinglet sector, one is not concerned about gluon-quark transition scenarios. Therefore, one can safely set the QCD quark current to zero, $j^\nu = 0$ and simplify the gluon equation of motion to just pure gluodynamics $D_\mu F^{\mu\nu} = 0$. Decomposing it in terms of Sudakov components, one get

$$(\partial^+)^2 A^{a-} - \partial_\top A^a_\perp - \partial_\perp A^a_\top - g f^{abc}(A^b_\perp A^c_\top + A^b_\top A^c_\perp) = 0\,, \tag{B.56}$$

$$\partial^+(F^{-\perp} \pm F^{-\top}) + D^-(F^{+\perp} \pm F^{+\top}) + \tfrac{1}{2}(D^\perp \mp D^\top)\big[\pm(F^{\perp\perp} + F^{\perp\top}) \mp (F^{\top\perp} + F^{\top\top})\big] = 0\,, \tag{B.57}$$

in the light cone gauge $A^+ = 0$. Here, one introduced conventional notations for helicity plus/minus gluon fields

$$A_\perp = A^1 + iA^2\,, \qquad A_\top = A^1 - iA^2\,. \tag{B.58}$$

The same notation will be used below for holomorphic and antiholomorphic components of any four-vector.

In practice, the use of gluonic equations of motion in Feynman graphs is employed by keeping contributions in numerators that cancel denominators of on-shell propagators, in a fashion identical to the one for quarks. Namely, giving these lines a small transverse momentum does the trick. Let us illustrate this methods with a few examples.

We start with a simple example of a two-to-two particle transition

$$f^a_{++}(x_1)\bar{f}^b_{++}(x_2) \to f^{a'}_{++}(y_1)\bar{f}^{b'}_{++}(y_2)$$

that, due to helicity-conservation, possesses an nontrivial annihilation channel as shown in Fig. B.5 (b). This graph yields

$$\mathcal{O}^{ab}(x_1,x_2) = \int \prod_{i=1}^{2} \frac{d^4p_i}{(2\pi)^4}\delta(p_i^+ - y_i) \prod_{j=1}^{2} \frac{d^4k_j}{(2\pi)^4}\delta(k_j^+ - x_j) \frac{k_1^+ k_2^+}{p_1^+ p_2^+} \times \Gamma^{\rho\mu\nu\sigma}\, \mathcal{V}^{b_1 b_2 a_1}_{\delta\lambda\alpha}(-k_2, p_1+p_2, -k_1)\mathcal{V}^{a'b'b_3}_{\rho\sigma\tau}(p_1, p_2, -p_1-p_2)$$

$$\times (-i)\Delta^{\mu\nu}_{aa_1}(k_1)(-i)\Delta^{\nu\delta}_{bb_1}(k_2)(-i)\Delta^{\lambda\tau}_{b_2b_3}(p_1+p_2)A^{a'}_{\perp}(p_1)A^{b'}_{\top}(p_2)\,, \qquad \text{(B.59)}$$

where one uses for convenience a projector in terms of the Dirac matrices $\Gamma^{\rho\mu\nu\sigma} = \gamma^{\rho}_{\perp}\gamma^{\mu}_{\top}\gamma_{\perp}\gamma^{\nu}_{\perp}\gamma^{\sigma}_{\top}$ on the transverse holomorphic and anti-holomorphic components of the gluon field, and the three-gluon vertex being

$$\begin{aligned}\mathcal{V}^{abc}_{\mu\nu\rho}(k_1,k_2,k_3) &= (2\pi)^4\delta^{(4)}(k_1+k_2+k_3) \qquad \text{(B.60)}\\ &\times g f^{abc}[(k_1-k_2)_\rho g_{\mu\nu}+(k_2-k_3)_\mu g_{\nu\rho}+(k_3-k_1)_\nu g_{\rho\mu}]\,.\end{aligned}$$

one also defined the transverse four vectors of Dirac matrices $\gamma^{\mu}_{\perp}$, $\gamma^{\mu}_{\top}$ and their (anti)holomorphic combinations $\gamma_{\perp}$ and $\gamma_{\top}$,

$$\gamma^{\mu}_{\perp} = (0,\gamma^1,\gamma^2,0)\,, \qquad \gamma^{\mu}_{\top} = (0,\gamma^1,-\gamma^2,0)\,, \qquad \gamma_{\perp} = \gamma^1+i\gamma^2\,, \qquad \gamma_{\top} = \gamma^1-i\gamma^2\,. \qquad \text{(B.61)}$$

After some algebra and integration, one arrives at the expression

$$\begin{aligned}\mathcal{O}^{ab}(x_1,x_2) &= \frac{g^2\ln\mu}{\pi^2} f^{bca}f^{a'b'c}\gamma_{\perp} \qquad \text{(B.62)}\\ &\times\int d\mathcal{M}_2 A^{a'}_{\perp}(p_1)A^{b'}_{\top}(p_2)\frac{x_1x_2(x_1-x_2)(y_1-y_2)(\vartheta(-x_2)-\vartheta(x_1))}{y_1y_2(y_1+y_2)^3}\,,\end{aligned}$$

with now two-particle measure

$$d\mathcal{M}_2 \equiv \prod_{i=1}^{2}\frac{dp_i^- d^2p_{i,\perp}}{(2\pi)^4}\delta\left(\sum_{i=1}^{2}y_i-\sum_{j=1}^{2}x_j\right). \qquad \text{(B.63)}$$

Above, $\vartheta(x)$ is the ordinary step function and $\gamma_{\perp}$ structure is maintained to the end as anticipated. The expression above is obtained through the cancellation of the denominator of the on-shell propagator $(p_1+p_2)^2 = -(p_1+p_2)^2_{\perp}$ and ignoring all terms that fail to cancel $(p_1+p_2)^{-2}$. In fact, the terms that remove the singular dependence on "divergent" propagator $(p_1+p_2)^{-2}$ are the only term that survive to the end.

Let us now outline the strategy for a two-to-three transitions, shown in Fig. B.5 (c). This graphs correspond to the a particular contribution to the transition $\frac{1}{2}D_{-+}\bar{\psi}^i_+(x_1)\bar{f}^a_{++}(x_2)\to$

$\bar{\psi}^i_+(y_1)\bar{f}^a_{++}(y_2)\bar{f}^d_{++}(y_3)$. Using the vertex $\Gamma^{\rho\chi} = \frac{\sqrt[4]{2}}{2}\gamma^+\gamma_\top\gamma^\rho_\top\gamma^\chi_\top$ in four-dimensional notations, one can write the momentum integrals for the transition in question as

$$\begin{aligned}\mathcal{O}^{ia}(x_1,x_2) = \int\prod_{i=1}^{3}\frac{d^4p_i}{(2\pi)^4}\delta(p_i^+ - y_i)\prod_{j=1}^{2}\frac{d^4k_1}{(2\pi)^4}\delta(k_j^+ - x_j)\bar{\psi}_{i'}(p_1)\\ \times i\mathcal{V}^{b_1}_{\mu}(p_1,-k_1,-k_3)i\mathcal{P}(k_1)\Gamma^{\rho\chi}k_{1\top}A^{d,\alpha}_{\perp}(p_3)\mathcal{V}^{b_2b_4b_3}_{\nu\sigma\lambda}(k_3,p_2+p_3,-k_2)\\ \times\mathcal{V}^{dab_5}_{\alpha\chi\tau}(p_3,p_2,-p_2-p_3)(-i)\Delta^{\mu\nu}_{b_1b_2}(k_1)(-i)\Delta^{\rho\sigma}_{cb_3}(k_2)(-i)\\ \times\Delta^{\lambda\tau}_{b_4b_5}(p_2+p_3)A^{a'}_{\top}(p_2)\,,\end{aligned} \tag{B.64}$$

where as before $k_{1\top} = k^1 - ik^2$ and $k_{1\perp} = k^1 + ik^2$. After some algebraic manipulations that cancel the on-shell propagator and straightforward integrations over the loop momentum, one ends up with the following expression

$$\begin{aligned}\mathcal{O}^{ia}(x_1,x_2) = -\frac{\sqrt[4]{2}ig^3}{8\pi^2}t^{b_1}_{ii'}f^{b_1b_4a}f^{da'b_4}\\ \times\int d\mathcal{M}_3V(x_1,x_2|y_1,y_2,y_3)\bar{\psi}_{i'}(p_1)\gamma^+\gamma_\top A^{a'}_{\top}(p_2)A^{d}_{\top}(p_3)\,,\end{aligned} \tag{B.65}$$

where the transition kernel stemming from the graph B.5 (c) reads

$$\begin{aligned}V(x_1,x_2|y_1,y_2,y_3) = \frac{x_2\big[(y_2+y_3)(y_1+2(y_2+y_3))-2y_3x_2\big]}{y_2y_3(x_1-y_1)(y_2+y_3)}\vartheta^0_{12}(x_1-y_1,-x_2)\\ +\frac{1}{y_2y_3(x_1-y_1)(y_2+y_3)}\Big\{2y_1y_2(y_2+y_3)-x_2(y_2-y_3)(y_1+2(y_2+y_3))\\ +2x_2^2(y_2-y_3)\Big\}\vartheta^0_{112}(x_1,x_1-y_1,-x_2)\\ +\frac{x_1x_2(y_3-y_2)\vartheta^0_{111}(x_1,x_1-y_1,-x_2)}{y_2y_3(x_1-y_1)(y_2+y_3)}-\frac{x_1y_1x_2\vartheta^1_{112}(x_1,x_1-y_1,-x_2)}{x_1y_2y_3-y_1y_2y_3}\,.\end{aligned} \tag{B.66}$$

Let us conclude this section by discussing the use of gluon equations of motion when the field is emitted from an internal off-shell line. The corresponding diagram is shown in Fig. B.6 (a) and reads

$$\begin{aligned}\mathcal{O}^{ia}(x_1,x_2) = \int\prod_{i=1}^{3}\frac{d^4p_i}{(2\pi)^4}\delta(p_i^+ - y_i)\prod_{j=1}^{2}\frac{d^4k_j}{(2\pi)^4}\delta(k_j^+ - x_j)\bar{\psi}_{i'}(p_1)\\ \times i\mathcal{V}^{b_1}_{\mu}(p_1,-k_2,k_2-p_1)i\mathcal{P}(k_1-p_2-p_3)i\mathcal{V}^{b_2}_{\rho}(p_1-k_2,p_2+p_3,-k_1)\end{aligned}$$

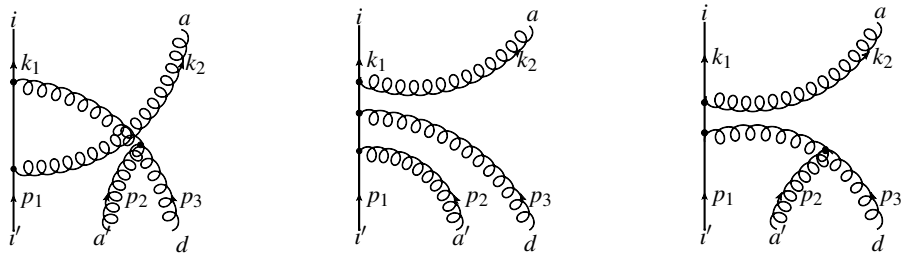

(a) (b) (c)

Figure B.6: In (a), the Feynman graph due to gluon equation of motion in the transition $\frac{1}{2}D_{-+}\bar{\psi}^{i}_{+}(x_1)f^{a}_{++}(x_2) \to \bar{\psi}^{i'}_{+}(y_1)f^{a'}_{++}(y_2)\bar{f}^{d}_{++}(y_3)$. In (b) and (c), diagrams corresponding to the double use of equations of motion for mixing $\frac{1}{2}D_{-+}\bar{\psi}^{i}_{+}(x_1)f^{a}_{++}(x_2) \to \bar{\psi}^{i'}_{+}(y_1)f^{a'}_{++}(y_2)\bar{f}^{d}_{++}(y_3)$ and $\frac{1}{2}D_{-+}\bar{\psi}^{i}_{+}(x_1)f^{a}_{++}(x_2) \to \bar{\psi}^{i'}_{+}(y_1)f^{a'}_{++}(y_2)\bar{f}^{d}_{++}(y_3)$, respectively.

$$\times i\mathcal{P}(k_1)\Gamma^{\nu\alpha}k_{1,\top}\mathcal{V}^{da'b_3}_{\chi\alpha\sigma}(p_3,p_2,-p_2-p_3)(-i)\Delta^{\mu\nu}_{ab_1}(k_2)(-i)$$
$$\times \Delta^{\rho\sigma}_{b_2b_3}(p_2+p_3)A^{a'}_{\perp}(p_2)A^{d,\chi}_{\perp}(p_3)\,, \tag{B.67}$$

where $\Gamma^{\nu\alpha} = \frac{1}{2\sqrt{2}}\gamma^{+}\gamma_{\top}\gamma^{\nu}_{\top}\gamma^{\alpha}_{\top}$. After dropping all terms that leave the divergent $(p_2+p_3)^2$ factor in the denominator intact, one finds

$$\mathcal{O}^{ia}(x_1,x_2) = -\frac{\sqrt{2}g^3\ln\mu}{4\pi^2}(t^at^c)_{ii'}f^{da'c} \tag{B.68}$$
$$\times\int d\mathcal{M}_3 V(x_1,x_2|y_1,y_2,y_3)\bar{\psi}_{i'}(p_1)\gamma^{+}\gamma_{\top}A^{a'}_{\perp}(p_2)A^{d}_{\top}(p_3)\,,$$

with the following nontrivial evolution kernel

$$V(x_1,x_2|y_1,y_2,y_3) = -\frac{\left(y_1^2-3y_1x_2+2x_2^2\right)\vartheta^0_{112}(x_1,y_1-x_2,-x_2)}{y_2y_3(y_2+y_3)}$$
$$+\frac{x_1(y_1-2x_2)\vartheta^0_{22}(y_1-x_2,-x_2)}{y_2y_3(y_2+y_3)}+\frac{(2x_2-y_1)(y_2-y_3)\vartheta^1_{122}(x_1,y_1-x_2,-x_2)}{y_2y_3}$$
$$+\frac{(y_1(y_3-3y_2)+2x_2(y_2-y_3))\vartheta^0_{122}(x_1,y_1-x_2,-x_2)}{y_2y_3(y_2+y_3)}$$
$$+\frac{4x_2(x_2-y_1)(-y_1-y_2-y_3+x_2)\vartheta^2_{122}(x_1,y_1-x_2,-x_2)}{y_2(y_2+y_3)}\,. \tag{B.69}$$

B.4.3 Double Equations of Motion

In certain mixing channels, one also has to account for graphs that involve double use of quark and/or gluon equations of motion. In these cases, the method advocated above works as well. Below, one gives a couple of examples to illustrate the point. First, one discusses the diagram, shown in Fig. B.6 (b), that possesses two quark on-shell propagators. Its integral representation reads

$$\begin{aligned}\mathcal{O}^{ia}(x_1,x_2) = \int\prod_{i=1}^{3}\frac{d^4p_i}{(2\pi)^4}\delta(p_i^+ - y_i)\prod_{j=1}^{2}\frac{d^4k_i}{(2\pi)^4}\delta(k_j^+ - x_j)\bar\psi^{i'}(p_1)\\ \times i\mathcal{V}^d_\rho(p_1,p_2,-p_1-p_2)i\mathcal{P}(p_1+p_2)i\mathcal{V}^{a'}_\chi(p_1+p_2,p_3,-p_1-p_2-p_3)\\ \times i\mathcal{P}(p_1+p_2+p_3)i\mathcal{V}^b_\mu(p_1+p_2+p_3,-k_1,-k_2)i\mathcal{P}(k_1)\Gamma^{\alpha\chi}_\top\\ \times(-i)\Delta^{\rho\sigma}_{ab}(k_2)k_{1\top}A^{a'}_\perp(p_2)A^\rho_{d\perp}(p_3)\,,\end{aligned}$$

where $\Gamma^{\alpha\chi}_\top = \frac{1}{2\sqrt{2}}\gamma^+\gamma_\top\gamma^\alpha_\top\gamma^\chi_\top$ projects the quark-gluon operator in question. Separating the terms with cancelled denominators $(p_1+p_2)^2(p_1+p_2+p_3)^2$ front the rest, one has the following contribution to the transition from double quark equation of motion,

$$\begin{aligned}\mathcal{O}^{ia}(x_1,x_2) = \frac{ig^3\ln\mu}{2\sqrt{2}\pi^2}(t^dt^{a'}t^a)_{ii'}\\ \times\int d\mathcal{M}_3\,\frac{x_1x_2\vartheta^0_{12}(x_1,-x_2)}{y_2y_3(x_1+x_2)}\bar\psi^{i'}(p_1)\gamma^+\gamma_\top A^{a'}_\perp(p_2)A^d_\top(p_3)\,.\end{aligned}\tag{B.70}$$

Last but not least, let us address the case involving both quark and gluon equations of motion. A representative graph in demonstrated in Fig. B.6 (c). It provided an additive contribution to the following two-to-three transition

$$\tfrac{1}{2}D_{-+}\bar\psi^i_+(x_1)f^a_{++}(x_2)\to\bar\psi^i_+(y_1)f^a_{++}(y_2)\bar f^d_{++}(y_3)$$

and gives

$$\mathcal{O}^{ia}(x_1,x_2) = \int\prod_{i=1}^{3}\frac{d^4p_i}{(2\pi)^4}\delta(p_i^+ - y_i)\prod_{j=1}^{2}\frac{d^4k_j}{(2\pi)^4}\delta(k_j^+ - x_j)k_{1,\top}A^{a'\rho}_\perp(p_2)A^{d\chi}_\perp(p_3)$$

$$\times \bar{\psi}(p_1) i\mathcal{V}^b_\lambda(p_1, p_2+p_3, -p_1-p_2-p_3) i\mathcal{P}(p_1+p_2+p_3)$$
$$\times i\mathcal{V}^c_\sigma(-k_1,-k_2,p_1+p_2+p_3) i\mathcal{P}(k_1)\Gamma_\top \mathcal{V}^{b'da'}_{\tau\chi\rho}(-p_2-p_3,p_3,p_2)$$
$$\times (-i)\Delta^{\alpha\sigma}_{ac}(k_2)(-i)\Delta^{\lambda\tau}_{bb'}(p_2+p_3)\,, \tag{B.71}$$

with $\Gamma_\top = \frac{1}{2\sqrt{2}}\gamma^+\gamma_\top$. Projecting on the channel in question, taking care of the symmetrization by swapping $A^{a'\rho}_\perp \leftrightarrow A^{d\chi}_\perp$ and finally dropping terms with uncancelled denominator $(p_2+p_3)^2(p_1+p_2+p_3)^2$, one gets

$$\mathcal{O}^{ia}(x_1,x_2) = -\frac{g^3\ln\mu}{8\sqrt{2}\pi^2}(t^b t^a)_{ii'} f^{ba'd} \tag{B.72}$$
$$\times \int d\mathcal{M}_3 \frac{x_1x_2(y_2-y_3)\vartheta^0_{12}(x_1,-x_2)}{(x_1+x_2)y_2y_3(y_2+y_3)} \bar{\psi}^{i'}(p_1)\gamma^+\gamma_\top A^{a'}_\perp(p_2) A^d_\top(p_3)\,.$$

B.5 Light-Ray Kernels in Section 3.4.3

Here one converts the diagrammatic results given in Sects. 3.4.3 and 3.4.3 into the coordinate space. This is done by inverse-Fourier transform the corresponding kernels in momentum space making use of formulas in Sect. 3.3.2 and applied in Appendix B.2.2.

B.5.1 Coordinate Kernels for Operators 3.145 in Sect. 3.4.3

We start with the operators involving transverse derivatives[13]

$$\mathbb{O}^{ia}(z_1,z_2) = \tfrac{1}{2} D_{-+}\bar{\psi}^i_+(z_1)\bar{f}^a_{++}(z_2)$$

and $\mathbb{O}^{ia}(z_1,z_2) = \bar{\psi}^i_+(z_1)\frac{1}{2}D_{-+}\bar{f}^a_{++}(z_2)$ evolving into

$$\mathbb{O}^{iad}(z_1,z_2,z_3) = g\sqrt{2}\bar{\psi}^i_+(z_1)\bar{f}^a_{++}(z_2)\bar{f}^d_{++}(z_3)\,.$$

For both of them, the transition gets decomposed into the same color-flow structures and reads

$$[\mathbb{H}^{(2\to3)}\mathbb{O}]^{ia}(z_1,z_2) = \sum_{c=1}^{6}[C_c]^{ia}_{a'i'd}[\mathbb{H}_c\mathbb{O}^{i'a'd}](z_1,z_2,z_3)\,, \tag{B.73}$$

[13] Here, $\mathbb{O}^{ia}$ and $\mathbb{O}^{i'a'd}$ corresponds to operator X and Y in Ref. [78], respectively.

where C_c are defined in Eq. (3.158). The kernels for the first operator, i.e., $\frac{1}{2}D_{-+}\bar{\psi}^i_+(z_1)\bar{f}^a_{++}(z_2)$ read

$$[\mathbb{H}_1\mathbb{O}]^{ia}(z_1,z_2) = z_{12}\Big\{\int_0^1 d\alpha\int_{\bar\alpha}^1 d\beta\,\frac{\bar\beta^2}{\beta}\,\mathbb{O}^{i'a'd}(z_{21}^\alpha,z_2,z_{12}^\beta) + 2\int_0^1 d\alpha\int_{\bar\alpha}^1 d\beta\,\alpha\bar\beta\,\mathbb{O}^{i'a'd}(z_1,z_{12}^\alpha,z_{21}^\beta) + \int_0^1 d\beta\bar\beta\,\mathbb{O}^{i'a'd}(z_1,z_2,z_{12}^\beta)\Big\}, \tag{B.74}$$

$$[\mathbb{H}_2\mathbb{O}]^{ia}(z_1,z_2) = z_{12}\int_0^1 d\alpha\int_{\bar\alpha}^1 d\beta\,\frac{\bar\alpha\beta}{\alpha}\left(2-\frac{\bar\alpha\bar\beta}{\alpha\beta}\right)\mathbb{O}^{i'a'd}(z_{12}^\alpha,z_2,z_{21}^\beta), \tag{B.75}$$

$$[\mathbb{H}_3\mathbb{O}]^{ia}(z_1,z_2) = -z_{12}\Big\{\int_0^1 d\alpha\int_{\bar\alpha}^1 d\beta\,\frac{\bar\beta^2}{\beta}\,\mathbb{O}^{i'a'd}(z_{21}^\alpha,z_{12}^\beta,z_2) + 2\int_0^1 d\alpha\int_{\bar\alpha}^1 d\beta\,\alpha\bar\beta\,\mathbb{O}^{i'a'd}(z_1,z_{21}^\beta,z_{12}^\alpha) + \int_0^1 d\beta\bar\beta\,\mathbb{O}^{i'a'd}(z_1,z_{12}^\beta,z_2)\Big\}, \tag{B.76}$$

$$[\mathbb{H}_4\mathbb{O}]^{ia}(z_1,z_2) = -2z_{12}\int_0^1 d\alpha\int_{\bar\alpha}^1 d\beta\,\bar\alpha\beta\,\mathbb{O}^{i'a'd}(z_2,z_{12}^\alpha,z_{21}^\beta), \tag{B.77}$$

$$[\mathbb{H}_5\mathbb{O}]^{ia}(z_1,z_2) = z_{12}\Big\{\int_0^1 d\alpha\int_{\bar\alpha}^1 d\beta\,\frac{\bar\alpha\beta}{\alpha}\left(2-\frac{\bar\alpha\bar\beta}{\alpha\beta}\right)\mathbb{O}^{i'a'd}(z_{12}^\alpha,z_{21}^\beta,z_2) - 2\int_0^1 d\alpha\int_0^{\bar\alpha} d\beta\,\bar\alpha\beta\,\mathbb{O}^{i'a'd}(z_2,z_{12}^\alpha,z_{21}^\beta)\Big\}, \tag{B.78}$$

$$[\mathbb{H}_6\mathbb{O}]^{ia}(z_1,z_2) = -z_{12}\int_0^1 d\alpha\int_{\bar\alpha}^1 d\beta\,\frac{\bar\alpha\beta}{\alpha}\left(2-\frac{\bar\alpha\bar\beta}{\alpha\beta}\right)\mathbb{O}^{i'a'd}(z_{12}^\alpha,z_{21}^\beta,z_2). \tag{B.79}$$

Here the symmetry of $a\leftrightarrow d, w_2\leftrightarrow w_3$ described in the main text of Sect. 3.4.3 becomes manifest. Notice that the kernels $\mathbb{H}_1$ and $\mathbb{H}_3$ can be mapped into each other by a simple exchange of the gluon fields $\mathbb{O}(w_1,w_2,w_3)\leftrightarrow\mathbb{O}(w_1,w_3,w_2)$. This serves as another check for the kernels.

For the $\mathbb{O}^{ia}(z_1,z_2) = \bar{\psi}^i_+(z_1)\frac{1}{2}D_{-+}\bar{f}^a_{++}(z_2)$ case, one finds

$$[\mathbb{H}_1\mathbb{O}]^{ia}(z_1,z_2) = z_{12}\Big\{\int_0^1 d\alpha\int_{\bar\alpha}^1 d\beta\,\frac{\bar\alpha^2\beta}{\alpha}\mathbb{O}^{i'a'd}(z_1,z_{12}^\beta,z_{21}^\alpha) + \int_0^1 d\alpha\int_{\bar\alpha}^1 d\beta\,\frac{\alpha\bar\beta^2}{\beta}\left(2-\frac{\bar\alpha\bar\beta}{\alpha\beta}\right)\mathbb{O}^{i'a'd}(z_1,z_{12}^\alpha,z_{21}^\beta) + \int_0^1 d\alpha\int_0^{\bar\alpha} d\beta\,\beta\,\mathbb{O}^{i'a'd}(z_{12}^\alpha,z_2,z_{21}^\beta)$$

$$- \int_0^1 d\beta\, \bar\beta\, \mathbb{O}^{i'a'd}(z_1, z_2, z_{12}^\beta) \Big\}, \tag{B.80}$$

$$[\mathbb{H}_2\mathbb{O}]^{ia}(z_1,z_2) = z_{12} \int_0^1 d\alpha \int_{\bar\alpha}^1 d\beta\, \beta\, \mathbb{O}^{i'a'd}(z_{12}^\alpha, z_2, z_{21}^\beta), \tag{B.81}$$

$$\begin{aligned}[\mathbb{H}_3\mathbb{O}]^{ia}(z_1,z_2) = -z_{12} \Big\{ & \int_0^1 d\alpha \int_{\bar\alpha}^1 d\beta\, \frac{\bar\alpha^2\beta}{\alpha} \mathbb{O}^{i'a'd}(z_1, z_{21}^\alpha, z_{12}^\beta) \\ & + \int_0^1 d\alpha \int_{\bar\alpha}^1 d\beta \frac{\alpha\bar\beta^2}{\beta} \left(2 - \frac{\bar\alpha\bar\beta}{\alpha\beta}\right) \mathbb{O}^{i'a'd}(z_1, z_{21}^\beta, z_{12}^\alpha) \\ & + \int_0^1 d\alpha \int_0^{\bar\alpha} d\beta\, \beta\, \mathbb{O}^{i'a'd}(z_{12}^\alpha, z_{21}^\beta, z_2) \\ & - \int_0^1 d\beta\, \bar\beta\, \mathbb{O}^{i'a'd}(z_1, z_{12}^\beta, z_2) \Big\}, \end{aligned} \tag{B.82}$$

$$\begin{aligned}[\mathbb{H}_4\mathbb{O}]^{ia}(z_1,z_2) = -z_{12} \Big\{ & \int_0^1 d\alpha \int_{\bar\alpha}^1 d\beta\, \bar\alpha\bar\beta\, \mathbb{O}^{i'a'd}(z_2, z_{12}^\alpha, z_{21}^\beta) \\ & + \int_0^1 \int_0^{\bar\alpha} d\beta\, \bar\alpha\bar\beta\, \mathbb{O}^{i'a'd}(z_2, z_{21}^\beta, z_{12}^\alpha) \Big\}, \end{aligned} \tag{B.83}$$

$$\begin{aligned}[\mathbb{H}_5\mathbb{O}]^{ia}(z_1,z_2) = -z_{12} \Big\{ & \int_0^1 d\alpha \int_{\bar\alpha}^1 d\beta\, \bar\alpha\bar\beta\, \mathbb{O}^{i'a'd}(z_2, z_{21}^\beta, z_{12}^\alpha) \\ & + \int_0^1 \int_0^{\bar\alpha} d\beta\, \bar\alpha\bar\beta\, \mathbb{O}^{i'a'd}(z_2, z_{12}^\alpha, z_{21}^\beta) \\ & + \int_0^1 d\alpha \int_{\bar\alpha}^1 d\beta\, \beta\, \mathbb{O}^{i'a'd}(z_{12}^\alpha, z_{21}^\beta, z_2) \Big\}, \end{aligned} \tag{B.84}$$

$$[\mathbb{H}_6\mathbb{O}]^{ia}(z_1,z_2) = -z_{12} \int_0^1 d\alpha \int_{\bar\alpha}^1 d\beta\, \beta\, \mathbb{O}^{i'a'd}(z_{12}^\alpha, z_{21}^\beta, z_2). \tag{B.85}$$

B.5.2 Coordinate Kernels for Operators 3.171 in Sect. 3.4.3

As in Sect. B.5.1, one presents here coordinate-space transition of $\mathbb{O}^{ai}(z_1,z_2) = \bar f^a_{++}(z_1)\psi^i_-(z_2)$ and $\mathbb{O}^{ai}(z_1,z_2) = \frac{1}{2} D_{-+} \bar f^a_{++}(z_1)\psi^i_+(z_2)$ into three-particle operator $\mathbb{O}^{aid} = g\sqrt{2}\bar f^a_{++}(z_1)\psi^i_+(z_2)\bar f^d_{++}(z_3)$. The action of the Hamiltonian yields the decomposition

$$[\mathbb{H}^{(2\to3)}\mathbb{O}]^{ai}(z_1,z_2) = \sum_{c=1}^{6} [C_c]^{ia}_{a'i'd} [\mathbb{H}_c \mathbb{O}^{a'i'd}](z_1,z_2,z_3), \tag{B.86}$$

where the color structures are introduced in Eq. (3.174).

Then for $\bar f^a_{++}(z_1)\psi^i_-(z_2)$, one gets

$$[\mathbb{H}_1\mathbb{O}]^{ai}(z_1,z_2) = -z_{12}^2 \Big\{ 2 \int_0^1 d\alpha \int_0^{\bar\alpha} d\beta \int_\beta^{\bar\alpha} d\gamma\, \bar\alpha\gamma\, \mathbb{O}^{a'i'd}(z_{12}^\alpha, z_{21}^\beta, z_{21}^\gamma)$$

$$+\int_0^1 d\alpha \int_{\bar\alpha}^1 d\beta\, \bar\beta\, \mathbb{O}^{a'i'd}(z_1, z_{12}^{\alpha}, z_{21}^{\beta})\Big\}, \tag{B.87}$$

$$[\mathbb{H}_2\mathbb{O}]^{ai}(z_1,z_2) = -z_{12}^2\Big\{2\int_0^1 d\alpha \int_0^{\bar\alpha} d\beta \int_{\bar\alpha}^1 d\gamma\, \bar\alpha\gamma\, \mathbb{O}^{a'i'd}(z_{12}^{\alpha}, z_{21}^{\beta}, z_{21}^{\gamma}) - \int_0^1 d\alpha \int_0^{\alpha} d\beta\, \alpha\, \mathbb{O}^{a'i'd}(z_{21}^{\alpha}, z_{21}^{\beta}, z_1)\Big\}, \tag{B.88}$$

$$[\mathbb{H}_3\mathbb{O}]^{ai}(z_1,z_2) = z_{12}^2\Big\{2\int_0^1 d\alpha \int_0^{\bar\alpha} d\beta \int_0^{\beta} d\gamma\, \bar\alpha\gamma\, \mathbb{O}^{a'i'd}(z_{12}^{\alpha}, z_{21}^{\beta}, z_{21}^{\gamma}) + \int_0^1 d\alpha \int_{\bar\alpha}^1 d\beta\, \frac{\bar\alpha\bar\beta}{\alpha}\, \mathbb{O}^{a'i'd}(z_1, z_{21}^{\alpha}, z_{12}^{\beta})\Big\}, \tag{B.89}$$

$$[\mathbb{H}_4\mathbb{O}]^{ai}(z_1,z_2) = 2z_{12}^2 \int_0^1 d\alpha \int_{\bar\alpha}^1 d\beta \int_0^{\bar\alpha} d\gamma\, \bar\alpha\gamma\, \mathbb{O}^{a'i'd}(z_{12}^{\alpha}, z_{21}^{\beta}, z_{21}^{\gamma}), \tag{B.90}$$

$$[\mathbb{H}_5\mathbb{O}]^{ai}(z_1,z_2) = z_{12}^2\Big\{2\int_0^1 d\alpha \int_{\bar\alpha}^1 d\beta \int_{\bar\alpha}^1 d\gamma\, \bar\alpha\gamma\, \mathbb{O}^{a'i'd}(z_{12}^{\alpha}, z_{21}^{\beta}, z_{21}^{\gamma}) + \int_0^1 d\alpha \int_{\bar\alpha}^1 d\beta\, \frac{\bar\alpha\bar\beta}{\alpha}\, \mathbb{O}^{a'i'd}(z_{12}^{\beta}, z_{21}^{\alpha}, z_1)\Big\}, \tag{B.91}$$

$$[\mathbb{H}_6\mathbb{O}]^{ai}(z_1,z_2) = -z_{12}^2\Big\{2\int_0^1 d\alpha \int_{\bar\alpha}^1 d\beta \int_{\beta}^1 d\gamma\, \bar\alpha\gamma\, \mathbb{O}^{a'i'd}(z_{12}^{\alpha}, z_{21}^{\beta}, z_{21}^{\gamma}) + \int_0^1 d\alpha \int_{\bar\alpha}^1 d\beta\, \frac{\bar\alpha\bar\beta}{\alpha}\, \mathbb{O}^{a'i'd}(z_{12}^{\beta}, z_{21}^{\alpha}, z_1)\Big\}. \tag{B.92}$$

Here the $w_1 \leftrightarrow w_3$ symmetry is readily observed. While for $\frac{1}{2}D_{-+}\bar f^a_{++}(z_1)\psi^i_+(z_2)$ case, the transitions are

$$\begin{aligned}[\mathbb{H}_1\mathbb{O}]^{ai}(z_1,z_2) = z_{12}\Big\{ &\int_0^1 d\alpha \int_{\bar\alpha}^1 d\beta \frac{\bar\alpha^2\beta}{\alpha}\mathbb{O}^{a'i'd}(z_{21}^{\beta}, z_2, z_{12}^{\alpha}) \\ &+ \int_0^1 d\alpha \int_0^{\bar\alpha} d\beta \int_{\beta}^{\bar\alpha} d\gamma\, \bar\alpha\gamma\Big(4 - \frac{\alpha\gamma}{\bar\alpha\bar\gamma}\Big)\mathbb{O}^{a'i'd}(z_{12}^{\alpha}, z_{21}^{\beta}, z_{21}^{\gamma}) \\ &+ \int_0^1 d\alpha \int_0^{\bar\alpha} d\beta \int_{\bar\alpha}^1 d\gamma\, \bar\alpha\gamma\Big(2 + \frac{\bar\alpha\bar\gamma}{\alpha\gamma}\Big)\mathbb{O}^{a'i'd}(z_{21}^{\gamma}, z_{21}^{\beta}, z_{12}^{\alpha}) \\ &+ \int_0^1 d\alpha \int_{\bar\alpha}^1 d\beta \frac{\alpha\bar\beta^2}{\beta}\Big(2 - \frac{\bar\alpha\bar\beta}{\alpha\beta}\Big)\mathbb{O}^{a'i'd}(z_{21}^{\alpha}, z_2, z_{12}^{\beta}) \\ &+ \int_0^1 d\beta\, \bar\beta\, \mathbb{O}^{a'i'd}(z_1, z_2, z_{12}^{\beta})\Big\}, \end{aligned} \tag{B.93}$$

$$\begin{aligned}[\mathbb{H}_2\mathbb{O}]^{ai}(z_1,z_2) = -z_{12}\Big\{ &\int_0^1 d\alpha \int_{\bar\alpha}^1 d\beta \frac{\bar\alpha^2\beta}{\alpha}\mathbb{O}^{a'i'd}(z_{12}^{\alpha}, z_2, z_{21}^{\beta}) \\ &+ \int_0^1 d\alpha \int_0^{\bar\alpha} d\beta \int_{\beta}^{\bar\alpha} d\gamma\, \bar\alpha\gamma\Big(4 - \frac{\alpha\gamma}{\bar\alpha\bar\gamma}\Big)\mathbb{O}^{a'i'd}(z_{21}^{\gamma}, z_{21}^{\beta}, z_{12}^{\alpha}) \\ &+ \int_0^1 d\alpha \int_0^{\bar\alpha} d\beta \int_{\bar\alpha}^1 d\gamma\, \bar\alpha\gamma\Big(2 + \frac{\bar\alpha\bar\gamma}{\alpha\gamma}\Big)\mathbb{O}^{a'i'd}(z_{12}^{\alpha}, z_{21}^{\beta}, z_{21}^{\gamma}) \end{aligned}$$

$$+\int_0^1 d\alpha \int_{\bar\alpha}^1 d\beta \frac{\alpha\bar\beta^2}{\beta}\left(2-\frac{\bar\alpha\bar\beta}{\alpha\beta}\right)\mathbb{O}^{a'i'd}(z_{12}^{\beta},z_2,z_{21}^{\alpha})$$
$$+\int_0^1 d\beta\,\bar\beta\,\mathbb{O}^{a'i'd}(z_{12}^{\beta},z_2,z_1)\Bigg\}, \tag{B.94}$$

$$[\mathbb{H}_3\mathbb{O}]^{ai}(z_1,z_2)=z_{12}\Bigg\{\int_0^1 d\alpha\int_0^{\bar\alpha} d\beta\int_0^{\beta} d\gamma\bar\alpha\gamma\left(4-\frac{\alpha\gamma}{\bar\alpha\bar\gamma}\right)\mathbb{O}^{a'i'd}(z_{12}^{\alpha},z_{21}^{\beta},z_{21}^{\gamma})$$
$$+\int_0^1 d\alpha\int_{\bar\alpha}^1 d\beta\int_{\beta}^1 d\gamma\bar\alpha\gamma\left(2+\frac{\bar\alpha\bar\gamma}{\alpha\gamma}\right)\mathbb{O}^{a'i'd}(z_{21}^{\gamma},z_{21}^{\beta},z_{12}^{\alpha})\Bigg\}, \tag{B.95}$$

$$[\mathbb{H}_4\mathbb{O}]^{ai}(z_1,z_2)=-z_{12}\Bigg\{\int_0^1 d\alpha\int_{\bar\alpha}^1 d\beta\int_0^{\bar\alpha} d\gamma\bar\alpha\gamma\left(4-\frac{\alpha\gamma}{\bar\alpha\bar\gamma}\right)\mathbb{O}^{a'i'd}(z_{12}^{\alpha},z_{21}^{\beta},z_{21}^{\gamma})$$
$$+\int_0^1 d\alpha\int_{\bar\alpha}^1 d\beta\int_{\bar\alpha}^1 d\gamma\bar\alpha\gamma\left(2+\frac{\bar\alpha\bar\gamma}{\alpha\gamma}\right)\mathbb{O}^{a'i'd}(z_{21}^{\gamma},z_{21}^{\beta},z_{12}^{\alpha})$$
$$-\int_0^1 d\alpha\int_{\bar\alpha}^1 d\beta\int_{\beta}^1 d\gamma\bar\alpha\gamma\left(2+\frac{\bar\alpha\bar\gamma}{\alpha\gamma}\right)\mathbb{O}^{a'i'd}(z_{21}^{\gamma},z_{21}^{\beta},z_{12}^{\alpha})\Bigg\}, \tag{B.96}$$

$$[\mathbb{H}_5\mathbb{O}]^{ai}(z_1,z_2)=-z_{12}\Bigg\{\int_0^1 d\alpha\int_0^{\bar\alpha} d\beta\int_0^{\beta} d\gamma\bar\alpha\gamma\left(4-\frac{\alpha\gamma}{\bar\alpha\bar\gamma}\right)\mathbb{O}^{a'i'd}(z_{21}^{\gamma},z_{21}^{\beta},z_{12}^{\alpha})$$
$$+\int_0^1 d\alpha\int_{\bar\alpha}^1 d\beta\int_0^{\bar\alpha} d\gamma\bar\alpha\gamma\left(4-\frac{\alpha\gamma}{\bar\alpha\bar\gamma}\right)\mathbb{O}^{a'i'd}(z_{21}^{\gamma},z_{21}^{\beta},z_{12}^{\alpha})$$
$$+\int_0^1 d\alpha\int_{\bar\alpha}^1 d\beta\int_{\bar\alpha}^1 d\gamma\bar\alpha\gamma\left(2+\frac{\bar\alpha\bar\gamma}{\alpha\gamma}\right)\mathbb{O}^{a'i'd}(z_{12}^{\alpha},z_{21}^{\beta},z_{21}^{\gamma})\Bigg\}, \tag{B.97}$$

$$[\mathbb{H}_6\mathbb{O}]^{ai}(z_1,z_2)=z_{12}\Bigg\{\int_0^1 d\alpha\int_{\bar\alpha}^1 d\beta\int_{\beta}^1 d\gamma\bar\alpha\gamma\left(2+\frac{\bar\alpha\bar\gamma}{\alpha\gamma}\right)\mathbb{O}^{a'i'd}(z_{12}^{\alpha},z_{21}^{\beta},z_{21}^{\gamma})$$
$$+\int_0^1 d\alpha\int_0^{\bar\alpha} d\beta\int_0^{\beta} d\gamma\bar\alpha\gamma\left(4-\frac{\alpha\gamma}{\bar\alpha\bar\gamma}\right)\mathbb{O}^{a'i'd}(z_{21}^{\gamma},z_{21}^{\beta},z_{12}^{\alpha})\Bigg\}. \tag{B.98}$$